Using *Caenorhabditis elegans* to identify succinimide-based neuroprotective compounds and their mechanisms of action

Shi Quan Wong

Thesis submitted in accordance with the requirements of the University of Liverpool for the degree of Doctor in Philosophy

September 2017

"…all the most acute, most powerful, and most deadly diseases, and those which are most difficult to be understood by the inexperienced, fall upon the brain."

Hippocrates

TABLE OF CONTENTS

ABSTRACT

Title: Using *Caenorhabditis elegans* to identify succinimide-based neuroprotective compounds and their mechanisms of action

Author: Shi Quan Wong

Neurodegenerative diseases such as Alzheimer's disease (AD) and amyotrophic lateral sclerosis (ALS) are associated with a significant socioeconomic burden. As age is a major risk factor for the development of these conditions, coupled with the fact that no disease-modifying treatments exist, the predicted ageing population growth in the next few decades is only expected to exacerbate this burden. The antiepileptic drug (AED) ethosuximide is a first-line treatment for absence seizures which exhibited neuroprotective and lifespan-extending effects in various models of neurodegeneration in *Caenorhabditis elegans* and rodents, making it a promising repurposing candidate for treating neurodegenerative diseases. As its molecular mechanism of action (MMOA) remains unclear despite being an established AED, delineating its MMOA may provide useful insights into the pathogenesis processes of these diseases. A most direct and informative strategy is to deconvolute the drug's molecular target(s), and this is classically performed with affinity-type binding approaches such as affinity chromatography, which requires appropriate drug derivatisation for subsequent immobilisation onto an affinity matrix. However, drug repurposing and target identification may prove difficult or unfeasible due to suggestive low potency from high therapeutic concentrations and doses required in models and humans. To improve the prospects of both approaches, the aim of the current project is to develop compounds with enhanced neuroprotective potency from ethosuximide as an alternative strategy. Using chemistry approaches, a selection of structurally-similar compounds to the drug were selected and screened for anticonvulsant activity in a *C. elegans* seizure model. This facilitated in-house insights into the structure-activity relationship (SAR) of the drug, which informs about appropriate molecular modifications on ethosuximide and/or its derivatives for further potency enhancement and for target identification studies. Furthermore, screens identified a candidate molecule with a two-fold enhanced anticonvulsant potency than the drug. This molecule, referred to as compound 9, was further verified for its neuroprotective and lifespan-extending properties in a *C. elegans* ALS model whereby it ameliorated locomotion defects, extended the reduced lifespan, and conferred direct protection against neurodegeneration. Comparable extent of protection was exerted at a 160-fold lower externally-administered concentration than ethosuximide. Further ^{1}H nuclear magnetic resonance (NMR) spectroscopy analysis of treated worms suggest that compound 9 had bioaccumulated below the detection limit of 5 µM whereas the internal concentration of ethosuximide was determined to be 143.8 µM, excluding improved bioaccumulation as an unlikely contributing factor towards the enhanced potency of the compound. Finally, both compounds required the DAF-16 forkhead box O (FOXO) transcription factor to exert protection in the ALS worms, demonstrating similar aspects of their MMOAs. Taken together, the current study has established important contributions towards expediting translational efforts for treating neurodegenerative diseases through the identification of compound 9.

ACKNOWLEDGEMENTS

First and foremost, I would like to thank my funder, the Wellcome Trust, and my supervisors, Alan Morgan and Bob Burgoyne. Thank you for making this project possible, and for your patience and guidance throughout my PhD. To Alan especially, thank you for being such an involved primary supervisor, for advising me on things PhD and non-PhD related, and for pushing me out of my comfort zone so much with this project - it hasn't been an easy one at all but I would not have traded this experience for anything else. I would also like to extend my gratitude to our collaborators Paul O'Neill, Neil Berry, and Chandra Pidathala from the Chemistry department, and Marie Phelan from the Technology Directorate/NMR centre, for the help and technical support they have given me throughout the project. To Marie especially, you have been so understanding and patient with me, and I really appreciate you for lending a listening ear. To the other members of Red Block past and present, Jeff, Lee, Charlotte, Nordine, Alistair, Rick, Iman, Paul, Dayani, Hannah, and all the MRes students who have spent time in our lab, it has been a tremendous pleasure to have worked alongside you all. Each and every one of you has made Red Block such a great place to be in, and I am truly going to miss it.

To my friends back home, thank you for the continuing presence in my life despite me having been away for so long. To my friends in Liverpool, Zohra, Charlotte, Helen, Francesca, Fiona, Louise, Erica, Hannah, Alistair, Rick, Ste, thank you playing such a positive role in my life for the past few years in this city. To Zohra, Charlotte, Fran, Helen, Fi, Nic, Dina, and Manda especially, thank you for being the physical presence and listening ear when I needed it. You've dealt with my highs and lows – especially my lows – and you've always made sure that I know it's fine to feel the way I did. I wouldn't have lasted final year without you.

To my family, thank you for everything. I would never have had the opportunity to experience a life abroad without your unwavering support. I'm sorry for all the times I've been "too busy" to call, and for not being more involved with what is happening back home. I hope that you are proud of what I have achieved.

This thesis is dedicated to my grandmother who passed away last year.

ABBREVIATIONS

1D	1-dimensional
^{1}H	Proton
6-OHDA	6-hydroxydopamine
Aa	Amino acid
Aβ	Amyloid beta
AcN	Acetonitrile
AD	Alzheimer's disease
ADME	Adsorption, distribution, metabolism, elimination
AKT	Protein kinase B
AED	Antiepileptic drug
ALS	Amyotrophic lateral sclerosis
ANCL	Adult-onset neuronal ceroid lipofuscinosis
APoE4	Apolipoprotein E type 4 allele
APP	Amyloid precursor protein
ARE	Antioxidant response element
ASCII	American Standard Code for Information Interchange
BSA	Bovine serum albumin
Ca^{2+}	Calcium ions
Ca_V	Voltage-gated calcium channel
cDNA	Complementary deoxyribonucleic acid
CIP	Cahn-Ingold-Prelog
CLogD	Calculated dissociation coefficient
CLogP	Calculated partition coefficient
CNS	Central nervous system
CNS MPO	Central nervous system multiparameter algorithm
CPMG	Carr-Purcell-Meiboom-Gill
CSF	Cerebrospinal fluid
CTF	C-terminal fragment
DAE	DAF-16-associated element
DARTS	Drug affinity responsive target stability
DBE	DAF-16-binding element
DD	Dorsal D

DMSO	Dimethyl sulfoxide
DNA	Deoxyribonucleic acid
DRS	Dent's Ringer solution
dsRNA	Double-stranded RNA
EEG	Electroencephalogram
eIF2α	Eukaryotic initiation factor 2α
EMS	Ethyl methanesulfonate
ER	Endoplasmic reticulum
FDA	Food and Drug Administration
FDG	Fluorodeoxyglucose
FOXO	Forkhead box O
FTD	Frontotemporal dementia
FTDP-17	Frontotemporal dementia with parkinsonism-17
FUDR	5-Fluoro-2′-deoxyuridine
FUS	Fused in sarcoma
GABA	Gamma-aminobutyric acid
$GABA_A$	GABA type A receptor
GAERS	Genetic Absence Epilepsy Rats from Strasbourg
GAT-1	Sodium- and chloride-dependent GABA transporter 1
GFP	Green fluorescent protein
GRR	Glycine-rich region
GWAS	Genome-wide association studies
HD	Huntington's disease
HPLC	High performance liquid chromatography
HT	High throughput
HTS	High throughput screening
HTT	Huntingtin
IGF-1	Insulin-like growth factor 1
IGFR	IGF-1 receptor
IIS	Insulin/IGF-1 signalling
ILP	Insulin-like peptide
iPSC	Induced pluripotent stem cell
K^+	Potassium ions
K_D	Dissociation constant

K_V7	*KCNQ*-encoded low-threshold voltage-gated potassium channels
MES	Maximal electroshock
MMOA	Molecular mechanism of action
MOO/MPO	Multi-objective optimisation/multiparameter optimisation
MPTP	1-methyl-4-phenyl-1,2,3,6-tetrahydropyridine
MRI	Magnetic resonance imaging
Na^{2+}	Sodium ions
Na_V	Voltage-gated sodium channel
NES	Nuclear export signal
NFT	Neurofibrillary tangle
NGM	Nematode growth media
NLS	Nuclear localisation signal
NMDA	N-methyl D-aspartate
NMR	Nuclear magnetic resonance
NOESY	Nuclear Overhauser Enhancement Spectroscopy
Nrf2	NFE2-related factor 2
OASIS	Online Application for the Survival Analysis of Lifespan Assays
PAGE	Polyacrylamide gel electrophoresis
PBS	Phosphate buffered saline
PCA	Principal component analysis
PCR	Polymerase chain reaction
PD	Parkinson’s disease
PEG	Polyethylene glycol
PERK	Protein kinase RNA-like ER kinase
PET	Positron emission topography
PI3K	Phosphoinositide 3-kinase
PIP_2	Phosphatidylinositol 4,5-bisphosphate
PIP_3	Phosphatidylinositol 3,4,5-triphosphate
PLS-DA	Partial least squares discriminant analysis
PolyQ	Polyglutamine

PP2A	Protein phosphatase 2A subunit
Ppm	Parts per million
PSEN	Presenilin
PSP	Progressive supranuclear palsy
PTEN	Phosphatase and tensin homolog
PTZ	Pentylenetetrazol
qPCR	Quantitative polymerase chain reaction
RAN	Repeat-associated non-ATG
RNA	Ribonucleic acid
RNAi	RNA interference
RRM	RNA recognition motif
SAR	Structure-activity relationship
SAM	Structure-based accumulation model
scMET	Subcutaneous metrazol
sAPP	Secreted APP
scPTZ	Subcutaneous pentylenetetrazol
SDS	Sodium dodecyl sulfate
SMN	Survival motor neuron
SOD1	Superoxide dismutase 1
SVA-1	Synaptic vesicle protein 2A
Tc	Tanimoto similarity coefficient
TDP-43	Transactive response DNA binding protein 43 kDa
TLC	Thin layer chromatography
TSP	Sodium trimethylsilyl-$^{2}H_{4}$-propionate
VD	Ventral D
WT	Wildtype
YFP	Yellow fluorescent protein

CHAPTER 1

INTRODUCTION

1.1 NEURODEGENERATIVE DISORDERS

Population ageing is a global phenomenon. The ageing population, defined as individuals aged 65 years and older, is predicted to double from 8 to 16 % globally from 2010 to 2050 (Global Health and Aging, 2017). Such a rapid rate of global population ageing is a great cause for concern as age is the major risk factor for the development of neurodegenerative diseases which are progressive in nature, examples of which include Alzheimer's (AD) and Parkinson's (PD) diseases, amyotrophic lateral sclerosis (ALS) or motor neurone disease, and tauopathies such as progressive supranuclear palsy (PSP) and the various types of frontotemporal dementias (FTDs). Intra- and/or extra-neuronal protein aggregates and inclusions are a fundamental feature of these conditions, and implicated proteins are typically aberrantly processed and exist in various forms in these deposits. However, the affected protein species and brain regions are mostly disease-specific, and affected proteins may spread between connected brain anatomical regions via a prion-like mechanism (Brettschneider *et al*., 2015). Furthermore, disease-causative mutations were uncovered in distinct genes, and risk loci identified from linkage analysis, genome-wide association studies (GWAS) and high throughput (HT) sequencing exhibit little commonality between the conditions despite overlapping clinical features. Adding to the layer of complexity, dysfunctions in multiple cellular and molecular processes have been implicated, such as epigenetic changes, defects in mitochondrial function, oxidative stress, dysregulation of protein homeostatic mechanisms such as autophagy, and neuroinflammation (Jellinger, 2010). The complex and multifactorial aetiology of most of these conditions makes delineation of the underlying pathogenic mechanisms difficult. Hence, efforts to develop disease-modifying treatments have been unsuccessful thus far. In the following sections, AD and ALS will be described in greater detail as they are the main form of dementia and motor neuron disease respectively; additionally, the current project utilises a *C. elegans* ALS model. The other forms of neurodegeneration as aforementioned will be briefly highlighted.

1.1.1 Alzheimer's disease (AD)

AD accounts for 40 to 80 % of all dementia, which is a major cause of disability in old age. Dementia is associated with a significant socioeconomic burden; annual expenditure to cope with dementia in the UK alone amounts to approximately £26.3 billion (Later Life in the United Kingdom, 2017) whilst the global cost of dementia is currently estimated at US$818 billion and is expected to become a trillion-dollar disease by 2018 (World Alzheimer Report, 2016). There are an approximate 47 million cases of dementia at present, and this number is projected to surpass 131 million by 2050, with every 1 in 85 individuals predicted to suffer from the condition by then. Six approved treatments for AD exist, four of them being acetylcholinesterase inhibitors (AChEIs; galantamine, rivastigmine, donepezil, and tacrine), an uncompetitive antagonist of the glutamatergic N-methyl D-aspartate (NMDA) receptor memantine (Anand *et al*., 2014), and a combination treatment of AChEI donepezil and memantine (Table 1.1); note that tacrine has been largely discontinued due to its associated hepatotoxicity. However, these drugs offer only symptomatic relief and do not alter disease progression. With the looming projected rise in AD and dementia cases, disease-modifying treatments are essential to counteract the consequential increase of the associated socioeconomic burden.

AD has two neuropathological hallmark features of extracellular senile plaques and intracellular cytoplasmic neurofibrillary tangles (NFTs), which consist of insoluble aggregates of respective amyloid beta (Aβ) (Glenner and Wong, 1984, Masters *et al*., 1985) and hyperphosphorylated forms of the microtubule-binding protein tau (Goedert *et al*., 1989, Goedert *et al*., 1992). These pathological lesions mainly affect brain regions involved in cognition and memory, such as the hippocampus and entorhinal cortex. In addition, it is associated with gliosis and cerebral atrophy, which is indicative of synaptic and neuronal losses. Clinically, three stages of AD have been described, consisting of the pre-symptomatic stage, the prodromal stage of mild cognitive impairment but not yet fully-fledged dementia, and the final stage of dementia (Jack *et al*., 2010).

Disease	Drug	Approval date by FDA	Date withdrawn	Tradename	Mechanism of action	Clinical benefits as evaluated in clinical trials
Alzheimer's disease (AD)	Galantamine	February 2001; for mild-to-moderate AD	NA	Razadyne® (former name Reminyl®)	Deficiencies in cholinergic neurotransmission are linked to Alzheimer's disease; acetylcholinesterase inhibitors (AChEIs) restore this deficiency by elevating acetylcholine levels and neurotransmission through the blockade of acetylcholinesterase-mediated degradation, but may also mediate therapeutic effects through anti-inflammatory activities (Tabet, 2006)	Analysis of 10 clinical trials showed cognitive improvements with galantamine treatment in patients with mild cognitive impairment and probable AD, but not recommended for use in the former due to an unexplained association in excess death rate (Loy and Schneider, 2006).
	Rivastigmine	April 2000; for mild-to-moderate AD	NA	Exelon®		Analysis of 7 clinical trials showed that rivastigmine treatment improved cognitive and functional outcomes, and reduced disease severity in mild-to-moderate patients (Birks *et al*., 2000).
	Donepezil	December 1996; for all stages of AD	NA	Aricept®		Analysis of 23 clinical trials showed overall beneficial effects on cognition, function, and behaviour, with less disease decline in donepezil-treated patients in all stages of disease (Birks and Harvey, 2006).
	Tacrine	September 1993; first approved drug for AD (mild-to-moderate)	Largely discontinued due to associated liver toxicity	Cognex®		Clinical trials showed improvements in cognition and quality of life in probable AD patients treated with tacrine (Farlow *et al*., 1992, Davis *et al*., 1992, Knapp *et al*., 1994).
	Memantine	October 2003; for moderate-to-severe disease	NA	Namenda®	Blocks glutamate excitotoxicity in AD by inhibiting tonic activation of glutamatergic N-methyl D-aspartate (NMDA) receptors (Gilling *et al*., 2009, Revett *et al*., 2013). Therapeutic effect may also be attributed to α7 nicotinic acetylcholine receptor inhibition; block shown to occur at therapeutic concentrations (Aracava *et al*., 2005)	Various clinical trials assessed the impact of memantine therapy in mild-to-moderate (Porsteinsson *et al*., 2008, Peskind *et al*., 2006, Bakchine and Loft, 2007) and moderate-to-severe patients (Reisberg *et al*., 2003, van Dyck *et al*., 2006, Tariot *et al*., 2004) by examining improvements in cognitive, functional, behavioural outcomes, and/or overall global outcomes. Trial findings demonstrated general significant benefits in moderate-to-severe patients but not mild-to-moderate ones.
	Donepezil/ memantine combination	December 2014; for moderate-to-severe disease	NA	Namzaric® (fixed-dose combination of both drugs in one capsule)	AChEI and NMDA inhibition (see above)	Approval status was based on findings from a phase III trial of memantine in moderate-to-severe AD patients on donepezil therapy; memantine/donepezil treatment significantly improved various aspects of cognitive function when compared to memantine/placebo therapy (Grossberg *et al*., 2013). In contrast, combination therapy showed no significant benefits in mild-to-moderate patients (Porsteinsson *et al*., 2008)
Amyotrophic lateral sclerosis (ALS)	Riluzole	December 1995	NA	Rilutek®	Therapeutic effect proposed to be mediated via its anti-glutamatergic effect; also shown to inhibit the persistent Na^{2+} current, delayed rectifier and voltage-gated K^{+} currents, voltage-gated Ca^{2+} currents, and neurotransmitter release, potentiate calcium-dependent K^{+} currents, and promote neuronal survival by increasing neurotrophic factor production at various concentrations, but therapeutic contribution unclear (Bellingham, 2011)	Phase III trials demonstrated significant improvements in patient survival rate with riluzole treatment as compared to placebo (Bensimon *et al*, 1994, Lacomblez *et al*., 1996), but the drug only modestly prolongs survival by 2-3 months.
	Edaravone	May 2017; first approved in Japan in June 2015	NA	Radicut® and Radicava®	Thought to protect neurons and glia from oxidative stress through its antioxidant action of free radical scavenging; oxidative stress proposed as a major pathological process of ALS (Watanabe *et al*, 2008, Takei *et al*, 2017)	Phase III trials demonstrated that edaravone treatment significantly reduced disease deterioration as compared to placebo (Abe *et al*., 2017).

Table 1.1. Drugs approved by the United States Food and Drug Administration (FDA) for the treatment of AD and ALS. Note that they are not curative and only provide symptomatic relief.

AD can be early- or late-onset. Less than 5 % of cases have an early onset prior to 65 years of age (Bertram and Tanzi, 2005), and is typically attributed to mutations in genes coding for amyloid precursor protein (APP) and the presenilins 1 and 2 (PSEN1 and 2) catalytic subunits of the APP-processing γ-secretase enzyme (Chartier-Harlin *et al*., 1991, Sherrington *et al*., 1995, Rogaev *et al*., 1995, Murrell *et al*., 1991, Goate *et al*., 1991, Levy-Lahad *et al*., 1995). Given the disease-causative nature of these mutations, it is noteworthy that a rare A673T mutation in the *APP* gene was reported to protect against AD and cognitive decline in an Icelandic population (Jonsson *et al*., 2012a). The majority of AD cases are late-onset and sporadic form, typically manifesting after 65 years. Although genetic causes have not been directly shown for this form of AD, risk loci have been uncovered through genetic association studies. The apolipoprotein E-encoding *APOE* gene has three alleles (ε2, ε3, ε4) encoding three different isoforms (ApoE2, ApoE3, and ApoE4 respectively). ApoE4 is the first AD risk factor to be identified by a genetic linkage study, with the age of disease onset greatly accelerated dependently on the number of ApoE4 alleles (Corder *et al*., 1993, Strittmatter *et al*., 1993). In contrast, ApoE2 is protective and delays disease onset (Corder *et al*., 1994). Although newer advances with GWAS and massive parallel resequencing has uncovered over 20 additional risk factors since the identification of ApoE4, ApoeE4 remains the most prominent and aggressive susceptibility factor to be identified for both early- and late-onset disease thus far (Van Cauwenberghe *et al*., 2015). Of these subsequently-identified risk factors, variants of the *TREM2* gene, which encodes the microglia triggering receptor expressed on myeloid cells 2, is noteworthy given the shared pathological feature of neuroinflammation in neurodegenerative diseases (Jonsson *et al*., 2012b, Guerreiro *et al*., 2012, Schmid *et al*., 2002). Furthermore, *TREM2* mutations cause early-onset neurodegeneration in Nasu-Hakola disease (Paloneva *et al*., 2002), and have been shown to confer risk for FTD (Cuyvers *et al*., 2014, Rayaprolu *et al*., 2013), PD (Rayaprolu *et al*., 2013), and ALS (Cady *et al*., 2014), lending further support to the role of microglia in neuroinflammatory processes in neurodegeneration

Despite the complex, multifactorial aetiology of AD (Anand *et al*., 2014, De Strooper and Karran, 2016), much of AD research and translational efforts have been based on the amyloid cascade hypothesis, which posits that dyshomeostasis of the APP processing pathway and consequential $A\beta_{42}$ production and aggregation are the critical initiating events in AD (Hardy and Allsop, 1991, Selkoe and Hardy, 2016). These events induce a pathological cascade, resulting in NFTs, neurodegeneration, and dementia in AD. The APP processing pathway can be non-amyloidogenic or amyloidogenic, depending on whether APP gets cleaved by α- or β-secretase respectively (Chow *et al*., 2010). APP is a single transmembrane protein which contains an Aβ peptide sequence. In the non-amyloidogenic pathway, APP gets cleaved by α-secretase within the Aβ sequence, releasing the secreted APP (sAPPα) N-terminal fragment into the extracellular space. The membrane-retained C-terminal fragment (CTFα) is subsequently cleaved sequentially by the γ-secretase proteolytic complex, forming the APP intracellular domain (AICD) and soluble N-terminal p3 fragment. In the amyloidogenic pathway, APP gets cleaved by β-secretase N-terminal to the Aβ sequence, releasing sAPPβ and a longer membrane-bound CTFβ sequence. Sequential proteolysis of CTFβ by γ-secretase generates the same AICD and soluble Aβ monomers of different lengths, such as $A\beta_{40}$, $A\beta_{42}$, and longer Aβ peptides. $A\beta_{40}$ was shown to prevent amyloid formation, whereas $A\beta_{42}$ and presumably longer Aβ peptides promote the aggregation process (Kim *et al*., 2007b). Figure 1.2 outlines both APP processing pathways.

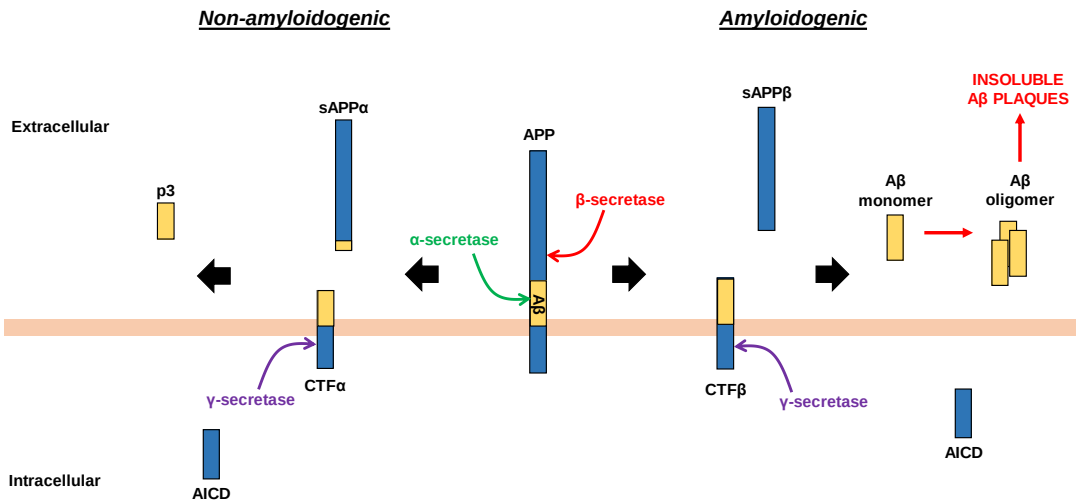

Figure 1.2. Non-amyloidogenic and amyloidogenic APP processing pathways. APP cleavage by α-secretase within its Aβ peptide sequence and subsequent proteolysis by γ-secretase produces non-amyloidogenic products, whereas β-secretase/γ-secretase cleavages generate Aβ peptides of varying lengths, of which the anti-amyloidogenic $A\beta_{40}$ and amyloidogenic $A\beta_{42}$ are the most common. Note that γ-secretase exist as a complex with the presenilins PSEN1 and 2 constituting the catalytic component.

Although evidence has supported the central role of Aβ in AD pathogenesis (Selkoe and Hardy, 2016), translational efforts targeting this arm of the disease has shown little success. The most recent example is solanezumab, a monoclonal antibody developed by Elli Lilly which targets soluble Aβ monomers and potentially oligomers, but not insoluble senile plaques. This is particularly promising as studies have suggested the soluble oligomeric form of Aβ to be the toxic species instead of the insoluble senile plaques (Murphy and LeVine, 2010). Additionally, phase III trials were conducted on mild AD patients. Given that pathological changes in AD were hypothesized to precede the onset of clinical symptoms by at least two decades (Jack *et al*., 2010, Bateman *et al*., 2012), there is increasing awareness of the importance of targeting the disease at the earlier presymptomatic or prodromal stages in order to elicit disease-modifying effects. Conversely, it might be too late when the condition is targeted at the symptomatic, clinical phase. As previous failures of Aβ-centric trials have been attributed to a myriad of reasons which include the predominant targeting of symptomatic patients, these phase III solanezumab trials hold great promise due to the targeting of patients at an earlier disease stage. Unfortunately, solanezumab failed to decelerate cognitive decline in this subset of patients and was abandoned from further development, adding to the string of failures which puts the validity of the amyloid cascade hypothesis in more jeopardy.

Despite disappointing trial outcomes, the possibility remains that early stage presymptomatic or prodromal targeting may render the practicality of disease modification through a single target. This is suggested by studies which showed that Aβ-lowering γ-secretase inhibitors were most efficacious at reducing Aβ load when delivered prior to plaque formation in transgenic mutant APP, Aβ-producing mice (Das *et al*., 2012, Brendel *et al*., 2015). However, a myriad of reliable biomarkers is essential to pinpoint the stages of the disease. At present, established AD biomarkers include cerebrospinal fluid (CSF) levels of $A\beta_{42}$ and tau, positron emission topography (PET) imaging of $A\beta_{42}$, structural magnetic resonance imaging (MRI) of cerebral atrophy to measure synaptic losses and neurodegeneration, and synaptic activity as revealed from fluorodeoxyglucose (FDG)-PET measurement of brain metabolism (Jack *et al*.,

2010). Given the complexity of AD (De Strooper and Karran, 2016), however, more biomarkers need to be established to encapsulate other pathologic features of AD aside from Aβ and tau, not only to stage the disease, but also to track disease progression after administration of a treatment. In addition, given the complexity of AD, current on-going efforts to develop therapies targeting the other pathological processes in AD need to remain continual (Anand *et al*., 2014). Despite the growing recognition of the importance of targeting early stages of the disease, translational efforts should not neglect late-stage disease either. To sum it up, a multipronged approach should be the adopted strategy for combating AD and dementia. Note that although this is discussed in detail for only AD herein, the necessity for early-stage intervention at the presymptomatic or prodromal stages, good biomarkers, and good disease models is the general consensus in the neurodegeneration research community for tackling the challenges associated with managing neurodegenerative diseases.

1.1.2 Amyotrophic lateral sclerosis (ALS)

ALS is the most common form of motor neuron disease and the third leading form of neurodegenerative disease behind AD and PD, with approximately 3 to 5 per 100,000 people suffering from the condition (Brown and Al-Chalabi, 2017, Chio *et al*., 2013). It results in rapid and progressive degeneration of the upper motor neurons, localized in the brain's motor cortex, and lower motor neurons, which populate the brain stem and spinal cord and innervate muscles. Degeneration of both groups of neurons causes gradual muscular atrophy and paralysis. Because diaphragmatic muscles are also affected, death eventually ensues as a result of respiratory failure within 3 to 5 years of diagnosis. The disease manifests typically in adulthood, with an age of onset in the mid- to late-50s.

ALS is largely sporadic, with 5 to 10% accounting for the familial form. Genetic mutations which are causative for the disease have been found, with the first discovery being made in *SOD1*; *SOD1* encodes the enzyme superoxide dismutase 1 which scavenges and converts harmful superoxide radicals to hydrogen peroxide (Rosen *et al*., 1993). *SOD1* mutations account for 12 % of familial ALS and 1 to 2 % of sporadic cases (Renton *et al*., 2014). The

discovery of these mutations led to the generation of the toxic gain-of-function G93A SOD1 ALS mouse model, which recapitulates aspects of the human disease (Gurney *et al*., 1994) and is still widely employed to study disease pathogenic mechanisms and for screening potentially therapeutic compounds. Following the initial discovery of *SOD1* mutations, numerous genetic causes of the condition were uncovered from familial ALS, with mutations identified in *ALS1, SETX, SPG11, VAPB, ANG, FIG4, OPTN, ATXN2, VCP, UBQLN2, SIGMAR1, CHMP2B, FUS, TARDBP, C9orf72, PFN1, ERBB4, hnRNPA1, MATR3, TBK1, SQSTM1*, and *TUBA4A* to date (Kenna *et al*., 2017). A number of these affected genes encode proteins involved in RNA processing (*TARDBP*, *FUS*, *C9orf72*, *MATR3, hnRNPA1*, *PFN1*) (Renton *et al*., 2011, DeJesus-Hernandez *et al*., 2011b, Kim *et al*., 2013, Johnson *et al*., 2014, Wu *et al*., 2012, Sreedharan *et al*., 2008, Vance *et al*., 2009, Kwiatkowski *et al*., 2009). Of these, *TARDBP*, *FUS*, and *C9orf72* mutations are noteworthy. *TARDBP* and *FUS* encode transactive response DNA binding protein 43 kDa (TDP-43) and fused in sarcoma (FUS), and mutations for either gene are rare and account for 4 % of familial and 1 % of sporadic ALS (Renton *et al*., 2014). On the other hand, mutations in *C9orf72* resulting from noncoding hexanucleotide GGGGCC repeat expansions are the most prominent, as they account for 40 % of familial and 7 % of sporadic cases (Majounie *et al*., 2012, DeJesus-Hernandez *et al*., 2011b, Renton *et al*., 2014). The hexanucleotide sequence may be repeated up to thirty times in normal humans, whereas hundred- and thousand-folds repeats have been found in ALS and FTD patients. The pathogenic mechanism of these repeat expansions towards disease is currently not understood, although both gain- and loss-of-function theories have been proposed. For instance, intranuclear RNA foci have been observed in *C9orf72* ALS patients, which may have a toxic gain-of-function by sequestering RNA-binding proteins and interfering with physiological RNA functions (DeJesus-Hernandez *et al*., 2011b). Noncanonical repeat-associated non-ATG (RAN) translation of the repeat expansions have also been reported, generating aggregating dipeptide repeat proteins which may have also have toxic gain-of-function roles (Mori *et al*., 2013). Alternatively, the mutation may cause haploinsufficiency, resulting in a loss of function. In addition to genes that regulate RNA processing, a subset of these causative

mutations have also been uncovered in genes that regulate protein homeostasis through components of the autophagy and ubiquitin-proteasome pathways (*UBQLN2*, *VCP*, *SQSTM1*, *OPTN, TBK1*) (Maruyama *et al*., 2010, Johnson *et al*., 2010, DeJesus-Hernandez *et al*., 2011a, Koppers *et al*., 2012, Deng *et al*., 2011, Fecto *et al*., 2011). Note that mutations in *TARDBP*, C9ORF72, *FUS*, *UBQLN2*, and *VCP* also account for cases of FTD, the second leading cause of early-onset dementia after AD which shares overlapping clinical features with ALS.

In addition to these known genetic causes of ALS, GWAS have uncovered various risk loci and variants (van Rheenen *et al*., 2016, Fogh *et al*., 2014, Shatunov *et al*., 2010, van Es *et al*., 2009, Hoglinger *et al*., 2011, Freischmidt *et al*., 2015, Cirulli *et al*., 2015). Of these, variation on chromosome 9 has the strongest genetic association (van Es *et al*., 2009, Shatunov *et al*., 2010), and since its identification has now shown to correspond with the *C9orf72* mutation in familial ALS (Renton *et al*., 2011). The occurrence of this mutation in both familial and sporadic disease, as was also observed for other affected genes as exemplified above with *TARDBP* and *FUS*, supports the view that both forms of the disease are not distinct and mutually-exclusive but instead exist on a spectrum (Al-Chalabi *et al*., 2016). Additionally, the genetic landscape of ALS is made even more complicated by the pleiotropy of various variants in ALS causative and associated genes, which can give rise to different conditions. For instance, *C9orf72* and the *UNC13A* risk variant are implicated in both ALS and FTD (Diekstra *et al*., 2014, Hsiung *et al*., 2012).

Despite a diverse aetiology and in addition to the similar implication of various genes, more than 90 % of ALS cases and a tau-negative form of FTD share a common neuropathological feature of cytoplasmic aggregates consisting of TDP-43 (Arai *et al*., 2006, Neumann *et al*., 2006). However, these TDP-43 inclusions are absent in *SOD1* and *FUS* ALS cases. Although FUS is the implicated protein in such aggregates in *FUS*-related ALS, neither pathological TDP-43 or FUS aggregates are present in *SOD-1* cases (Tateishi *et al*., 2010, Suzuki *et al*., 2010, Mackenzie *et al*., 2007, Vance *et al*., 2009, Tan *et al*., 2007). Additionally, *TARDBP* mutations are rare despite this shared pathological feature. TDP-43 is a DNA/RNA-binding protein (Figure 1.3) which

resides primarily in the nucleus to regulate RNA processing, such as mRNA splicing and microRNA biogenesis (Buratti and Baralle, 2012). In addition to regulating a diverse number of transcripts (Tollervey *et al*., 2011, Polymenidou *et al*., 2011), TDP-43 autoregulates its own mRNA expression (Avendaño-Vázquez *et al*., 2012). In response to cellular stressors, it translocates from the nucleus to the cytoplasm where it associates with stress granules, non-membrane bound complexes consisting of mRNA binding proteins which sequester transcripts with halted translation (Liu-Yesucevitz *et al*., 2010). In ALS and tau-negative FTD, TDP-43 is cleared from the nucleus and deposited as misfolded, hyperphosphorylated, and ubiquitinated full-length and fragmented forms in insoluble cytoplasmic inclusions (Neumann *et al*., 2006). As for *C9ORF72* repeat expansions, the mechanisms underlying TDP-43 proteinopathy are not understood. Both TDP-43 gain- and loss-of-function theories have been proposed to account for TDP-43-mediated neurotoxicity, and as evidence exists to support both sides of the argument, it appears that a combination of both mechanisms are in play (Scotter *et al*., 2015, Vanden Broeck *et al*., 2014, Lee *et al*., 2011, Xu, 2012).

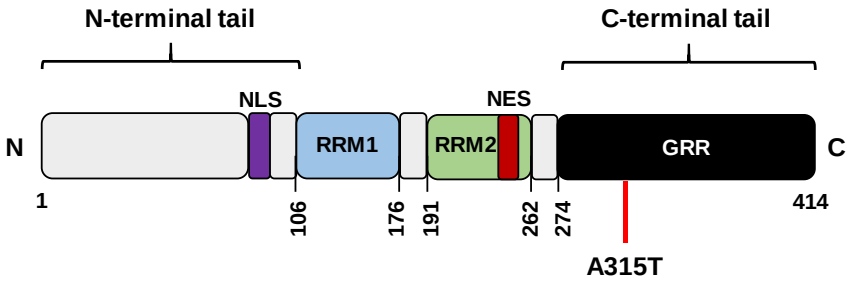

Figure 1.3. Human TDP-43 protein. The protein has nuclear localisation (NLS) and export (NES) signals, which enables nuclear and cytoplasmic shuttling of TDP-43. DNA and RNA binding are mediated through the two RNA recognition motifs (RRM 1 and 2). Finally, the C-terminal glycine-rich region (GRR) has a hypothesized prion domain, and is important for protein-protein interactions. ALS-causative autosomal dominant mutations in the TDP-43 gene *TARDBP*, which typically cluster within this domain, promotes the misfolding and aggregation of the protein (Johnson *et al*., 2009a). As indicated within this region is the A315T mutation (Gitcho *et al*., 2008, Sreedharan *et al*., 2008); the current study utilises an A315T TDP-43 transgenic ALS *C. elegans* model (Liachko *et al*., 2010) which will be described in chapters 4 and 5. Numbers represent amino acids.

There are currently only two approved treatments for ALS, riluzole and edaravone (Table 1.1) (Brown and Al-Chalabi, 2017). Riluzole was first approved by the FDA in 1995 and prolongs the survival by only two to three months. It is thought to have anti-glutamatergic properties, but this mechanism of action is controversial. Instead, the drug may have multiple mechanisms of action. For instance, it appears to act on various ion channels (Bellingham, 2011). Edaravone was approved in Japan in 2015, and only recently approved by FDA in May 2017. It is an antioxidative molecule which acts to remove free radicals, thereby offering protection against oxidative stress (Watanabe *et al*., 2008, Takei *et al*., 2017). Oxidative stress is thought to contribute to disease pathology, but whether the antioxidative mechanism of the drug plays a role in disease amelioration is unknown. As neither drug modifies disease and provide only symptomatic relief, it is paramount to develop new therapies which alter the course of disease. As aforementioned, the G93A SOD1 ALS mouse model is still widely used to understand disease pathogenesis and for drug screening. However, as the shared pathological feature of TDP-43 inclusions are absent in *SOD1* ALS, this ALS subset may have a distinct pathology from the majority of ALS cases. Hence, *SOD1* models may not have a general utility for discovering ALS disease-modifying treatments for ALS. In the same vein, C9ORF72 and TDP-43-related ALS constitute the majority of ALS cases and may be better therapeutic targets; however, the pathogenic mechanisms behind these mutations need to be delineated for effective targeting.

1.1.3 Other neurodegenerative diseases

PD is the second most common neurodegenerative disease behind AD, affecting every 13 per 100,000 people (Williams-Gray and Worth, 2016). It is defined pathologically by dopaminergic neuronal losses in the substantia nigra, a midbrain region with an important role in regulating movement, and intracellular cytoplasmic eosinophilic-dense inclusions consisting primarily of α-synuclein called Lewy bodies or Lewy neurites (Spillantini *et al*., 1998, Spillantini *et al*., 1997); note that Lewy bodies and neurites are also found in dementia with Lewy body, which is the second most common cause of dementia after AD. PD is a movement disorder with motor symptoms such as bradykinesia, resting tremor, and postural instability, and non-motor symptoms such as mood disturbances and cognitive deficits (Williams-Gray and Worth, 2016). The disorder affects 2 to 3 % of the global population, is typically late-onset at 65 years and older, and is largely sporadic with 10 % accounting for familial forms. Genetically, disease-causing mutations in the α-synuclein gene *SCNA*, *LRRK2, EIF4G1*, *VPS35, DNAJC13, and CHCHD2*, *Parkin*, *PINK1*, *DJ-1*, and *ATP-13A2* have been identified (Klein and Westenberger, 2012, Kalia and Lang, 2015, Williams-Gray and Worth, 2016). PD therapies mainly act to ameliorate motor symptoms by replenishing dopaminergic signalling, albeit with little effectiveness and various side effects (Williams-Gray and Worth, 2016, Kalia and Lang, 2015). This can be exemplified by levodopa, which is administered as a precursor for dopamine synthesis. Levodopa is currently the most effective of these therapies, but its long-term use is complicated with a progressive reduction of its effectiveness and motor side effects such as dyskinesia.

Huntington's disease (HD) is a rare neurodegenerative disease affecting 5 to 10 per 100,000 individuals in the Caucasian populace, with a mid-onset age of 40 years (Ross and Tabrizi, 2011). It is an autosomal dominant disorder caused by repeated trinucleotide CAG expansions in the huntingtin (HTT) protein, resulting in a polyglutamine (polyQ) tract within the encoded protein. As such, it is classified as a polyQ disease, which includes other conditions such as the different types of spinocerebellar ataxias (Orr, 2012). The repeat expansions occur in different proteins in these polyQ diseases, with specific

neurons and brain regions being affected. In normal individuals, HTT CAG expansions varies and occurs up to 35 times (Kremer *et al*., 1994). In HD patients, however, expansions exceed 35 times, with the longer expansions predicting for earlier ages of onset. Pathologically, HD is characterised by aggregates of the polyQ HTT, which can be found in neuronal nuclei, cytoplasm, dendrites, and axon terminals, and neurodegeneration in particularly the striatum (Ross and Tabrizi, 2011). Clinically, the condition typically manifests in a triad of motor, psychiatric, and cognitive deficits such as bradykinesia, depression, and cognitive decline respectively. Therapies exist to provide symptomatic relief, but as with other neurodegenerative diseases, no disease-modifying treatments are available.

Tauopathies are a group of neurodegenerative disorders which are pathologically characterised by insoluble intraneuronal aggregates of tau (Orr *et al*., 2017). As such, AD is considered a tauopathy. Other tauopathies include the FTDs such as frontotemporal dementia with parkinsonism-17 (FTDP-17), PSP, corticobasal degeneration, and chronic traumatic encephalopathy. Despite this pathological commonality, affected brain regions and clinical phenotypes are typically heterogeneous, the latter comprising a range of motor, psychiatric, and cognitive defects. Disease-causing mutations in tau-encoding *MAPT* have been identified in familial FTDP-17, implicating aberrant tau in the pathogenic process of tauopathies (Goedert and Jakes, 2005). Although the exact mechanism is still unclear, a toxic gain-of-function of the dysregulated protein is a prevailing hypothesis, and various tau dyshomeostasis processes are currently investigated as potential therapeutic targets (Khanna *et al*., 2016).

Table 1.4 summarises the aforementioned neurodegenerative diseases by the major proteins implicated in the pathological aggregates.

Disease	Protein species implicated in aggregates	Gene	Disease-causing mutations in gene?
Alzheimer's disease	Amyloid beta (Aβ)	*APP* (encodes amyloid precursor protein, which gets processed aberrantly to produce aggregation-prone $A\beta_{42}$ in disease)	Yes
	Tau	*MAPT*	No
Amyotrophic lateral sclerosis	Superoxide dismutase 1 (SOD1)	*SOD1*	Yes
	Fused in sarcoma (FUS)	*FUS*	Yes
	Transactive response DNA binding protein 43 kDa (TDP-43)	*TARDBP*	Yes
	C9orf72 dipeptide repeat proteins (result from noncanonical repeat-associated translation of noncoding hexanucleotide GGGGCC repeat expansions in encoding gene)	*C9orf72*	Yes
Parkinson's disease	α-synuclein	*SCNA*	Yes
Huntington's disease	Huntingtin	*HTT*	Yes
Tauopathies	Tau	*MAPT*	Yes

Table 1.4. Summary of the main protein species implicated in neurodegenerative diseases mentioned in text. Familial forms of these diseases facilitated the identification of disease-causing mutations in many genes encoding for these proteins. Note that in Alzheimer's disease, aberrant processing of amyloid precursor protein (APP) into Aβ can also be due to mutations in *PSEN1* and PSEN2, which encodes the presenilins 1 and 2 catalytic subunits of the APP-processing γ-secretase enzyme. In amyotrophic lateral sclerosis, the different implicated proteins do not co-occur in pathological aggregates. SOD1 and FUS aggregates, but not TDP-43, are only found in respective *SOD1*- and *FUS*-mutated forms of the condition, whereas TDP-43 aggregation is the predominant pathological feature of the majority of both familial and sporadic forms of the disease. In Hungtington's disease, pathological trinucleotide CAG repeat expansions in *HTT* results in long polyglutamine tracts in huntingtin which coalesce into aggregates. Such CAG expansions are also a shared and defining feature of other polyglutamine diseases, albeit differing by the implicated genes, encoded proteins, and brain regions; these conditions are not elaborated on herein due to their relative rarity.

1.1.4 Targeting common pathways in neurodegenerative diseases

As illustrated from the various neurodegenerative diseases above, no disease-modifying treatments exist, and available therapeutics provide only symptomatic relief. Development of therapies has been largely impeded by a poor understanding of these conditions despite extensive research, and this is attributed to the complex aetiology and multifactorial nature of neurodegenerative diseases. Although the conditions have disease-specific features, a common theme is the aberrant processing and aggregation of proteins. Notwithstanding the fact that the pathogenic roles of protein dyshomeostasis in neuronal degeneration for each disorder are still not clearly resolved overall, the shared processes contributing to this pathological feature can be potentially targeted as a general therapeutic approach for neurodegenerative diseases. Additionally, other processes which may not directly relate to protein homeostasis are implicated in neurodegenerative diseases as briefly aforementioned, such as the prion-like spreading of disease-associated proteins and neuroinflammation, may also contain common aspects which underlie neurodegeneration and may be potential therapeutic targets.

The notion of targeting common themes which underlie neurodegeneration is appealing especially since overlapping clinical phenotypes may exist between conditions, which when combined with the general lack of complete biomarker arsenals, may impede precise diagnosis. Additionally, the idea of treating neurodegenerative diseases as one condition instead of separate entities makes this proposition even more attractive, given the difficulty in comprehending each disease. Various work has lended support to this concept. For instance, our group has previously identified overlapping genes which were found to regulate neurodegenerative phenotypes from small and large scale genetic screens in *Caenorhabditis elegans*, *Drosophila melanogaster*, and *Saccharomyces cerevisiae* AD, PD, ALS, and polyQ models from other studies (Chen and Burgoyne, 2012). All genes within this overlapping subset have a human ortholog, hence findings may translate to the clinical setting. In line with the shared pathological feature of aberrant protein processing and aggregation, overlapping genes include those encoding protein homeostasis

regulatory components, such as heat shock transcription factors, molecular chaperones, and components which mediate post-translational modification such as ubiquitination and phosphorylation. In addition, aberrant protein regulatory processes and other common elements of neurodegeneration have been described elsewhere, such as neuroinflammation and dysregulations in mitochondrial function, protein recycling, and the unfolded protein response (UPR) (Halliday and Mallucci, 2015, Smith and Mallucci, 2016, Rubinsztein, 2006, Lin and Beal, 2006, Frank-Cannon *et al*., 2009). Of these, the UPR is a notable example. The UPR is a cellular response to endoplasmic reticulum (ER) stress which is induced by the presence of unfolded and/or misfolded proteins in the ER. In response to ER stress, protein translation is temporarily halted, lipid synthesis and chaperone protein production increase, and the ER-associated protein degradation (ERAD) pathway becomes activated (Halliday and Mallucci, 2015). Three arms of the UPR exist, and of these, activated protein kinase RNA-like ER kinase (PERK) mediates the translational inhibition component of the response by phosphorylating and activating downstream eukaryotic initiation factor 2α (eIF2α). Enhanced levels of activated PERK and eIF2α were previously shown in affected anatomical regions in the brains of AD, PD, and PSP patients, (Hoozemans *et al*., 2007, Hoozemans *et al*., 2009, Stutzbach *et al*., 2013). Additionally, there are multiple lines of evidence linking the UPR to AD, PD, HD, PSP, FTD, and ALS, prion diseases, and memory formation (Halliday and Mallucci, 2015). In mouse models of prion disease and FTD, chronic translational inhibition by constitutive activation of PERK/eIF2α resulted in synaptic protein losses, neurodegeneration, and behavioural deficits (Moreno *et al*., 2013, Halliday *et al*., 2015, Halliday *et al*., 2017, Moreno *et al*., 2012). Protection against these defects were conferred by both experimental compounds and approved drugs by inhibition of the PERK/eIF2α pathway (Moreno *et al*., 2013, Halliday *et al*., 2015, Halliday *et al*., 2017). In addition, pharmacological inhibition of this pathway protected against TDP-43 proteotoxicity in *D. melanogaster* and primary neuronal ALS models (Kim *et al*., 2014). Overall, these findings demonstrate the feasibility of modulating the PERK/eIF2α component of the UPR pharmacologically for the therapeutic intervention of neurodegenerative diseases, and support the proposition of targeting common pathogenic processes of these conditions.

Aside from common pathogenic processes of neurodegeneration, promising therapeutic targets include protective factors which have been uncovered from studies on ageing. A notable example is the sirtuin SIRT1, a beta-nicotinamide adenine nucleotide-dependent class III histone deacetylase. SIRT1 and its orthologs were shown to mediate the lifespan-extending effects of caloric restriction in rodents, *C. elegans*, *D. melanogaster*, and *S. cerevisiae*, although contradictory evidence exists as well (Hubbard and Sinclair, 2014, Cantó and Auwerx, 2009). Despite the controversial role of SIRT1 in mediating longevity, its neuroprotective effects have been demonstrated in *C. elegans*, mouse, and cellular neurodegeneration models of AD, PD, ALS, and polyQ diseases (Kim *et al*., 2007a, Jiang *et al*., 2012, Jeong *et al*., 2012, Wu *et al*., 2011, Marvanova and Nichols, 2007). Furthermore, the *C. elegans sir-2.1* ortholog was one of the overlapping genetic regulators of neurodegeneration identified from our analysis as aforementioned (Chen and Burgoyne, 2012).

Alternative to targeting common themes of neurodegeneration, a converse approach is to identify compounds which exert general neuroprotection. Such compounds can then be used in chemical genetics screen to facilitate insights into shared pathogenic processes. This can be well exemplified by the naturally-occurring polyphenol resveratrol, a known activator of the aforementioned SIRT1, which has demonstrated neuroprotection in *C. elegans*, mouse, and mammalian models of AD, PD, ALS, polyQ diseases, and a *C. elegans* model of the rare autosomal dominant neurodegenerative disease adult-onset neuronal ceroid lipofuscinosis (ANCL) which was characterised by our group; refer to section 1.2.2.2 for more information on the ANCL model (Kashyap *et al*., 2014, Tauffenberger *et al*., 2013, Karuppagounder *et al*., 2009, Parker *et al*., 2005, Kim *et al*., 2007a, Wu *et al*., 2011). It is worth noting that the neuroprotective effect of resveratrol in the *C. elegans* ANCL model was shown to be *sir-2.1*-independent (Kashyap *et al*., 2014), demonstrating the possibility of dissecting undiscovered neuroprotective mechanisms via chemical genetics screens with such compounds; however this was not further explored within our group.

In addition to resveratrol, some antiepileptic drugs (AEDs), namely valproic acid, ethosuximide, trimethadione, and levetiracetam, were demonstrated to

mediate neuroprotection in different neurodegeneration models (van Bergeijk *et al*., 2006, Pan *et al*., 2005, Kautu *et al*., 2013, Teixeira-Castro *et al*., 2011, Qing *et al*., 2008, Yi *et al*., 2013, Rouaux *et al*., 2007, Crochemore *et al*., 2009, Sugai *et al*., 2004, Monti *et al*., 2010, Monti *et al*., 2012, Kidd and Schneider, 2011, Ximenes *et al*., 2015, Carriere *et al*., 2014, Wildburger *et al*., 2009b, Tiwari *et al*., 2015, Chen *et al*., 2015b, Erbaş *et al*., 2016, Bezard *et al*., 2004, Sanchez *et al*., 2012, Tauffenberger *et al*., 2013). Of these, the wide-ranging neuroprotective effects of valproic acid and ethosuximide have been the most studied, the latter also having been shown within our group. Protective effects of ethosuximide and other AEDs will be further elaborated in section 1.3 and chapter 4 respectively.

1.2 *CAENORHABDITIS ELEGANS*

1.2.1 Characteristics

C. elegans is a free-living, soil-dwelling nematode which was first introduced by Sydney Brenner as a model organism in 1965 (Brenner, 1974). The nematode exists in two genders, hermaphrodites and males. The self-fertilising hermaphrodite is the predominant gender, whereas the abundance of males in the population is extremely rare and occurs at about 0.02 %. Both hermaphrodites and male nematodes have six diploid autosomes. However, hermaphrodites are diploid for the *X*-chromosome whereas males are haploid for it. Note that as the behaviour, development, and anatomy of male worms differ from hermaphrodites, general features as outlined herein pertain specifically to the predominant sex. The anatomy of the nematode is extremely well characterised, with adult hermaphrodites having exactly 959 somatic cells and 302 neurons. Additionally, *C. elegans* is the first multicellular organism to have its genome completely sequenced, and it contains homologs for over two-thirds of the human genome ('Genome sequence of the nematode *C. elegans*: a platform for investigating biology,' 1998, Lai *et al*., 2000). The nematode feeds on various forms of bacteria including *Escherichia coli*, and develops through four larval stages L1 to L4 before reaching a gravid, adulthood stage with a body length of approximately 1 mm. The developmental rate and lifespan of the worm is dependent on the growth temperature, with higher temperatures inducing faster development to adulthood and shorter lifespans (Byerly *et al*., 1976). At a typical maintenance temperature of 20°C, however, the developmental life cycle and lifespans are approximately 3 to 4 days and 2 to 3 weeks respectively. Nematodes can be maintained on solid agar or in liquid culture in the presence of *E. coli* as the food source. Note that food scarcity causes nematodes to arrest development at the L1 or L2 stages. Developmental arrest may be sustained up to 4 months, with normal development ensuing in the presence of food which does not affect post-dauer lifespan. Food scarcity in adulthood has been shown to cause lifespan extension through caloric restriction (Walker *et al*., 2005).

There are various advantages to using *C. elegans* as a model system, especially in regard to the study of ageing and age-related neurodegenerative

diseases. For instance, its relatively short lifespan and generation time as compared to more complex model systems like rodents makes it comparatively easier and quicker to assess lifespan and neurodegenerative phenotypes. A completely mapped nervous system, fully sequenced genome, and genetic amenability facilitates the development of genetic disease models of neurodegeneration and to delineate disease processes via chemical and genetic screens (see section 1.2.2 below). Additionally, *C. elegans* has a transparent body which enables fluorescently-labelled neurons to be studied *in vivo*.

In terms of drug screening, the nematode enables the systemic effects of drug administration to be addressed at a preliminary stage, as opposed to the traditional use of cellular models which typically provides unicellular biochemical readouts to inform of drug effects. Additionally, the ease of culture, low cost of maintenance, quick generation time, and the development of automation for handling the nematodes and for tracking behavioural and electrophysiological changes (Lockery *et al*., 2012, Stroustrup *et al*., 2013, Swierczek *et al*., 2011, Flavell *et al*., 2013, Ben Arous *et al*., 2009, Boyd *et al*., 2010, Buckingham and Sattelle, 2009, Yemini *et al*., 2013, Tsibidis and Tavernarakis, 2007), makes *C. elegans*-based screens highly amenable for high throughput screening (HTS). Indeed, the feasibility of HT chemical screens in *C. elegans* have been demonstrated (Kwok *et al*., 2006, Burns *et al*., 2006, Sleigh *et al*., 2011, Gosai *et al*., 2010, McCormick *et al*., 2013, Schwendeman and Shaham, 2016, Leung *et al*., 2013, Ellerbrock *et al*., 2004). These qualities make *C. elegans* a better alternative to rodent model systems in early stage, whole organism screening. The latter, although typically considered the gold standards for preclinical evaluation, are associated with prohibitive high costs and time-consuming experimental designs, hence are neither suitable for early-stage nor HTS. Additionally, *C. elegans* experimentation is devoid of ethical issues as opposed to the use of rodents.

Despite such attractive features, there are various limitations of using *C. elegans*. For instance, drug treatment of nematodes is performed typically by culturing them on agar plates in the presence of the drug, which can be taken up via ingestion, exposed sensory nerve endings, and permeation

through the exoskeletal cuticle (Kaletta and Hengartner, 2006). However, the cuticle is weakly permeable and impedes drug accumulation, hence high concentrations of treatment need to be administered externally, which can become prohibitively costly. In addition, poor bioaccumulation can result in false negatives. Despite this limitation, a worm structure-based accumulation model (SAM) has been developed to computationally predict the bioaccumulation propensities of drugs so that the best predicted accumulating ones can be prioritised for screening (Burns *et al*., 2010); this is further elaborated in chapter 3.

1.2.2 Modelling neurodegeneration in *C. elegans*

1.2.2.1 Genetic manipulation

As aforementioned, the fully sequenced genome and genetic amenability of *C. elegans* makes it an ideal model organism to study the functions of genes in physiology and disease. This is commonly performed via forward and reverse genetics approaches. In forward genetics, random and permanent null mutations are introduced in the worm genome via exposure to a mutagen (Figure 1.5) (Jorgensen and Mango, 2002). Homozygous progenies of mutagenized animals which exhibit phenotypes of interest are identified and isolated, followed by genetic mapping of the mutation on the genome to locate the defective gene which was responsible for the phenotype. As mutagenesis may introduce other mutations in additional loci in isolated progenies, it is paramount and common practice to backcross them multiple times with wildtype (WT) strains to clean up the genetic background before the causative gene(s) can be confirmed. Ethyl methanesulfonate (EMS) is a commonly used mutagen which introduces mutations in the gametes of the hermaphrodites (Jorgensen and Mango, 2002).

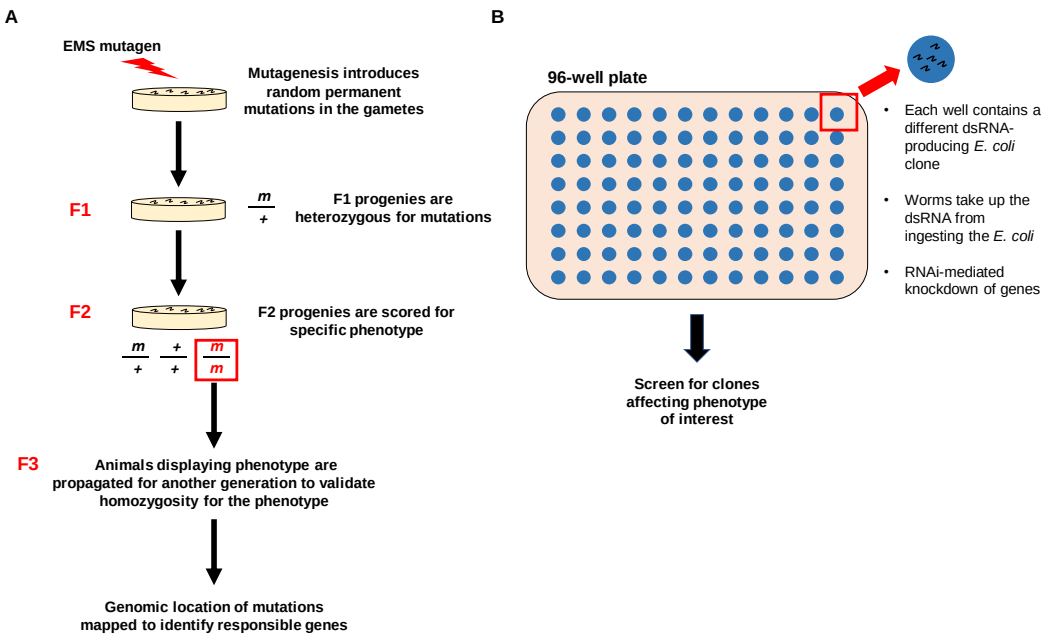

Figure 1.5. Forward and reverse genetics screens. (A) Forward genetics screen with EMS mutagenesis. EMS induces null mutations from deletions, G to C, and A to T mutations. Parental worms are typically exposed to the mutagen for 4 hours, which inactivates approximately 10 to 20 genes in the genome. (B) Genome-wide RNAi reverse genetics screens are performed in 96-well plates and are amenable to high throughput, automated procedures.

Unlike forward genetics screens which delineates gene functions by identifying genes associated with a specific phenotype, reverse genetics employ a directed approach of manipulating known candidate genes to identify the phenotypic consequences. RNA interference (RNAi) is a commonly used reverse genetics approach which induces post-transcriptional gene silencing via double stranded RNA (dsRNA)-mediated neutralization of target mRNA (Fire *et al*., 1998). Unlike EMS mutagenesis, gene function is reduced but not completely abolished with RNAi. Additionally, it may be used to knockdown gene expression at various stages of the life cycle, whereas mutations from EMS mutagenesis are stably present at all stages once induced. Further temporal control of gene knockdown by RNAi may be finetuned with the use of temperature-sensitive strains, whereby RNAi can be induced at permissive temperatures but inhibited at restrictive ones (Calixto *et al*., 2010b). RNAi can be performed in several ways, namely by direct injection of the dsRNA, soaking in dsRNA, or by feeding with *E. coli* clones which produce dsRNA, the latter being a typical approach (Timmons *et al*., 2001, Timmons and Fire, 1998, Tabara *et al*., 1998, Fire *et al*., 1998). Given the ease of performing RNAi in *C. elegans*, HT genome-wide RNAi screens have been developed to enable RNAi-mediated knockdown of the majority of *C. elegans* genes with RNAi libraries of dsRNA-producing bacterial clones (Kamath *et al*., 2001, Fraser *et al*., 2000, Rual *et al*., 2004, Kamath and Ahringer, 2003). This is typically performed on 96-well plates, and automated procedures have been developed to facilitate such screens (Figure 1.5) (Squiban *et al*., 2012). An important caveat of RNAi is the increased potential for false negatives since gene expression is only reduced but not completely knocked out, hence RNAi may be insufficient to induce obvious phenotypes. Additionally, neurons are poor responders to RNAi, although this can be circumvented with strains with enhanced neuronal sensitivity to RNAi (Calixto *et al*., 2010a, Simmer *et al*., 2002, Kennedy *et al*., 2004).

An important feature of both forward and reverse genetics approaches is the ability to employ them in enhancer and suppressor screens to identify genes which exacerbate or protect against specific phenotypes. Such screens are extremely useful in the context of understanding disease pathogenesis, as

genes which regulate disease-associated phenotypes can be identified, which may potentially have direct pathogenic roles. Forward and reverse genetics may additionally be performed with chemical compounds to identify genes which confer resistance or hypersensitivity to a phenotypic effect of the compound. Such chemical genetics screens can shed light onto processes which mediate a particular effect and the compound's mechanism of action (MMOA), as identified genes may encode the putative target(s) or act in protective or pathological pathways. This is particularly useful for compounds identified as hits from phenotype-driven screens, where the MMOA responsible for the phenotype is not known. In the following section, the utility of such screens in established models of neurodegeneration in *C. elegans* will be exemplified.

1.2.2.2 Neurodegeneration models and screens

Models of neurodegenerative diseases have been generated in rodents, *C. elegans*, *D. melanogaster*, *S.* cerevisiae, and in culture systems with mammalian- or human-derived cell lines, primary neurons, stem cells, and induced pluripotent stem cells (iPSCs) (Gitler *et al*., 2017, Li and Le, 2013, Wong *et al*., 2002, Khurana and Lindquist, 2010, Bilen and Bonini, 2005, Han *et al*., 2011, Jakel *et al*., 2004, Schlachetzki *et al*., 2013, Chen *et al*., 2015a). Due to the breadth of this topic, selected studies of genetic and/or chemical screens which have been performed in *C. elegans* models will be elaborated on herein to further highlight the utility of the nematode as a model organism for drug discovery.

Neurodegeneration models in *C. elegans* can be generated genetically or induced chemically (Chen *et al*., 2015a, Li and Le, 2013). The latter approach has been used to derive PD models by exposure to dopaminergic neurodegeneration-causing neurotoxins such as 6-hydroxydopamine (6-OHDA) and 1-methyl-4-phenyl-1,2,3,6-tetrahydropyridine (MPTP), herbicides and insecticides such as paraquat and rotenone which cause the PD pathological features of mitochondrial dysfunction and oxidative stress, and environmental toxins such as manganese and bacterial secondary metabolites which are associated with PD development (Caldwell *et al*., 2009, Braungart

et al., 2004, Settivari *et al*., 2009, Ruan *et al*., 2010, Liu *et al*., 2015, Ved *et al*., 2005, Saha *et al*., 2009, Samann *et al*., 2009).

Genetic models are common, and in large part driven by the identification of disease-causing genetic mutations from familial forms of the disorders. These models are typically generated either by manipulating the ortholog of a human disease gene, or by transgenically overexpressing the affected human gene. Using the former approach and as aforementioned, our group has characterised a model of ANCL which was generated by introducing null mutations in the *C. elegans DNAJC5* ortholog, *dnj-14* (Kashyap *et al*., 2014); *DNAJC5* encodes cysteine string protein α and mutations in the gene cause ANCL (Noskova *et al*., 2011). Several aspects of human ANCL were recapitulated, such as reduced lifespan, and progressive neuronal degeneration and dysfunction. Focused chemical screens revealed the SIRT1 activator resveratrol (Kashyap *et al*., 2014) and the AED ethosuximide (Chen *et al*., 2015b) as neuroprotective compounds. As briefly mentioned before, the effects of resveratrol were found to be *sir-2.1*/SIRT1-independent as introducing *sir-2.1* null mutations into the mutant *dnj-14* background did not affect the lifespan-extending effect of the compound (Kashyap *et al*., 2014). For more information on ethosuximide, refer to section 1.3.2 and chapter 5.

Other examples include models of spinal muscular atrophy generated via a null deletion, or a missense mutation in the *C. elegans smn-1* ortholog which mimics the *SMN-1* mutation found in a patient (Sleigh *et al*., 2011). *SMN-1* encodes survival motor neuron (SMN) protein, and its reduced expression and function results in lower motor neurodegeneration and progressive paralysis. The models recapitulated aspects of the disease such as reduced lifespan, and impaired motility and synaptic transmission, in addition to other phenotypic defects like reduced egg-laying and hatching, albeit at differing severities; phenotypes were more severe in the null mutant. Due to the lethality of the null mutation which impedes large scale screening, chemical screens were performed on the other strain with a National Institute of Neurological Disorders and Stroke library of 1040 compounds. The screens identified compounds which ameliorated motility defects, and further characterization in both models revealed gaboxadol hydrochloride, 4-aminopyridine, and N-

acetylneuraminic acid as the best neuroprotective candidates as potential treatments for the condition.

On the other hand, transgenic “humanized” models predominate the field, and are derived by typically expressing human transgenes in body wall muscles or neurons with muscle- or neuron-specific promoters. Most transgenic models are based on constitutive transgene expression, although transgene expression by temperature upshift or heat shock in a few AD and ALS models have been developed (Oeda *et al*., 2001, Paiva *et al*., 2015, Link *et al*., 2003, Florez-McClure *et al*., 2007, Drake *et al*., 2003, Diomede *et al*., 2013, McColl *et al*., 2012). An example of a muscle-type transgenic model is an AD strain which constitutively expresses the pathologic $A\beta_{42}$ peptide in body wall muscles under the myosin *unc-54* promoter, and exhibits intramuscular $A\beta_{42}$ aggregation and progressive paralysis (Link, 1995). The model has been utilised by several studies to screen for compounds which protected against $A\beta_{42}$ proteotoxicity and/or mediated lifespan extension, revealing protective effects from natural compounds such as soy-derived isoflavone glycitein (Gutierrez-Zepeda *et al*., 2005), the green tea extract epigallocatechin gallate (Abbas and Wink, 2010), Gingko biloba (Smith and Luo, 2003), caffeine, tannic acid, baicalein (Lublin *et al*., 2011), ferulic acid, curcumin (Jagota and Rajadas, 2012), and approved drugs such as bacitracin, ciclopirox olamine, acetaminophen (Lublin *et al*., 2011), fluoxetine (Keowkase *et al*., 2010), reserpine (Arya *et al*., 2009), and the amyloid-binding dye thioflavin T (Alavez *et al*., 2011). In a PD muscle type model which expresses *unc-54*-driven yellow fluorescent protein (YFP)-fused α-synuclein in body wall muscles, a reverse suppressor screen was performed with genome-wide RNAi to identify genes which enhanced the number of YFP-α-synuclein inclusions when silenced (van Ham *et al*., 2008). Notably, the sirtuin *sir-2.1* as aforementioned, was one of the suppressors identified via this screen along with other ageing-associated genes, highlighting the link between ageing and neurodegeneration and the protective effects of such genes. In the same vein, a focused RNAi screen was performed in a separate study on another PD model with *unc-54*-driven muscle expression of green fluorescent protein (GFP)-fused α-synuclein, with hypothesized gene targets guided by bioinformatic analysis (Hamamichi *et al*.,

2008). Aside from the abovementioned AD and PD models, muscle expression models for ALS have been generated with mutant *SOD1* transgenes (Gidalevitz *et al*., 2009), and polyQ-expressing polyQ disease and HD models (Satyal *et al*., 2000, Morley *et al*., 2002, Wang *et al*., 2006, Yamanaka *et al*., 2004).

A caveat of such transgenic models with muscle-specific expression is that they may not recapitulate human neurodegeneration as well as the neuronal expression types, since neurons are the primary pathological sites. Hence, neuronal-type models may have better predictive validity for dissecting disease pathogenic processes and for discovering protective compounds. As a matter of fact, most transgenic neurodegeneration models are of the neuronal type. Examples include two FTDP-17 tauopathy models which were generated by pan-neuronal expression of human P301L and V337M *MAPT* disease-causing mutants driven by the *aex-3* promoter (Kraemer *et al*., 2003). These animals phenocopy several aspects of human tauopathies, such as reduced lifespans, accumulation of detergent-insoluble and hyperphosphorylated tau, and progressive age-dependent locomotory defects and neurodegeneration. Using these models, a forward enhancer screen was performed to identify mutations which exacerbate the tau-induced locomotion defect (Kraemer and Schellenberg, 2007). The screen identified *sut*-1 as an enhancer, a gene encoding a novel protein with uncharacterised functions. Further yeast two hybrid screens (Fields and Song, 1989) identified protein-protein interactions between SUT-1 and UNC-34, the *C. elegans* homolog of the conserved Ena/VASP actin regulatory proteins. Although SUT-1 has no human homolog, these findings suggest that actin regulatory components may be potential therapeutic targets. Chemical screens were also performed with the V337M model to uncover neuroprotective compounds (McCormick *et al*., 2013). Initial screens with the Prestwick chemical library of 1120 compounds identified six candidates, namely azaperone, trazodone, nefopam, clofazimine, isoniazid, and lorglumide with protective effects against age-dependent locomotory decline, but only the typical antipsychotic azaperone additionally reduced levels of detergent-insoluble tau and ameliorated neurodegeneration. Subsequent focused screens of other typical antipsychotics showed that a

handful of them displayed the same protective effects. As typical antipsychotics are known to antagonize the D2 dopamine receptors, these receptors were investigated as potential therapeutic targets. Knockouts of the *C. elegans* D2-like receptors DOP-2 and DOP-3 in the model ameliorated motility defects, protected against neuronal losses, and reduced insoluble tau levels, suggesting the therapeutic potential of targeting the D2 receptors for neurodegeneration treatment.

Aside from these FTDP-17 models, a neuronal type ALS model which pan-neuronally expresses the A315T disease-causing missense mutation in the human *TARDBP* TDP-43 gene by the *snb-1* promoter is primarily utilised in the current study (Figure 1.3) (Gitcho *et al*., 2008, Sreedharan *et al*., 2008, Liachko *et al*., 2010). The model, referred to as CK426, exhibits a reduced lifespan, and age-dependent and severe locomotory defects and neurodegeneration. Furthermore, hyperphosphorylated, ubiquitinated, and truncated forms of TDP-43 were detected in detergent-insoluble aggregates in the model, mimicking the TDP-43 pathology in humans (Arai *et al*., 2006, Neumann *et al*., 2006). This model is further described in chapter 4, section 4.2.2.

Other neuronal models of tauopathies, ALS, polyQ disorders and HD, AD, PD, prion diseases, and spinocerebellar ataxia type 3 have been generated as well and have been reviewed elsewhere (Chen *et al*., 2015a, Li and Le, 2013). Aside from pan-neuronal expression, transgenes may also be expressed in specific neuronal groups which are pathologically affected in the human disease. For instance, as AD is associated with glutamate dysregulation, an AD model was generated which expresses $A\beta_{42}$ specifically in the glutamatergic neurons of the worms with the *eat-4* vesicular glutamate transporter promoter (Treusch *et al*., 2011).

As a concluding note for this section, like all disease models generated in other organisms, *C. elegans* models are not complete representations of the human diseases although they may recapitulate various pathological and phenotypic features. Despite this, the aforementioned studies exemplify the utility of the nematode for facilitating insights into disease pathological processes and

discovering chemical compounds which confer protection against disease pathology. Additionally, the amenability of such screens for a HT format and the fact that they are performed at a whole organism, systemic level, makes such screens in *C. elegans* extremely suitable for early-stage drug discovery.

1.3 ANTIEPILEPTIC DRUGS (AEDS)

1.3.1 Epilepsy and AEDs

Epilepsy is a heterogeneous group of brain disorders which are commonly linked by persistent vulnerability to epileptic seizures, which are transient occurrence of signs and/or symptoms as a result of abnormal hypersynchronous neuronal activity in the brain (Fisher *et al*., 2005). Epileptic seizures are generally thought to be due to an imbalance between neuronal excitation and inhibition (Figure 1.6). Epilepsy and seizures have different classifications, the former categorized based on genetic, structural or metabolic, or unknown causes, and the latter classified as either focal (partial) or generalised depending on whether seizures originated in neuronal networks within one cerebral hemisphere or bilaterally without specific foci respectively (Berg *et al*., 2010). Epilepsy affects 65 million individuals globally and is the most common neurological condition (Ngugi *et al*., 2010). Although an arsenal of more than 20 AEDs exists, they only relieve seizures and are neither disease-modifying nor act to prevent epileptogenesis, the process which propagates the development of epilepsy (Figure 1.6 and Table 1.7) (Schmidt and Schachter, 2014, Moshe *et al*., 2015, Santulli *et al*., 2016, Brodie *et al*., 2011). Additionally, although 70 % of patients respond to AED treatment, the remaining 30 % are pharmacoresistant.

AEDs are discovered serendipitously, empirically from screening-based approaches in seizure models, or derived as derivatives of pre-existing AEDs (Bialer, 2012a). Screening-based discovery is typically initiated with two gold standard rodent acute seizure tests, the maximal electroshock (MES) and subcutaneous metrazol/pentylenetetrazol (scMET/scPTZ) tests (Löscher, 2011). In the MES model, seizures are induced electrically by typical transcorneal administration of 0.2-second, 50 or 150 mA electrical stimuli in mice and rats respectively, resulting in tonic hindlimb extension. Inhibition of hindlimb extension is generally thought to be predictive of protection against

tonic-clonic seizures. In the scMET/scPTZ model, clonic seizures which last for at least 5 seconds in 97 % of the animals are induced chemically via subcutaneous administration of a convulsive dose of MET/PTZ. Protection against these seizures are considered to be predictive of activity against non-convulsive absence seizures. Once anticonvulsant activity is established in these initial tests, further evaluation requires more sophisticated models. The kindling model is a chronic seizure model which is commonly employed at these secondary stages of screening. Seizures are induced via repeated electrode-administered electrical stimuli in the amygdala or hippocampus which progressively increases seizure susceptibility, resulting in exacerbation of seizures. The kindling test is considered to predict for protection against focal seizures.

AEDs possess rich chemical diversities and multiple mechanisms of actions, which is reflected in the repurposing of various AEDs as treatments for non-epileptic neurological and psychiatric conditions such as bipolar and anxiety disorders and neuropathic pain (Table 1.7) (Schmidt and Schachter, 2014, Bialer, 2012b). This can be exemplified by the broad-spectrum AED valproic acid, which mediates its anti-seizure effect by inhibiting voltage-gated sodium (Na_V) and calcium (Ca_V) channels, and by activating gamma-aminobutyric acid (GABA) type A ($GABA_A$) receptors (Figure 1.6). Its multiple mechanisms of action have led to it being approved as a prophylaxis for migraine and for managing mood disorders (Bialer, 2012b). In addition, it has also demonstrated neuroprotective and lifespan-extending effects in a range of neurodegenerative disease models (refer to chapter 4), and such neuroprotective effects are attributed to its actions on other molecular targets such as histone deacetylase (Monti *et al*., 2009). As aforementioned, other AEDs namely trimethadione, levetiracetam, and ethosuximide have also exhibited such protective effects. With the exception of ethosuximide which will be discussed in the following section, these findings will be discussed in chapter 4.

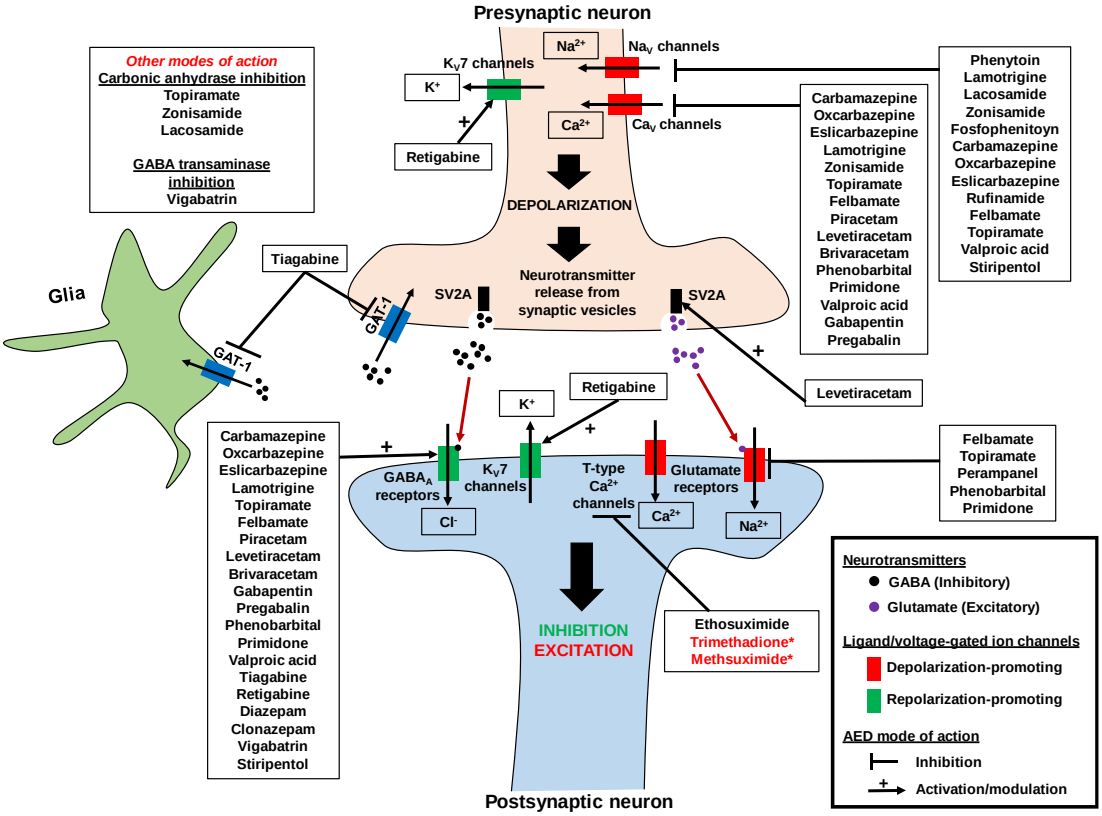

Figure 1.6. Epileptic seizures due to an imbalance between neuronal inhibition and excitation. At the presynaptic neuron terminal, depolarization induces exocytosis and release of neurotransmitters from synaptic vesicles into the synaptic cleft. GABA and glutamate, the major inhibitory and excitatory neurotransmitters, mediate postsynaptic inhibition and excitation by binding to respective ionotropic receptors. Seizures are thought to arise from neuronal hyperexcitability, and various ionotropic receptors and ion channels which promote (red) or inhibit (green) neuronal excitation are shown alongside AEDs which putatively target them. Other targets include carbonic anhydrase and GABA transaminase. *Trimethadione is no longer prescribed whilst methsuximide is infrequently prescribed. Na^{+}, sodium ions; Ca^{2+}, calcium ions; K^{+}, potassium ions; Na_V, voltage-gated sodium channel; Ca_V, voltage-gated calcium channel; K_V7, *KCNQ*-encoded low-threshold voltage-gated potassium channels; SV2A, synaptic vesicle protein 2A; GAT-1, sodium- and chloride-dependent GABA transporter 1.

AED	Type of seizure/epilepsy	Other conditions
Phenobarbital	Focal and generalised convulsive seizures	Anxiety and sleep disorders
Primidone	Focal and generalised convulsive seizures	-
Phenytoin	Focal and generalised convulsive seizures	-
Carbamazepine	Focal and generalised convulsive seizures	Bipolar disorder, trigeminal pain
Valproic acid	Focal and generalised convulsive seizures, absence seizures	Migraine (prophylaxis), bipolar disorder
Diazepam	Convulsive disorders, status epilepticus	Anxiety disorders, alcohol withdrawal
Clonazapam	Lennox-Gastaut syndrome, myoclonic seizures	Panic disorders
Clobazam	Lennox-Gastaut syndrome	Anxiety disorders
Lamotrigine	Focal and generalised convulsive seizures, Lennox-Gastaut syndrome	Bipolar disorder
Vigabatrin	Infantile spasms, focal and generalised convulsive seizures	-
Oxcarbazepine	Focal and generalised convulsive seizures	-
Topiramate	Focal and generalised convulsive seizures, Lennox-Gastaut syndrome	Migraine (prophylaxis)
Levetiracetam	Focal and generalised convulsive seizures, juvenile myoclonic epilepsy	-
Zonisamide	Focal and generalised convulsive seizures	-
Gabapentin	Focal and generalised convulsive seizures	-
Pregabalin	Focal and generalised convulsive seizures	Neuropathic pain, generalized anxiety disorder, fibromyalgia
Stiripentol	Dravet syndrome	-
Rufinamide	Lennox-Gastaut syndrome	-
Lacosamide	Focal and generalised convulsive seizures	-
Perampanel	Focal and generalised convulsive seizures	-
Escarbazepine	Focal and generalised convulsive seizures	-
Trimethadione	Absence seizures	-
Methsuximide	Focal and generalised convulsive seizures, absence seizures	-
Ethosuximide	Absence seizures	-

Table 1.7. Epileptic and non-epileptic uses of AEDs.

1.3.2 Ethosuximide

1.3.2.1 General features

Ethosuximide is a succinimide derivative which was approved in 1958 for the treatment of generalised absence seizures, and remains the first-line treatment for the condition (Figure 1.8) (Zimmerman and Burgemeister, 1958). Valproic acid and lamotrigine are the other two AEDs currently prescribed for absence seizures, whereas trimethadione and the succinimide derivatives phensuximide and methsuximide are no longer prescribed for the condition (Hughes, 2009) (Figure 1.8). Absence seizures are non-convulsive and are characterised by brief lapses of awareness lasting between 9 to 12 seconds (Hughes, 2009). They are classified as either childhood or juvenile, depending on the ages of onsets at 6 and 12 years respectively, and may co-occur with generalised convulsive tonic-clonic seizures whereby patients experience loss of consciousness, muscle stiffening, and jerking movements.

The reported therapeutic range of the drug is 280 to 700 µM, with a half-life ranging from 30 to 60 hours (Browne *et al*., 1975, Buchanan *et al*., 1969). Ethosuximide is primarily metabolized by the phase I cytochrome P450 enzyme CYP3A4 and to a minor extent, CYP2E1 (Bachmann *et al*., 2003). Five phase I primary hydroxymetabolites of the drug have been identified, which mainly undergo phase II glucuronidation and urinary excretion (Millership *et al*., 2005, Pettersen, 1978, Horning *et al*., 1973b, Preste *et al*., 1974, Goulet *et al*., 1976, Millership *et al*., 1993). As the drug is administered as a racemic mixture, chiral characteristics of its metabolites have been studied and is briefly discussed in chapter 4. Early adverse effects associated with ethosuximide mainly involve the gastrointestinal and central nervous systems (CNS), such as abdominal discomfort, diarrhea, nausea and vomiting, dizziness, and somnolence (Schmidt and Schachter, 2014, Gaitatzis and Sander, 2013). Late adverse effects from chronic administration are more serious, and patients may suffer from psychiatric conditions such as depression and psychosis. Immunological effects such as leukopenic and aplastic anemia have also been reported.

Ethosuximide has demonstrated efficacy in the scMET/scPTZ test but not in the MES or kindling tests, correlating with its anticonvulsant activity against

absence seizures only (Löscher, 2011). Electroencephalogram (EEG)-detectable generalised spike-wave discharges in the thalamocortical regions of the brain are the characteristic waveform discharges in absence seizures which has been recapitulated in various models, such as the Genetic Absence Epilepsy Rats from Strasbourg (GAERS) (Marescaux *et al*., 1992), and in rodent thalamocortical slices by perfusion with magnesium-free medium (Zhang *et al*., 1996b). Ethosuximide controlled spike-wave discharges in such models, further corresponding with its anti-absence activity (Manning *et al*., 2004, Zhang *et al*., 1996b).

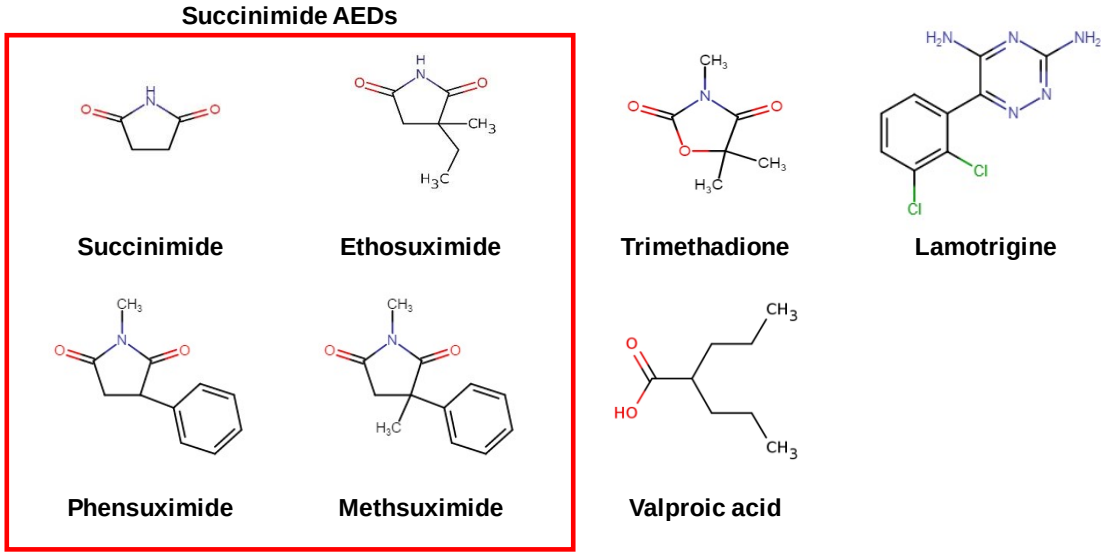

Figure 1.8. Ethosuximide and other AEDs for the treatment of absence seizures. Ethosuximide, phensuximide, and methsuximide are derivatives of the inert compound succinimide; the latter two and trimethadione are no longer prescribed for absence seizures.

1.3.2.2 Neuroprotective and lifespan extension properties

As stated previously in section 1.1.4, ethosuximide has demonstrated neuroprotective and lifespan-extending effects in addition to its anticonvulsant activity. Work performed within our group has demonstrated that the drug induced a concentration-dependent extension of the reduced lifespans in V337M *MAPT* FTDP-17 and ANCL *C. elegans* models, both of which were described in section 1.2.2.2 (Chen *et al*., 2015b). At optimal concentrations, mean lifespans were increased by at least 40 % in comparison to vehicle-treated controls. In addition to a shortened lifespan and progressive neurodegeneration, the ANCL model also suffered from sensory defects, which was characterised by a reduced rate of travel to a food source (refer to chapter 2, sections 2.3.4 and Figure 2.4 for details of assay) (Kashyap *et al*., 2014). As the ANCL worms had minimal motility defects, this reduction was attributed to a reduced ability to sense the food. Ethosuximide ameliorated the sensory defects as it improved the rate of travel to the food source whilst having no effect on the locomotion rate, indicating that the protective effect of the drug was not in part attributed to an improvement in locomotion rate. Ethosuximide additionally improved the defective locomotion of the FTDP-17 model, and reduced levels of detergent-insoluble tau whilst concurrently increasing soluble tau levels. To assess the translational value of these findings in *C. elegans*, the effect of the drug on polyQ aggregation in a mouse neuroblastoma N2A cell line was evaluated. The cell was transfected with EGFP-tagged polyQ25 or 97 constructs, with the latter forming cytoplasmic fluorescent punctae which was indicative of polyQ aggregation. Punctae formation was reduced by 20 % in comparison to vehicle controls, showing that ethosuximide protects against polyQ aggregation, suggesting the feasibility of translating its protective effects into humans.

In separate studies, ethosuximide also extended the lifespans of WT worms (Evason *et al*., 2005, Collins *et al*., 2008) and an A315T TDP-43-expressing transgenic *C. elegans* ALS strain (Tauffenberger *et al*., 2013), providing further evidence for its lifespan-extending effects. Interestingly, it should be noted that the drug did not induce lifespan extension of WT worms in work performed within our group (Chen *et al*., 2015b)

The neuroprotective and neurogenic properties of ethosuximide was additionally demonstrated in a rat model of AD-like symptoms (Tiwari *et al*., 2015). The model was generated by bilateral stereotaxic intrahippocampal injection of $A\beta_{42}$, and immunohistochemical analyses of hippocampal brain slices demonstrated marked reductions of neural stem cell proliferation and differentiation into new born neurons, in addition to reduced survival of mature neurons. Furthermore, there was an increase in neuronal degeneration and apoptosis. Behaviourally, these rats displayed cognitive defects. Remarkably, these effects were ameliorated by treating the animals with ethosuximide.

The neuroprotective and lifespan-extending effects of ethosuximide in WT *C. elegans* and in different models of neurodegenerative diseases in *C. elegans*, mammalian cells, and rats, suggest the potential for the drug to be repurposed as a general neuroprotective drug. Drug repurposing is an attractive alternative to the tedious and lengthy traditional drug discovery and development process, as approved drugs have already undergone preclinical evaluation and so can be expedited to clinical testing in humans. However, the mechanism of action of ethosuximide is largely unclear, although it has been proposed to mediate its anticonvulsive effects by blocking T-type calcium, and voltage-gated sodium and potassium channels, and lifespan extension and neuroprotection by acting on chemosensory function, forkhead box O (FOXO) transcription factors, and the phosphoinositide 3-kinase (PI3K)/protein kinase B (AKT)/Wnt/β-catenin pathway; these putative mechanisms of action will be discussed in chapter 5. As the pathogenic mechanisms which underlie both neurodegenerative diseases and epilepsy/seizures are still currently poorly understood, drugs like ethosuximide are extremely useful for facilitating insights into disease pathogenesis. As aforementioned, this can be performed via chemical genetics screens in genetically tractable organisms like *C. elegans*, but a more direct approach would be to utilise the drug to identify molecular binding targets which may be disease-modifying. This is traditionally performed via an affinity chromatography approach whereby a derivatised version of a drug is immobilised onto an affinity column, followed by subsequent incubation with protein extracts and extensive washes to remove nonspecific binding (Terstappen *et al*., 2007). Bound proteins are eluted and

analysed with sodium dodecyl sulfate (SDS)-polyacrylamide gel electrophoresis (PAGE) and identification by mass spectrometry. The success of this approach depends on various factors, including high affinity of a drug for its target(s) such that nonspecific binding is reduced and to ensure sufficiently tight binding to endure washing steps. The dissociation constant (K_D), which is a measure of the binding affinity of a ligand for its binding partner, typically has values ranging from femtomole to nanomole concentrations for high affinity ligands (Terstappen *et al*., 2007). In spite of the *C. elegans* cuticle which impedes drug permeation, high mM externally-administered concentrations were required to elicit protective effects of ethosuximide in the aforementioned studies. Although the internal lifespan-extending concentration of ethosuximide was reported by one such study to be within the µM range at approximately 220 µM, this value still deviates far from the desired K_D range (Evason *et al*., 2005). Furthermore, therapeutic effects of the drug in humans are also elicited at high µM concentrations, as extrapolated from the reported minimum therapeutic dose of 40 µg/ml which translates to approximately 280 µM. Hence, this suggests that target identification may prove unfeasible or difficult with ethosuximide. Moreover, the drug will have to be derivatised with a linker molecule to affix it to the affinity column, which may further diminish its affinity for its target(s) if structural modifications are made in the bioactive part of the molecule. To facilitate appropriate derivatisation, tedious structure-activity relationship (SAR) studies must be performed. In addition, there is a possibility of low clinical neuroprotective efficacy, which may make repurposing an unideal strategy.

Aside from the classic affinity chromatography approach for target identification, alternative approaches such as protein microarrays and yeast three-hybrid systems may be employed, although most of them necessitates molecular derivatisation for immobilization to matrices as well and may similarly be potentially unfeasible with ethosuximide (Terstappen *et al*., 2007, Lomenick *et al*., 2011). Drug affinity responsive target stability (DARTS) is an approach which does not require tedious SAR studies and molecular derivatisation, as it relies on the enhanced stability and increased proteolytic resistance of drug-bound targets to identify molecular targets through the

enhanced proteolysis of unbound proteins (Pai *et al*., 2015, Lomenick *et al*., 2011, Lomenick *et al*., 2009). Although such a technique may improve the prospect of target identification with ethosuximide, existing limitations such as the choice and specificities of protease, and the rate and extent of proteolysis, can influence the success of target identification. The pros and cons of these different approaches need to be taken into consideration to select the most appropriate one for target identification with ethosuximide. However, given that most approaches require molecular derivatisation, a derivatised version of the drug may have broader utility and hence may improve the prospects of target identification. Given the potential low affinity of the drug, however, alternative strategies will have to be considered to optimise the success of such approaches.

1.4 PROJECT AIMS

In view of the possible low affinity of ethosuximide and the consequent possible issues with repurposing and utilising it to identify binding targets, the main aims of the current work are as follows:

1) To utilise the drug as a scaffold to derive a structurally-similar candidate compound with enhanced neuroprotective potency. Such a candidate molecule may improve the prospect of deriving new therapies and for identifying potential disease-modifying targets in neurodegenerative diseases
2) To understand the SAR of ethosuximide for appropriate molecular modifications for target identification
3) To compare the MMOAs between ethosuximide and the candidate compound

CHAPTER 2

MATERIALS AND METHODS

2.1 CHEMICALS AND COMPOUNDS

All chemicals and reagents listed were obtained from Sigma-Aldrich Ltd (Dorset, UK) unless stated otherwise in the text.

2.2 *C. ELEGANS* METHODS

2.2.1 Strains and maintenance

The *dnj-14 (tm3223)* strain was supplied by the National BioResource Project (Tokyo Women's Medical University School of Medicine, Japan) whilst the following strains were obtained from the *Caenorhabditis* Genetics Center (University of Minnesota, USA): WT Bristol N2, *unc-49 (e407) III*, *cca-1 (ad1650) X*, and *daf-16 (mu86) I*. Transgenic tau-expressing CK10–bkIs10 [P*aex-3*::Tau–337^{M}, P*myo-2*::GFP] (hereafter referred to as CK10), and transactive response DNA binding protein 43 kDa (TDP-43)-expressing strains CK405 [P*snb-1*::TDP-43 (WT), P*myo-2::*dsRED] and CK426 [P*snb-1*::TDP-43^{A315T}, P*myo-2::*dsRED] were generated and kindly donated by Dr. Brian Kraemer (University of Washington, USA) (Kraemer *et al*., 2003, Kraemer and Schellenberg, 2007, Liachko *et al*., 2010), who also provided the CZ1200 strain [P*unc-25*::GFP] from Prof. Yishi Jin (University of California, San Diego, USA). Compound mutant strains *unc-49*/*cca-1* and *unc-49*/*daf-16* were generated via genetic crosses of *unc-49 (e407) III* with *cca-1 (ad1650) X* and *daf-16 (mu86) I* respectively by Douglas Grimes (University of Liverpool, UK), whilst CK426/CZ1200 strain was generated in the same manner with CK426 and CZ1200 strains by Matthew Pontifex (University of Liverpool, UK). Crosses of the CK426/CZ1200 worms with *daf-16 (mu86) I* strain were made with Beth Atherton (University of Liverpool, UK) to generate the triple mutant *daf-16*/CK426/CZ1200. Note that as denoted, *daf-16 (mu86) I* is an autosomal mutation on chromosome I whereas *cca-1 (ad1650) X is X*-chromosome-linked. CK426 and CZ1200 are transgenic strains with integrated extrachromosomal arrays containing transgenes and additionally the P*myo-2::*dsRED red pharyngeal co-injection fluorescent marker for the former. The genomic locations of these integrated arrays were not determined, and locations were assumed to be autosomal. Figures 2.1 and 2.2 show the general crossing strategies used for autosomal mutants and between autosomal and *X*-linked mutants respectively. All mutants were genotyped with polymerase chain

reaction (PCR) and subsequent agarose gel electrophoresis (sections 2.4.2 and 2.4.5 respectively; genotyping primers listed in Table 2.3), except CK426/CZ1200 worms which were verified for human TDP-43 protein expression with western blotting (section 2.4.1). Specific details about the genetic crosses should be referred to in the results chapters 4 and 5.

Strains were maintained under standard conditions at 20°C on Nematode Growth Media agar culture plates (NGM; 1 mM each of $CaCl_2$ and $MgSO_4$, 25 mM KH_2PO_4, 5 µg/mL cholesterol, and in w/v 2 % agar, 0.25 % peptone, and 0.3 % NaCl) seeded with 100 µL of the OP50 *E. coli* bacteria strain acting as the food source (Brenner, 1974). Maintenance was performed every 3 to 5 days by transferring 5 to 10 egg-laying adult worms onto the OP50 lawn of freshly seeded NGM plates with a worm tungsten pick (World Precision Instruments Inc., Hertfordshire, UK). Chunking was performed in the event of starvation or near-starvation, whereby sections of NGM agar-containing worms were removed and transferred to freshly seeded plates; chunked worms will detect and move towards OP50 on freshly seeded plates.

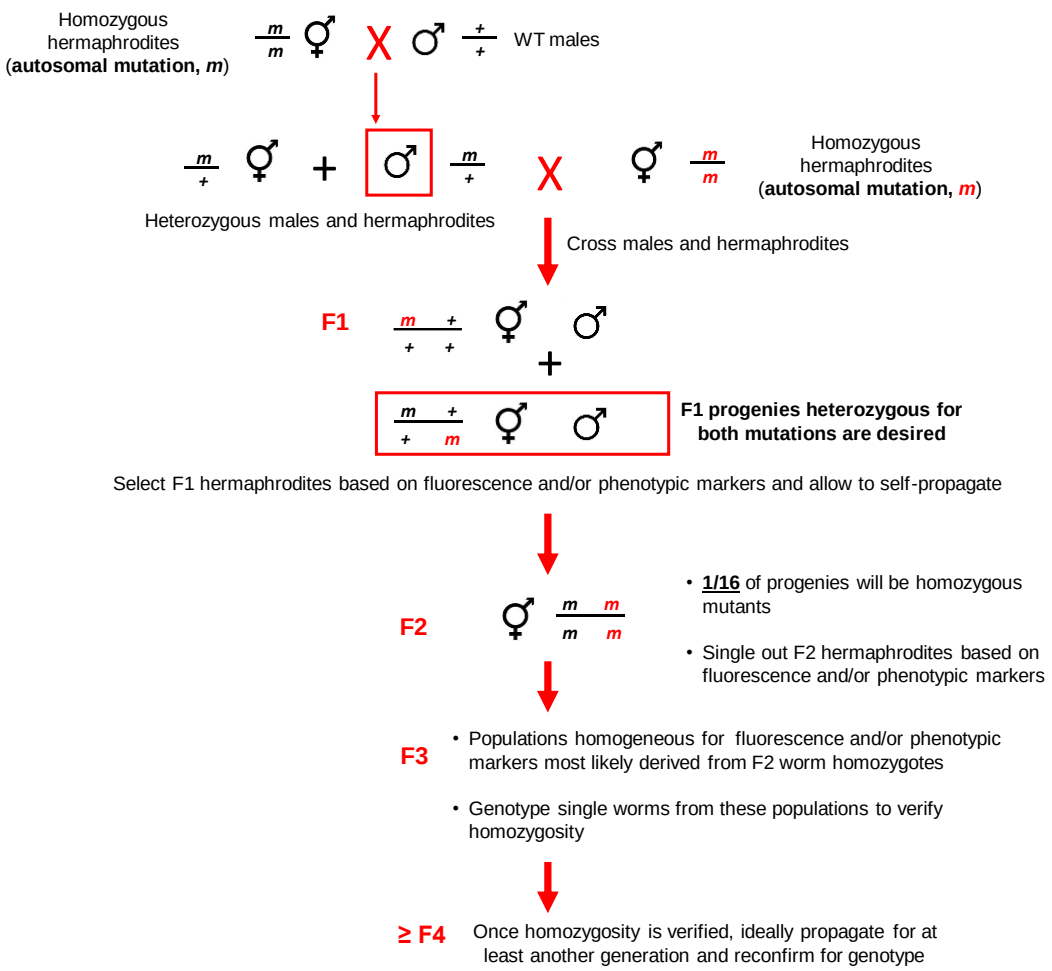

Figure 2.1. Worm crossing strategy for autosomal mutations.

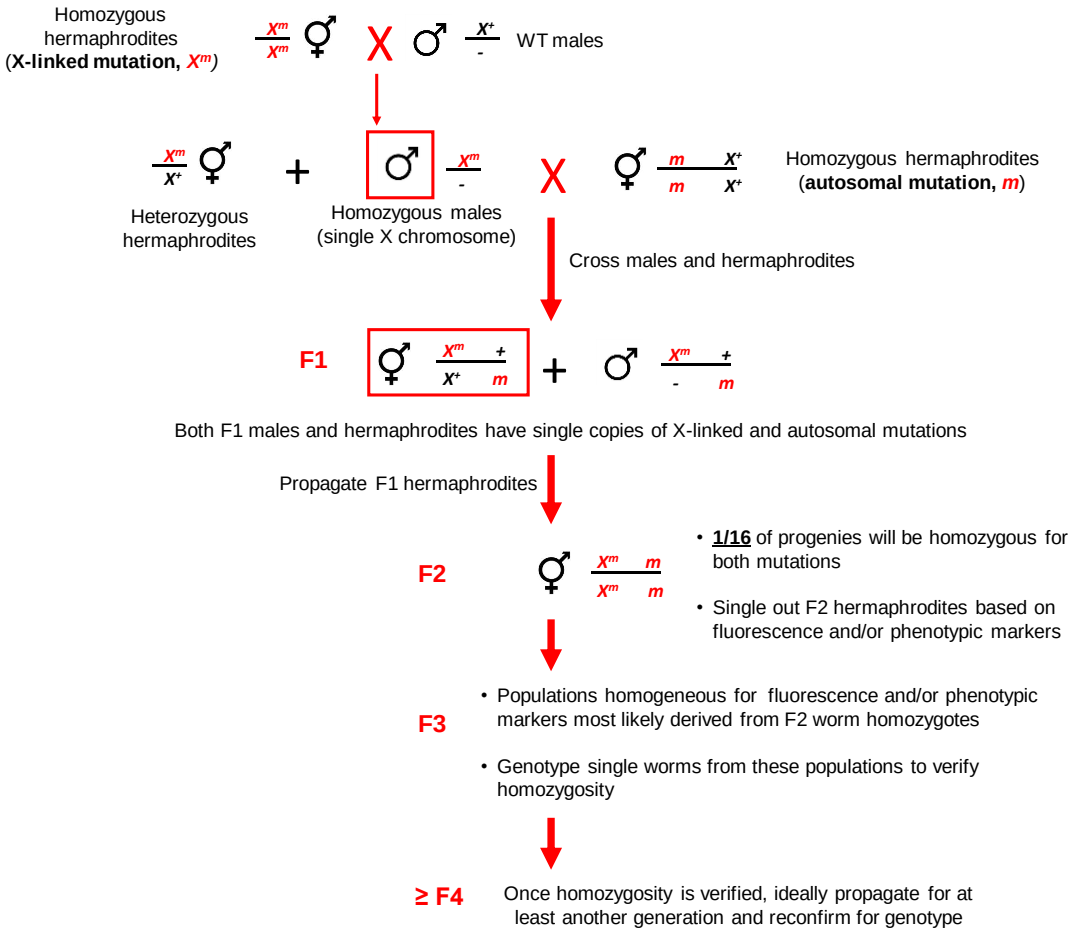

Figure 2.2. Strategy for crossing *X*-linked and autosomal mutant strains.

PCR (genotyping)				
Primer	**Sequence (5'-3')**	**Annealing temperature (ºC)**	**Amplicon size (bp)**	**Genotyped strains**
TARDBP forward (human TDP-43)	CTGAATATATTCGGGTAACCG	47	1231	*daf-16* (*mu86*) /CK426/CZ1200
TARDBP reverse (human TDP-43)	CAGCCAGAAGACTTAGAATCC			
daf-16 (mu86) forward	CCCACATTCGTGTGGGTTTTCTAGTCG	55	635 (wildtype *daf-16*)	*daf-16* (*mu86*) /CK426/CZ1200
daf-16 (mu86) internal reverse	GCGTCAGTTCCGATCTGATATGAAC			
daf-16 (mu86) forward	CCCACATTCGTGTGGGTTTTCTAGTCG	54	405 (*daf-16 (mu86)*)	
daf-16 (mu86) external reverse	CGTTATCAAATGCTCCTTGCATTGAATC			
daf-16 forward (new)	GTAGACGGTGACCATCTAGAG	50	950 (*daf-16 (mu86)*)	*unc-49*/*daf-16*
daf-16 reverse (new)	GACGATCCAGGAATCGAGAG			
daf-16 forward (new)	GTAGACGGTGACCATCTAGAG		1470 (wildtype *daf-16*)	
daf-16 internal (new)	CGGGAATTTCAGCCAAAGAG			
cca-1 (*ad1650*) forward	CCGCAATTTGCCCTCCACAT		3310 (wildtype *cca-1*); 930 (*cca-1* (*ad1650*))	*unc-49*/*cca-1*
cca-1 (*ad1650*) reverse	ATGAGGATGGCGAAGAGGACC			
unc-49 forward	ATGACCAAGGTTAGGCGACG	55	431 (both wildtype and e407 alleles)	*unc-49*/*daf-16* *unc-49*/*cca-1*
unc-49 reverse	TCTGGCTACATAACGGCACG			

Table 2.3. PCR primers for genotyping of mutant strains.

2.2.2 Freezing and revival of frozen worm strains

As adapted from previously-described procedures, *C. elegans* was frozen in a cryoprotective agent at -80°C for long-term preservation (Brenner, 1974, Stiernagle, 2006). Strains were propagated and starved to obtain and arrest progenies at the L1 and/or L2 larval stages which best survive freezing. Worms were then washed off NGM agar with 3 ml M9 buffer (1 mM $MgSO_4$, 3 g/L KH_2PO_4, 5 g/L NaCl, and 6 g/L Na_2HPO_4) and mixed with an equal volume of freezing solution (30 % (w/v) glycerol, 3 mM $MgSO_4$, 5.5 mM NaOH, 50 mM KH_2PO_4, and 100 mM NaCl) before aliquoting to cryovials. Worms were subjected to slow freezing overnight at -80°C in polystyrene boxes followed by long-term storage at the same temperature. To recover frozen stocks, frozen aliquots were thawed at room temperature and transferred to freshly seeded plates followed by continued propagation of recovered worms.

2.2.3 Decontamination of strains

Worm populations can be contaminated with mould, bacteria, or yeast. Decontamination was carried out either by transferring contaminated chunks onto freshly seeded plates and further transferral of worms which had crawled off chunks onto freshly seeded plates, or by bleaching as adapted from established protocols (Porta-de-la-Riva *et al*., 2012). With bleaching, contaminated populations washed off plates with 3.5 mL water were combined with 1.5 mL bleach mixture (2 parts 8 % commercial alkaline hypochlorite bleach and 1 part 5 M NaOH). Eggs were released from gravid adult worms through lysis by vortexing the mixture every 2 mins for 10 mins, and pelleted via centrifugation (1 min, 1300 g). The egg pellet was resuspended in 1 mL M9 buffer after a triple wash with 5 mL M9 buffer, and incubated for 24 hours on a nutating shaker at room temperature to arrest the hatched progenies at the L1 larval stage. The L1 suspension was then transferred to the edges of freshly seeded plates to allow continuation of development; worms of locomotion-defective CK10, CK426, CK426/CZ1200, and *daf-16* null CK426/CZ1200 strains were transferred directly onto OP50 lawns instead.

2.2.4 Age synchronisation

Strains were age-synchronised by bleaching or timed egg lay. Bleaching was performed as described in the preceding section with procedures as adapted from established protocols (Porta-de-la-Riva *et al*., 2012). To obtain a desired worm population size per plate, the number of L1 worms were counted per µL of suspension and appropriate volumes of suspension transferred onto freshly seeded plates. With timed egg lay, approximately 60 gravid worms per strain were transferred and left onto freshly seeded plates for 6 hours for egg laying, following which they were removed so that only eggs remained on the plates. Depending on the procedure used, the duration from egg to adulthood is approximately 4 days at 20°C, whereas it takes about 3 days from the L1 stage. Bleaching was the preferred method of age synchronisation, as it prevented contamination of strains and kept synchronised populations free from contamination for further experimentation.

2.3 *C. ELEGANS* ASSAYS

All assays were performed at 20°C.

2.3.1 Plate-based pharmacological treatment

Treatment NGM plates containing water-soluble compounds were prepared by dissolving sterile-filtered 10X stocks in NGM without the agar component, followed by further dilution to 1X working concentrations in molten NGM agar before transferral into 60 mm culture plates. Treatment plates containing hydrophobic compounds were prepared by diluting sterile-filtered stocks (100X of the working concentration in 40 % dimethyl sulfoxide (DMSO) in NGM without agar) with molten NGM agar to obtain the working concentration in 0.4 % DMSO. Corresponding DMSO vehicle control plates were prepared in the same manner. Treatment and vehicle plates with the thymidylate synthase inhibitor 5-Fluoro-2′-deoxyuridine (FUDR) were prepared as described above, with the addition of 49.5 µM of FUDR as reported previously (Sutphin and Kaeberlein, 2009).

All freshly poured plates were stored in the dark at 4°C after drying at room temperature overnight, and transferred to room temperature and seeded up to 4 days before use. FUDR plates were seeded with overnight cultures of 10X

concentrated OP50 with the same concentration of FUDR, as adapted from previously published protocols (Sutphin and Kaeberlein, 2009, Anderson *et al*., 2016). Plates older than 2 weeks since preparation were not used to ensure that plates were kept as fresh as possible.

2.3.2 Liquid thrashing assay

The motility of worms in liquid was assessed via quantification of their thrashing rates in Dent's Ringer solution (DRS pH 7.4; 1 mM $MgCl_2$, 3 mM $CaCl_2$, 6 mM KCl, 10 mM HEPES, and 140 mM NaCl), as previously described (Johnson *et al*., 2009b). A thrash is typically scored as a head to tail sinusoidal movement in WT worms. However, the current study assessed the thrashing phenotype of the locomotion-defective CK10 strain which does not exhibit typical thrashes, with sinusoidal movements apparent only in the anterior halves of these worms whereas the posteriors are paralysed. These worms also exhibit uncoordinated and minimal movements in liquid. To improve comparisons between pharmacological treatments, the phenotype was scored differently for this strain. A thrash was scored when a worm moves laterally or sinusoidally in their anterior halves, whereas lateral movements in the head only were not scored. Thrashes were quantified over 1 min after a 10-min acclimatisation period in 0.1 % (w/v) bovine serum albumin (BSA) / DRS.

2.3.3 Body bend assay

Locomotion on a solid medium was assessed by quantifying the number of body bends made, adapted as previously described (Sleigh, 2010). Depending on the treatments administered, corresponding unseeded plates were used to acclimatise worms for 20 s followed by scoring of body bends over a duration of 1 minute, and to ensure chronic treatment exposure during throughout the assay. The current study assessed the body bends of the locomotion-defective CK426 and *daf-16*/CK426/CZ1200 strains. Unlike WT worms which move sinusoidally on solid medium, these strains generally display limited locomotion with movement primarily manifesting in the posterior part of the body. Body bends for these worms were scored when the posterior half moves laterally, sinusoidally, or coils at maximum angle away from the central axis of the body. Reversion of the movement back to the central body axis is not

scored as another body bend, and a bend would have to be made away from the central axis again to be scored.

2.3.4 Food race assay

The food race assay, which measures sensory neuron function by determining the rate of movement towards an OP50 food source (Figure 2.4), was based on established protocols (Kashyap *et al*., 2014, Mitchell *et al*., 2010). Before commencement of the assay, 20 to 30 worms were washed twice in 0.1 % BSA / M9 buffer. This was performed by picking them into the wash buffer and allowing them to thrash for 5 mins each time. Depending on the treatment administered to the assayed worms, the same concentration of the treatment was included in the wash buffer to ensure continuous treatment exposure.

2.3.5 Lifespan assay

Assays were adapted as previously described (Chen *et al*., 2015b) and were initiated with 60 age-synchronised adult day 1 worms on freshly-seeded treatment or vehicle plates, and concluded when all assayed worms were dead. Worms were scored for survival every alternate day throughout the assay. To prevent contamination with progenies especially during the fertile period of the first 2 weeks, and to prevent or reduce plate contamination, worms were transferred to freshly seeded plates on each scoring day. Worms were scored as alive if they display spontaneous locomotion, or in the absence of that, locomotive responses to touch stimulation with a worm pick and/or pharyngeal pumping. Dead worms were accounted for per scoring day, whereas missing worms, those with internally-hatched progenies, and worms damaged from picking which were evident from visible spillage of body contents, were censored from analysis.

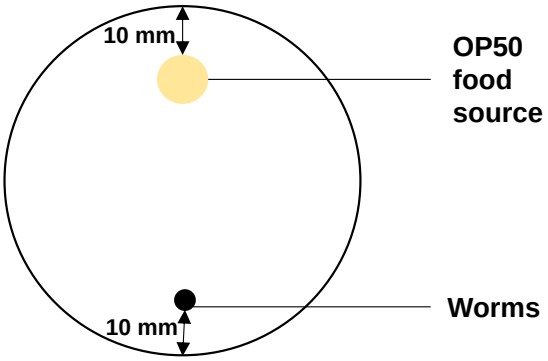

Figure 2.4. Food race assay. Worms and a 30 µL lawn of the OP50 food source were placed at opposite ends of a 60 mm treatment or vehicle plate, 10 mm from the edges. The number of worms at the food source was noted every 10 mins up to 2 hours, and removed from the food each time after counting.

2.3.6 *In vivo* imaging of GABAergic motor neurons

Worms expressing GFP in GABAergic neurons were imaged as previously described (Kashyap *et al*., 2014). Worms were immobilised in a 3 µL droplet of polyethylene glycol (PEG)/glycerol solution in 1X phosphate buffered saline (PBS) (20 % each of PEG (w/v) and glycerol) on a 22 x 40 mm imaging slide (VWR International, Pennsylvania, USA), and mounted with a 13-mm coverslip (Paul Marienfeld GmbH & Co. KG, Germany). Worms were then imaged immediately under fluorescence with the Nikon Eclipse Ti S microscope (Nikon Instruments Europe BV, Netherlands). Quantification of cell bodies and breaks of the GABAergic D-type motor neurons in the ventral nerve cord was carried out at 40 or 60 X objective, whereas images were acquired at 200X magnification on the 20X objective with the NIS-Elements imaging software version 3.2 (Nikon Instruments Europe BV, Netherlands). As previously described, cell bodies of the neurons were scored when intact and clear punctate fluorescence was observed, whilst neuronal breaks were quantified from fluorescence breaks (Liachko *et al*., 2010).

2.3.7 Pentylenetetrazol (PTZ)-induced seizure assay

2.3.7.1 Assay optimisation

A PTZ-induced seizure model was previously described in a GABAergic-deficient and synaptic transmission mutant strain, *unc-49*, which exhibits a seizure-type phenotype when exposed to the convulsant PTZ (Williams *et al*., 2004). This model was further adapted herein to develop a screening assay for antiseizure protection. Seizures are defined as head bobbing movements manifested by head extension from the body followed by shrinkage back into the body, and were stringently scored herein in a qualitative and/or quantitative manner. Qualitative scoring is a ‘yes/no’ assessment of whether the worm is seizing or not in general over the course of 30 s, whereby seizing was scored when the worm exhibits three repetitive head bobs. This was then followed by subsequent determination of the seizing proportion in the assayed population. On the other hand, the quantitative approach scores the number of head bobs over the same duration. Both scoring approaches complement each other and concurrent usage strengthens the assessment of the phenotype.

Previous work by Steven Dodd (University of Liverpool, UK) established a liquid-based protocol for inducing seizures in the *unc-49* strain by incubating the worms in 50 mM PTZ in 0.1 % BSA / DRS for an optimal seizure-inducing duration of 15 mins. Further work was performed herein to identify the optimal seizure-inducing concentration of PTZ at this treatment duration via concentration-response assessments of the compound. To identify the optimal treatment duration and the ballpark concentration at which compounds would be initially screened at to assess their activity in regard to protection against PTZ-induced seizures, the antiepileptic drug ethosuximide was used as the reference molecule to assess these parameters. Note that given the differences in molar mass, screens were initiated at a standardised mg/mL concentration of 4 mg/mL, which is equivalent to the optimal protective 28 mM concentration of ethosuximide, unless stated otherwise. The resultant optimised protocol for primary screens is as follows: *unc-49* worms were pretreated with 4 mg/mL compound in 0.1 % BSA / DRS for 2 hrs, followed by exposure to 50 mM PTZ with the same drug treatment concentration in 0.1 % BSA / DRS for 15 mins to induce seizures. Seizing phenotypes were scored concurrently with video recordings of the worms performed with a Zeiss Stemi 2000-C microscope (Carl Zeiss Limited, Cambridge, USA) mounted on a Prior OptiScanII™ motorised microscope stage (Prior Scientific Inc, Massachusetts, USA) on the Worm Tracker software version 2.0.3.1. For detailed description of assay optimisation, refer to chapter 3, section 3.2.2.

2.3.7.2 Primary screens and concentration-response assessment of active compounds

As abovementioned, screens were performed at a standardised optimal seizure-protecting mg/mL concentration of ethosuximide at 4 mg/mL. However, screening concentration was reduced to 2 mg/mL if toxicity was observed. Hydrophobic compounds were screened at 1 % DMSO, with activities compared against ethosuximide and succinimide controls at the same vehicle concentration. If inactivity was observed at 4 mg/mL in the absence of toxicity, re-screening was performed at a higher 70 mM-equivalent concentration of ethosuximide at 10 mg/mL to verify inactivity; confirmation of inactivity was also performed for succinimide to substantiate its use as the negative control.

As the objective of these primary screens were to get a quick preliminary assessment of a compound's activity, identified compounds were subsequently subjected to further in-depth concentration-response assessments to assess and compare their potencies. At this stage, molar concentrations were assessed to account for molar mass differences, for more accurate comparisons. Except 1-Benzylpyrrolidine-2,5-dione (AK Scientific Inc., California, USA), 3,3-diethylpyrrolidine-2,5-dione and 4-ethyl-4-methylpyrrolidin-2-one (Enamine Ltd, New Jersey, USA), and 2,5-Pyrrolidinedione,3-ethyl-1,3-dimethyl which was synthesized in the current study (section 2.5.2), all compounds were obtained from Sigma.

2.4 MOLECULAR BIOLOGY TECHNIQUES

Procedures involving genetic material (sections 2.4.2 – 2.4.5) were performed with nuclease-free water (ThermoFisher Scientific Inc., Waltham, MA, USA) to prevent genetic degradation.

2.4.1 SDS-PAGE, western blotting, and coomassie blue staining

Procedures were based on previously established protocols (Duerr, 2006). Human TDP-43 protein expression in CK426/CZ1200 double mutants was verified with western blot by Matthew Pontifex (University of Liverpool; section 2.2.1). Briefly, 100 worms per sample were picked into 25 µL water, followed by addition of an equivalent volume of Tris-Glycine SDS 2X sample buffer (ThermoFisher Scientific Inc). Samples were lysed via a freeze-thaw cycle at -80ºC for at least 30 mins, boiled at 100ºC for 20 mins, and resolved via SDS-PAGE alongside 5 µL of the SeeBlue® Plus2 pre-stained protein standard on precast NuPAGE™ Bis-Tris 4-12 % protein gels in 1X NuPAGE™ MOPS SDS running buffer (all components from ThermoFisher Scientific Inc) at 165 V for 1 hr. Proteins were transferred onto nitrocellulose membranes in transfer buffer (0.025 M Tris, 0.192 M glycine, 20 µL methanol) with a BioRad Trans-blot Electrophoresis Transfer Cell (Bio-Rad Laboratories Ltd, Hertfordshire, UK) at 25 V overnight. The membrane was then blocked with 3 % (w/v) skimmed milk in 1X PBS for 1 hr, followed by incubation with a mouse monoclonal anti-TDP-43 primary antibody (Abcam, Cambridge, UK) at 1:1000 dilution for another hour. After three 5-min 1X PBS washes, the membrane was incubated for 1 hr with goat anti-mouse IgG peroxidase secondary antibody at 1:500 dilution. After rinsing of the membrane with 1X PBS, chemiluminescent detection of immunoreactivity was performed with Clarity™ Western ECL Blotting Substrates (Bio-Rad Laboratories Ltd) according to manufacturer's instructions. For 1-dimensional (1D) proton (^{1}H) nuclear magnetic resonance (NMR) analysis of bioaccumulated treatment concentrations (see section 2.6.3.3 and Figure 2.17), samples prepared for SDS-PAGE were lysed and resolved via SDS-PAGE at 200 V for 45 mins. Gels were stained with InstantBlue™ coomassie stain (Expedeon Ltd, Cambridge, UK) by microwaving on high heat for 40 s followed by incubation for 30 mins on a nutating shaker prior to analysis of staining intensities. Imaging and analysis

of gels, blots, and gel staining intensities were performed on the ChemiDoc™ XRS+ imaging system with Image Lab™ version 6.0 (Bio-Rad Laboratories Ltd).

2.4.2 Single worm PCR

Lysis of single worms were adapted as previously described (Ahringer, 2006) in 10 µL lysis buffer (1X Phusion® HF buffer, New England Biolabs Ltd, Hitchin, UK; 1 mg/mL proteinase K) to extract genomic material via initial freezing at -80ºC for at least 30 mins and subsequent heating at 65ºC for 90 mins. Samples were stored long-term at -80ºC after proteinase K was inactivated at 95ºC for 15 mins. PCR was performed on 2 µL of template DNA in a 25 µL reaction with One*Taq*® Quick-Load® 2X Master Mix with Standard Buffer (New England Biolabs Ltd) according to manufacturer's instructions. Annealing temperatures, derived with the online NEB Tm calculator (New England Biolabs Ltd), are shown per primer pair in Table 2.3.

2.4.3 RNA extraction and reverse transcription to complementary deoxyribonucleic acid (cDNA)

RNA was extracted from worms (Figure 2.5) and purified with the RNeasy mini kit and RNase-Free DNase Set (Qiagen, Manchester, UK) according to manufacturer's instructions, followed by measurement of concentration and purity with a NanoDrop™ Lite spectrophotometer (ThermoFisher Scientific Inc). Reverse transcription to cDNA was then performed with 3 µL template RNA with the GoScript™ Reverse Transcription kit according to manufacturer's instructions (Promega, Southampton, UK).

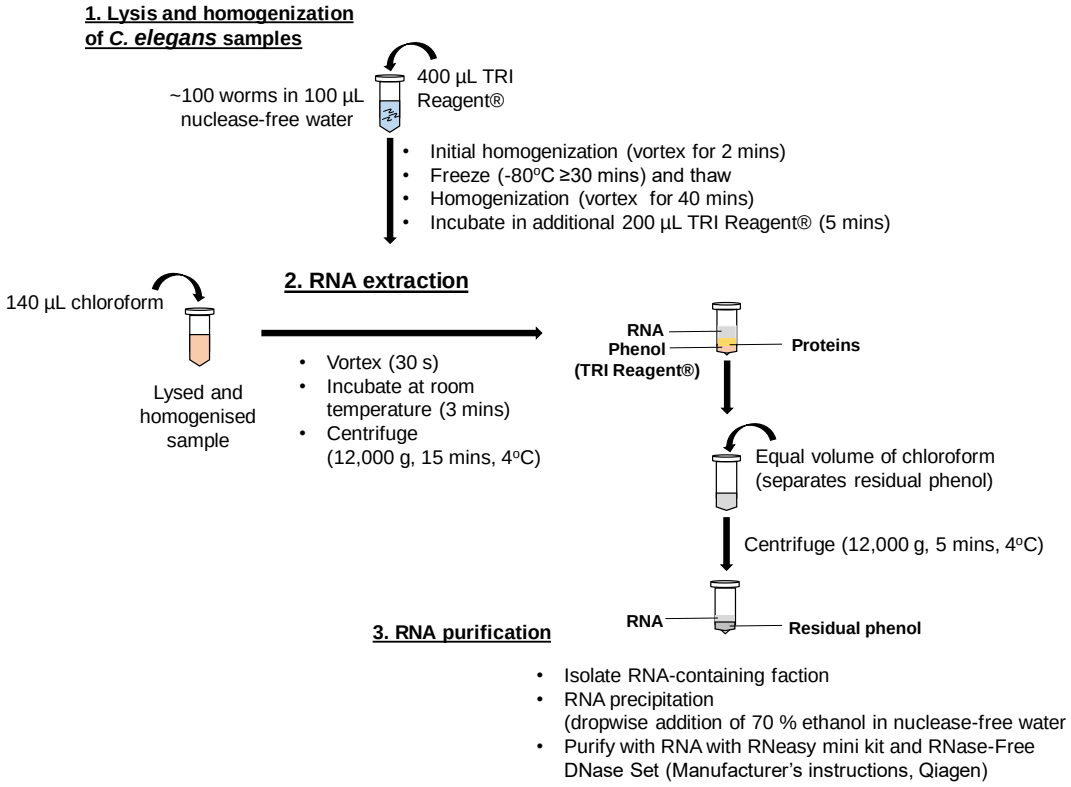

Figure 2.5. RNA extraction from *C. elegans*.

2.4.4 Quantitative PCR (qPCR)

Procedures were adapted as previously described (Chen *et al*., 2015b), and equipment and reagents were obtained from Bio-Rad Laboratories Ltd unless stated otherwise. One µL of cDNA samples were prepared in 10 µL reactions on white well Hard-Shell® 96-well PCR plates, at primer concentrations of 0.5 µM in iTaq™ Universal SYBR® Green Supermix according to manufacturer's instructions. qPCR analysis was performed with the CFX Connect™ Real-Time PCR Detection System and CFX Manager 3.1, with thermocycling conditions as follows: Initial denaturation at 95ºC for 2 mins, followed by 40 cycles of 30-sec 95ºC denaturation, 55ºC annealing, and 72ºC extension steps, and final extension at 72ºC for 5 mins. *cdc-42* and *pmp-3* were previously verified as appropriate *C. elegans* internal controls and their geometric mean was used for normalizing expression levels of sampled genes (Hoogewijs *et al*., 2008). All qPCR primers used (Table 2.6) have melting temperatures between 55 and 60ºC and were specific for cDNA templates due to the intron-spanning priming sites on one or both primers in the primer pair. Primer design was carried out with DNA Dynamo Sequence Analysis Software (Blue Tractor Software, Llanfairfechan, UK), and secondary structures were checked with Beacon™ Designer (PREMIER Biosoft, Palo Alto, California, USA). Primer specificities were confirmed via a single melt temperature with melt curve analysis at the end of a qPCR and presence of single band on agarose gel.

2.4.5 Agarose gel electrophoresis

DNA and cDNA amplicons from PCR and qPCR experiments were resolved on 2 % agarose gels containing SYBR® Safe DNA gel stain (ThermoFisher Scientific Inc) at 80 V for 45 mins. cDNA amplicons were loaded into gel wells in combination with 6X DNA gel purple loading dye (Bio-Rad Laboratories Ltd), whereas the use of the One*Taq*® Quick-Load® reagent (New England Biolabs Ltd) for PCR enables direct loading of DNA amplicons. The HyperLadder™ 1kb molecular weight marker (Bioline Reagents Limited, London, UK) was resolved alongside products as a guide for amplicon size. Resolved bands were visualized with UV light on the ChemiDoc™ XRS+ imaging system with Image Lab™ version 6.0 (Bio-Rad Laboratories Ltd).

qPCR	
Primer	**Sequence (5'-3')**
pmp-3 forward	TGGTGTCGCGATTACTGTAG
pmp-3 reverse	GATTTGTTGTCGCAGAGTGG
cdc-42 forward	GGTGGCGAGCCATACACATTAGG
cdc-42 reverse	CTCTCCAACATCCGTTGACACTGG
pph-6 forward	ACATGGAGGACTTTCACCTG
pph-6 reverse	ATAGCAGTAGTTTGGAGCCG
cyp-34A9 forward	CGAGACTCTTGCCGTAGACC
cyp-34A9 reverse	TTCCACCGGTAACCTCTGTC
cyp-35B1 forward	CAAAGATGGAGCAGGAGAGG
cyp-35B1 reverse	ATTGAATCCTGCGACCAAAG
cyp-14A3 forward	CAAAGGACCGTTACCATTGC
cyp-14A3 reverse	TTGAAGCCTCCAGTTGTCTC
ugt-25 forward	ATGACTCACGGAGGTCTTGG
ugt-25 reverse	TGCAAGCATATTCGCATTTC
ttr-44 forward	GACGTCTGATCTGTGGAGAC
ttr-44 reverse	TCCAGGTTGAGAACTCCAAG
dhs-26 forward	AACATCTGCAGGATCTTGGG
dhs-26 reverse	CACAAAGTGATTGCCCATCC
dod-3 forward	GCCCAGCCAACAGTCTATC
dod-3 reverse	CATGAACACCGGCTCATTC
dod-6 forward	TCCTCGTCATCATGTCTGTC
dod-6 reverse	CACTTTCCGCAAGTCTTTGG
asm-3 forward	GCACTTCACTTGACCGACC
asm-3 reverse	GGGCTTCTCCTTCCCATCTC
tir-1 forward	GATAACTGTGAGGATTGGGTG
tir-1 reverse	CATTTCTTTGGTGGTCGGTG

Table 2.6. qPCR primers.

2.5 CHEMISTRY APPROACHES

All procedures described in this section were carried out with the expertise and supervision of collaborators Professor Paul O'Neill and Drs Neil Berry and Chandrakala Pidathala from the Chemistry Department at the University of Liverpool (UK). Synthesis reactions were performed with Dr Chandrakala Pidathala, who subsequently confirmed successful formation of reaction products from the analyses of concluded reactions by 1D ^{1}H NMR spectroscopy and small molecule mass spectrometry. The Appendices section contains information on product-derived peaks from 1D ^{1}H NMR spectroscopy, and an additional mass spectrometry spectra for the final reaction of compound 9 *(R)*-enantiomer synthesis.

2.5.1 Selection of compounds via computational chemistry

Compounds similar to ethosuximide were selected with computational and empirical approaches, although the procedures described herein applies primarily to the former approach since empirical selection was performed by Professor Paul O'Neill and Dr Neil Berry. Computational identification of similar compounds was performed on ZINC database version 12 (Irwin and Shoichet, 2005), a repository of commercially-available compounds for virtual screening. Similar compounds were identified on the database by applying in-built filters for substructure (Barnard, 1993) and similarity searching (Stumpfe and Bajorath, 2011, Bender and Glen, 2004), with the criteria for similarity search specified at Tanimoto similarity coefficient (Tc) similarities of 70 to 90 %; refer to chapter 3.1.2.1 for further information. Selection of identified compounds from both computational and empirical approaches for screening was facilitated computationally with the Accelrys Pipeline Pilot^{TM} software version 9.0 (Accelrys Software Inc., California, USA) via the multiobjective/multiparameter optimisation (MOO/MPO; (Ekins *et al*., 2010) "pareto sort" function which ranks the compounds based on the following parameters: 1) predicted CNS permeability from computed CNS MPO scores (Wager *et al*., 2010b), 2) structural similarity to ethosuximide, and 3) predicted *C. elegans* bioaccumulation propensity from the worm SAM (Burns *et al*., 2010). Physicochemical information required to compute CNS MPO scores were derived from ChemDraw Professional version 15.0 (PerkinElmer

Informatics, Coventry, UK) and ACD/I-lab (National Chemical Database Service, UK). As a similarity reference, the structure of ethosuximide was included in the analysis via the software's "Similarity Filter" component as a MOL file (.mol), which was generated from ChemDraw Professional version 15.0 (PerkinElmer Informatics). Chemical structures of compounds selected for screening as represented herein were drawn using the Marvin JS chemical editor from ChemAxon (Budapest, Hungary).

2.5.2 Synthesis of an N-methylated ethosuximide derivative for primary screening

The N-methylated form of ethosuximide (2,5-Pyrrolidinedione,3-ethyl-1,3-dimethyl) was generated from a single step reaction with the methylating agent iodomethane in anhydrous conditions as adapted from a previously reported procedure (Khan *et al*., 2001). The reaction was initially left to react at room temperature for 3 nights with the listed reagents (Figure 2.7), and continued for an additional night with half the original amount of iodomethane (6.8 mM). Analytical thin layer chromatography (TLC) performed on a silica gel-coated aluminium plate (Figure 2.8) was used to verify successful generation of the N-methylated product. The reaction mixture was then subjected to filtration and reduced pressure to remove K_2CO_3 and acetone respectively. The product was purified by silica gel column chromatography at hexane/ethyl acetate = 4/1 (Figure 2.9), and confirmed for its identity after solvent removal from combined appropriate fractions (Appendix 1).

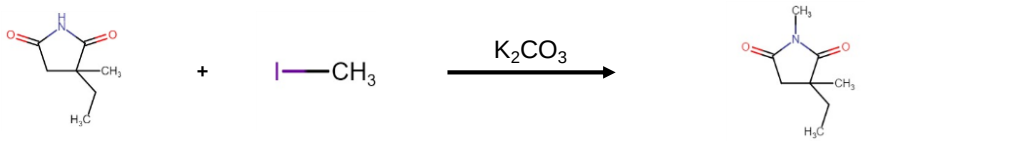

Chemical	Purpose of chemical	mmol	g	Volume (ml)
Ethosuxmide	Starting compound	3.4	0.489	-
Iodomethane (liquid)	Methylating agent	13.6	1.931	0.846
Anhydrous potassium carbonate	Weak base for deprotonating	5.1	0.704	-
Anhydrous acetone	Solvent	-	-	10

Figure 2.7. Single step synthesis of an N-methylated derivative of ethosuximide. Ethosuximide was N-methylated in the presence of the methylating agent iodomethane and weak base potassium carbonate (K_2CO_3). In the presence of K_2CO_3, the nitrogen atom in ethosuximide was deprotonated, facilitating the transfer of the methyl group ($-CH_3$) from iodomethane to the nitrogen. As nitrogen is an effective hydrogen bond donor, the reaction was performed in anhydrous conditions to prevent nitrogen reprotonation from hydrogen bonding between nitrogen and water. The amounts of chemicals and reagents used for the reaction are indicated in the given table.

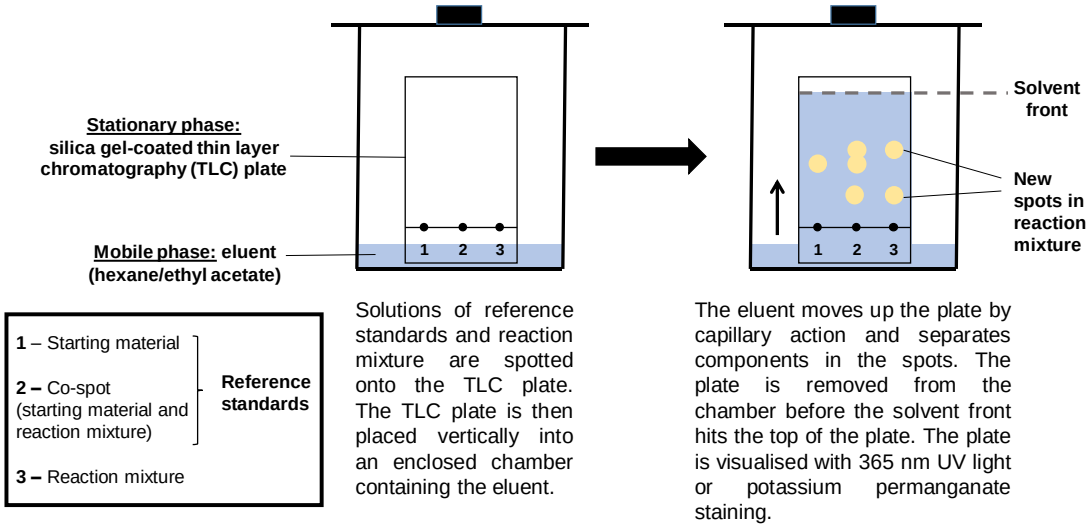

Figure 2.8. Analytical thin layer chromatography (TLC). Polarity of spotted samples and both stationary and mobile phases affect the mobility of samples up the TLC plate, and hence the extent of component separation in samples. Due to the polar silica gel coating on the TLC plate, increased polarity of samples results in stronger interaction with this stationary phase and reduced mobility up the plate. Therefore, the polarity of the eluent was increased to simultaneously weaken this interaction and strengthen that with the eluent to allow for better separation of components. This was performed by decreasing the ratio of non-polar hexane to polar ethyl acetate.

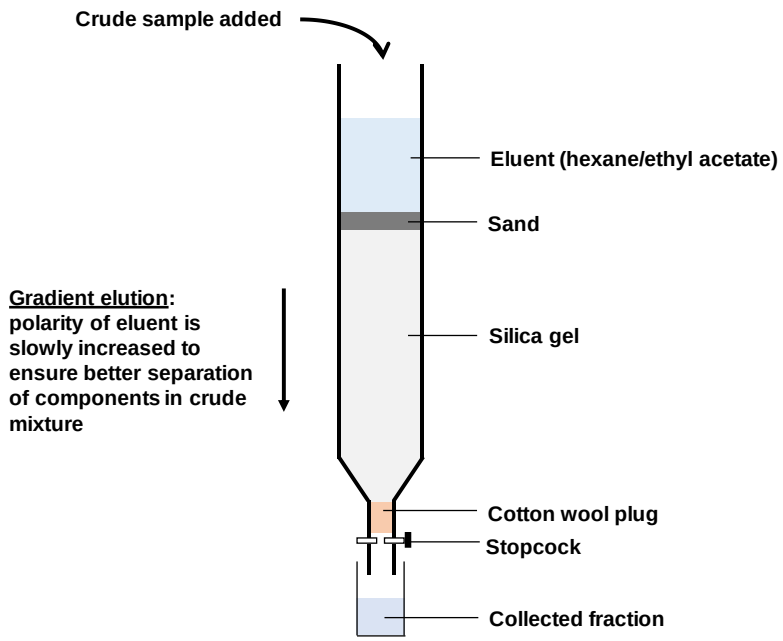

Figure 2.9. Silica gel column chromatography for the purification of crude mixtures. The silica gel was packed into the column with hexane after a cotton wool plug was inserted at the bottom to prevent the gel from washing out, followed by addition of sand at the top of the packed gel to maintain surface tension. The column was flushed with hexane after the crude mixture was applied, and a gradient elution performed with hexane/ethyl acetate to collect fractions of eluate.

2.5.3 Synthesizing (R)-enantiomer of compound 9

Three sequential reactions were performed to synthesize the (*R)*-enantiomer (Figure 2.10 and Table 2.11). Chemical procedures for the first two and third reactions were adapted from Shintani *et al* (2006) and Carniato *et al* (2009) respectively. In the first reaction, the synthesis of the substrate for isomeric generation, 1-benzyl-3-methylmaleimide, was carried out at 125°C for 2 hours in acetic acid. Following removal of the acid and verification of product formation, the product was separated with silica gel column chromatography at hexane/ethyl acetate = 9/1 and purified.

Reaction 2 involved isomer generation from 1-benzyl-3-methylmaleimide. The chiral ligand (*R*)-binap and chiral rhodium catalyst $RhCl(C_2H_4)_2]_2$ were stirred in 1,4-dioxane at room temperature for 15 mins, followed by addition of $PhB(OH)_2$ and KOH and further stirring for 3 mins at room temperature. 1-benzyl-3-methylmaleimide and additional 1,4-dioxane of the same volume were added, and the reaction was continued at 50°C overnight. The reaction mixture was filtered through a silica gel pad to remove the rhodium catalyst. (*R*)-1-benzyl-3-methyl 3-phenylsuccinimide and *trans*-1-benzyl-3-methyl-4-phenylsuccinimide were reported to elute closely to each other (Shintani *et al*., 2006) and were separated with gradient silica gel column chromatography at hexane/ethyl acetate = 9/1, followed by purification. 1D ^{1}H NMR peaks from reaction 1 and 2 products are shown in Appendix 2.

The last reaction involved debenzylation of the co-eluting products with $AlCl_3$ to increase the polarities and improve separation of the desired product (*R*)-1-benzyl-3-methyl 3-phenylsuccinimide from the other isomer. This final reaction was performed on a small scale with only 50 mg of the starting material to assess the feasibility of the procedure for debenzylation. The reaction was carried out at 120°C overnight and subsequent analytical TLC (hexane/ethyl acetate = 9/1) to assess the success of debenzylation via the presence of new spots which may be product-derived. A lower eluting spot was present which was likely from debenzylated products due to an increase in polarity and a consequently slower elution rate. The reaction was confirmed to be successful, although it did not go into completion as traces of starting benzylated materials

were detectable by 1D ^{1}H NMR spectroscopy and small molecule mass spectometry (Appendices 3 and 4). The reaction was not continued to completion, neither were debenzylated products separated as the amount of product recovered from the scale of the reaction would be insignificant. In addition, the reaction was not repeated on a larger scale due to the departure of Dr Chandrakala Pidathala.

2.5.4 Prediction of 1D ^{1}H NMR spectra

1D ^{1}H NMR spectra for compound 9 and its hydroxylated metabolite α-(*p*-hydroxyphenyl)-α-methylsuccinimide were predicted on ACD/I-lab (National Chemical Database Service) at a resonance frequency of 600 MHz. Molecular structures of both compounds were uploaded as MOL files, which were generated from ChemDraw Professional version 15.0 (PerkinElmer Informatics).Spectra were predicted from the “H NMR Predictor” with the resonance frequency specified as 600 MHz, and extracted from the database as a JCAMP file (.jdx) before being imported onto TopSpin^{TM} version 3.5pl6 (Bruker BioSpin Gmbh, Germany) for further spectral processing to be as presented herein in Appendix 7.

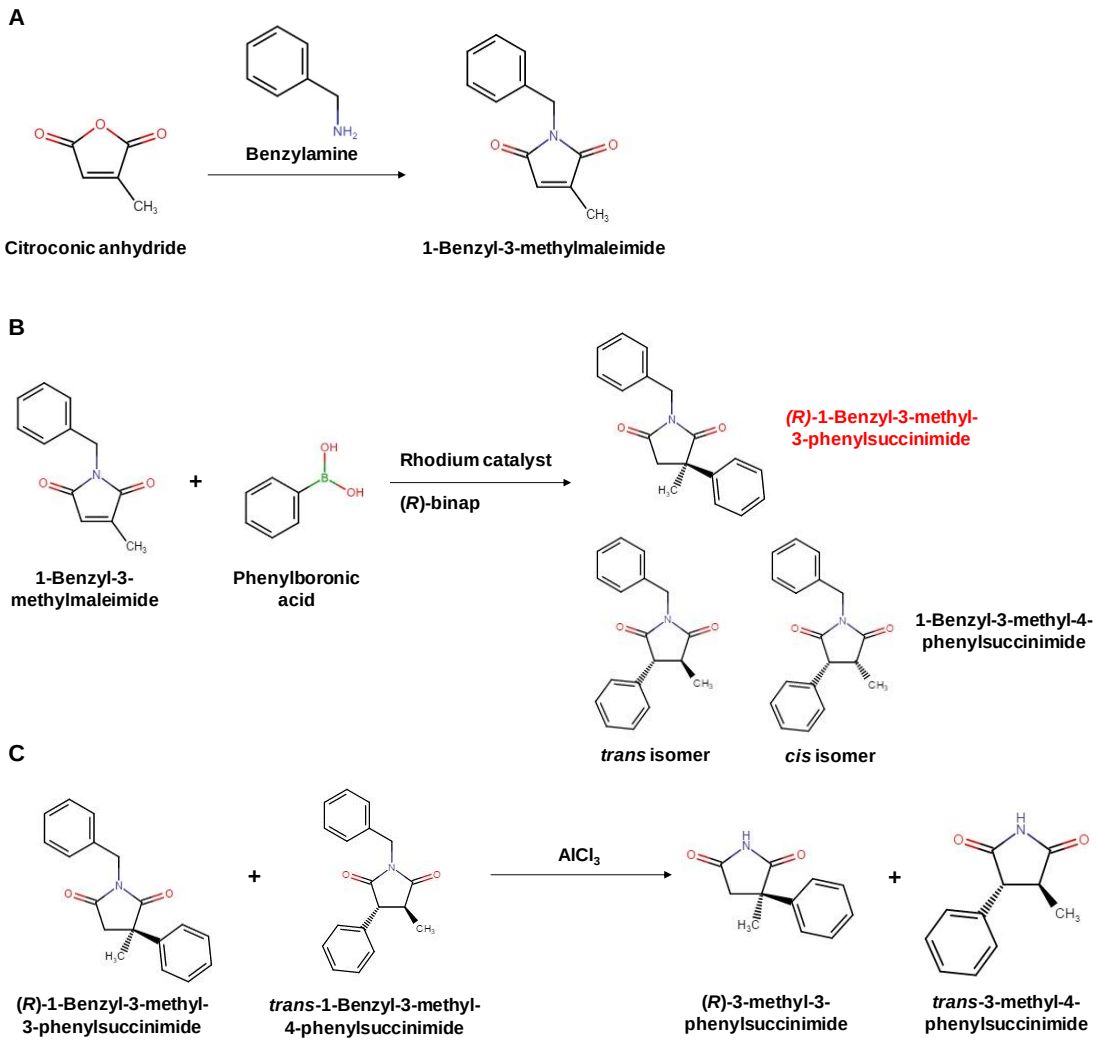

Figure 2.10. *(R)*-compound 9 synthesis. (A) Reaction 1, synthesis of starting substrate 1-benzyl-3-methylmaleimide. (B) Reaction 2, synthesis of isomers. Regioselective transfer of phenyl from phenylboronic acid onto the 1-benzyl-3-methylmaleimide was catalysed by the chiral rhodium catalyst and (*R*)-binap ligand, forming minor products *trans*/cis-1-benzyl-3-methyl-4-phenylsuccinimide and major product (*R*)-1-benzyl-3-methyl-3-phenylsuccinimide (compound 9). (C) Reaction 3, debenzylation of isomers with $AlCl_3$. The *cis* isomer is not shown as it does not elute closely with the others.

Reaction	Chemical	Purpose	mmol	g	Volume (ml)
1	Citroconic anhydride	Starting material	10	1.12	-
	Benzylamine	Donates benzyl group	10	-	1.09
	Acetic acid	Solvent	-	-	15
2	1-Benzyl-3-methylmaleimide	Starting material; product from reaction 1	1	201	-
	Rhodium catalyst	Chiral catalyst	0.0255	5	-
	(*R*) – binap	Chiral ligand	0.0275	17.5	-
	1,4-Dioxane	Solvent	-	-	2.5
	Phenylboronic acid	Phenyl group donor	3	366	-
	Potassium hydroxide	Base	0.5	-	0.5
3	(*R*)-1-benzyl-3-methyl 3-phenylsuccinimide; *trans*-1-benzyl-3-methyl-4-phenylsuccinimide	Starting materials; co-eluting products from reaction 2	0.18	50	-
	Aluminium chloride	Debenzylating agent	0.9	110	-
	Toluene	Solvent	-	-	5

Table 2.11. Chemicals for *(R)*-compound 9 synthesis. Reaction 2 for the stereoselective synthesis of isomers was conducted on a 1 mmol scale, and under oxygen-free and anhydrous conditions to prevent/reduce loss of catalytic activity from the rhodium catalyst due to oxidation.

2.6 METABOLITE ANALYSIS OF TREATED *C. ELEGANS* WITH 1D ^{1}H NMR SPECTROSCOPY

Procedures were performed with advice from Dr Marie Phelan (Technology Directorate, University of Liverpool, UK).

2.6.1 General procedure for metabolite extraction from whole *C. elegans* samples and analysis with 1D ^{1}H NMR spectroscopy

Metabolites were extracted from thawed *C. elegans* samples in 50 % (v/v) water and ice-cold acetonitrile (AcN) via sonication with the MSE Soniprep 150 Plus sonicator/cell disruptor (Wolf Laboratories Ltd, York, UK) with conditions adapted as previously described (Beckonert *et al*., 2007); AcN disrupts membranes, acts as a solubilising agent for water-soluble metabolites, and aggregates and precipitates proteins in the samples. Extraction was performed on samples kept in an ice bath to prevent overheating, for three 30 s durations at 30 s intervals and 10 % amplitude. Samples were then vortexed for 30 s and centrifuged at 21,000 g for 5 mins at 4°C to pellet cell debris and insoluble components. Metabolite-containing supernatants were snap frozen in liquid nitrogen for 2 minutes, lyophilised to completion with a Heto PowerDry LL1500 freeze dryer (ThermoFisher Scientific Inc), and stored long-term at -80°C.

After extraction and immediately prior to analysis by NMR spectroscopy, NMR buffer prepared in deuterated water (Goss Scientific Instruments, Cheshire, UK) was added to thawed solutions and lyophilised extracts (Table 2.12). All components of the buffer were added after metabolite extraction, whereas the reference compound sodium trimethylsilyl-$^{2}H_{4}$-propionate (TSP) was added prior to it to account for extraction-induced sample losses unless specified otherwise. Following the addition of NMR buffer, solutions were vortexed for 1 min, and centrifuged at 12,000 g for 2 mins at 20 to 25°C to pellet any remaining cell debris or insoluble components. 200 µL resuspensions of lyophilised extracts and 600 µL of fluids were then transferred to clean 3- and 5- mm outer diameter NMR SampleJet tubes (Bruker BioSpin Gmbh) respectively.

Components	%	Final concentration (mM)
<u>Sample</u> **1. Lyophilised extracted metabolites (resuspended in deuterated H_2O)** ***OR*** **2. Solution (in protonated H_2O)**	**89.8**	**-**
1 M sodium phosphate pH 7.4	10	100
100 mM sodium trimethylsilyl-$^2H_4$-propionate (TSP)	0.1	0.1
1.2 mM sodium azide	0.1	0.0012

Table 2.12. Components of NMR samples prepared prior to spectral acquisition. The NMR buffer constitutes the sodium phosphate buffer, the reference compound TSP, and sodium azide to prevent sample contamination. Constituents were prepared in deuterated water to reduce interfering signals from protonated water in 1D ^1H NMR spectroscopy. Note that TSP is added prior to extraction to account for extraction-induced sample losses. The highlighted section of the table displays the sample type, which is either extracted metabolites or solutions.

Samples were analysed by 1D ^{1}H NMR spectroscopy with the Bruker Avance III NMR spectrometer equipped with the 5 mm TCI CryoProbe with a proton resonance frequency of 600 MHz (Bruker BioSpin Gmbh). 1D ^{1}H spectra were acquired at 25ºC on TopSpin™ version 3.5pl6 (Bruker BioSpin Gmbh), with the manufacturer-provided nuclear Overhauser enhancement spectroscopy (NOESY) pulse sequence (noegpr1d) which provides suppression of the water signal and gives an overview of all types of molecules present in the sample. In addition, the manufacturer-provided Carr-Purcell-Meiboom-Gill (CPMG) pulse sequence (cpmgpr1d) which again provides suppression of the water signal, and enhances small molecule metabolite signals by removing any contribution from larger molecules over 5 kDa such as proteins and carbohydrates. NOESY and CPMG experiments were used to analyse solutions and extracted metabolites from samples respectively. Initial processing of acquired spectra was performed automatically on TopSpin™, such as baseline correction and phasing, prior to splitting up the spectra into buckets using AMIX™ software version 3.9.14 (Bruker BioSpin Gmbh); note that processing procedures vary depending on the purpose of analysis and should be referred to in the respective subsections for more detail. In general, however, the intensities of specific peaks such as the TSP signal (0.1 to -0.1 ppm) or treatment-derived peaks were derived by specifying the spectral region of interest on AMIX™. On the other hand, the entire ^{1}H resonance region between 10 to 0.10 ppm can be processed either by integrating the total spectral intensity, or by division into uniform buckets with widths of 0.005 ppm followed by subsequent integration of each bucket. The protonated water-occupied region at 4.8 to 4.6 ppm is excluded from analysis. Figure 2.13 provides a simple schematic for spectral bucketing and integration of peak intensities on AMIX™. Unless otherwise specified, integrated signal intensities were scaled manually to the TSP signal to account for extraction-induced sample losses.

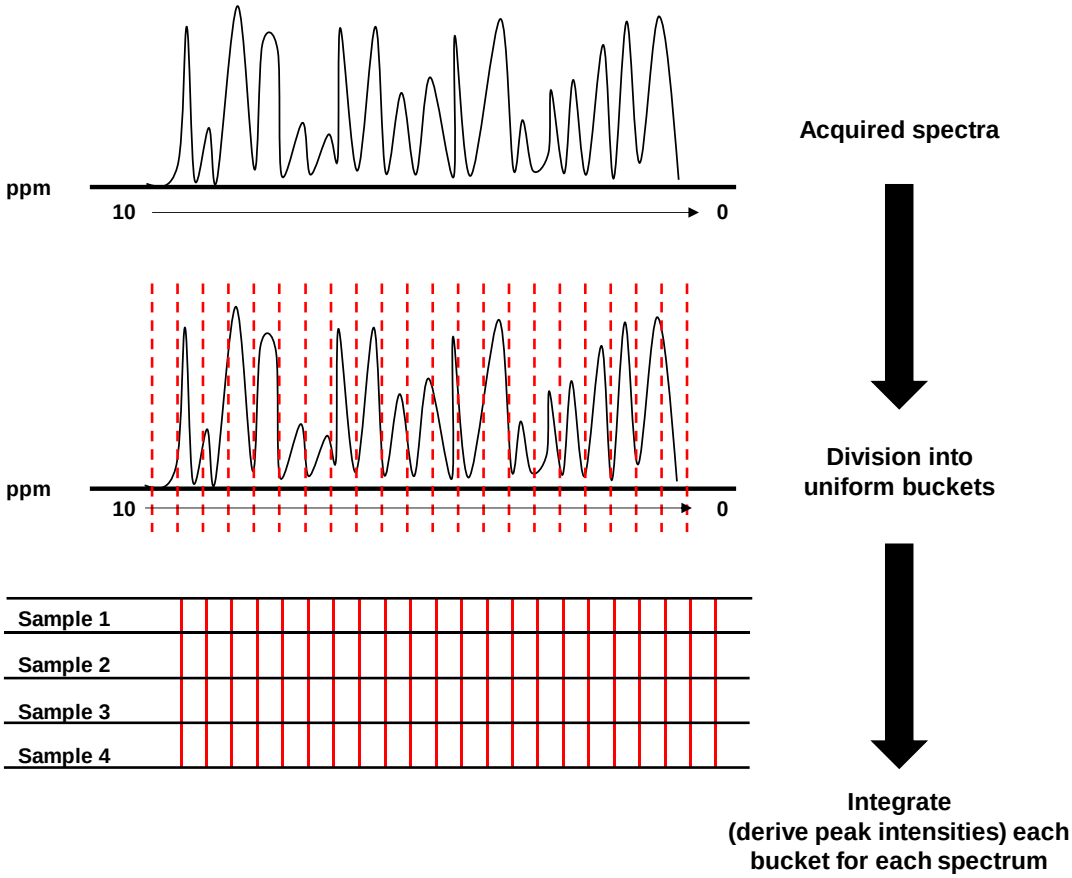

Figure 2.13. Processing of acquired 1D ^{1}H NMR spectra by division and integration of uniform buckets. This excludes the protonated water region at 4.8 to 4.6 ppm. Integrated buckets are scaled to the signal from the reference molecule TSP from the corresponding spectrum.

2.6.2 Optimisation of extraction procedures

2.6.2.1 Comparison of extraction methods

Sonication and bead-beating were the available resources for metabolite extraction in the current study. Although various extraction methods were previously compared for their extraction efficiencies of *C. elegans* samples (Geier *et al*., 2011), no comparisons were made between sonication and bead-beating, hence this was addressed in the current study to select an extraction method. Both procedures were evaluated on day 1 CK426 samples of similar estimated sizes. Sonication was performed as outlined in the previous section. Bead-beating was performed by shaking samples at 2000 rpm for 2 mins with 425 to 600 µm acid-washed glass beads in 2 mL round bottom cryogenic vials (Corning Inc, Wiesbaden, Germany) on a Mikro-Dismembrator S (B. Braun Biotech Gmbh, Berlin, Germany). Following this, three holes were generated at the bases of the vials, and centrifugation was performed at 5000 rpm for 5 mins at 4°C in 15 mL centrifuge tubes (Grenier Bio-one Ltd, Stonehouse, UK) to remove the resultant lysate into the tubes. Pelleting of cell debris and insoluble cell components, followed by lyophilisation of supernatant were then carried out as described in the previous section. TSP was added to lyophilised samples after extraction so that it does not reflect extraction-induced losses. This trial was performed to compare extracted yields based on a known concentration of the reference molecule. As described before, levels of extracted metabolites were compared from TSP-scaled total spectral intensities (see section 2.6.1).

2.6.2.2 Assessing suitability of AcN as an extraction medium for hydrophobic compounds

AcN was recommended for the extraction of water-soluble metabolites (Beckonert *et al*., 2007), hence it might be inefficient for extracting hydrophobic compound 9 from treated *C. elegans* samples. To address this, the suitability of AcN as an extraction medium for the compound was investigated as outlined in Figure 2.14.

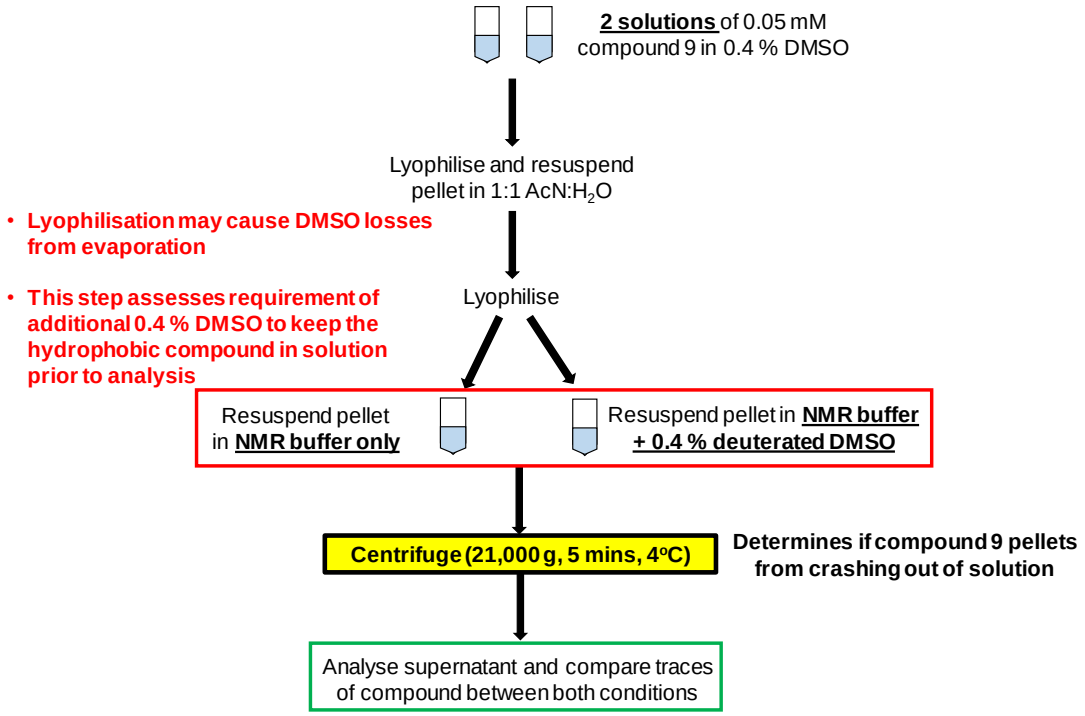

Figure 2.14. Procedure for investigating the suitability of AcN as an extraction medium for the hydrophobic compound 9. Note that the concentration of the compound prepared for this purpose corresponds with the chronic treatment concentration administered to CK426 ALS worms in this study. The centrifugation step (highlighted in yellow) is important for determining if the compound stays in solution for subsequent analysis. Signal intensities of the strongest compound-derived TSP-scaled peak at 1.758 to 1.746 ppm (see section 2.6.3.1) were compared between conditions.

2.6.2.3 Assessing extent of sample loss from sonication

Day 1 CK426 samples of similar estimated sample sizes were prepared (Figure 2.16) and TSP was added at the required concentration (Table 2.12) before or after sonication. Following procedures as previously outlined for metabolite extraction with sonication, the various constituents of NMR buffer were added to lyophilised extracts with or without TSP depending on whether it was added before extraction or not. As described in section 2.6.1 above, total intensities of acquired ^{1}H spectra were derived on AMIX^{TM}. Instead of scaling to the TSP signals, the inverse was performed whereby resultant TSP signals were scaled against total spectral intensities to compare extent of sample losses from sonication, assuming minor changes in overall metabolite content between samples.

2.6.3 Determining internal concentrations of pharmacological treatments in treated *C. elegans* samples

2.6.3.1 Reference spectra for compounds and concentration calibration curves

Compound-derived peaks on 1D ^{1}H NMR spectra were derived by analysing 1 mM solutions of each compound prepared in water. The highest singlet peak for each compound was selected for further analysis as they provide the best signal-to-noise ratio for detection. Chemical shifts of these peaks are as follows: succinimide, 2.820 to 2.787 ppm; ethosuximide, 1.299 to 1.294 ppm; compound 9, 1.758 to 1.746 ppm; refer to chapter 3, Figure 3.2.19 for reference spectra.

2.6.3.2 Preparation of treated *C. elegans* samples

Acutely-treated *unc-49* and chronically-treated CK426 samples were prepared and processed for subsequent 1D ^{1}H NMR analysis as illustrated in Figures 2.15 and 2.16. 2000 *unc-49* and 3000 CK426 L1 larval worms were cultured on plates seeded with 100 µL OP50 and processed at adulthood day 1 approximately 63 and 70 hours post L1-plating; number of worms were estimated by counting from 1 µL of L1 worm suspension. The number of post-plating hours was selected based on knowledge of the duration required for the WT strain to attain life cycle progression from L1 to pre-gravid young adult

stage (Gonzalez-Moragas *et al*., 2015) and observations of the differences in growth rates between both strains, such that maximal OP50 depletion was present by the time of processing without causing visible worm starvation so as to improve efficiency of bacterial removal during washes. This was additionally to prevent or reduce the population of laid eggs, since these may present an additional source of variability when co-processed. Due to the slower growth and OP50 ingestion rate of the CK426 worms, this strain was cultured at a higher density on the same volume of OP50 than *unc-49* worms as they deplete the bacteria at a slower rate. The rationale for increasing the population density rather than decreasing the volume of OP50 was based on the advantage of having a bigger sample size for analysis. It should be noted that conditions for the protocol shown for preparing day 5 CK426 samples were not yet optimised due to time constraints (Figure 2.16).

Treatment conditions were performed to mirror procedures conducted for assaying *unc-49* and CK426 worms in their respective behavioural assays. Although *unc-49* worms were not age-synchronised for the PTZ-induced seizure assays, synchronised worms were used in the current protocol to ease scale-up; day 1 was selected as the age of processing to closely reflect the use of young day 1 to 3 worms in the PTZ-induced seizure assay. As illustrated, liquid-based acute treatment of these worms was performed in Corning® Costar® Spin-X® tube filters (Corning Inc) (Figure 2.15). Due to the hydrophobic nature of compound 9, potential precipitation in tube filters might result in artefact signals in addition to possible adherence to *C. elegans* cuticle (Burns *et al*., 2010). The feasibility of the designed protocol was hence assessed with compound 9 as illustrated in Figure 2.15b.

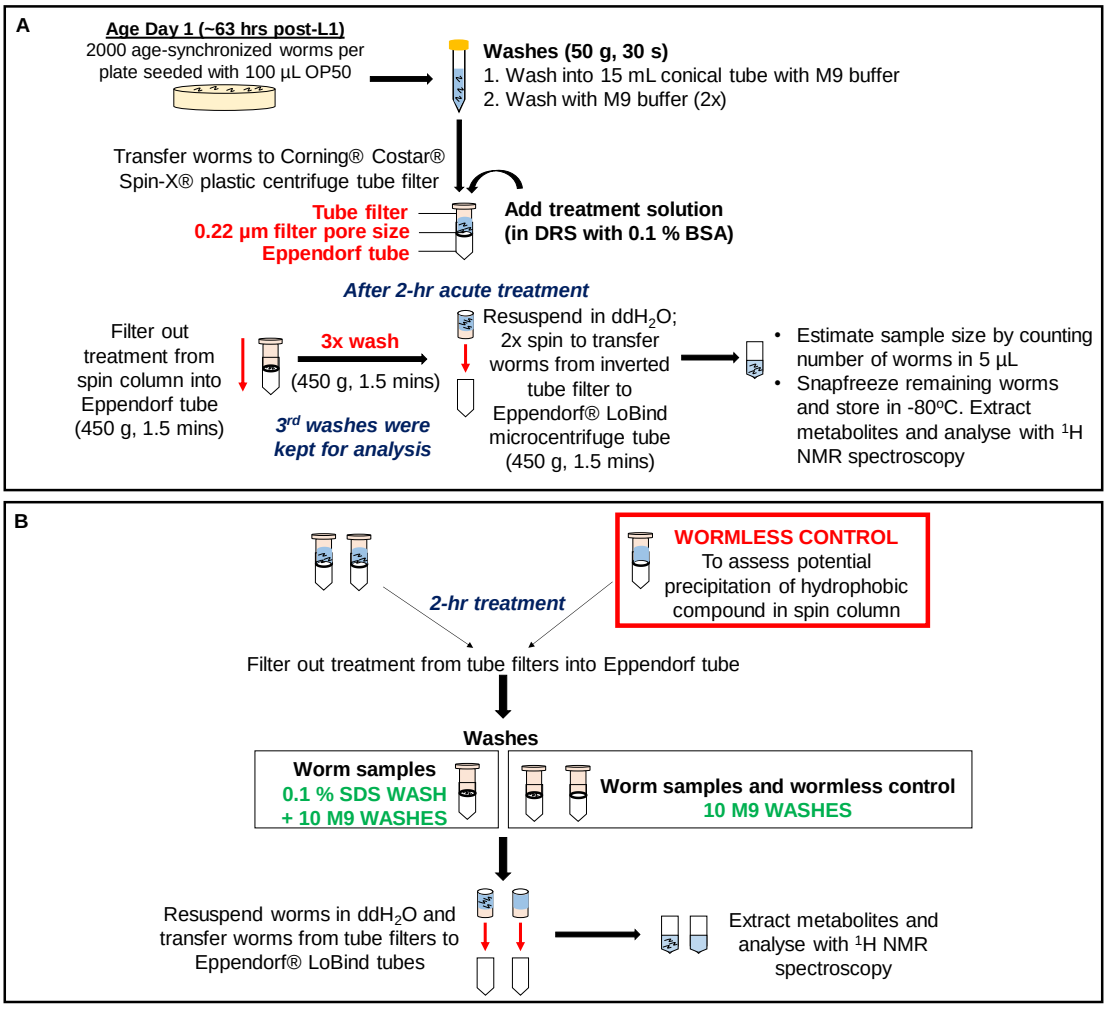

Figure 2.15. Preparation of acutely-treated day 1 *unc-49* worms for 1D ^{1}H NMR spectroscopy. (A) Protocol for sample processing in Corning® Costar® Spin-X® tube filters. Processed worms were kept in Eppendorf® LoBind microcentrifuge tubes to prevent adherence to tube walls to obtain a uniform worm suspension for estimating sample sizes. DRS, Dent's Ringer solution; BSA, Bovine serum albumin. (B) Protocol was tested with compound 9 to address potential precipitation of hydrophobic compounds in tube filters and adherence to *C. elegans* cuticles, and to determine wash conditions to reduce the impact of these undesirable effects.

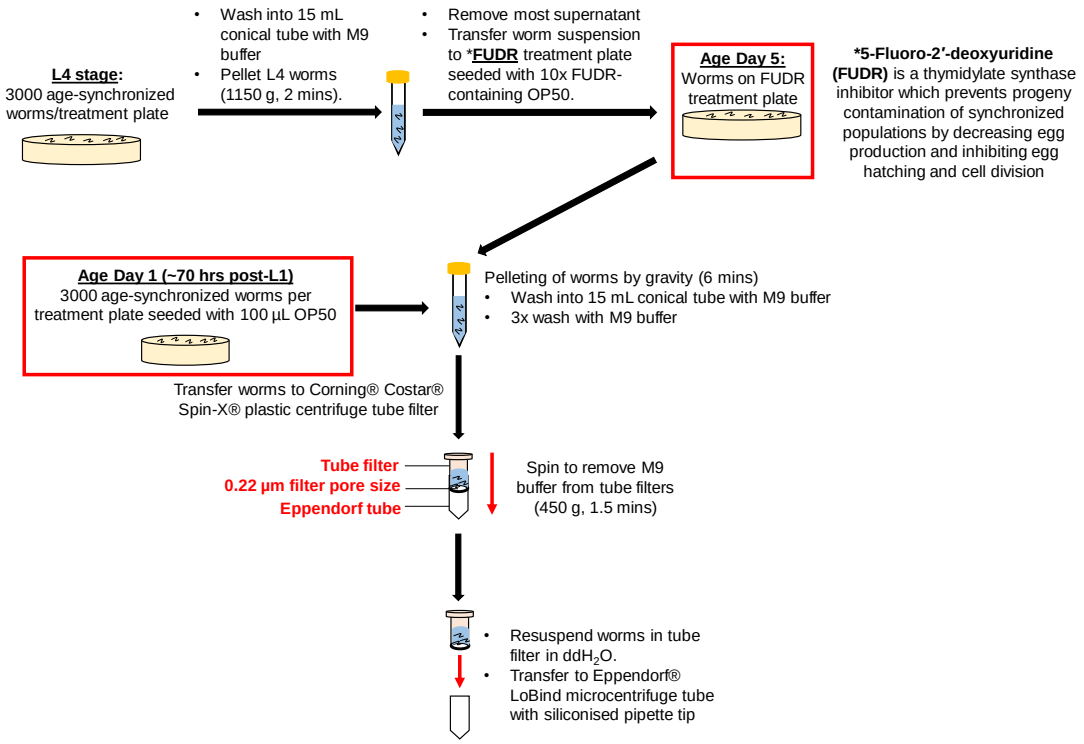

Figure 2.16. Protocol for preparing chronically-treated CK426 amyotrophic lateral sclerosis worms at adult ages days 1 and 5. Chronic exposure to treatment was initiated from the L1 larval stage. Note that siliconized pipette tips were used to reduce sample losses from worms adhering to internal pipette tip walls.

2.6.3.3 Determining bioaccumulated concentrations of treatments in *C. elegans*

The procedure for measuring the internal concentration of each treatment compound in day 1 CK426 *C. elegans* is outlined in Figure 2.17, and requires standard curves for deriving total bioaccumulated concentrations and sample sizes per analysed batch of worms. Note that the ballpark volume of 4 nL for a day 1 adult worm was estimated from the published growth curve for the WT N2 strain at approximately 85 hours post-hatch (Hirose *et al*., 2003), based on the sum of approximate 15 hours for development to L1-arrest after hatching at 20°C (Gonzalez-Moragas *et al*., 2015) and sample processing at 70 hours post L1-arrest (section 2.6.3.2). Concentration standard curves were derived from a range of concentrations of each compound (0.001 to 1 mM) by linear fits of data plotted from spectral intensities of the highest TSP-scaled compound-derived singlet peaks against the corresponding concentrations from which they were derived; water-soluble succinimide and ethosuximide were prepared in water alone whereas the hydrophobic compound 9 was prepared in a final concentration of 0.4 % deuterated DMSO.

Reference samples for generating the sample size standard curve were obtained by preparing various ratios of known number of worms to 1X Tris-Glycine SDS sample buffer (diluted in water from the 2X supplied reagent; ThermoFisher Scientific Inc), and were resolved and stained with InstantBlue^{TM} coomassie stain (Expedeon Ltd) on the same NuPAGE^{TM} Bis-Tris 4-12 % protein gel (Bio-Rad Laboratories Ltd) alongside samples to preserve staining consistency for accurate interpolation of sample sizes (refer to section 2.4.1 for SDS-PAGE and coomassie staining procedures); curve was plotted as a function of staining intensity against various dilutions of number of worms in 1X SDS buffer.

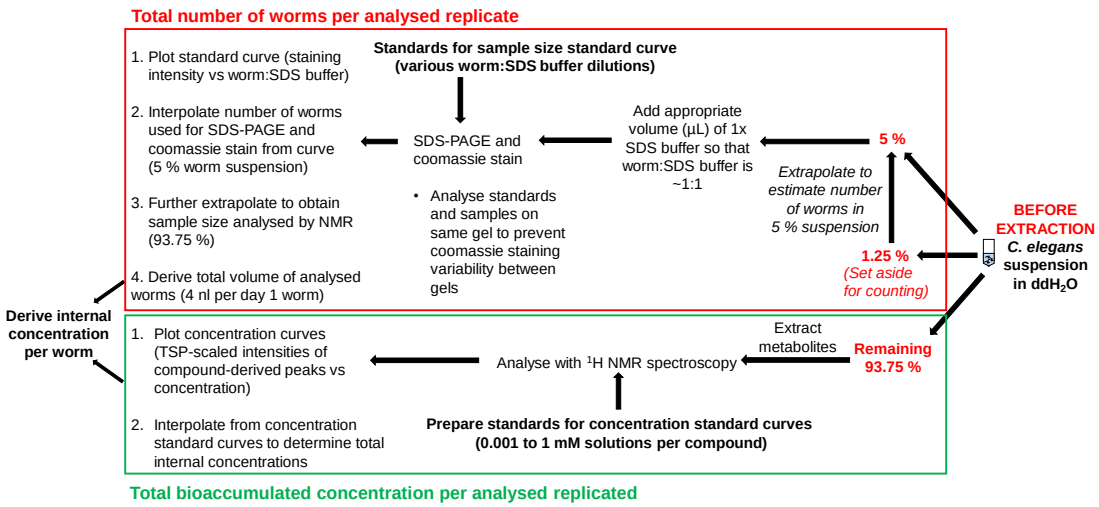

Figure 2.17. Workflow for determining bioaccumulated concentration of compound in day 1 CK426 *C. elegans* after treatment.

2.6.3.4 Metabolome comparison between treatments

^{1}H spectra acquired from chronically-treated day 1 CK426 samples were processed using TopSpin™ and AMIX™ by division into 2000 uniform buckets or integrals and scaled to TSP signals as described in section 2.6.1. Additionally, to account for signal intensity differences as a result of variable sample sizes, the TSP-scaled buckets were further scaled to the largest population size from all analysed samples; see Figure 2.13 for bucket division and integration on AMIX™ and Figure 2.17 for sample size determination.

The processed data was then exported for analysis on MetaboAnalyst v3.0 (Xia and Wishart, 2002) in a comma-separated values format. Following mean-centering and Pareto scaling of the data, statistical analyses were carried out with uni- and multi-variate analyses of one-way ANOVA with *post-hoc* Tukey's test and principal component analysis (PCA) respectively.

2.7 STATISTICAL ANALYSIS

All general statistical analyses were performed on GraphPad Prism version 6 (GraphPad Software Inc.,California, USA), except analyses and comparison of lifespan which were carried out with the log-rank test on the Online Application for the Survival Analysis of Lifespan Assays 2 (OASIS 2; Han *et al*., 2016). Concentration-response curves were fitted with GraphPad Prism 6 via nonlinear regression with the variable slope model, followed by subsequent derivation and statistical comparison of $LogEC_{50}$ values. Data is presented as mean values, with standard error of mean when appropriate. Statistical analysis for metabolome comparisons from NMR is described in the preceding section.

CHAPTER 3

IDENTIFICATION AND SELECTION OF COMPOUND 9 AS A CANDIDATE SCAFFOLD

3.1 INTRODUCTION

3.1.1 SAR of succinimide derivatives

The neuroprotective effect of ethosuximide in several neurodegeneration models (Chen *et al*., 2015b, Tauffenberger *et al*., 2013, Tiwari *et al*., 2015) highlights potential for the AED to be repurposed for neurodegeneration treatment, however this is yet to be clinically explored. High concentrations of the drug reported to exert neuroprotection in models suggest probable low clinical neuroprotective efficacy and/or potency which may make repurposing an unideal strategy. Additionally, this might also impede insights into its poorly understood MMOA and consequent understanding of the pathogenic processes which underlie neurodegeneration as identification of molecular binding targets through affinity approaches may prove to be difficult. To circumvent such potential issues surrounding ethosuximide, the drug may be utilised as a scaffold to derive structurally-similar compounds with enhanced potencies. This may not only improve the prospect of deriving new therapies, but also in the identification of potential disease-modifying targets in neurodegenerative diseases. In addition, SAR knowledge of the succinimide backbone is mandatory for pinpointing appropriate molecular modifications to either derivatise these structurally-similar compounds for target identification studies, or to further enhance the potencies. Pre-existing SAR studies were mostly performed in gold standard rodent models of electrically- (MES test) and/or chemically-induced (scMET/scPTZ) test seizures, which are generally deemed to predict for protection against generalized tonic-clonic and absence seizures respectively; ethosuximide is only effective in the scPTZ test (Löscher, 2011). However, some of these SAR findings may not be generally applicable for succinimide-based compounds due to the large structural diversity of the derivatives evaluated (Klunk *et al*., 1982b, Klunk *et al*., 1982a, Klunk *et al*., 1982c, Poupaert *et al*., 1984, Kaminski and Obniska, 2008, Obniska *et al*., 2009, Obniska *et al*., 2010, Obniska *et al*., 2012, Rybka *et al*., 2014, Kaminski *et al*., 2013); Figure 3.1.1 summarises these studies. For the purposes of utilising ethosuximide as a scaffold for development, single changes to the succinimide backbone may be preferable to best delineate the SAR.

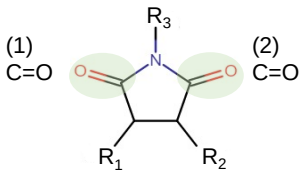

References	General SAR findings	Tests/assays used to evaluate activity
Poupaert *et al*., 1984	Intact -NH and C=O groups are important for preserving anticonvulsive potency • Methyl R_3 decreases potency (N-methylation) • Substitution of one C=O group further decreased potency	Rodent MES test
Klunk *et al*., 1982a Klunk *et al*., 1982b Klunk *et al*., 1982c **NOTE: Observations based from derivatives which exhibited either convulsive or anticonvulsive activity; conclusions given pertain to structural features important for bioactivity in general**	1) Presence of **both R_1 AND R_2 substituents** switches activity from anticonvulsant to convulsant 2) Intact –NH (no R_3 substituent or complete substitution of N) is important for preserving convulsive potency 3) Convulsive potency is affected by chemical nature of R_1/R_2 substituent • Hydrophobic substituent increases potency • Hydrophilic substituent decreases potency	• Convulsive behaviours in mice (initial myoclonic twitch and generalized clonic seizures) • EEG-detectable epileptiform discharges in guinea pigs • Electrical activity of incubated guinea pig hippocampal slices • Seizures induced by PTZ, MES, and other known convulsants (bicuculline, picrotoxin) in mice and guinea pigs *Anticonvulsant activities were additionally tested against seizures induced by proconvulsant compounds which were investigated in the studies
Kamiński and Obniska.,2008 Obniska *et al*., 2009 Obniska *et al*., 2010 Obniska *et al*., 2012 Kamiński *et al*., 2013 Rybka *et al*., 2014 **NOTE: SAR findings should be interpreted with caution due to the diverse structural modifications of molecules assessed in this series of studies**	Compounds studied in this series of studies contain diverse $R_1/R_2/R_3$substituents, and direct comparison and inference of the SAR are difficult. **Structural requirements at R_1/R_2 seem to depend on the type of N-substituent at R_3. However, the following SAR rules may generally apply:** 1) Intact –NH was not essential for activity • All assessed compounds have diverse R_3 N-substituents of the piperazine, phenylpiperazine, benzylpiperidine, and morpholine moieties (structures shown below), which in addition contain different substituents themselves. However, these N-substituent compounds were generally active in the MES test. 2) At least one aromatic substituent at R_1/R_2 is required for activity, whereas alkyl substituents render compound inactive **N-substituents of succinimide derivatives assessed in studies**  **Morpholine** 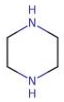 **Piperazine** 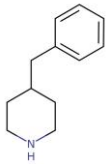 **4-benzylpiperidine** 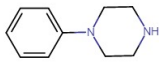 **Phenylpiperazine**	Rodent MES and scPTZ tests • Compounds were primarily evaluated in the MES test • In general, when activities were assessed in both tests, most compounds with anti-MES activity exhibited no anti-PTZ activity

Figure 3.1.1. Summary of pre-existing anticonvulsive SAR studies of succinimide derivatives.

3.1.2 *In silico* approaches for optimizing compound selection

3.1.2.1 Identifying similar compounds

Molecules similar to a compound may be screened to facilitate SAR knowledge of the compound. Various *in silico* approaches exist to facilitate identification and/or virtual screening of similar molecules based on a query compound. One of the earliest approaches is substructure searching, which specifies the query compound as a substructure and identifies all molecules containing this structural feature (Barnard, 1993). Substructure searching can be performed by comparisons of compounds represented structurally in a 2D SMILES format, which essentially depicts the atoms and bonds via linear strings of ASCII (American Standard Code for Information Interchange) characters (Weininger, 1988). Such molecular representations of compounds are called descriptors. Similarity searching is another widely used and newer approach, and a particular component of it has evolved from substructure searching through the utilisation of substructure-based bit string-type descriptors called molecular fingerprints (Stumpfe and Bajorath, 2011, Bender and Glen, 2004). A general outline of the principle of similarity searching is given in Figure 3.1.2 below.

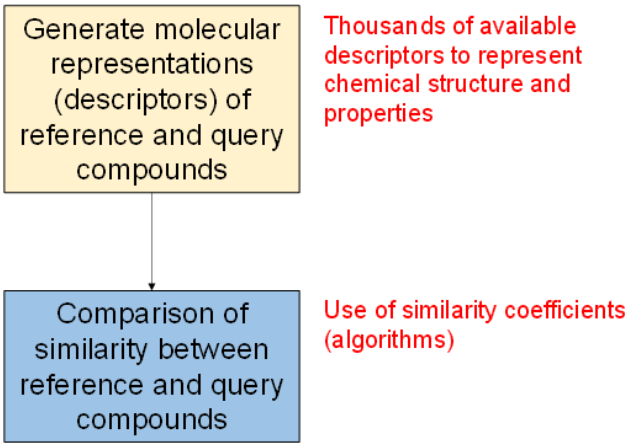

Figure 3.1.2. Outline of similarity searching.

These substructure-based fingerprints typically represent substructural features in a binary format by assigning a specific position to each feature in a bit string and indicating their presence or absence in a compound with 1 or 0 respectively (Stumpfe and Bajorath, 2011, Bender and Glen, 2004). Comparison and measurement of similarity between query and database compounds via these bit string fingerprints are popularly performed in a pairwise manner by applying the Tanimoto similarity coefficient (Tc) (Holliday *et al*., 2002), of which the formula is shown below.

$$\text{Tc} = \frac{C}{(A+B)-C}$$

Where *A* and *B* refer to the sum of '1' bits in compounds 1 and 2, and *C* the sum of '1' bits in both compounds. Similarity between two compounds increases from a Tc value of 0 to 1, and a Tc value of at least 0.7 is generally considered to represent high similarity.

Both substructure and similar search approaches are based on the Similarity Property Principle which associates molecular similarity with similar bioactivity (Klopmand, 1992), and are particularly useful ligand-centric approaches when little or no information is known about the target(s) of a molecule.

3.1.2.2 Multiobjective/Multiparameter optimisation (MOO/MPO)

Bioactivity is not the sole prerequisite for successful drug discovery, and other parameters affecting the attributes and safety of a compound should be simultaneously considered, such as the physicochemical properties. Such parallel consideration of multiple parameters is called MOO or MPO, and it facilitates the selection of the most optimal structures fulfilling the best characteristics for considered parameters for early-stage screens, whereas those deemed unsuitable can be excluded. This improves the efficiency of the drug discovery and development process by enabling only suitable compounds to be synthesized and screened, thus reducing or avoiding late-stage attrition from unfavourable compounds. MOO is performed *in silico*, and an example of a widely-used MOO approach is Pareto optimisation which identifies compounds with the best trade-offs by putting equal weightage on all

specified parameters i.e. all parameters are as important as each other (Ekins *et al*., 2010).

3.1.2.3 Prediction of CNS permeability and druglike attributes

This CNS MPO algorithm predicts the CNS permeability and druglike attributes of compounds from the following six key physicochemical properties commonly considered by medicinal chemists in drug design and CNS penetration: calculated partition (ClogP) and dissociation (ClogD) coefficients, molecular weight, topological polar surface area, number of hydrogen bond donors, and dissociation constant (pK_a) (Wager *et al*., 2010b). Mathematical functions were applied to yield individual desirability transformed scores (T0) based on undesirable to optimal range of values for each parameter for CNS-targeting compounds as defined by medicinal chemistry experts. T0s range from 0 to 1 depending on the optimality for each property. The same weightage or importance was given to each parameter, and the summation of T0s yields the overall CNS MPO desirability score (0 to 6) which increases with CNS permeability and druglikeness. When applied to a set of approved CNS drugs, the majority of them were assigned high scores of ≥4 (74%), showing a good prediction for the survival rate of new compounds. Further validation performed with *in vitro* adsorption, distribution, metabolism, elimination, (ADME) and toxicity assays, including determination of P-glycoprotein liability which affects CNS penetration, showed that high scoring compounds displayed desirable safety and ADME characteristics, and most importantly low CNS drug efflux potential. In conclusion, this algorithm facilitates the selection of optimal compounds to be tested in the drug discovery and development pipeline.

3.1.2.4 Prediction of bioaccumulation in *C. elegans*

An important factor to consider when using *C. elegans* for drug screens is the permeability of compounds across the external cuticle. The cuticle is a weakly-permeable exoskeletal layer which physically hinders drug bioaccumulation in the worm, consequently affecting bioavailability and bioactivity. In this regard, poor bioaccumulation can result in the identification of false negatives from screens. To reduce the chances of this happening, an *in silico* structure-based

accumulation model (SAM) was developed to predict the bioaccumulation propensity of compounds in *C. elegans* (Burns *et al*., 2010). Using compounds previously categorised as accumulating or non-accumulating in *C. elegans* after a 6-hour treatment, the SAM was trained to recognise over- and under-represented structural features in the accumulating subset. Positive and negative scores were assigned to over- and under-represented features and the summation of scores represents the overall accumulation score; simply put, bioaccumulation propensity is predicted to increase with the score. The predictive value of the model was validated by experimentally determining the bioaccumulations of the top- and bottom-scoring 5 % of compounds from a separate test library as these compounds represented the predicted best and worst accumulating compounds in worms. SAM predictions were largely accurate with most positively-scored compounds shown to bioaccumulate and *vice versa*. Although the minority of wrong predictions revealed that complete reliance should not be placed on the model, the exclusion of potential false negatives prior to screening nevertheless reduces cost and time of drug screens in worms.

3.1.3 Chapter aims

The aims of the chapter are to select and screen compounds similar to ethosuximide in a suitable screening platform in *C. elegans*, so as to derive a candidate molecule for further generation of compounds and to understand the SAR of ethosuximide.

3.2 RESULTS

3.2.1 Identification and selection of compounds similar to ethosuximide for primary screening

A dual chemical approach was employed to identify compounds similar to ethosuximide for primary screening in *C. elegans*. Results from these screens will not only potentially identify more potent compounds than ethosuximide, but also improve understanding of the currently limited SAR of ethosuximide to facilitate the identification of its molecular target. The first approach used was to computationally identify compounds similar to both ethosuximide and its inert parent compound succinimide from the ZINC database, an online repository for virtual screening compounds. This was performed based on both substructure search and similarity searching at Tc thresholds of 70 to 90 %; as aforementioned, Tc scores of at least 70 % are generally considered to represent high similarity. Note that both searching methods are used to get a wider coverage of identification as molecules may be identified by one method and not the other (Sheridan and Kearsley, 2002). Figure 3.2.1 illustrates a screenshot of how similar compounds were identified from the database via these approaches. Compounds similar to both ethosuximide and its inert parent compound succinimide were first extracted from the database at 70 to 90 % Tc similarities and substructure. An initial scoping activity was performed to get an idea of the numbers of potentially suitable identified compounds which can be carried forward for screening based on the aqueous solubilities of compounds. Solubility is an important parameter for consideration as it influences ADME and toxicity of the drug. Previously, 98 CNS marketed drugs were experimentally assessed for their aqueous solubilities with the aim of establishing the solubility criteria for guiding CNS drug development (Alelyunas *et al*., 2010). The study demonstrated that more than 85 and 90 % of these CNS drugs have LogS values which were greater than -4 and -5 respectively; solubility (S) values were in mol/L. In contrast, the remaining drugs with LogS<-5 were withdrawn due to associated toxicity, establishing LogS>-5 as the cutoff solubility value for maximizing the chances of deriving CNS drugs with good safety features. In view of this reported LogS threshold, identified compounds were subjected to a solubility filter on the Pipeline Pilot™ software with an intermediate LogS cutoff of at least -4.5. Molecules not

fulfilling this solubility criterion were deemed unsuitable and removed. The resultant analysis yields the number of retained compounds with good predicted aqueous solubilities for CNS molecules (Figure 3.2.1). As ZINC only provides the supplier information of compounds, pricings of compounds had to be manually compiled. This initial scoping activity was helpful in determining if further MOO was required to optimise compound selection, so that purchasing information need only be extracted for the best compounds if the numbers of retained compounds range in the hundreds to thousands. From this analysis, the numbers of compounds with desirable solubilities at the various levels of similarity were reported to be between 1 to 2478 for succinimide-similar compounds, and 36 to 4433 for ethosuximide-similar ones (Figure 3.2.1).

Due to the large numbers of suitable compounds with ideal solubilities, initial MOO was performed via the Pareto Sort function on Pipeline Pilot™ (Figure 3.2.2A). Since succinimide and ethosuximide are themselves structurally similar, and as the objective was to derive bioactive compounds similar to ethosuximide for screening, compounds similar to inert succinimide were removed from pooled molecules. The remaining ethosuximide-similar compounds were again subjected to the solubility filter, and retained compounds were subsequently ranked for their optimality via Pareto Sort by maximising for the extent of structural similarity to ethosuximide, and SAM-predicted *C. elegans* bioaccumulation propensity. The CNS permeability of compounds were not considered at this point, as predicted CNS MPO scores from the CNS MPO algorithm had to be calculated and compiled manually for analysis by Pipeline Pilot™, making it unnecessarily tedious for the large number of analysed compounds at this stage. Pareto sorting was performed for all identified compounds at the various levels of similarities (70 to 90 % Tc and substructure).

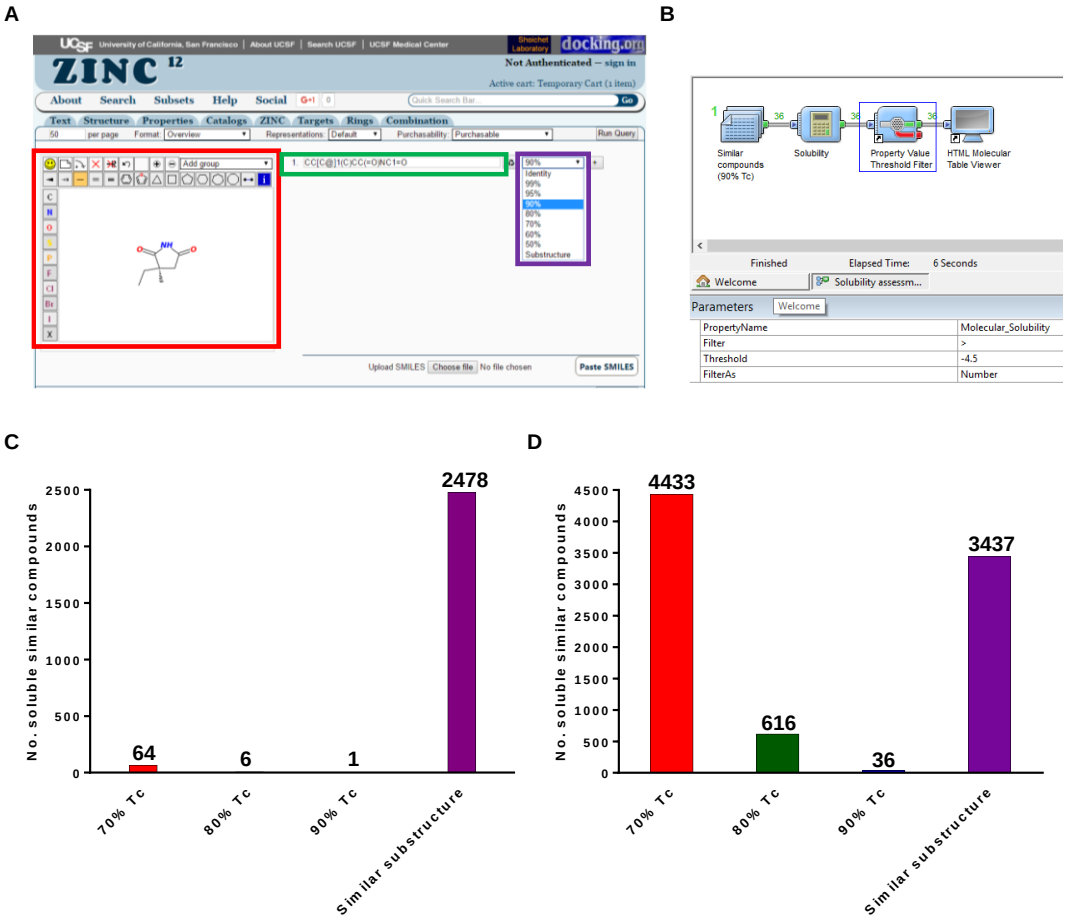

Figure 3.2.1. Initial scoping activity to assess numbers of similar compounds with acceptable aqueous solubilities. (A) Compounds from the ZINC database with similarity to query compounds ethosuximide and inert succinimide (represented herein as ethosuximide; red box) were identified at various criteria of similarity (purple box). The SMILES representation of query molecule is depicted (green box). (B) Identified compounds with LogS≤-4.5 were filtered by the aqueous solubility filter on Pipeline Pilot^{TM}. The number of retained compounds with acceptable solubilities were reported at the end of the analyses and indicated with the histograms for compounds similar to (C) succinimide and (D) ethosuximide, and ranged from 1 to 4433 compounds. Due to the large number of compounds, they had to be subjected to further MOO to identify the most optimal ones for obtaining purchasing information.

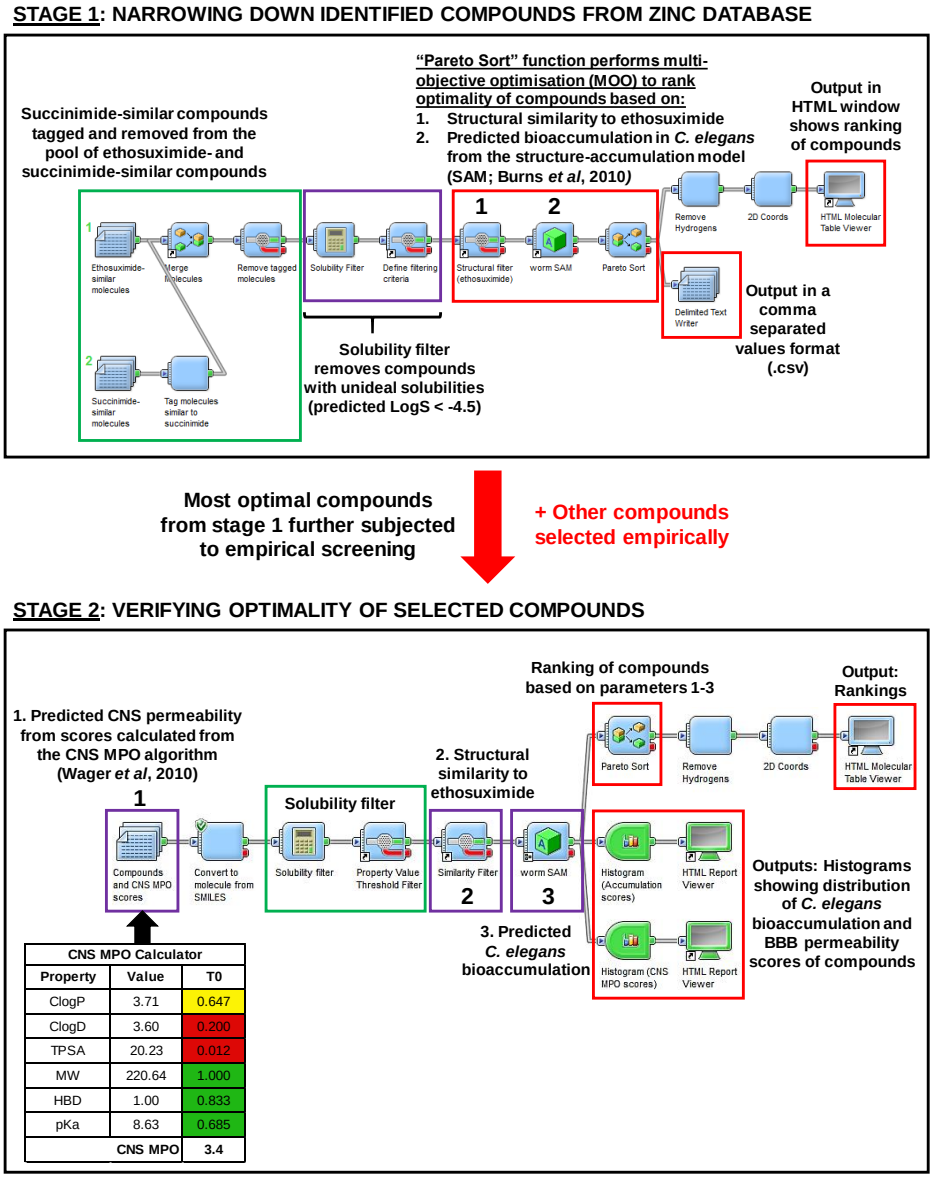

Figure 3.2.2. Multi-objective optimisation (MOO) of ethosuximide-similar compounds on Pipeline Pilot™. (A) Due to the large number of compounds identified from the ZINC database, initial MOO was performed to identify the most optimal ones amongst them based on structural similarity to ethosuximide and predicted *C. elegans* bioaccumulation; succinimide-similar compounds were removed from analysis to optimise chances of finding active compounds. (B) Empirical selection of the most optimal ones from (A) initial MOO and other similar compounds which may potentially be excluded from ZINC identification resulted in a final group of compounds which were further verified for their optimality with MOO. This final MOO stage included consideration of their predicted CNS permeabilities in addition to the aforementioned parameters.

A second empirical approach was utilised to further optimise selection of the best molecules from the abovementioned computational approach, and to identify additional chemical spaces which may have potentially been excluded by computation. This requires medicinal chemistry knowledge and was performed by Professor Paul O'Neill and Dr Neil Berry (University of Liverpool, UK).

Utilising both computational and empirical approaches and considering costs of potential compounds, a total of 16 compounds were selected for screening in addition to ethosuximide and succinimide, which will be utilised as positive and negative controls respectively (Figure 3.2.3); note that approved antiepileptic drugs 5,5-diphenylhydantoin sodium salt (phenytoin), trimethadione, methsuximide, and phensuximide were included in the selection.

To confirm their optimality, the compounds were subjected to a final analysis via MOO on Pipeline Pilot™ (Figure 3.2.2B). Due to the small number of compounds analysed at this stage, CNS MPO scores for each compound were calculated with the CNS MPO algorithm, manually compiled, and included as a parameter for MOO in the pipeline in addition to the compounds' structural similarity to ethosuximide and predicted *C. elegans* bioaccumulation propensities (Figure 3.2.2B and Table 3.2.4). A screenshot of the analytic output is given in Figure 3.2.5, and summarised in Table 3.2.6. Histograms showing the distributions of predicted CNS permeability and *C. elegans* bioaccumulation scores are shown in Figure 3.2.7.

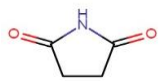

(1) Succinimide

(2) Ethosuximide

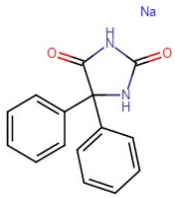

(3) 5,5-Diphenylhydantoin sodium salt (Phenytoin)

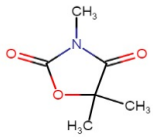

(4) 3,5,5-Trimethyloxazolidine-2,4-dione (Trimethadione)

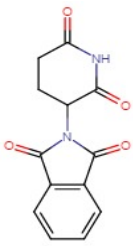

(5) Thalidomide

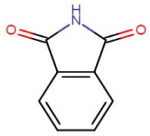

(6) Phthalimide

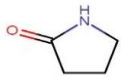

(7) 2-Pyrrolidine

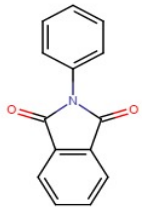

(8) N-Phenylphthalimide

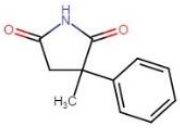

(9) α-Methyl-α-phenylsuccinimide

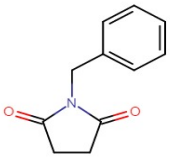

(10) 1-Benzylpyrrolidine-2,5-dione

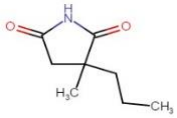

(11) α-Methyl-α-propylsuccinimide

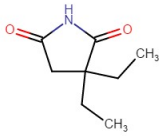

(12) 3,3-Diethylpyrrolidine-2,5-dione

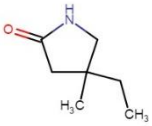

(13) 4-Ethyl-4-methylpyrrolidin-2-one

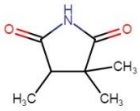

(14) α,α-Dimethyl-β-methylsuccinimide

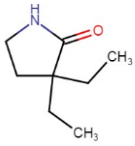

(15) 3,3-diethylpyrrolidin-2-one

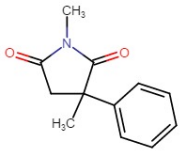

(16) Methsuximide

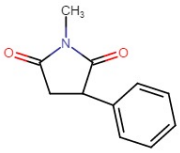

(17) Phensuximide

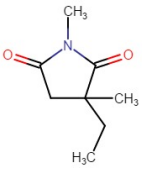

(18) 2,5-Pyrrolidinedione,3-ethyl-1,3-dimethyl

Figure 3.2.3. Compounds for primary screens. Alongside ethosuximide and its inactive parent compound succinimide, 16 similar compounds were selected for initial screens (numbered). All compounds were obtained from commercial sources, except compound 18 (2,5-Pyrrolidinedione,3-ethyl-1,3-dimethyl) which was generated from the N-methylation of ethosuximide.

All selected compounds had acceptable aqueous solubilities with LogS values ranging from -3.025 to 0.035, whereas predicted worm bioaccumulation scores ranged from -1.686 to 1.660. Although bioaccumulation is predicted to improve with increasing scores, it is difficult to infer the differences in bioaccumulation between the compounds at this point until it is experimentally determined. Compounds were also predicted to possess good CNS permeability as evident from high CNS MPO scores from 4.3 to a perfect score of 6; scores of ≥4 were considered to be high (Wager *et al*., 2010b). Finally, all compounds were ranked 4th and above, indicating a small difference in optimality between them. Overall the selected compounds displayed good predicted permeation of the CNS, small differences in predicted *C. elegans* bioaccumulation, and a good overall ranking, confirming their optimality for screening.

With the exception of compound 18 (2,5-Pyrrolidinedione,3-ethyl-1,3-dimethyl), all selected compounds were deemed reasonably priced based on allocated budgets and were hence purchased from commercial suppliers. Compound 18 was synthesized from a single step N-methylation reaction of ethosuximide (refer to chapter 2, section 2.5.2).

No.	Name	SMILES	CLogP		CLogD		TPSA		MW		HBD		pKa		CNS MPO Score
				T0		T0		T0		T0		T0		T0	
1	Succinimide	C1CC(=O)NC1=O	-1.17	1	-0.67	1	46.2	1	99.1	1	1	0.83	9.62	0.19	5.0
2	Ethosuximide	CCC1(CC(=O)NC1=O)C	0.4	1	0.4	1	46.2	1	141	1	1	0.83	9.7	0.15	5
3	5,5-Diphenylhydantoin sodium salt	C1=CC=C(C=C1)C2(C(=O)[N-]C(=O)N2)C3=CC=CC=C3.[Na+]	2.09	1	2.47	0.77	58.2	1	252	1	2	0.5	14.8	0	4.3
4	Trimethadione	CC1(C(=O)N(C(=O)O1)C)C	-0.12	1	-0.06	1	46.6	1	143	1	0	1	-2.18	1	6
5	Thalidomide	C1CC(=O)NC(=O)C1N2C(=O)C3=CC=CC=C3C2=O	0.53	1	0.53	1	83.6	1	258	1	1	0.83	10.7	0	4.8
6	Phthalimide	C1=CC=C2C(=C1)C(=O)NC2=O	1.15	1	1.1	1	46.2	1	147	1	1	0.83	10.4	0	4.8
7	2-Pyrrolidone	C1CC(=O)NC1	-0.97	1	-0.64	1	29.1	0.46	85.1	1	1	0.83	16.6	0	4.3
8	N-Phenylphthalimide	C1=CC=C(C=C1)N2C(=O)C3=CC=CC=C3C2=O	2.39	1	2.33	0.84	37.4	0.87	223	1	0	1	-0.54	1	5.7
9	α-Methyl-α-phenylsuccinimide	CC1(CC(=O)NC1=O)C2=CC=CC=C2	0.91	1	1.36	1	46.2	1	189	1	1	0.83	9.17	0.42	5.2
10	1-Benzylpyrrolidine-2,5-dione	C1CC(=O)N(C1=O)CC2=CC=CC=C2	0.97	1	1.43	1	37.4	0.87	189	1	0	1	-1.37	1	5.9
11	α-Methyl-α-propylsuccinimide	CCCC1(CC(=O)NC1=O)C	0.92	1	0.91	1	46.2	1	155	1	1	0.83	9.7	0.15	5
12	3,3-Diethylpyrrolidine-2,5-dione	CCC1(CC(=O)NC1=O)CC	0.92	1	1.25	1	46.2	1	155	1	1	0.83	9.7	0.15	5
13	4-Ethyl-4-methylpyrrolidin-2-one	CCC1(CC(=O)NC1)C	0.59	1	1.31	1	29.1	0.46	127	1	1	0.83	16.7	0	4.3
14	α,α-Dimethyl-β-methylsuccinimide	CC1C(=O)NC(=O)C1(C)C	0.39	1	0.3	1	46.2	1	141	1	1	0.83	9.74	0.13	5
15	3,3-Diethylpyrrolidin-2-one	CCC1(CCNC1=O)CC	1.12	1	0.86	1	29.1	0.46	141	1	1	0.83	16.7	0	4.3
16	Methsuximide	CC1(CC(=O)N(C1=O)C)C2=CC=CC=C2	1.46	1	1.67	1	37.4	0.87	203	1	0	1	-1.81	1	5.9
17	Phensuximide	CN1C(=O)CC(C1=O)C2=CC=CC=C2	0.94	1	1.68	1	37.4	0.87	189	1	0	1	-1.86	1	5.9
18	2,5-Pyrrolidinedione,3-ethyl-1,3-dimethyl	CCC1(CC(=O)N(C1=O)C)C	0.95	1	0.75	1	37.4	0.87	155	1	0	1	-1.25	1	5.9

Table 3.2.4. CNS MPO scores of compounds gives a prediction of CNS permeability. Actual and transformed (T0; highlighted in yellow) values of various physicochemical properties are shown and computed using the CNS MPO algorithm (Wager *et al*., 2010b) for each compound. Summation of the six T0 scores yielded the final CNS MPO score, which gives a numerical measure of how well compounds are predicted to permeate the CNS; the greater the score is to 6 the better the predicted permeability. The CNS MPO score for the phenytoin sodium salt (compound 3; highlighted in green) was derived based on physicochemical properties for phenytoin due to the difficulty for *in silico* modelling of the salt.

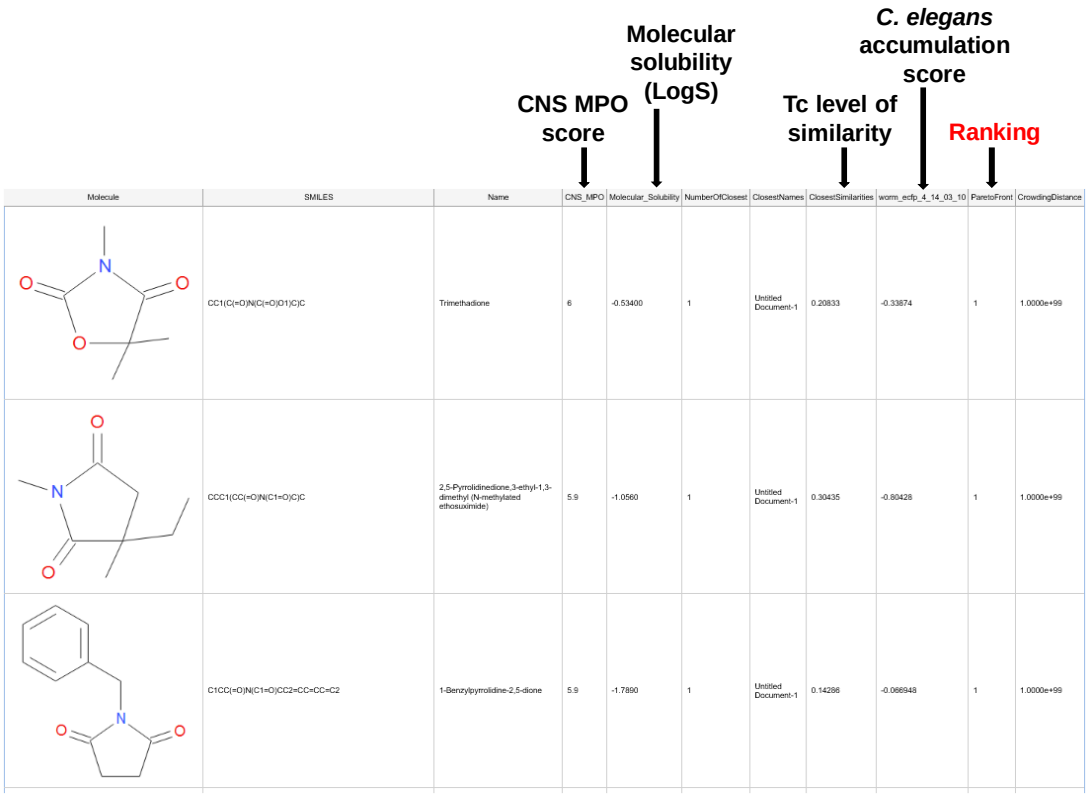

Molecule	SMILES	Name	CNS_MPO	Molecular_Solubility	NumberOfClosest	ClosestNames	ClosestSimilarities	worm_ecfp_4_14_03_10	ParetoFront	CrowdingDistance
	CC1(C(=O)N(C(=O)O1)C)C	Trimethadione	6	-0.53400	1	Untitled Document-1	0.20833	-0.33874	1	1.0000e+99
	CCC1(CC(=O)N(C1=O)C)C	2,5-Pyrrolidinedione,3-ethyl-1,3-dimethyl (N-methylated ethosuximide)	5.9	-1.0560	1	Untitled Document-1	0.30435	-0.80428	1	1.0000e+99
	C1CC(=O)N(C1=O)CC2=CC=CC=C2	1-Benzylpyrrolidine-2,5-dione	5.9	-1.7890	1	Untitled Document-1	0.14286	-0.086948	1	1.0000e+99

Figure 3.2.5. Screenshot of the MOO analytic output of selected compounds on Pipeline Pilot™. Predicted solubility (LogS) values, CNS MPO and *C. elegans* accumulation scores, similarity score as computed by the Tanimoto coefficient (Tc), and ranking of compounds as determined by the Pareto Sort function based on the latter three parameters are indicated in the output. Optimality decreases as the ranking number increases.

Compound	No.	Solubility (LogS)	CNS MPO score	Similarity (Tc value)	Predicted *C. elegans* bioaccumulation score	Pareto ranking
3,5,5-Trimethyloxazolidine-2,4-dione (Trimethadione)	4	-0.534	6	0.208	-0.339	1
2,5-Pyrrolidinedione,3-ethyl-1,3-dimethyl	18	-1.056	5.9	0.304	-0.804	1
1-Benzylpyrrolidine-2,5-dione	10	-1.79	5.9	0.143	-0.0670	1
Ethosuximide	2	-1.11	5	1	-0.203	1
Phthalimide	6	-1.44	4.8	0.261	1.66	1
3,3-Diethylpyrrolidin-2-one	15	-1.71	4.3	0.550	0.154	1
α-Methyl-α-phenylsuccinimide	9	-2.43	5.2	0.400	0.322	1
3,3-Diethylpyrrolidine-2,5-dione	12	-1.46	5	0.875	-0.127	1
N-Phenylphthalimide	8	-3.03	5.7	0.148	0.0538	1
Methsuximide	16	-2.39	5.9	0.172	-0.279	1
Phensuximide	17	-1.95	5.9	0.13333	-1.06	2
α-Methyl-α-propylsuccinimide	11	-1.53	5	0.824	-1.10	2
5,5-Diphenylhydantoin sodium salt (Phenytoin)	3	-3.53	4.3	0.222	1.10	2
4-Ethyl-4-methylpyrrolidin-2-one	13	-1.33	4.3	0.632	-0.350	2
Succinimide	1	0.0350	5	0.563	-0.643	2
α,α-Dimethyl-β-methylsuccinimide	14	-1.16	5	0.526	-1.29	3
2-Pyrrolidine	7	-0.0560	4.3	0.400	-0.666	3
Thalidomide	5	-2.11	4.8	0.300	-1.69	4

Table 3.2.6. Pareto rankings of screening compounds based on structural similarity to ethosuximide, and CNS MPO and *C. elegans* bioaccumulation scores. Predicted molecular solubility (LogS) values for each compound are also indicated. The CNS MPO score for the phenytoin sodium salt (compound 3) was derived based on physicochemical properties for phenytoin due to the difficulty for *in silico* modelling of the salt.

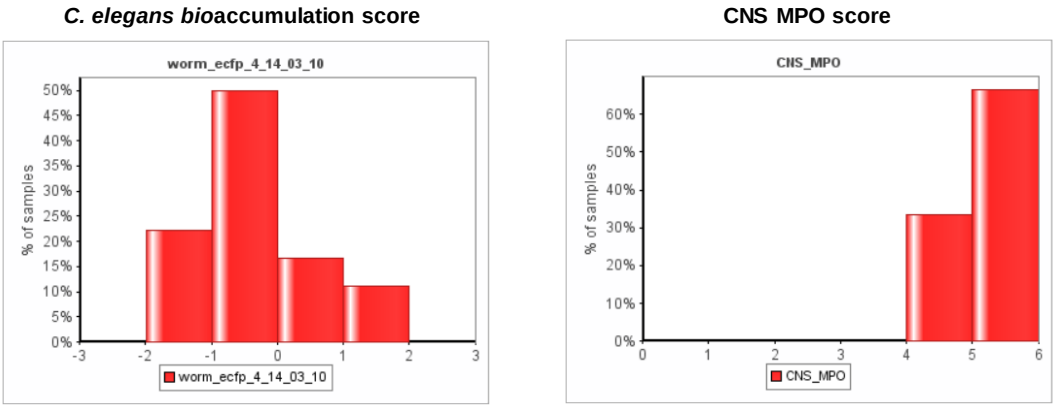

Figure 3.2.7. Histograms showing the distributions of predicted *C. elegans* bioaccumulation and CNS MPO scores of selected compounds. The range of accumulation scores is small, suggesting that differences between the compounds for *C. elegans* bioaccumulation is minimal. All compounds had high CNS MPO scores of more than 4, suggesting good CNS permeation.

3.2.2 *C. elegans* neurodegeneration assays are unfeasible for primary screening

Ethosuximide was previously shown by work from our group to ameliorate the locomotion defect of the FTDP-17 CK10 strain and sensory defect of the ANCL *dnj-14 (tm3223)* strain through neurodegenerative phenotypic readouts from liquid thrashing and food race assays respectively. In addition, the drug extended the shortened lifespans of both strains (Chen *et al*., 2015b, Kashyap *et al*., 2014). Although the feasibility of using the CK10 liquid thrashing phenotype for chemical genetic screens was previously demonstrated (McCormick *et al*., 2013), direct comparisons between these neurodegeneration assays have yet to be made to identify the most suitable one for drug screening. In the current study, this comparison was made between liquid thrashing and food race assays, but not for the lifespan assay due to the nature of its low throughput. The suitability of both assays was assessed with succinimide and ethosuximide with consideration of their throughputs and whether the assessed phenotypes exhibit robust and reproducible improvements in response to ethosuximide treatment.

Previous work demonstrated optimal neuroprotectiveness by ethosuximide at 1 mg/mL (Chen *et al*., 2015b), hence the drug and the inert control succinimide were administered at their corresponding molar concentrations at 7 and 10 mM. Note that the disparity between given molar concentrations was intended at this stage to verify the inert neuroprotective property of succinimide at a higher concentration. Following this initial confirmation stage, both compounds were assessed as controls at equal molar concentrations from chapter 4 onwards. In the liquid thrashing assay, ethosuximide appeared to ameliorate the locomotion defects of the CK10 worms at most assessed ages in comparison to succinimide-treated worms, however these effects were not significant (Figure 3.2.8). In addition, it should be noted that the locomotive responses to ethosuximide treatment were observed to be quite variable between worms, suggestive of an unideal signal-to-noise ratio.

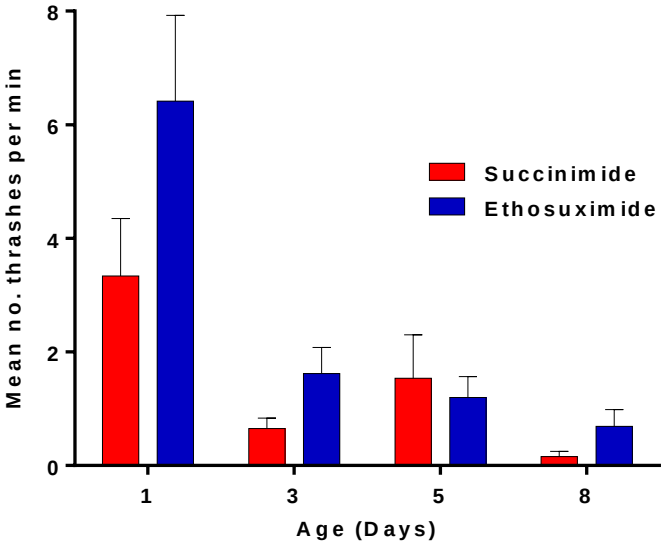

Figure 3.2.8. Liquid thrashing assay with the locomotion-defective CK10 strain. Age-synchronised CK10 worms were chronically treated with 7 and 10 mM ethosuximide or succinimide respectively. Ethosuximide appeared to improve thrashing rates in comparison to succinimide on days 1, 3, and 8, although this was not demonstrated to be significant ($p>0.05$). Data shown was pooled from three biological replicates, with comparisons made via the Kruskal-Wallis test with Dunn's multiple comparison. Ethosuximide, days 1 and 3 (n = 60 each), day 5 (n = 40), day 8 (n = 32); succinimide, day 1 (n = 59), day 3 (n = 60), day 5 (n = 39), day 8 (n = 32).

The food race assay assesses sensory neuron function of the *dnj-14* ANCL worms by measuring the rate of travel to an *E. coli* food source (Figure 3.2.9 and 3.2.10). Succinimide-treated *dnj-14* worms were significantly slower at getting to the food source than their WT counterparts at ages day 1 to 8 as previously reported (Kashyap *et al*., 2014). Ethosuximide had no effect on the sensory neuron function of WT N2 worms across the same ages, but restored the sensory defect of *dnj-14* worms to WT levels at days 1 and 3. Additionally, days 1 to 5 *dnj-14* worms exhibited improved sensory function with the drug as compared to succinimide treatment. However, this drug-mediated protective effect against sensory decline was lost at the older age of day 8. Although ethosuximide exerted a more robust and reproducible neuroprotective effect on this phenotypic readout than observed for the liquid thrashing phenotype, the throughput of the food race assay is of a medium nature at best. For the purposes of initial screens, it is far from ideal.

The need for generating and maintaining age-synchronised strains for studying age-dependent neurodegenerative phenotypes is time-consuming, and is a major reason impeding the throughputs of these assays. Additionally, drug exposure via treatment plates is economically unfeasible especially for pricier compounds, since a large amount goes into preparing the numerous required plates. Therefore, an alternative assay needs to be identified for primary screening which overcomes such issues associated with these plate-based treatment, age-dependent assays.

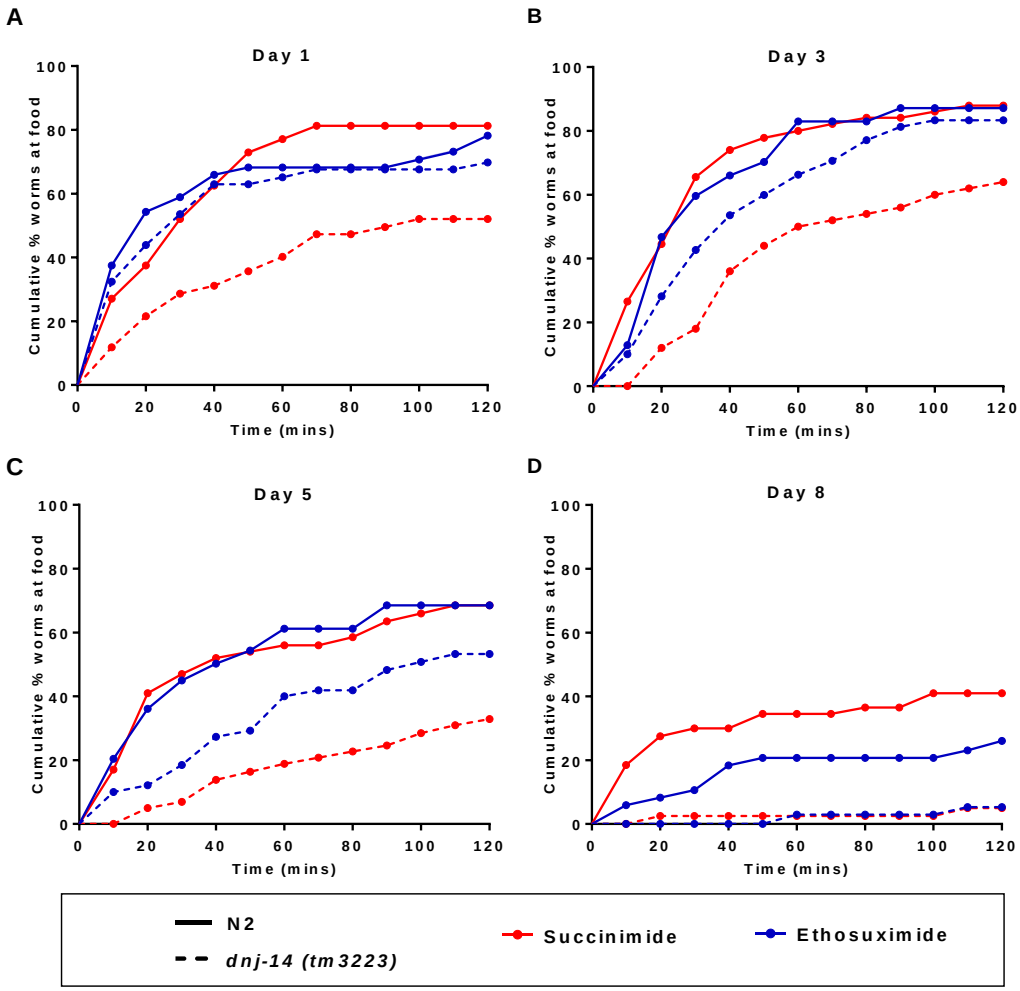

Figure 3.2.9. Food race assay with the sensory neuron-defective *dnj-14 (tm3223)* ANCL strain. The sensory neuron function of age-synchronised worms chronically-treated with 7 and 10 mM of respectively ethosuximide or succinimide was assessed by the travel rate from a starting position to an OP50 spot at the opposite end of the agar plate. The number of worms at OP50 was scored at 10-minute intervals up to 2 hours. Ethosuximide had no effect on the sensory function of wildtype N2 worms, but ameliorated the defect in *dnj-14* worms at days 1 to 5 ($p<0.05$)., following which protection was abolished at day 8 when sensory function had visibly declined in both strains. Data was pooled from two biological repeats and was analysed via the log-rank test. N2; ethosuximide, day 1 (n = 42), day 3 (n = 47), day 5 (n = 43), day 8 (n = 38); succinimide, day 1 (n = 48), day 3 (n = 49), day 5 (n = 45), day 8 (n = 45). *dnj-14;* ethosuximide, day 1 (n = 43), day 3 (n = 48), day 5 (n = 46), day 8 (n = 38); succinimide, day 1 (n = 42), day 3 (n = 50), day 5 (n = 46), day 8 (n = 38).

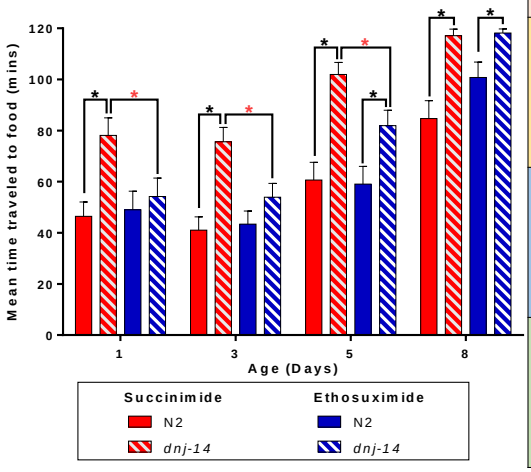

Age (Day)	Strain	Treatment	Mean time taken to travel to food (mins)	S.E.M
1	N2	PBS	49.79	6.06
		Succinimide	46.46	5.63
		Ethosuximide	49.05	7.26
	dnj-14 (tm3223)	PBS	76.22	6.62
		Succinimide	78.10	6.87
		Ethosuximide	54.19	7.25
3	N2	PBS	37.50	5.01
		Succinimide	41.02	5.25
		Ethosuximide	43.40	5.12
	dnj-14 (tm3223)	PBS	68.04	5.82
		Succinimide	75.60	5.64
		Ethosuximide	53.96	5.41
5	N2	PBS	46.44	5.64
		Succinimide	60.67	6.95
		Ethosuximide	59.07	6.89
	dnj-14 (tm3223)	PBS	99.76	5.20
		Succinimide	101.96	4.70
		Ethosuximide	81.96	6.00
8	N2	PBS	91.02	6.17
		Succinimide	84.67	7.06
		Ethosuximide	100.79	6.03
	dnj-14 (tm3223)	PBS	110.44	3.94
		Succinimide	117.11	2.60
		Ethosuximide	118.16	1.57

Figure 3.2.10. Rate of travel to a food source during food race assays is a readout of sensory neuron function. The time taken for succinimide-treated *dnj-14* worms to the food source was significantly longer than their WT counterparts at all ages, whereas ethosuximide restored the sensory defect of these worms to WT levels at days 1 and 3 ($p<0.05$, black asterisks). Additionally, the rate of travel to the food was significantly faster for ethosuximide-treated *dnj-14* worms as compared to succinimide-treated ones from days 1 to 5 ($p<0.05$, red asterisks). Data was pooled from two biological repeats and was analysed via the log-rank test; *, $p<0.05$. N2; ethosuximide, day 1 (n = 42), day 3 (n = 47), day 5 (n = 43), day 8 (n = 38); succinimide, day 1 (n = 48), day 3 (n = 49), day 5 (n = 45), day 8 (n = 45). *dnj-14;* ethosuximide, day 1 (n = 43), day 3 (n = 48), day 5 (n = 46), day 8 (n = 38); succinimide, day 1 (n = 42), day 3 (n = 50), day 5 (n = 46), day 8 (n = 38).

3.2.3 The *C. elegans* PTZ-induced seizure assay is a suitable primary screening assay

An alternative assay for primary screening purposes is the PTZ-induced seizure assay, which was previously established with the synaptic transmission mutant strain *unc-49 (e407)* (Williams *et al*., 2004). The *unc-49 (e407)* mutation is a point mutation in the *C. elegans unc-49* $GABA_A$ receptor gene which results in a premature stop codon (Q179stop) at the N-terminus, hence this mutation is null and causes defective GABA signalling at the neuromuscular junction (Bamber *et al*., 1999). Treatment with a known seizure-inducing agent PTZ causes characteristic and robust head bobbing seizures with immobile posterior ends in the *unc-49* mutants (Williams *et al*., 2004). Previous work in the laboratory had initially employed this model to screen for anticonvulsive activities in compounds via a plate-based treatment approach. However, preliminary work demonstrated the feasibility of liquid-based treatment whereby a 1-hour acute incubation of the *unc-49* worms in ethosuximide-containing liquid droplets provided seizure protection against PTZ (unpublished data), negating the need for chronic plate-based treatment. In addition, age-synchronised worms were not required since seizures were induced through a chemical agent. Such features of this liquid-based protocol suggest the potential for increased throughput and reduced associated costs with preparing treatment plates as compared to the neurodegeneration assays, making it a potential primary screening platform despite the major caveat of not being able to infer information about neuroprotective properties.

Assay optimisation was performed to enhance its efficiency for primary screening. A stringent scoring system was devised to score seizures qualitatively and quantitatively, by determining the overall presence or absence of seizures and number of head bobs in individual worms respectively over each scoring duration of 30 seconds. The PTZ treatment conditions were then assessed to evaluate the requirements for optimal seizure induction in the worms. PTZ treatment at 50 mM for 15 minutes was previously shown to be optimal for inducing seizures in other seizure-prone strains (unpublished data). Although this treatment duration induced maximal seizures in *unc-49* worms, this was demonstrated at a PTZ concentration below 50 mM without a

thorough concentration-response assessment. Therefore, the concentration-response relationship of PTZ in this strain was evaluated herein. Findings demonstrated a concentration-dependent induction of seizures up to 36 mM, after which higher concentrations up to 50 mM had similar effects (Figure 3.2.11). Together with previous observations, this verified that 50 mM was indeed optimal at reproducibly inducing seizures in several seizure-prone strains after a 15-min treatment duration.

To derive the best signal-to-noise ratio for differentiating active from inactive compounds, ethosuximide was utilised to determine the best drug pretreatment conditions prior to PTZ exposure (Figure 3.2.12). Duration of pretreatment was optimised with 14 mM ethosuximide as this concentration previously offered the best seizure protection in *unc-49* worms on a chronic 2-day plate-based treatment (unpublished data). The proportion of seizing worms reduced time-dependently until 55 minutes of pretreatment, after which increased pretreatment durations offered no further protection. As throughput is a major consideration, 2 hours was selected as the minimum pretreatment duration to robustly and reproducibly reduce seizures. This was sequentially applied to determine the optimal seizure-inducing concentration of ethosuximide (Figure 3.2.12). The drug concentration-dependently protected against seizures until seizures were fully obliterated at both 28 and 56 mM. Previous findings determined an internal drug concentration of 213 µM when 14 mM of the drug was administered to WT worms (Goren and Onat, 2007, Evason *et al*., 2005). Given the previously reported linear relationship between ethosuximide plasma levels and administered doses (Patsalos, 2005), 28 mM of the drug was selected as the optimal treatment concentration for this assay as it was assumed to translate to an internal concentration of 425 µM, mirroring the human therapeutic range of 280 to 700 µM (Goren and Onat, 2007, Evason *et al*., 2005).

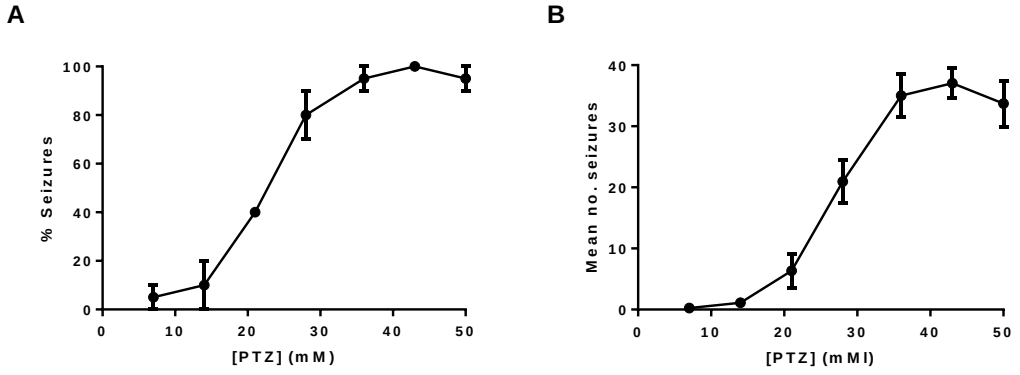

Figure 3.2.11. Determining the optimal seizure-inducing concentration of pentylenetetrazol (PTZ) in *unc-49* worms. The seizing phenotype was scored after exposure to various concentrations of PTZ (7 – 50 mM) for 15 mins. The (A) proportion of seizing worms and (B) number of seizures increased concentration-dependently up to 36 mM PTZ, which stabilised thereafter (*n* = 17 - 20 per concentration). Data was pooled from two biological replicates with contribution from Alistair Jones (University of Liverpool, UK).

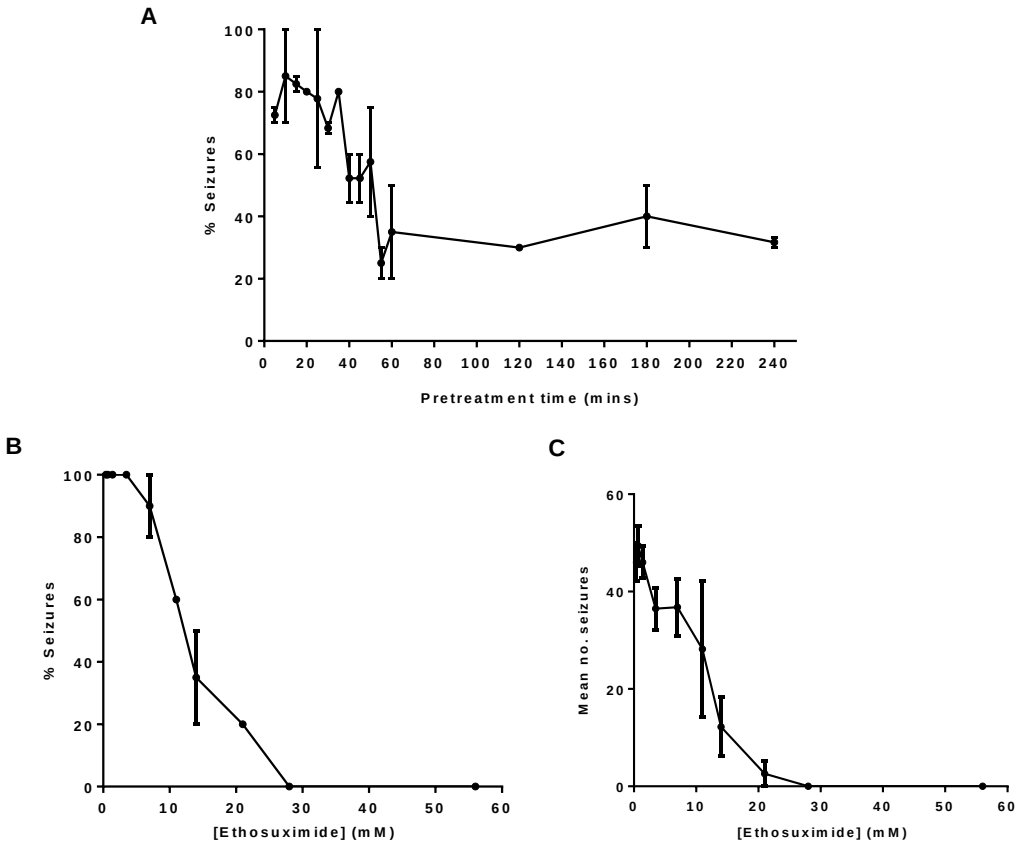

Figure 3.2.12. Optimisation of the PTZ-induced seizure assay in the synaptic transmission defective *unc-49* strain with ethosuximide. Prior to PTZ exposure, pretreatment with ethosuximide at various (A) lengths of time (5 – 240 mins) and (B and C) concentrations (0.4 – 56 mM) were performed to identify the optimal drug treatment conditions for seizure protection. (A) The proportion of seizing worms decreased as the length of pretreatment with 14 mM ethosuximide increased, with no further reductions after 55 mins (*n* = 17 – 20 per length of preincubation). A 2-hr acute ethosuximide pretreatment concentration-dependently reduced both (B) percentage of seizing worms and (C) number of seizures (*n* = 5 – 10 per concentration), with complete protection against seizures at 56 mM. All data shown was pooled from two biological replicates.

3.2.4 Primary screens identified one inactive and ten active compounds

Primary screens of selected compounds (Figure 3.2.3) were performed with the optimised assay. Compounds excluded from analysis due to problems with solubility include compounds 3 (phenytoin), 5 (thalidomide), 6 (phthalimide), 8 (N-phenylphthalimide), and 10 (1-benzylpyrrolidine-2,5-dione). The remaining compounds had no apparent solubility issues and were screened against ethosuximide and succinimide at the optimal 28 mM-equivalent ethosuximide concentration of 4 mg/mL, or a lower 14 mM-corresponding concentration of 2 mg/mL in the event of observed toxicity. Toxicity was determined by visual observations of abnormal stiff movement or immobility, and a weak response to touch or death as indicated by the absence of response to touch at the end of drug pretreatment and/or PTZ exposure. Conversely, a therapeutic effect was defined by a reduction or abolishment of seizures in the presence of movement and response to touch. If absence of seizures was observed with immobility, a non-seizing phenotype was scored only if a robust response to touch was observed, indicative of non-toxicity. Note that despite molar mass differences, standardised mg/mL concentrations were screened at this initial stage for a quick preliminary assessment of activity. As explained in the following section, concentration-response analysis of identified active compounds at molar concentrations were performed thereafter to account for these differences for an in-depth comparison of potencies.

Prior to screening DMSO-soluble compounds, the maximum tolerable concentration of the vehicle that does not cause toxicity and affect normal seizing responses to PTZ was determined (Figure 3.2.13). Pretreatment with up to 2 % DMSO did not result in any observable abnormality in the worms' behaviour, as they generally displayed spontaneous movement by the end of DMSO pretreatment, with 100 % of worms seizing in response to PTZ. (Figure 3.2.13A). However, seizure rate was reduced in worms pretreated with 2 % DMSO (Figure 3.2.13B). Further increases in DMSO concentrations resulted in concentration-dependent reduction of seizures and observable toxicity as defined above, which were likely a consequence of intolerable levels of DMSO as the behaviour of these worms were in stark contrast to those treated with

ethosuximide. In support of this likelihood, worms exposed to lower percentages of DMSO behaved similarly to ethosuximide-treated ones, highlighting that decreasing sensitivity to PTZ above a threshold of DMSO was a consequence of DMSO toxicity. Since the weakening of seizing responses to PTZ was already evident from 2 % DMSO, compound 9 was screened at the lower DMSO concentration of 1 %.

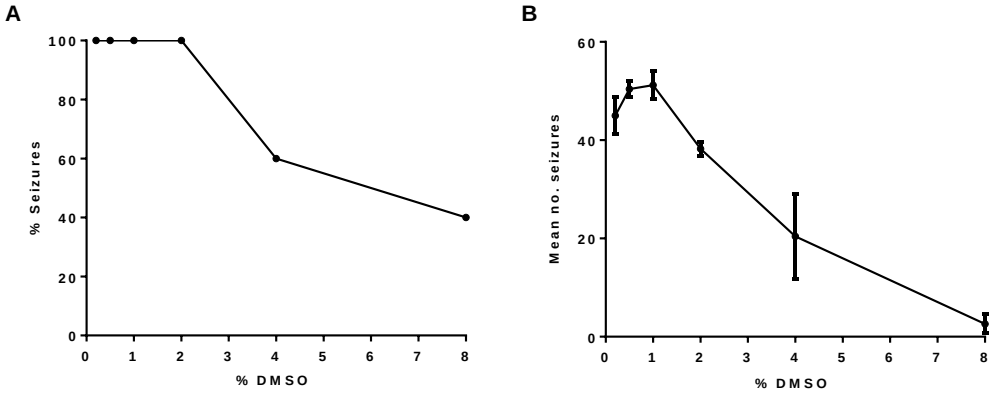

Figure 3.2.13. Concentration-response relationship of DMSO. Worms were exposed to 0.2 to 8 % DMSO throughout the length of time taken for drug pretreatment and PTZ exposure. To determine the maximum tolerable level of DMSO, seizing responses to PTZ were assessed. Treatment with up to 1 % DMSO resulted in comparable (A) percentages of seizing worms and (B) seizure rates in response to PTZ, which declined concentration-dependently from 2 %, indicative of the increasing toxicity of DMSO and consequential decreasing sensitivity to PTZ. The maximum tolerable concentration of DMSO was therefore identified to be 1 %. Data shown was from a single experiment (n = 4 – 5 worms per DMSO concentration).

The primary screens identified active compounds 9 (α-methyl-α-phenylsuccinimide), 11 (α-methyl-α-propylsuccinimide), 12 (3,3-diethylpyrrolidine-2,5-dione), 13 (4-ethyl-4-methylpyrrolidin-2-one), 14 (α,α-dimethyl-β-methylsuccinimide), 15 (3,3-diethylpyrrolidin-2-one), 16 (methsuximide), 17 (phensuximide), and 18 (2,5-pyrrolidinedione,3-ethyl-1,3-dimethyl) (Figures 3.2.15 and 3.2.16). Like ethosuximide, these active compounds protected against seizures when screened at 2 or 4 mg/mL, or when re-screened at a higher concentration of a 70 mM-equivalent ethosuximide concentration of 10 mg/mL if activity was not demonstrated at the lower concentrations. A reference of mg/mL-corresponding molar concentrations for each screened compound is displayed in Table 3.2.14.

As shown herein, compound 4 (trimethadione) did not exhibit an overall anticonvulsive effect in the population assayed when screened at 4 mg/mL, but hints of activity were observed as it protected against seizures in some but not all the worms (Figure 3.2.15). Hence, re-screening was not performed at 10 mg/mL to verify activity, and it was classified as potentially active for further concentration-response evaluation. Like succinimide, compound 7 (2-pyrrolidine) was not protective against induced seizures even at 10 mg/mL, and was classified as inactive (Figure 3.2.15). It should be noted that although it is possible that inactive compounds may exhibit bioactivity at concentrations higher than 10 mg/mL, such concentrations are likely well out of therapeutically relevant ranges in reference to ethosuximide.

Compound	No.	Molar mass (g/L)	Screened concentration (mg/mL)	Molar concentration (mM)
Succinimide	1	99.09	4	40
Ethosuximide	2	141.17	4	28
Trimethadione	4	143.14	4	28
2-Pyrrolidine	7	85.11	4	47
			10	117
α-Methyl-α-phenylsuccinimide	9	189.21	2	11
α-Methyl-α-propylsuccinimide	11	155.19	2	13
3,3-Diethylpyrrolidine-2,5-dione	12	155.19	4	26
4-Ethyl-4-methylpyrrolidin-2-one	13	127.18	4	31
α,α-Dimethyl-β-methylsuccinimide	14	141.17	4	28
3,3-Diethylpyrrolidin-2-one	15	141.21	4	28
			10	71
Methsuximide	16	203.24	2	10
Phensuximide	17	189.21	2	11
2,5-Pyrrolidinedione,3-ethyl-1,3-dimethyl	18	155.19	4	26
			10	64

Table 3.2.14. Standardised mg/mL screening concentrations of assayed compounds and corresponding molar concentrations.

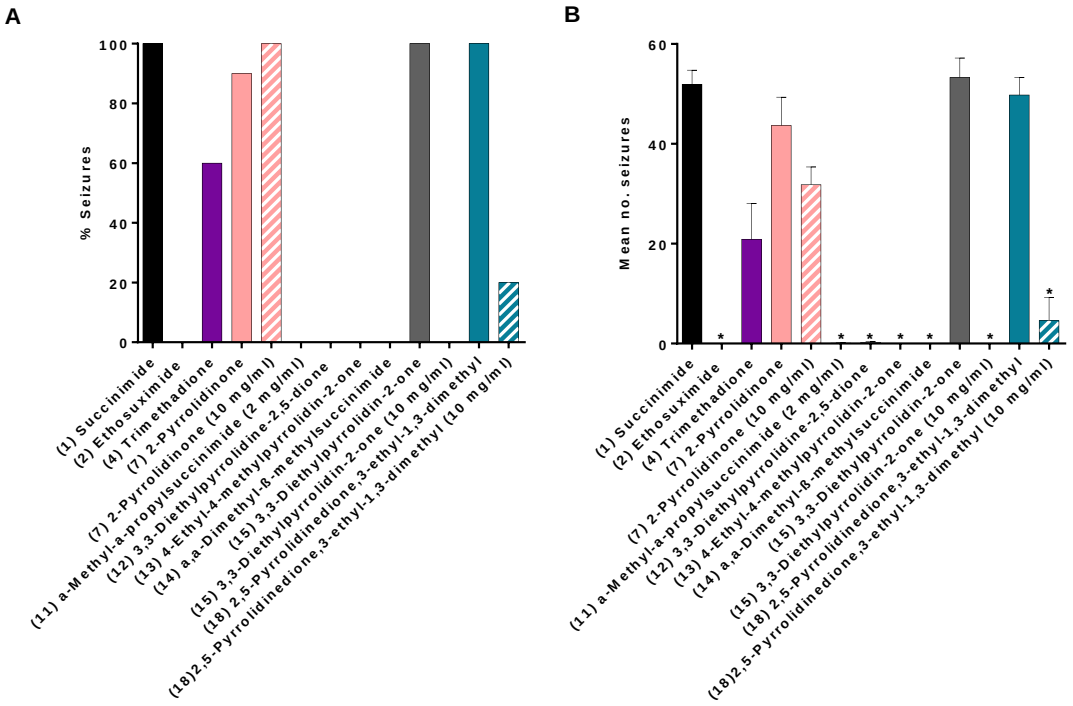

Figure 3.2.15. Water-soluble compounds were subjected to primary screens in the PTZ-induced seizure assay in the synaptic transmission defective *unc-49* strain. Compounds were screened at the optimal ethosuximide 28 mM-equivalent concentration of 4 mg/mL, or at a lower 14 mM-equivalent concentration of 2 mg/mL in the event of evident toxicity at the former concentration. Compounds not exhibiting activity at 4 mg/mL were re-screened at a higher concentration of 10 mg/mL to verify or disprove inactivity. With the exception of compounds 4 (trimethadione) and 7 (2-pyrrolidine), all compounds reduced both (A) percentage of seizing worms and (B) frequency of seizures ($p<0.05$). Compound 4 was not consistently active but displayed anticonvulsive protection in some worms, therefore it was herein classified as partially active. Seizure rates were compared with the Kruskal-Wallis test with Dunn's multiple comparison; *, $p<0.05$. Data shown was pooled from five biological replicates for ethosuximide and succinimide (n = 23 – 25 per condition), two biological replicates for compounds 4, 7, 14, 15 (n = 10 per condition), 11 (n = 20), 12 (n = 9), and 13 (n = 7) at 4 mg/mL, and single experiments for compound 18 at both 4 mg/mL and 10 mg/mL, and compounds 7 and 15 at 10 mg/mL (n = 5 per condition).

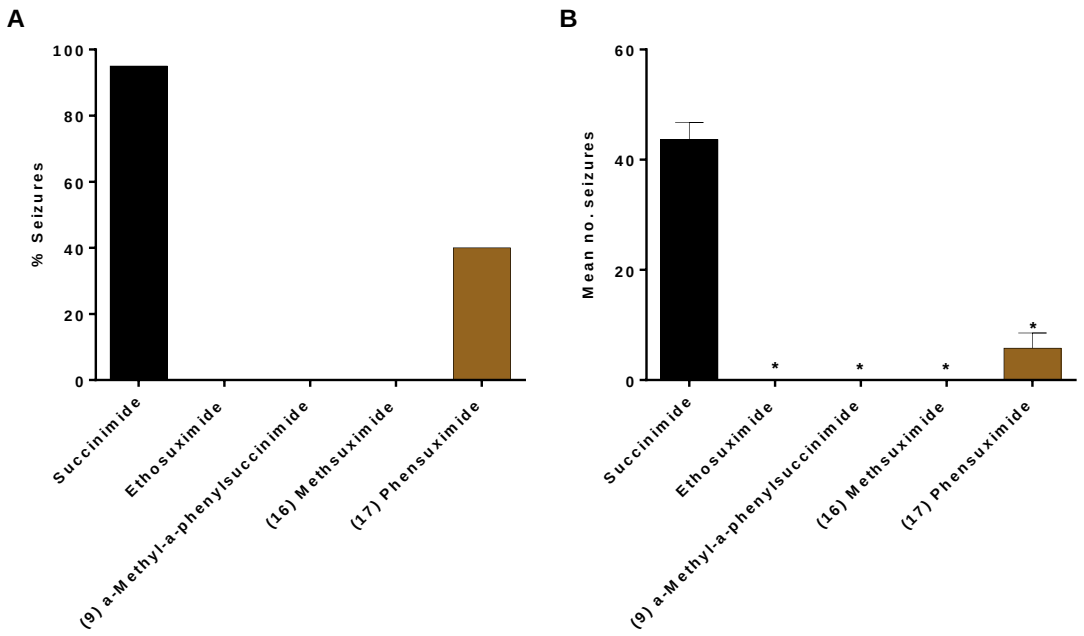

Figure 3.2.16. Primary screens of DMSO-soluble compounds. Compounds were screened at a ethosuximide 14 mM-equivalent concentration of 2 mg/mL at 1 % DMSO, as the optimal 28 mM-equivalent concentration of 4 mg/mL conferred visible signs of toxicity. Screening was performed against succinimide and ethosuximide controls prepared at the same concentration of the vehicle. Similar to ethosuximide, all compounds reduced both (A) percentage of seizing worms and (B) frequency of seizures in comparison to succinimide ($p<0.05$). Seizure rates were compared with the Kruskal-Wallis test with Dunn's multiple comparison; *, $p<0.05$. Data shown was pooled from four biological replicates for ethosuximide and succinimide (n = 20 per condition), two biological replicates for compounds 16 and 17 (n = 9 - 10 per condition), and a single experiment for compound 9 (n = 5).

3.2.5 Compound 9 was more potent than ethosuximide and selected as a candidate molecule

As explained in the preceding section, the concentration-response relationships of identified active compounds from primary screens were further evaluated at molar concentrations for in-depth analysis and comparisons of potencies (Figure 3.2.17). Resultant concentration-response curves appear to generally exhibit the same shift patterns from ethosuximide for both qualitative (% of worms seizing in the population) and quantitative (number of seizures) scoring approaches. Of focus are curves shifted to the left of ethosuximide, as leftward shifts are indicative of lower $LogEC_{50}$ values and enhanced potencies. Of the compounds assessed, this phenomenon was observed consistently for compounds 9, 14, and 16.

To better emphasize the potency differences, anticonvulsive effects were compared at a selected concentration of 7.5 mM (Figure 3.2.18). As expected from the direction of curve shifts, seizure protection by compounds 9, 14, and 16 were remarkably improved in comparison to ethosuximide. Comparison of $LogEC_{50}$ values which were derived from curve fits further corroborated the significant 2-fold increases in potencies from these compounds relative to ethosuximide, and identified compounds with similar or reduced potencies, as summarized in Table 3.2.19. Note that although compound 11 also showed enhanced anticonvulsive protection from ethosuximide at 7.5 mM (Figure 3.2.18), its overall potency was demonstrated to be similar to the drug (Table 3.2.19).

Of the three compounds with enhanced potencies, compound 9 was selected as a candidate by Professor Paul O'Neill and Dr Neil Berry for future generation of secondary compounds, as the presence of an aromatic phenyl moiety facilitates flexible structural modifications to be made to improve potencies and physicochemical properties (personal communication, Professor Paul O'Neill and Dr Neil Berry). Note that although compound 16 (methsuximide) also has a phenyl moiety, it was not selected as the candidate molecule as it is the AED pro-drug of compound 9; refer to discussion (section 3.3) for further details.

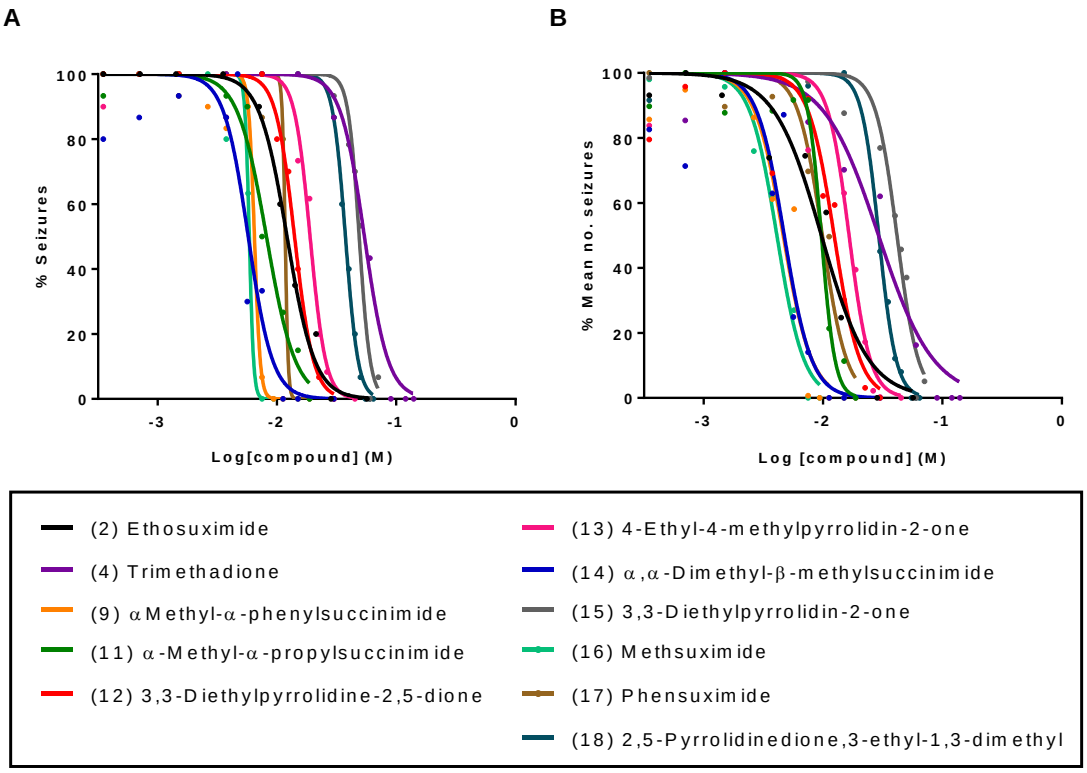

Figure 3.2.17. Concentration-response relationships of active compounds. Concentration-response curves were derived from scoring of (A) percentages of seizing worms and (B) frequencies of seizures in *unc-49* worms. Significant leftward shifts of curves from compounds 9, 14, and 16 in comparison to that of ethosuximide are indicative of enhanced potencies in comparison to the drug ($p<0.05$). Data shown was pooled from three biological replicates. Curve fit and significance of shifts, as derived from comparisons of fitted $LogEC_{50}$ values, were performed via nonlinear regression analysis on GraphPad Prism 6 (n = 5 - 15 worms per concentration per compound).

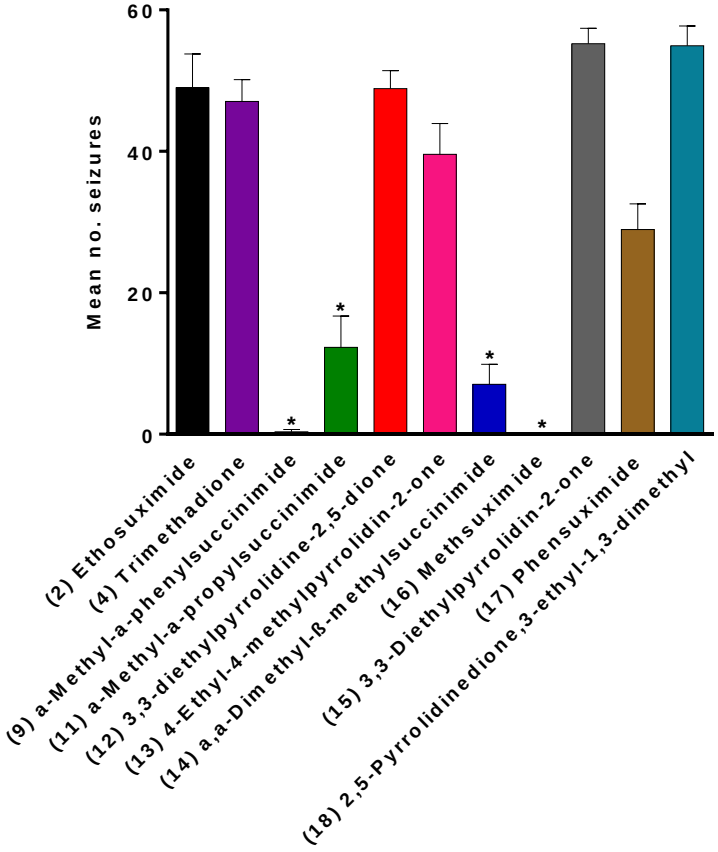

Figure 3.2.18. Seizure-protecting activities of active compounds at a single molar concentration. At 7.5 mM, compounds 9, 11,14, and 16 drastically reduced seizure rates as compared to ethosuximide ($p<0.05$). All data shown was pooled from three biological replicates, with comparisons made via the Kruskal-Wallis test with Dunn's multiple comparison (n = 14 - 15 worms per concentration per compound); *, $p<0.05$.

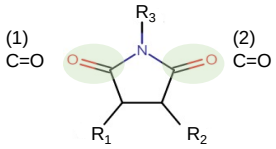

Compound	No.	Structure	R_1	R_2	R_3	(1) C=O	(2) C=O	Active?	EC_{50} (mM)	Potency against ethosuximide
Ethosuximide	2		X	✓	X	✓	✓	**ACTIVE**	9.7	-
Succinimide	1	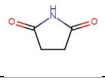	X	X	X	✓	✓	**Inactive**	-	-
2-Pyrrolidine	7		X	X	X	✓	X		-	-
Trimethadione	4		X	✓	✓	✓	✓	**Active but no differences in potency or less potent than ethosuximide**	29.2	3-fold lower
α-Methyl-α-propylsuccinimide	11	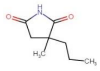	X	✓	X	✓	✓		9.7	No significant difference
3,3-Diethylpyrrolidine-2,5-dione	12	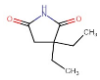	X	✓	X	✓	✓		12.4	No significant difference
4-Ethyl-4-methylpyrrolidin-2-one	13	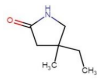	X	✓	X	✓	X		16.5	2-fold lower
3,3-diethylpyrrolidin-2-one	15	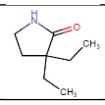	X	✓	X	X	✓		41.6	*** 3-fold lower than Compound 12**
Phensuximide	17	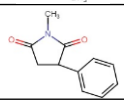	X	✓	✓	✓	✓		9.9	No significant difference
2,5-Pyrrolidinedione,3-ethyl-1,3-dimethyl	18	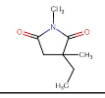	X	✓	✓	✓	✓		29.3	3-fold lower
α-Methyl-α-phenylsuccinimide	9		X	✓	X	✓	✓	**Active and more potent than ethosuxmimide**	4.6	2-fold higher
α,α-Dimethyl-β-methylsuccinimide	14		✓	✓	X	✓	✓		4.7	2-fold higher
Methsuximide	16	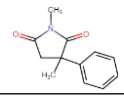	X	✓	✓	✓	✓		4.1	2-fold higher

Table 3.2.19. Summary of primary screens and concentration-response relationships of active compounds. Presence or absence of carbonyl groups (C=O) and other substituents as indicated on the top scaffold are summarized per compound. Note that compound 15 was compared against compound 12 due to a shared R_2 diethyl moiety whereas ethosuximide has a methyl-ethyl one.

3.2.6 SAR of ethosuximide

Knowledge of the SAR of ethosuximide is important for facilitating the development of secondary compounds from the candidate molecule, compound 9. Findings from primary screens and concentration-response assessments performed herein, as summarized in Table 3.2.19, provides an additional and in-house insight into the anticonvulsive SAR of ethosuximide using a non-rodent seizure model. SAR analysis was performed by considering the chemical structures of both active and inactive compounds, and the relative potency differences between active molecules.

Three interpretations were derived from these analyses, which can be illustrated with the scaffold structure shown at the top of Table 3.2.19. Firstly, anticonvulsive activity requires the presence of the R_1 and/or R_2 substituents at the carbon groups. This is supported by the observation that inactive compounds succinimide and compound 7 do not possess these substituents, whereas all active compounds have either one or both.

Secondly, carbonyl (C=O) groups are not essential for anticonvulsive activity *per se*, but they contribute to the potency of the compound. This is best exemplified from compounds 13 and 15 which lack a C=O group at opposing positions. These compounds exhibited 2- and 3-fold reductions of potencies when compared against their carbonyl-intact counterparts. Note that compound 15 was compared against compound 12 instead of ethosuximide due to the shared R_2 diethyl moiety, whereas ethosuximide has a methyl-ethyl one at that position. Although the inactive compound 7 has a missing C=O as well, this interpretation cannot be directly extrapolated from it since the absence of R_1 and R_2 substituents renders it inert.

Thirdly, substituents on the nitrogen atom of the scaffold (R_3) may play a contributory role towards the potency as well as the C=O groups. This can be best demonstrated by the relatively reduced potency of the R_3 methyl-possessing compound 18 against ethosuximide. Compound 4 possesses the same substituent and was also shown to be less potent than ethosuximide, however no direct inferences can be made based on this molecule due to the presence of additional structural disparities relative to the drug. Lastly and

contradictorily enough, the presence of the same substituent did not reduce the potencies of compounds 16 and 17 relative to ethosuximide.

3.2.7 Bioaccumulation of compound 9 in *C. elegans* after an acute treatment

Although compound 9 exhibited a 2-fold enhancement of potency relative to ethosuximide (section 3.2.6), this might be a direct result of improved bioaccumulation in the worms. As predicted from the worm SAM (Burns *et al*., 2010), bioaccumulation scores were -0.643, -0.203, and 0.322 for succinimide, ethosuximide, and compound 9 respectively (Table 3.2.6). As explained previously, it is difficult to get a solid grasp of the bioaccumulation differences between compounds based on assigned scores. Additionally, SAM predictions were not demonstrated to be always accurate. Hence, bioaccumulation of these compounds was addressed experimentally with proton (^{1}H) NMR spectroscopy.

Preliminary 1D ^{1}H NMR analysis of the compounds generated the reference spectra for each of them; succinimide was included for comparison to exclude poor bioaccumulation as a contributory factor for inactivity (Figure 3.2.20). Each compound yielded a unique pattern or signature of peaks deriving from various ^{1}H-containing chemical groups, with different spectral positions or rather, chemical shifts (ppm). Peak patterns and intensities depend on the chemical environment and the number of ^{1}H constituting them. For the best detectable signal-to-noise ratio from worm-derived metabolites, singlet peaks with the highest intensity for each compound were selected for further analysis.

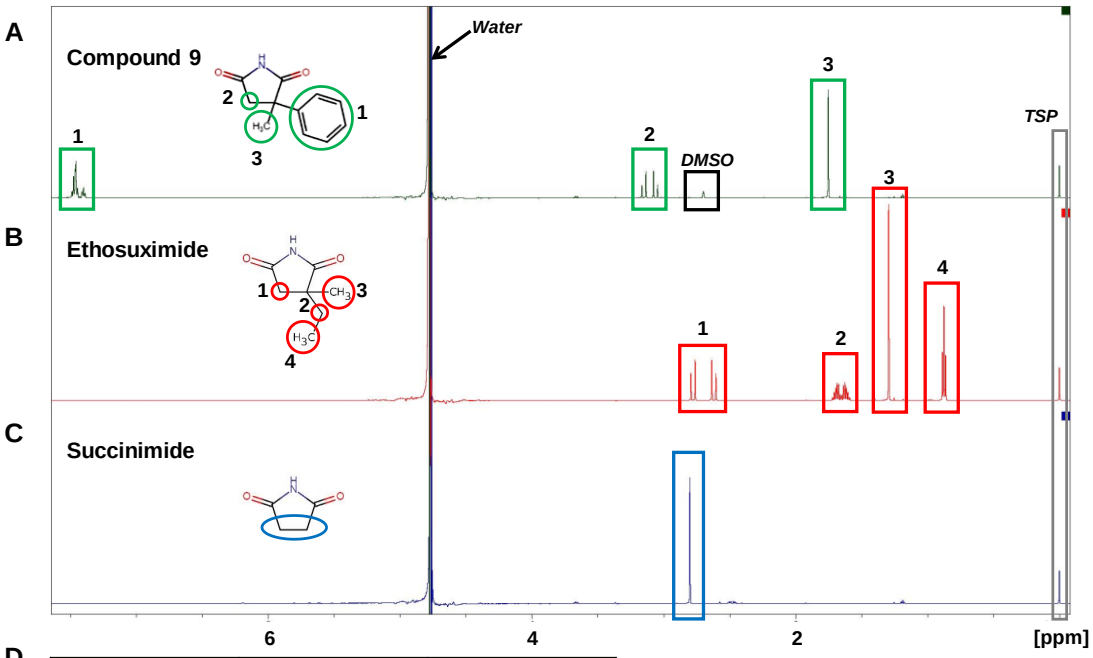

D

Compound	Chemical group no.	^{1}H Chemical shift (ppm)
Succinimide	-	2.820 – 2.787
Ethosuximide	1	2.798 - 2.593
	2	1.730 - 1.580
	3	1.299 – 1.294
	4	0.90 - 0.85
Compound 9	1	7.50 - 7.37
	2	3.18 - 3.03
	3	1.758 -1.746
DMSO	-	2.743 – 2.730

Figure 3.2.20. Compound-derived 1D ^{1}H NMR spectra. One mM solutions of compounds (A, compound 9; B, ethosuximide; C, succinimide) were analysed with 1D ^{1}H NMR spectroscopy. Chemical groups from each compound yielded a distinct pattern of peaks at various chemical shifts, which enables the differentiation of one compound from another; groups and corresponding peaks are numbered. Note that the DMSO-derived peak from the compound 9-derived spectrum was from the residual 1 % protonated component of a 99 % deuterated form of the vehicle used for solubilising the compound. Peaks from protonated water and the reference compound TSP are also indicated. (D) Table indicating spectral regions at which peaks appear. Peaks with the highest intensities were selected for future analysis (peaks number 3 for ethosuximide and compound 9, and singlet peak for succinimide). Data shown was from a single experiment of a single preparations.

To adhere to the liquid-based treatment conditions in the PTZ seizure assay and to scale up the sample size, the protocol was designed for the use of Corning® Costar® Spin-X® tube filters. Acute treatment and sequential washing of the *unc-49* worms were performed in these tube filters, which enable liquid treatments and washes to be filtered out via centrifugation. The initial protocol comprised three sequential washes in the tube filters following treatment to remove compounds from tube filters and worm surfaces. The sufficiency of these washes was evaluated by 1D ^{1}H NMR spectroscopy with succinimide and compound 9 by comparing the residual signals in the final wash, and in extracted metabolites from the worms following the washes. These two compounds were used to evaluate a broad protocol due to their different chemical propensities, as succinimide is water-soluble whereas compound 9 is hydrophobic. Resultant 1D ^{1}H NMR spectra showed detectable levels of both compounds in extracts, however these signals were unlikely to be derived exclusively from the bioaccumulated fractions as traces of the compounds were also distinct in the final wash (Figure 3.2.21). Moreover, levels of compound 9 was evidently higher than succinimide in the final wash, highlighting the difficulty in washing away compounds of a hydrophobic nature with an aqueous buffer.

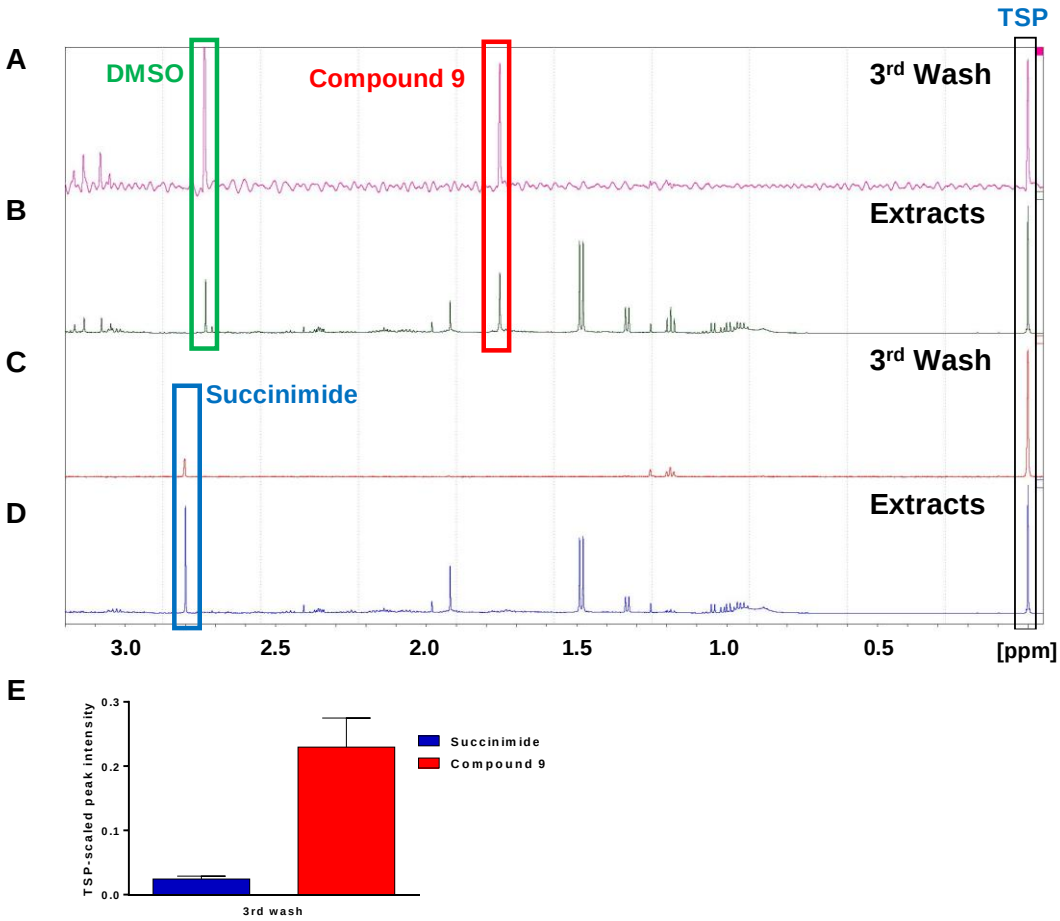

Figure 3.2.21. Comparison of levels of compounds between final washing steps and extracted metabolite fractions. *unc-49* worms were acutely-treated with the optimal 28 mM-corresponding 4 mg/mL seizure-protecting ethosuximide concentration of the hydrophilic succinimide or hydrophobic compound 9, and washed thrice in spin columns prior to metabolite extraction and analysis; final washes were analysed for traces of compounds to assess washing efficiencies. (A – D) Representative spectra showing detectable traces of compounds and the DMSO vehicle from extracted metabolites (A, compound 9; C, succinimide) and final washes (B, compound 9; D, succinimide). (E) A higher amount of compound 9 as compared to relatively low traces of succinimide in final washes suggest ineffectiveness of washing conditions for hydrophobic compounds which can contribute artefact signals to extracts. Data shown is from a single experiment of two technical replicates per condition.

Due to the apparent inadequacy of these wash conditions for hydrophobic compounds, the protocol was further evaluated with compound 9 for a series of ten washes. As mild detergent (0.1 % SDS) was previously utilised to remove adhered compounds from worm cuticle (Burns *et al*., 2010), an additional SDS pre-wash step was also assessed herein. Lastly, a wormless control was included to investigate the level of compound remaining in the tube filter after ten washes. The resultant analysis demonstrated wash-dependent reduction of the compound in both wormless control and treated worms (Figure 3.2.22). The SDS pre-wash was not any more effective at removing the compound, as comparable levels of the compound were present in the pre-wash and first washes from the wormless control and treated worms. In all conditions, levels of the compound started to stabilise from the fifth wash and remained detectable at residual levels in the final wash, suggestive of persisting presence of the compound in tube filters. Post-wash analysis of tube filter contents from the wormless control demonstrated that the compound was still present, highlighting the occurrence of precipitation in the tube filters (Figure 3.2.22). Quite alarmingly, this detected level constituted approximately half of signals from the metabolite extracts of treated worms, revealing that contaminant signals comprise a large proportion of bioaccumulation-derived ones.

Due to the inherent issues associated with the removal of compound 9 from tube filters, the procedure was deemed too prone to error and as such, unfit for the purpose herein. The decision was made to focus on measuring bioaccumulation in chronically-treated samples instead due to the plate-based nature of administering compounds, hence circumventing the issues of compound precipitation in tube filters associated with the liquid-based treatment approach (see chapter 4).

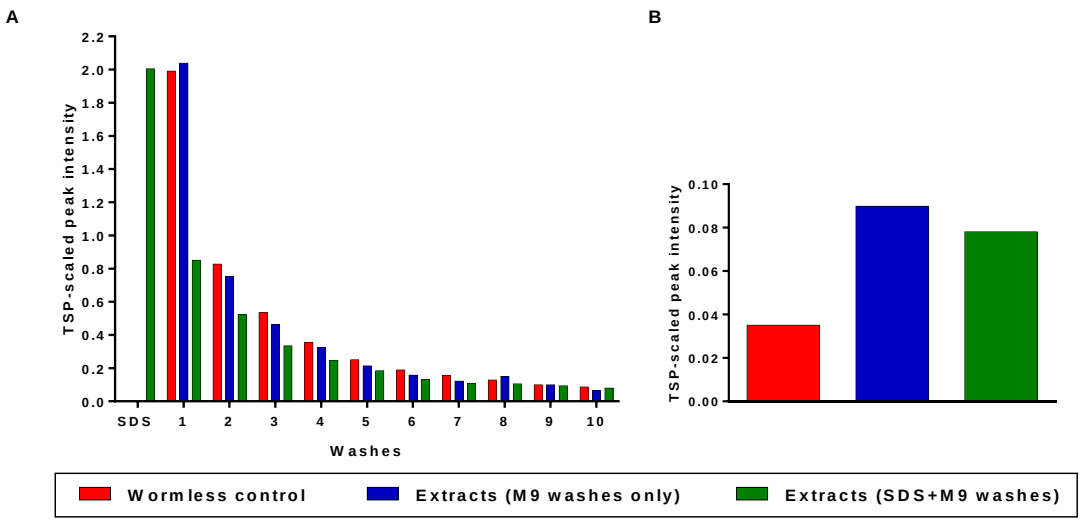

Figure 3.2.22. Optimising washing conditions for hydrophobic compound 9. (A) A series of washes with M9 buffer alone or with an additional detergent pre-wash with 0.1 % SDS were performed in tube filters on acutely-treated *unc-49* worms and a wormless compound 9 solution control. Detected levels of the compound started to stabilise from the fifth M9 wash, which were consistently present even by the final wash. (B) A residual amount of the compound remained detectable from the wormless control after all washes. This contaminant signal constituted approximately half of signals from the extracted metabolites of treated worms. Data shown is from a single experiment of single preparations.

3.3 DISCUSSION

In addition to identifying a candidate molecule, compound 9, which exhibited a 2-fold enhancement of anticonvulsive potency than ethosuximide, findings herein have also provided an in-house assessment of the SAR of succinimide-like compounds. These SAR observations facilitate appropriate structural modifications to be made to compound 9 to generate further derivatives with enhanced potencies. To verify that enhanced potency of the compound was not due to better bioaccumulation than ethosuximide, a protocol was designed to measure bioaccumulated concentrations in *unc-49* worms via 1D ^{1}H NMR spectroscopy following acute treatment in tube filters. However, the hydrophobic nature of the compound resulted in problematic artefact signals which were difficult to remove, hence the work was halted and a decision was made to focus on determining bioaccumulation after chronic treatments instead (see chapter 4). At this point, the bioaccumulations of compound 9 and ethosuximide may be assumed to be quite similar from worm SAM-predicted bioaccumulation scores

An obvious caveat of using the PTZ-induced seizure assay as a primary screening platform herein is the inability to infer information about the neuroprotective qualities of screened compounds. However, associations between seizures and neurodegenerative diseases have been reported in both humans and animal models, suggesting the potential utility of the platform as a predictive tool for neuroprotectiveness. For instance, seizures are a common clinical manifestation of the neuronal ceroid lipofuscinoses (Schulz *et al*., 2013), and although rare, have also been reported in PD patients as well (Son *et al*., 2016). Epidemiological studies have also reported increased prevalence or incidence of seizures in AD patients (Sjogren *et al*., 1952, Letemendia and Pampiglione, 1958, Sulkava, 1982, Hauser *et al*., 1996, Amatniek *et al*., 2006, Heyman *et al*., 1987, Romanelli *et al*., 1990, Risse *et al*., 1990, Förstl *et al*., 1992, Mendez *et al*., 1994, Volicer *et al*., 1995, Samson *et al*., 1996, Lozsadi and Larner, 2006, Scarmeas *et al*., 2009, Rao *et al*., 2009, Bernardi *et al*., 2010, Bell *et al*., 2011, Irizarry *et al*., 2012, Vossel *et al*., 2013, Imfeld *et al*., 2013, Sherzai *et al*., 2014, Cook *et al*., 2015, Cheng *et al*., 2015). In a transgenic mutant human APP-overexpressing J20 AD mouse model, spontaneous and

abnormal non-convulsive spike discharges were also frequently detected in various brain regions via EEG, including the hippocampus which is pathologically affected in AD (Palop *et al*., 2007).

As seizures have not been reported for other neurodegenerative disorders, it appears they might be disease-specific. However, various evidence has pointed towards the causative role of seizures in neuronal damage. For example, in induced rodent models of seizures elicited by the administration of various proconvulsive agents including PTZ, behavioural deficits associated with learning and memory and hippocampal damage have been observed (Jia *et al*., 2006, Muller *et al*., 2009, Groticke *et al*., 2008). Although PTZ-evoked seizures in the worms herein were only scored over a short duration of 30 s, evidence has shown that even brief single non-convulsive seizures were sufficient to induce brain neuronal apoptosis in rodent models (Bengzon *et al*., 2002). This suggests that compounds conferring seizure protection may also by extension possess potential neuroprotective properties, although this would likely only be applicable to neurodegenerative conditions with an underlying seizure pathology; however subclinical seizures may also be present in other forms of neurodegeneration. Note that the predictive power of this assay for neuroprotectiveness will be briefly explored in the following chapter.

SAR findings herein showed that R_1 and/or R_2 substituents are essential for anticonvulsive activity, and that intact C=O groups are important for preserving potency. These are in agreement with findings from Poupaert *et al* (1984), which demonstrated reduced potencies against MES-induced seizures in rodents from succinimide derivatives with only one C=O group in comparison to counterparts which have both intact C=O groups. In contrast, compound 15 which possess only one C=O group was demonstrated to mediate a larger lifespan extension effect in WT worms as compared to ethosuximide (Evason *et al*., 2005), although SAR findings in the current study showed a lower anticonvulsive potency; this suggests that SAR findings herein might be specific to anticonvulsant properties.

Quite intriguing was a key observation from a series of studies performed by Klunk *et al* that anticonvulsant activity depended on either R_1 or R_2 alkyl

substituents, whereas the presence of alkyl substituents at both positions induced a switch to proconvulsant activity (Klunk *et al*., 1982a, Klunk *et al*., 1982b, Klunk *et al*., 1982c). These anti- and pro-convulsant activities were assessed in a number of ways in mice and guinea pigs, such as the convulsive behaviours of mice, EEG monitoring of epileptic discharges in guinea pig brains, electrical activity of guinea pig hippocampal slices, and seizures induced by the standard methods PTZ and MES in addition to those evoked by known convulsant agents picrotoxin, bicuculline, and compounds shown to exhibit proconvulsant activities in the studies. In contrast, a series of pre-existing studies contradicted these observations by demonstrating anticonvulsant activities in rodent MES and scPTZ tests by R_1 and R_2 substituted derivatives (Miller *et al*., 1951, Miller and Long, 1953). The reason for these discrepancies are unclear, but it could be attributed to differences in the type and number of substituents at these positions. Pertaining to findings herein at least, the proconvulsant activity of compound 14, which fulfils the structural criteria of both R_1 and R_2 substituents, was previously verified in an *in vitro* seizure model whereby it exacerbated spontaneous discharges in rodent thalamocortical slices which resembled patterns observed in generalized seizures (Zhang *et al*., 1996b). However, compound 14 protected against PTZ-induced seizures in the worms at a two-fold enhanced potency in comparison to ethosuximide herein. Additionally, compound 13 was previously reported by Klunk *et al* to exhibit proconvulsant activity, which again contradicted with the demonstrated anticonvulsant activity of the compound herein. Reasons for the reported differences in activities of these molecules are unclear, but a likely explanation could be the use of rodents in the contradicting studies versus the use of *C. elegans* herein to evaluate the pro- or anti-convulsant properties of these molecules. Many AEDs have been documented to block seizures through the inhibition of voltage-gated sodium channels (Lasoń *et al*., 2013), so it is possible that these proconvulsant effects may be elicited through the activation of these channels. However, *C. elegans* do not express these channels (Hobert, 2013), which might explain the absence of proconvulsant effects from these molecules herein. Another possibility is the absence of the inhibitory GABA receptor in *unc-49* worms due to the null mutation in the GABA receptor-encoding *unc-49* gene (Bamber *et*

al., 1999). As hypothesized by by Klunk *et al*, proconvulsant substituents mediate seizure induction by enabling binding to the picrotoxin site at $GABA_A$ receptors and blocking inhibitory chloride ion flow through the receptor. A homomeric form of the *unc-49* GABA receptor is also picrotoxin-sensitive (Bamber *et al*., 1999), but since the gene has a null mutation in this strain, compounds 13 and 14 were unable to exert their proconvulsant effects. These hypotheses seem to suggest that subtle structural differences can shift the binding preference and mode of activity at the preferred binding site, and when preferred sites are absent compounds may adopt other sites and different modes of activity.

SAR findings herein suggest a less obvious role of the nitrogen in the succinimide backbone, as methyl substituents on it were demonstrated to preserve (compound 17; phensuximide), reduce (compounds 4; trimethadione, and 18), and enhance (compound 16; methsuximide) potencies in comparison to ethosuximide; AEDs as named. Corroborating the observation on compound 18, N-methylation of succinimide derivatives was reported to reduce potencies (Poupaert *et al*., 1984, Klunk *et al*., 1982c). However, a separate series of studies demonstrated protection against MES-induced seizures and to a lesser extent, PTZ-induced seizures, in rodents by diverse set of N-substituted succinimide derivatives (Kaminski and Obniska, 2008, Kaminski *et al*., 2013, Obniska *et al*., 2009, Obniska *et al*., 2010, Obniska *et al*., 2012, Rybka *et al*., 2014). However, a key observation from one such study from this series seemed to lend some support to the importance of the unsubstituted nitrogen of the succinimide backbone in retaining anticonvulsive activity (Obniska *et al*., 2012). In the study, N-substituted derivatives protected against MES-induced seizures in rodents only when R_1/R_2 substituents were diphenyl or methylphenyl moieties, whereas the presence of an alkyl methyl-ethyl moiety abolished seizure protection. As ethosuximide has the same alkyl substituent as well, taken together this corroborates observations herein with compound 18, which is essentially an N-methylated derivative of the drug. However, findings from these studies showed that anticonvulsive activity depended on the type of structural modifications at both nitrogen and R_1/R_2 positions. As modifications at these structural positions were made

concurrently, it was difficult to establish the molecular requirements for activity and potency. In addition, it should also be noted that anticonvulsant activities were mostly assessed singularly in the rodent MES test. When compounds were assessed in both MES and scPTZ tests, most compounds only protected against seizures in the former but not the latter. As compounds in the current study were studied for their protective activities against PTZ-induced seizures, albeit in *C. elegans*, this raises questions about the applicability of SAR findings from this series of studies to the work performed herein. Despite this caveat, these studies demonstrated that the type of nitrogen and R_1/R_2 modifications collectively influence the anticonvulsant activity and potency of a molecule. Pertaining specifically to observations herein, however, the loss of activity observed with the N-methylated compound 18 may be explained by the loss of the ionisable N-bonded hydrogen which likely partakes in hydrogen bonding of the molecule to its target, resulting in a reduced affinity and consequent reduced potency.

The other N-methylated compounds herein are AED prodrugs trimethadione, methsuximide, and phensuximide, which require N-demethylation for their active metabolites to exert anticonvulsant activity (Porter *et al*., 1979, Chamberlin *et al*., 1965). The observed discrepancies in the potencies with these compounds herein can be attributed to a combination of ADME-related factors such as the N-demethylation rate to active metabolites, half-lives of these metabolites, and rate of elimination in the worms over the drug and PTZ treatment window. As aforementioned, it is noteworthy that the candidate molecule compound 9 is the N-demethylated active metabolite of methsuximide (Dobrinska and Welling, 1977, Nicholls and Orton, 1972, Muni *et al*., 1973). Although both molecules exhibited similar anti-seizure potencies, the active metabolite was selected as the candidate compound since prodrug activation is not required. Additionally, it has an extremely long reported half-life of 38 hours as opposed to 1.4 hours for methsuximide, and good accumulation in human plasma at levels averaging about 700-fold higher than its parent molecule in patients on chronic methsuximide treatment (Porter *et al*., 1979, Strong *et al*., 1974). Taken together, this suggests that retention of the -NH group is important at least for the current derivatives which do not yet

deviate far away from the succinimide backbone. However, as exemplified above by the series of studies which demonstrated seizure protection from diverse N-substituted succinimide derivatives (Kaminski and Obniska, 2008, Kaminski *et al*., 2013, Obniska *et al*., 2009, Obniska *et al*., 2010, Obniska *et al*., 2012, Rybka *et al*., 2014), further comprehensive SAR analyses will have to be carried out with secondary compounds synthesized from the selected candidate compound 9.

As a further point of discussion, SAR requirements uncovered in the current study do not corroborate with the chemical structures of the structurally-similar AED levetiracetam (Figure 3.3.1). Although levetiracetam lacks R_1 or R_2 substituents which are inferred herein to be essential for anticonvulsive activity, the drug has a broad spectrum of anticonvulsive activity and is effective against generalized and focal seizures. Additionally, the drug possesses a single C=O group and an N-substituent. Levetiracetam is effective in the electrically-induced 6-Hz pyschomotor rodent seizure model, which is predictive for focal seizures and possibly for pharmacoresistant epilepsy as well (White, 2003, Löscher, 2011). However, it is not active in the gold standard MES and scPTZ seizure models. Conversely, ethosuximide displayed a 9-fold reduced potency in the 6-Hz model as compared to levetiracetam (Obniska *et al*., 2012), and is effective in the scPTZ but not MES model. It should be noted that in addition to both drugs, no one AED exhibits uniform activity across seizure models (White, 2003, Löscher, 2011). Additionally, levetiracetam but not ethosuximide reduced the EEG-detectable non-convulsive spike discharges In the brains of the APP-overexpressing J20 AD mouse model as mentioned previously (Sanchez *et al*., 2012). Taken together, this suggests that both the PTZ seizure model used herein and SAR findings obtained from it may only be applicable to a select group of compounds like the succinimide-based compounds. Furthermore, it emphasizes the complexity of trying to extrapolate SAR information from studies performed in different seizure models.

In conclusion, SAR findings herein are useful in facilitating the development of secondary compounds from the candidate molecule compound 9, but this information might only pertain specifically to anticonvulsant activity against

PTZ-induced seizures, and might not be extrapolated fully for neuroprotection. Further comprehensive SAR studies are required in the future for secondary compounds generated from compound 9.

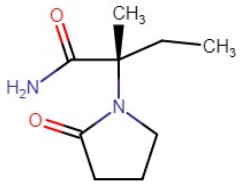

Levetiracetam

Figure 3.3.1. Chemical structure of levetiracetam.

CHAPTER 4

NEUROPROTECTIVE AND LIFESPAN-EXTENDING EFFECTS OF COMPOUND 9

4.1 INTRODUCTION

4.1.1 Neuroprotective effects of AEDs

In addition to the neuroprotective and lifespan extending effects of ethosuximide (Chen *et al*., 2015b, Tiwari *et al*., 2015, Evason *et al*., 2005, Tauffenberger *et al*., 2013, Collins *et al*., 2008), a number of other AEDs have been reported to protect against neurodegeneration associated with seizures, strokes, ischemia, and traumatic brain injury in experimental models (Trojnar *et al*., 2002, Pitkanen and Kubova, 2004, Czuczwar *et al*., 2007).

In neurodegenerative disorders *per se*, protective effects of a handful of AEDs have been reported. Of these, the structurally-unrelated broad-spectrum AED valproic acid has been most extensively studied and its neuroprotective actions have been shown in models of ALS, PD, AD, spinocerebellar ataxia type 3, and spinal muscular atrophy which were generated in cells, *C. elegans*, and rodents (van Bergeijk *et al*., 2006, Pan *et al*., 2005, Kautu *et al*., 2013, Teixeira-Castro *et al*., 2011, Qing *et al*., 2008, Yi *et al*., 2013, Rouaux *et al*., 2007, Crochemore *et al*., 2009, Sugai *et al*., 2004, Monti *et al*., 2010, Monti *et al*., 2012, Kidd and Schneider, 2011, Ximenes *et al*., 2015, Carriere *et al*., 2014). Valproate also extended the lifespan of WT *C. elegans* (Evason *et al*., 2008), although these longevity effects were not apparent in rodent ALS models (Rouaux *et al*., 2007, Crochemore *et al*., 2009). Trimethadione, an AED which is structurally-similar to ethosuximide, was once prescribed for the treatment of absence seizures but is now no longer in use due to its associated toxicity. It was reported to effect lifespan extension in WT worms (Evason *et al*., 2005) and protected against cell death of primary mouse hippocampal and cortical neuronal cultures (Wildburger *et al*., 2009a). Last but not least, the broad-spectrum AED levetiracetam was previously shown to ameliorate PD-associated behavioural deficits, dopamine neuronal losses, and oxidative stress in a rotenone-induced model of PD in rats (Erbaş *et al*., 2016). Levetiracetam was also shown to alleviate the dyskinesia which is associated with L-DOPA treatment of PD in a MPTP-induced primate PD model (Bezard *et al*., 2004). In a transgenic mutant human APP-overexpressing J20 AD mouse model, the drug protected against behavioural, cognitive, and hippocampal synaptic defects (Sanchez *et al*., 2012). In human studies, it was

most recently reported to normalize aspects of abnormal EEG patterns in a small group of mild AD patients, although cognitive improvements were not evident (Musaeus *et al*., 2017).

Some AEDs possess neuroprotective properties and have the potential to be repurposed as treatments for neurodegenerative disorders and other conditions associated with neuronal damage, such as stroke. Additionally, their chemical diversities and rich pharmacologies, especially of the new generation AEDs, also meant that they have the potential to be used as treatments for other conditions as well, as exemplified for instance by their protective effects in neuropathic pain and mood disorders (Bialer, 2012b). As neither methsuximide nor compound 9 have been yet documented to mediate neuroprotective and/or lifespan-extending effects, it will be interesting to assess these properties of compound 9 herein and to compare them with its succinimide family member ethosuximide.

4.1.2 Drug chirality

Chirality occurs when the mirror images of a molecule are non-superimposable. Chiral molecules or enantiomers possess chiral centres, which are usually but not exclusively carbon atoms. Different substituents bonded to such chiral centres have different spatial arrangements which leads to the configurational designation of enantiomers as either *R* or *S* based on the Cahn-Ingold-Prelog priority (CIP) system (Cahn *et al*., 1956). Additionally, enantiomers are also optical isomers designated + or - depending on the right or left rotation of plane-polarized light respectively. Aside from the direction of plane-polarized light, enantiomers share the same empirical formula and chemical and physical properties.

Chirality is an important parameter for consideration in the development of new drugs, as enantiomers can have different pharmacological activities, toxicities, ADME properties and pharmacokinetics (Nguyen *et al*., 2006). These properties determine if a drug is to be introduced as a racemic mixture of both enantiomers or as an enantiopure treatment. With regard to pharmacological activity, it is less common for both enantiomers to possess equal activity, whereas one enantiomer is usually the primary active species whilst the other

is less active or completely inactive. On the other hand, identical or different toxic or side effects may reside in one or both enantiomers, and is not exclusive to only the bioactive species; differential toxicity may also be mediated from chiral drug-derived metabolites.

Such chiral differences can be exemplified by the drug (*R*)-(-)-apomorphine, a nonselective dopamine receptor agonist which is approved for PD treatment (Quinn, 1995). Unlike (*R*)-(-)-apomorphine, its enantiomer (*S*)-(+)-apomorphine does not stimulate these receptors (Lehmann *et al*., 1983). Additionally, whilst emesis is an undesired side effect of (*R*)-(-)-apomorphine, this was not induced with (*S*)-(+)-apomorphine even at 10-fold higher doses when administered to dogs (Saari *et al*., 1973). A noteworthy study with (*S*)-(+)-apomorphine exemplifies the importance and utility of chiral consideration in developing new therapies for neurodegeneration (Mead *et al*., 2013). In that study, the therapeutic potential of immobilizing the NFE2-related factor 2 (Nrf2)-antioxidant response element (ARE) antioxidant pathway as a neuroprotective strategy against ALS was investigated. Compound screens for Nrf2-ARE inducing activity via a reporter cell line unveiled (*R*)-(-)-apomorphine as a hit molecule, and additional screening of (*S*)-(+)-apomorphine demonstrated equipotent Nrf2-ARE activation. Due to the lack of undesirable side effects associated with (*R*)-(-)-apomorphine, (*S*)-(+)-apomorphine was selected for further evaluation and was shown to protect against oxidative stress-induced losses of both primary motor neurons fibroblasts from mice and ALS patients respectively. Furthermore, it ameliorated motor function decline in an ALS mouse model. Given the preferable pharmacological tolerability of (*S*)-(+)-apomorphine and its demonstrated Nrf2-ARE activation and neuroprotection against oxidative stress in the various ALS models, it was deemed a more attractive and obvious candidate for clinical testing as an ALS therapeutic since dosing can be performed with an improved safety margin.

Given the importance of considering chirality-associated implications as illustrated above, regulatory agencies around the world have established mandatory guidelines to enforce chiral assessments of potential drugs before they are introduced into the market (Strong, 1999, Daniels *et al*., 1997).

Ethosuximide is a chiral drug and is used in its racemic form for the treatment of absence seizures. Although the pharmacological activities of its enantiomers have not been individually assessed and compared, the chiral aspects of its ADME and pharmacokinetics have been previously studied. For instance, enantioselective metabolism and elimination of (*R*)-ethosuximide was previously shown in rats (Mifsud *et al*., 2001). In humans, however, both enantiomers were detected at roughly equivalent ratios in blood plasma, suggesting the lack of enantioselective metabolism and elimination (Villen *et al*., 1990, Tomson and Villen, 1994). Unlike ethosuximide, the chiral characteristics of methsuximide or its active metabolite α-methyl-α-phenylsuccinimide (compound 9) remain unexplored.

4.1.3 Chapter aims

As neuroprotective and longevity properties of compound 9 or its AED prodrug methsuximide have not been documented, the primary aim of the current work is to investigate these characteristics of the compound in the CK426 *C. elegans* ALS model. As additionally discussed in the preceding chapter, the potential predictive value of the PTZ-induced seizure assay in the GABA-defective *unc-49* strain will be further explored herein. Lastly, in view of the importance of chirality on various aspects of a molecule's properties, a secondary aim is to derive enantiomers of compound 9 for further comparisons of their biological properties.

4.2 RESULTS

4.2.1 Generating enantiomers of compound 9

As detailed in the preceding chapter, compound 9 was the candidate molecule selected for further derivation of compounds with enhanced neuroprotective efficacies and/or potencies. However, as highlighted, the neuroprotective properties of the molecule remained unelucidated at this point due to the utilisation of the PTZ-induced seizure assay as the primary screening platform. As the compound was screened in its racemic form, and due to potential pharmacological and toxicological differences between enantiomeric forms as aforementioned, the objective herein is to obtain the separate enantiomers of the compound to facilitate a more thorough investigation of its neuroprotective features.

Direct enantiomer separation from a racemate can be performed with a preparative chiral high performance liquid chromatography (HPLC) column, however it was not possible for the current study due to the unavailability of this equipment. Additionally, this approach is associated with high costs and low yield. Hence, the synthesis route was taken to first derive the (*R*)-enantiomer via a series of three reactions as adapted from reported procedures (Shintani *et al*., 2006, Carniato *et al*., 2009). As described previously (chapter 2, section 2.5.2), the process involved initial generation of 1-benzyl-3-methylmaleimide, an N-benzylated substrate for chiral synthesis; N-benzylation blocks nitrogen from partaking in bonding reactions. This was followed by the stereospecific derivation of N-benzylated isomers *(R)*-compound 9 and *cis*/*trans*-1-benzyl-3-methyl-4-phenylsuccinimide from the substrate. In the last reaction of the series, $AlCl_3$-mediated N-debenzylation was attempted to remove the N-benzyl blocking group from N-benzylated *(R)*-compound 9 and *trans*-1-benzyl-3-methyl-4-phenylsuccinimide; compounds eluted closely and separated easily from the *cis* isomer. Removal of the lipophilic benzyl group at this stage will enhance polarity differences between the two compounds and facilitate separation of *(R)*-compound 9. Despite the success of N-debenzylation, however, *(R)*-compound 9 was not recovered for further investigation due to the tiny scale of the reaction which meant that recovered amounts will be minute. Unfortunately, further repeats were not

made on a larger scale, hence subsequent analysis of neuroprotection and lifespan extension herein were carried out with the racemate. Regardless, this provides a proof of concept for future replication of the procedure.

4.2.2 Rationale for utilising the CK426 ALS model and characteristics of TDP-43 pathology

Despite the unfeasibility of the CK10 FTDP-17 and *dnj-14* ANCL models for primary screens as described in preceding chapters, they are potential platforms for investigating the neuroprotective and lifespan-extending properties of compound 9. A key objective herein was to address the direct protective effect of the compound against neurodegeneration by assessing the integrity of the GABAergic D-type inhibitory motor neuronal subtype, since these neurons play a key role in mediating worm locomotion (Jorgensen, 2005, McLntire *et al*., 1993). GABAergic-specific expression of fluorescent markers would be required to study this. Hence, these models were unsuitable for the following reasons: 1) Previous attempts to express GFP in GABAergic neurons of the CK10 strain for this purpose demonstrated reversion to WT which was evident from intact neurons and WT thrashes. 2) Degeneration of these neurons manifest in *dnj-14* worms around adulthood day 9 (Kashyap *et al*., 2014). Due to the shortened lifespan of the strain, it was technically challenging to propagate sufficient worms up to this age and older ages to assess age-dependent changes in neuronal integrity. For such reasons, an alternative model had to be considered.

We decided to use a transgenic model of ALS, the CK426 strain, which was generated and kindly donated by our long-standing collaborator, Dr. Brian Kraemer (University of Washington, USA), as neuronal imaging work was previously described for this particular model (Liachko *et al*., 2010). The CK426 strain pan-neuronally expresses an *snb-1* promoter-driven A315T missense mutation in the TDP-43-encoding gene *TARDBP* which was identified in familial ALS (Gitcho *et al*., 2008, Sreedharan *et al*., 2008). Characterisation of this model was performed in comparison against WT worms and the CK405 transgenic control strain which express WT human TDP-43 (Liachko *et al*., 2010). Although CK405 transgenic control strains had

reduced lifespans and mild locomotion defects which exacerbated progressively with age in comparison to WT worms, these phenotypes were considerably augmented with the CK426 worms. When the integrity of the GABAergic D-type inhibitory motor neurons was assessed, CK405 control worms did not exhibit significant neurodegeneration in comparison to non-transgenic WT controls, whereas cell body losses and neuronal breaks were evident in the CK426 worms. These features of the CK426 worms mimic the shortened lifespan, motor deficits, and extensive neurodegeneration of ALS patients, hence recapitulating various aspects of the human disease. Importantly, the lifespan-extending and neuroprotective effects of ethosuximide were previously demonstrated in this model in a separate study (Tauffenberger *et al*., 2013), providing strong support to the justification of its use herein.

Longevity and direct neuroprotective effects of compound 9 can be investigated by the standard analyses of lifespans and neuronal integrity respectively. However, assessment of its protection against locomotory defects is less straightforward, as a suitable phenotypic readout with a good signal-to-noise ratio must be selected to best distinguish these effects. Preliminary work performed by Matthew Pontifex (University of Liverpool) compared the suitability of liquid thrashing and body bend frequencies as locomotion readouts. As the CK426 ALS worms mostly do not thrash at all in liquid as compared to WT and CK405 controls, the thrashing phenotype is hence a poor readout for distinguishing the effects between treatments (Figure 4.2.1). Body bend frequency on solid medium was assessed with the different treatments (Figure 4.2.1). CK426 worms exhibited markedly reduced body bend frequency than CK405 controls. Neither ethosuximide nor compound 9 had any effect on the body bend frequency of the CK405 controls. In contrast, movement was significantly improved with both compounds in CK426 worms, demonstrating the feasibility of using body bends as a readout for assessing the treatment effects on locomotion. Additionally, this provides the first evidence of the neuroprotective effects of compound 9.

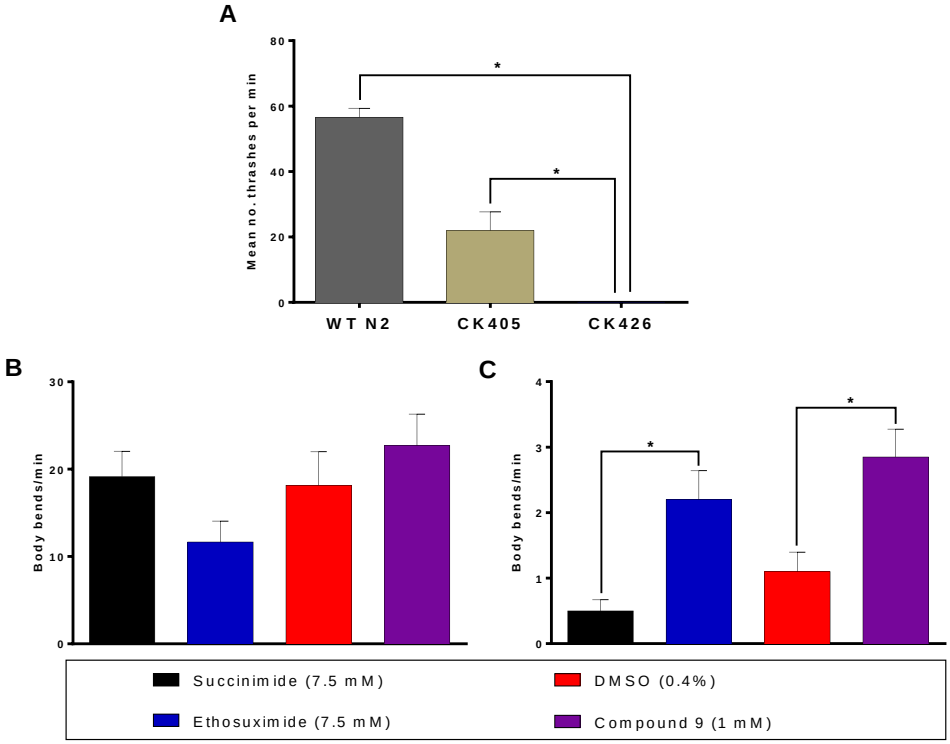

Figure 4.2.1. Assessment of suitable locomotory readout for CK426 ALS worms. (A) CK426 worms exhibited little to no thrashes in liquid as compared to WT N2 and CK405 WT human TDP-43-expressing transgenic control ($p<0.05$). Body bend frequencies of (B) CK405 controls and (C) CK426 ALS worms on solid medium were assessed as a locomotory readout. Body bend frequencies of (B) CK405 controls were not affected by treatments ($p>0.05$), whereas (C) improvements in CK426 worms were mediated by ethosuximide and compound 9 ($p<0.05$); note the different *y*-axis scales. CK405 thrashing data was derived from a single experiment (n = 10), whereas N2 and CK426 data were pooled from two biological replicates (n = 28 - 30). CK405 (n = 20) and CK426 (n = 13 - 15) body bend data were pooled from three and four biological replicates respectively; *, $p<0.05$.

Note that in addition to a lack of liquid thrashing and reduced body bends on solid agar, the CK426 worms exhibited apparent uncoordinated movement, partial paralysis, and a coiling phenotype. However, locomotory defects were observed to vary between batches, and appeared to improve after several generational propagations, potentially a result of genetic drift. To counteract this phenomenon, the worst moving worms were selected at each propagation, and new frozen stocks utilised whenever required.

4.2.3 Compound 9 is neuroprotective and lifespan-extending

Preliminary data on the body bend readout above evidenced the neuroprotective effect of compound 9 in CK426 ALS worms (Figure 4.2.1). However, a comprehensive concentration-response evaluation was required to enable an elaborate assessment of the compound's protective properties. To get an idea of the range of concentrations that could be assessed, preliminary re-assessment of the body bend readout with a 20-fold lower 0.05 mM concentration of the compound revealed an improvement even at this lower concentration. To proceed from this, the concentration-response relationship of the compound was evaluated to identify the optimal neuroprotective concentration. Findings showed that the concentration-response relationship was not established at younger ages of adulthood days 1 and 3, whereby none of the assessed concentrations significantly improved the locomotion defect of the worms (Figure 4.2.2). At older ages of days 5 to 9, the concentration-response relationship became more pronounced up to logarithmic concentrations (M) of -4.6 (0.025 mM) and/or -4.3 (0.05 mM) which ameliorated body bend frequencies. Further increases in the treatment concentration had negative instead of additional protective effects as locomotion rates declined, albeit seemingly to baseline levels. Hence, it appears that high concentrations used abolish the protective effects of the compound rather than inducing toxicity, as no differences in behaviour were displayed from worms treated at these concentrations in comparison to counterparts treated with lower concentrations. From these experiments, 0.05 mM was selected as the optimal concentration to be carried forward with further evaluations of the compound's properties. Comparisons of the compound's neuroprotective effects were made with a 160-fold higher

concentration of 8 mM ethosuximide which was identified to be the optimal neuroprotective concentration from concentration-response assessments performed previously with the same locomotory readout by Matthew Pontifex (University of Liverpool); note that this corresponds approximately to the optimal neuroprotective concentration of 1 mg/mL in previous work carried out with the CK10 and *dnj-14* strains (Chen *et al*., 2015b).

At these optimal concentrations, both compound 9 and ethosuximide improved the frequency of body bends made by the CK426 worms (Figure 4.2.3). Additionally, these effects were exerted to a comparable extent between the two compounds despite the considerable 160-fold difference of the concentrations given.

As aging is intimately linked with the development of neurodegenerative diseases, the longevity effect of the compound was also investigated. Despite the protective effects of ethosuximide on locomotion, the drug failed to mitigate the shortened lifespan of these worms as it only induced an insignificant 5 % increase of the mean lifespan in comparison to succinimide (Figure 4.2.4). In contrast, compound 9 increased the mean lifespan by 25 % as compared to the DMSO controls. This effect from the compound was shown to be significant.

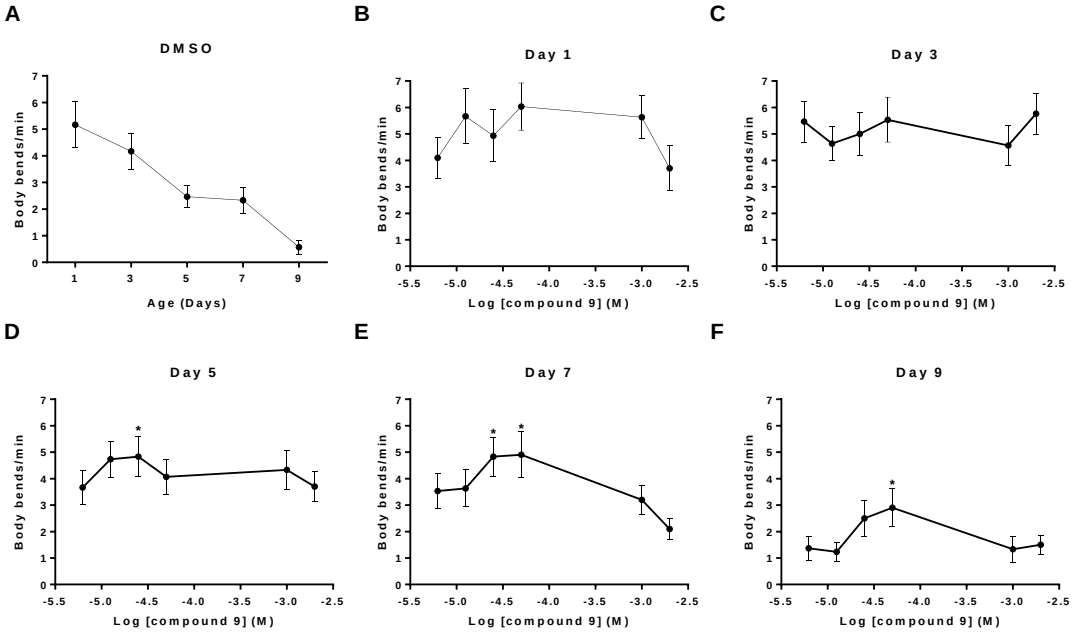

Figure 4.2.2. Concentration-response relationship of compound 9. Body bend frequencies of chronically-treated, age-synchronised CK426 ALS worms were assessed to determine the concentration-response relationship of the compound at various ages of adulthood. (A) Body bends of control worms treated with the 0.4 % DMSO vehicle (0 M compound) at all ages. Although control values were not incorporated into concentration-response curves on the logarithmic scale as a logarithmic value cannot be obtained for 0 M of the compound, body bend frequencies for each day were compared against respective control values. Locomotion defects were not ameliorated at any concentration on (B) days 1 and (C) 3 ($p>0.05$). (D - F) At older ages, locomotion rate was significantly improved with logarithmic concentrations (M) of -4.6 (0.025 mM) and/or -4.3 (0.05 mM) ($p<0.05$), although higher concentrations reduced it instead. Data shown was pooled from three biological replicates, and comparisons were made with the Kruskal-Wallis test with Dunn's multiple comparisons (n = 30 per day per concentration); *, $p<0.05$.

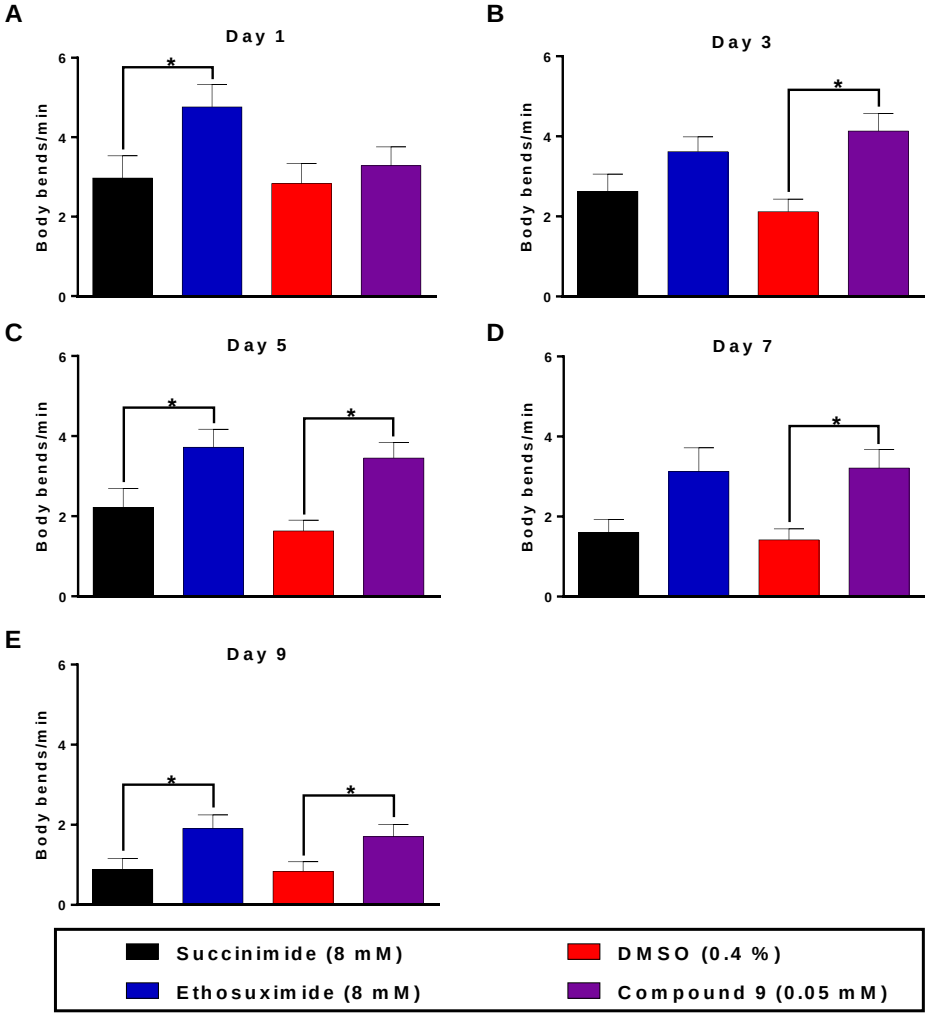

Figure 4.2.3. Compound 9 ameliorates locomotion defects of the CK426 ALS strain. Age-synchronised worms were chronically treated with 8 mM succinimide or ethosuximide, 0.4 % DMSO vehicle, or 0.05 mM compound 9 in 0.4 % DMSO from the L1 larval stage. Ethosuximide improved the frequency of body bends at most ages except days (B) 3 and (D) 7, whilst compound 9 consistently ameliorated locomotion from day 3 onwards (B-E; $p<0.05$). Comparisons were performed via the Kruskal-Wallis test with Dunn's multiple comparisons; *, $p<0.05$. Data shown was pooled with contributions from Matthew Pontifex (University of Liverpool). Number of biological replicates for pooled data and *n* (per day per treatment); four, *n* = 40, ethosuximide (days 7 and 9) and succinimide; five, *n* = 60, ethosuximide (days 1 to 5); six, *n* = 60, DMSO and compound 9 (days 1 to 7)

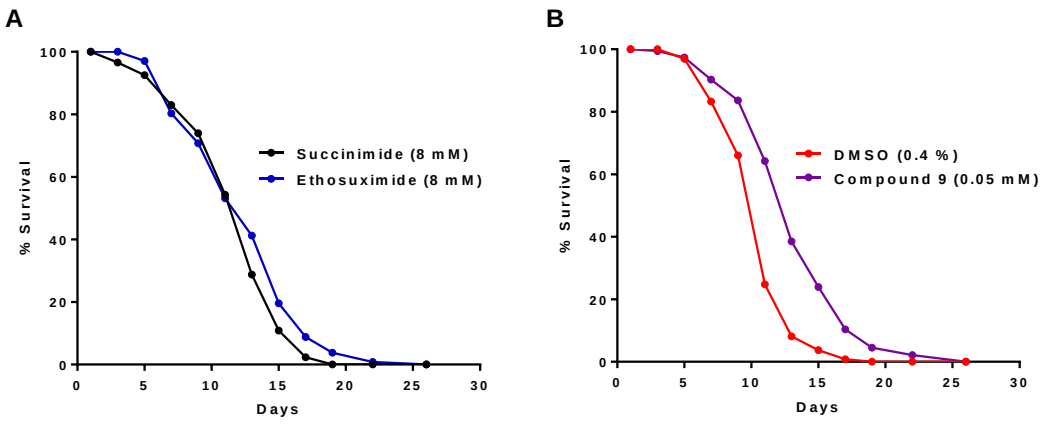

Figure 4.2.4. Compound 9 extends lifespan of the CK426 ALS worms. Lifespan analyses were performed on age-synchronised worms chronically treated from the L1 larval stage onwards. Worms were scored as dead in the absence of pharyngeal pumping or response to touch, with physically damaged and bagged worms censored from analysis. (A) Ethosuximide had no effect on the lifespan ($p>0.05$), (B) whereas compound 9 improved the longevity of the worms when compared to the DMSO control ($p<0.05$). Mean lifespans (number of adulthood days) are as follows: succinimide, 12.45 ± 0.37 (n = 141); ethosuximide, 13.08 ± 0.39 (n = 139); DMSO, 11.51 ± 0.35 (n = 131); compound 9, 14.37 ± 0.41 (n = 138). Data shown was pooled from three biological replicates, with comparisons of lifespans carried out with the log-rank test. Total n per biological replicate; first replicate, 39 succinimide, 42 ethosuximide, 36 DMSO, 46 compound 9; second replicate, 45 succinimide, 42 ethosuximide, 42 DMSO, 39 compound 9; third replicate, 52 succinimide, 53 ethosuximide, 49 DMSO, 46 compound 9.

ALS is characterised by the degeneration of upper and lower motor neurons in the brain and spinal cord. To investigate if compound 9 has a direct protective effect against neuronal degeneration, the integrity of the GABAergic D-type inhibitory motor neurons was studied. These neurons innervate the body wall muscles of the nematode, and are required for ventral and dorsal muscle relaxation during locomotion. Normal sinusoidal locomotion requires opposing excitatory and inhibitory neurotransmission on ventral and dorsal sides, and ablation of inhibitory D-type neurons resulted in movement defects due to the muscle walls receiving only excitatory input (Schuske *et al*., 2004). In other words, this neuronal subset plays an essential role in mediating normal locomotion. Since progressive loss of movement and eventual paralysis is a characteristic clinical feature of ALS, and this is in part recapitulated by the locomotion defects of the CK426 strain, the integrity of these neurons will be informative in relating underlying pathology with clinical phenotypes.

To facilitate the assessment of these neurons, CZ1200 worms which express GFP in GABAergic neurons were crossed with CK426 worms to introduce this genetic feature into the background of the latter strain to create the CK426/CZ1200 double mutant strain (refer to chapter 2; section 2.2.1 and Figure 2.1). GABAergic neuronal-specific expression of GFP in CZ1200 worms was driven by the promoter for the *unc-25* gene ([P*unc-25*::GFP]) which encodes glutamic acid decarboxylase, the enzyme which catalyses GABA biosynthesis from glutamate (Jin *et al*., 1999). Due to the transparency of *C. elegans*, the GFP-expressing GABAergic neurons can be visualised *in vivo* at various adult ages to track age-dependent neuronal changes.

From the cross, hermaphroditic F1 progenies heterozygous for the CK426 and CZ1200 transgenes were further propagated based on their respective P*myo-2::*dsRED red pharyngeal and P*unc-25*::GFP green fluorescence markers. Homozygous F2 hermaphrodites were singled out and propagated for a further generation based on the brightest red and green fluorescences, due to diploid copies of both transgenes. F3 lines which homogenously express both markers at the same intensities were most likely derived from a single homozygous F2 parent, and were retained for further verification. For the

obvious reason that worms were already selected based on GABAergic GFP expression, retained lines were not further genotyped for the expression of the CZ1200-derived P*unc-25*::GFP transgene. On the other hand, although red pharyngeal fluorescence was a selection marker for the CK426-derived TDP-43-encoding *TARDBP* transgene, expression of the TDP-43 protein was examined by Matthew Pontifex (University of Liverpool) to verify transgene expression (Figure 4.2.5). The protein was confirmed to be expressed in the CK426/CZ1200 worms, demonstrating success of the crosses.

The cell bodies of the 19 GABAergic D-type inhibitory motor neurons lie along the ventral nerve cord and consist of 13 ventral (ventral D; VD) and 6 dorsal (dorsal D; DD) type neurons which innervate the respective ventral and dorsal body wall muscles of *C. elegans*. The integrity of this neuronal subset was assessed herein by quantifying the number of cell bodies and neuronal breaks in the ventral nerve cord (Liachko *et al*., 2010); cell bodies were evident from GFP punctae fluorescence whereas discontinuities in the GFP fluorescence highlight neuronal breaks. Observations herein demonstrated clear differences between the CZ1200 controls and CK426/CZ1200 worms across all assessed ages. In general, CZ1200 worms displayed little to no cell body losses and neuronal breaks even at an older adult age of day 7 whereas CK426/CZ1200 fared significantly worse for these quantifications for all treatments even at the youngest assessed age of day 1, verifying the neurodegenerative effect of the *TARDBP* mutation (Figures 4.2.6 and 4.2.7).

.

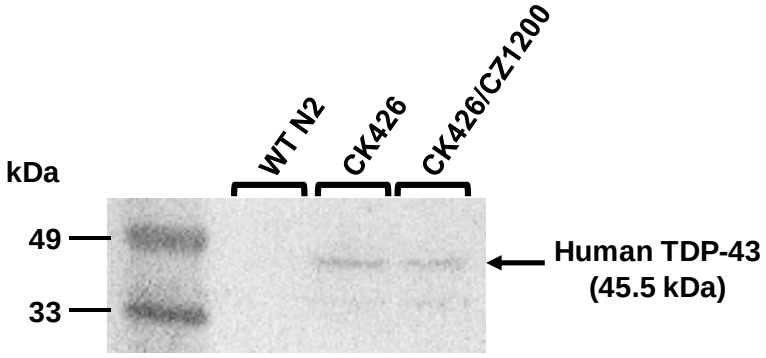

Figure 4.2.5. Representative western blot verifying expression of the human TDP-43 protein in the CK426/CZ1200 double mutant. Blots were probed with an antibody which recognizes amino acid (aa) residues 1 to 161 of the 414-aa human TDP-43 protein. WT N2 and CK426 single mutant strains were analysed alongside as negative and positive controls for TDP-43 expression. The 45.5 kDa protein was detected with the antibody in both the CK426 positive control and the CK426/CZ1200 double mutant from the genetic cross, verifying that the genetic cross had successfully generated the human TDP-43-expressing desired mutants. Western blots were performed by Matthew Pontifex (University of Liverpool).

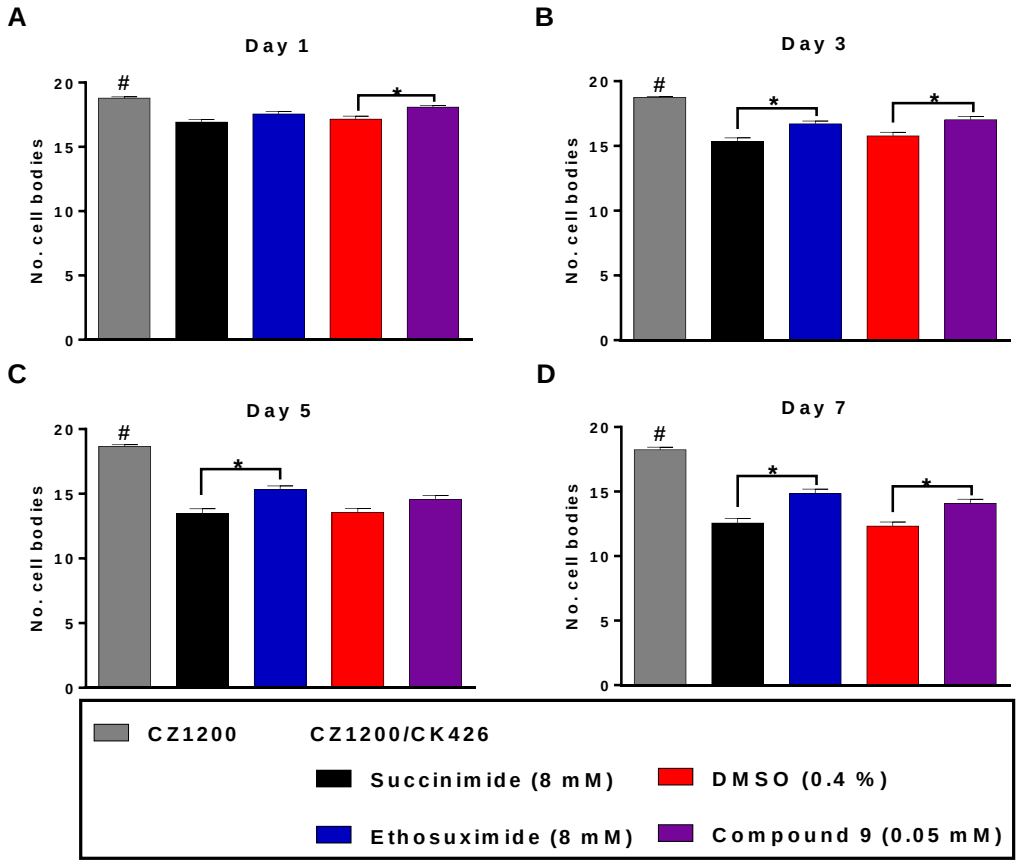

Figure 4.2.6. Compound 9 prevents GABAergic cell body losses in the CK426/CZ1200 strain. CK426/CZ1200 worms generated from mating of the CK426 ALS strain with the GABAergic-specific GFP-expressing CZ1200 strain were chronically treated from the L1 larval stage onwards. (A-D) CZ1200 worms consistently preserved more of the 19 D-type motor neuronal cell bodies than CK426/CZ1200 ones at all assayed ages, verifying neurodegenerative effect of the CK426 background (#, $p<0.05$). Both (B-D) ethosuximide and (A, B and D) compound 9 protected against cell body losses in CK426/CZ1200 worms when compared against respective succinimide and DMSO controls ($p<0.05$). Data for CZ1200 and CK426/CZ1200 strains were pooled from two and three biological replicates respectively, with comparisons made via the Kruskal-Wallis test with Dunn's multiple comparisons. CZ1200 (n = 30 per age), CK426/CZ1200 (n = 33 - 47 per age); #, *, $p<0.05$.

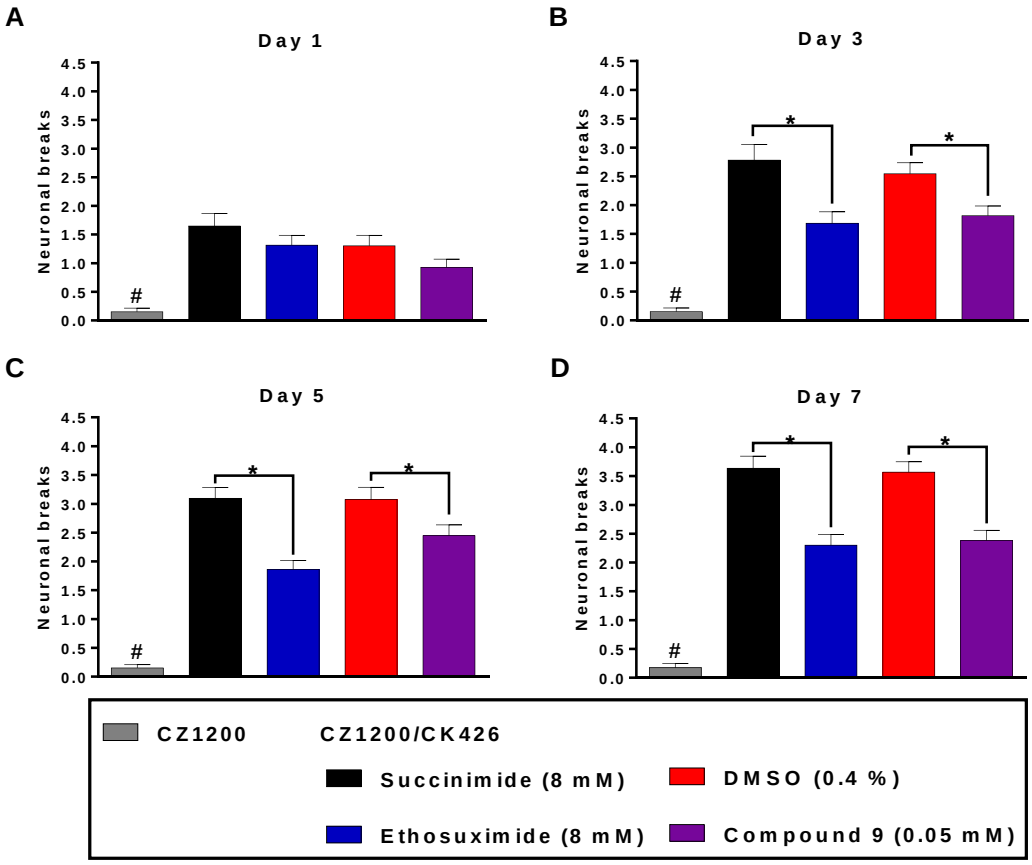

Figure 4.2.7. Compound 9 protects against breaks in D-type GABAergic motor neurons in the CK426/CZ1200 strain. CK426/CZ1200 worms generated from mating of the CK426 ALS strain with the GABAergic-specific GFP-expressing CZ1200 strain were chronically treated from the L1 larval stage (A-D) CZ1200 control worms had fewer neuronal breaks than CK426/CZ1200 worms at all ages, verifying the neurodegenerative effect of the CK426 background (#, $p<0.05$). (B-D) Both ethosuximide and compound 9 reduced the number of neuronal breaks in CK426/CZ1200 worms from day 3 onwards as compared to succinimide and DMSO controls ($p<0.05$). Data for CZ1200 and CK426/CZ1200 strains were pooled from three and four biological replicates respectively, with comparisons made via the Kruskal-Wallis test with Dunn's multiple comparisons. CZ1200 (n = 40 per age), CK426/CZ1200 (n = 43 - 56 per age); #, *, $p<0.05$.

When neurodegeneration was compared between differentially-treated CK426/CZ1200 worms, both ethosuximide and compound 9 protected against cell body losses and breaks within this motor neuronal subset (Figures 4.2.6 and 4.2.7). Effects appeared to be more apparent for neuronal break reduction than for cell body preservation as both compounds consistently protected against breaks from age 3 onwards, whereas protection against cell body losses were less consistent. This was likely to be a direct consequence of the difficulty in quantifying cell bodies especially with age, as punctae fluorescence becomes progressively less prominent and distinguishable. Representative images as shown in Figure 4.2.8 demonstrate the absence of neurodegeneration in the CZ1200 worms at younger and older ages of days 3 and 7, whereas Figures 4.2.9 and 4.2.10 represent the clear differences in neuronal deterioration between the differentially-treated CK426/CZ1200 worms at days 1 and 7; representative images for days 3 and 5 are shown in Appendices 5 and 6.

Taken together, overall findings demonstrated that compound 9 possesses both neuroprotective and lifespan-extending properties. Most importantly, neuroprotection and lifespan extension were mediated at a concentration which was 160-fold lower than the administered concentration for ethosuximide, displaying the enhanced potency of the compound relative to the starting scaffold.

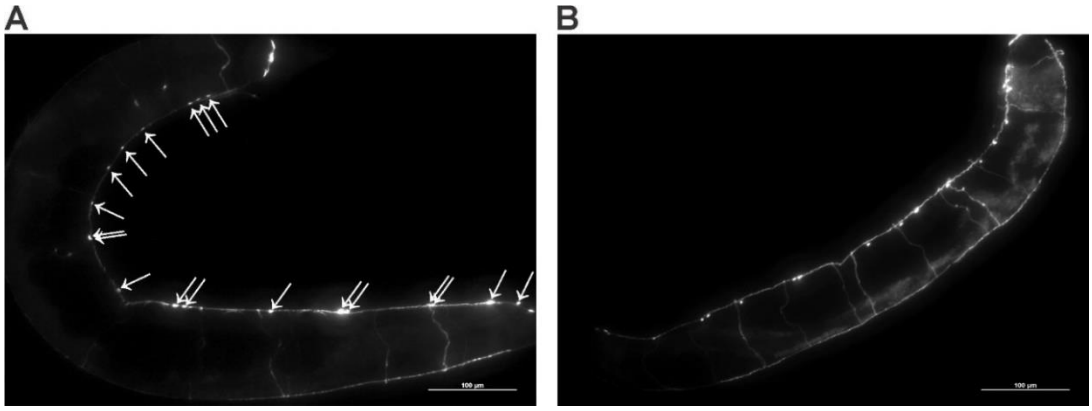

Figure 4.2.8. Representative images of control CZ1200 worms which express GFP in GABAergic neurons. Age-synchronised worms at adult ages of (A) day 3 and (B) day 7 are shown to compare the appearance of D-type GABAergic motor neurons in the ventral nerve cord. The 19 cell bodies of this neuronal subset and neuronal breaks manifest as puntae fluorescence (indicated with arrows in A) and discontinuities in GFP fluorescence respectively. (B) Aging did not cause observable physical neuronal deterioration, which was evident from intact neurons and discernible cell bodies. Images were taken at 200X magnification, scale bars = 100 µm.

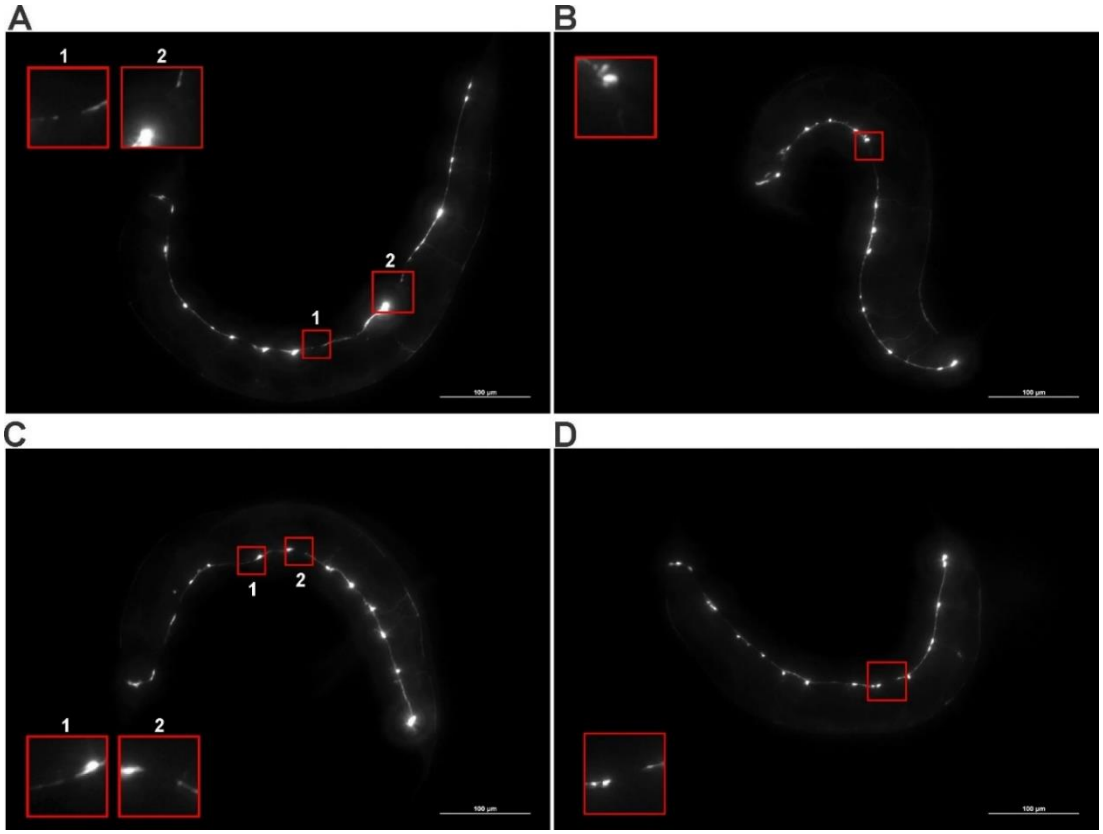

Figure 4.2.9. Representative images of day 1 CK426/CZ1200 worms. Age-synchronised worms were chronically treated with 8mM (A) succinimide or (B) ethosuximide, (C) 0.4 % DMSO vehicle or (D) 0.05 mM compound 9 in 0.4 % DMSO from the L1 larval stage. Breaks within the D-type GABAergic motor neurons in the ventral nerve cord are indicated and emphasized with red boxes. Images were taken at 200X magnification, scale bars = 100 µm.

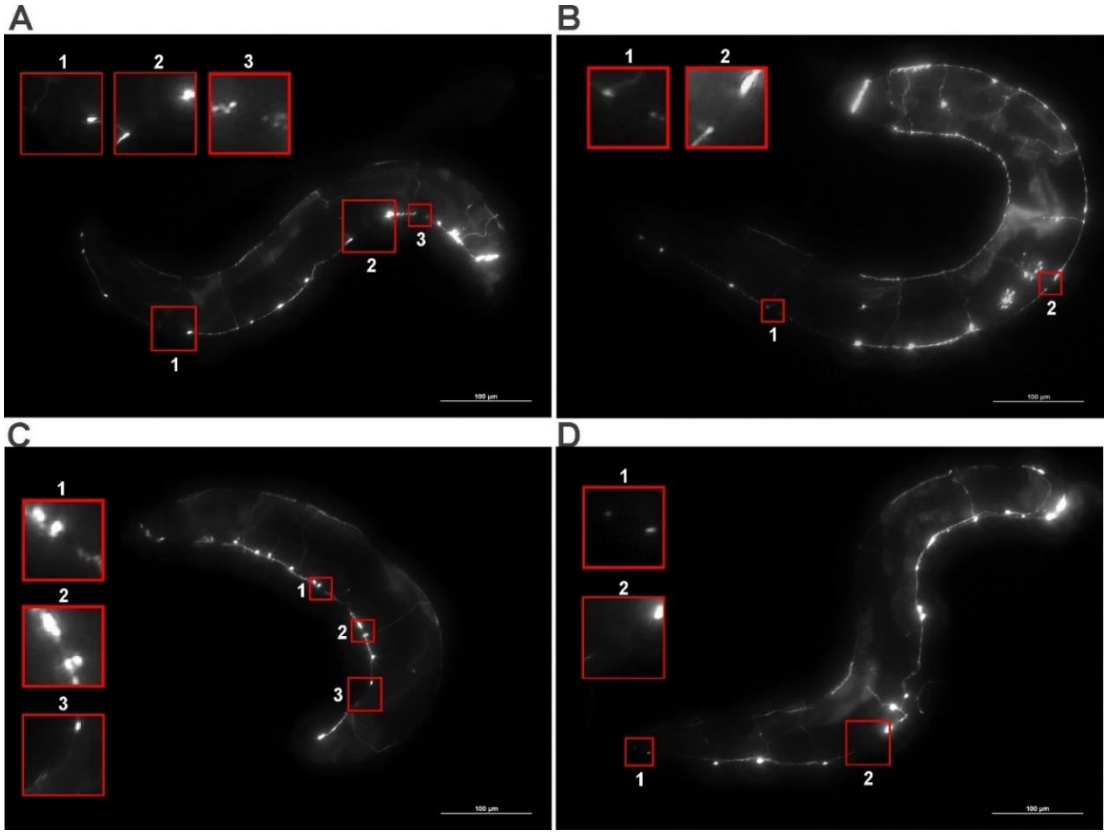

Figure 4.2.10. Representative images of day 7 CK426/CZ1200 worms. Age-synchronised worms were chronically treated with 8mM (A) succinimide or (B) ethosuximide, (C) 0.4 % DMSO vehicle or (D) 0.05 mM compound 9 in 0.4 % DMSO from the L1 larval stage. Breaks within the D-type GABAergic motor neurons in the ventral nerve cord are indicated and emphasized with red boxes. Bagged worms were commonly observed at this age. Images were taken at 200X magnification, scale bars = 100 µm.

4.2.4 Insights into the predictive value of the PTZ-induced seizure assay for neuroprotective characteristics of compounds

The trend observed with compound 9, which showed enhanced anticonvulsant potency in PTZ-induced seizure assays than ethosuximide, and subsequently enhanced neuroprotective and lifespan-extending activities herein, supported the argument for the potential predictive value of the PTZ-induced seizure assay for neuroprotectiveness as discussed in the preceding chapter. To explore this further, two active anticonvulsant compounds, compounds 4 (trimethadione) and 14, were selected on the basis of their reduced and enhanced seizure-protecting potencies in comparison to ethosuximide respectively. The neuroprotective properties of these compounds were assessed by their effects on the body bend frequencies of the CK426 worms.

At the same concentration administered for ethosuximide and the succinimide control, compound 14 only showed a significant improvement in locomotion at day 7 whereas trimethadione consistently ameliorated locomotion from ages 1 to 7; these protective effects were lost on day 9 (Figure 4.2.11). Although the effects of both compounds were not different from ethosuximide herein, primary screens from the PTZ-induced seizure assay showed a less consistent anticonvulsive effect from trimethadione whereas ethosuximide and compound 14 reproducibly and robustly protected against seizures. As aforementioned, trimethadione and compound 14 were less and more potent than ethosuximide in the seizure assay. Taken together, these findings suggest a poor or lack of correlation between seizure- and neuro-protection with the PTZ-induced seizure assay.

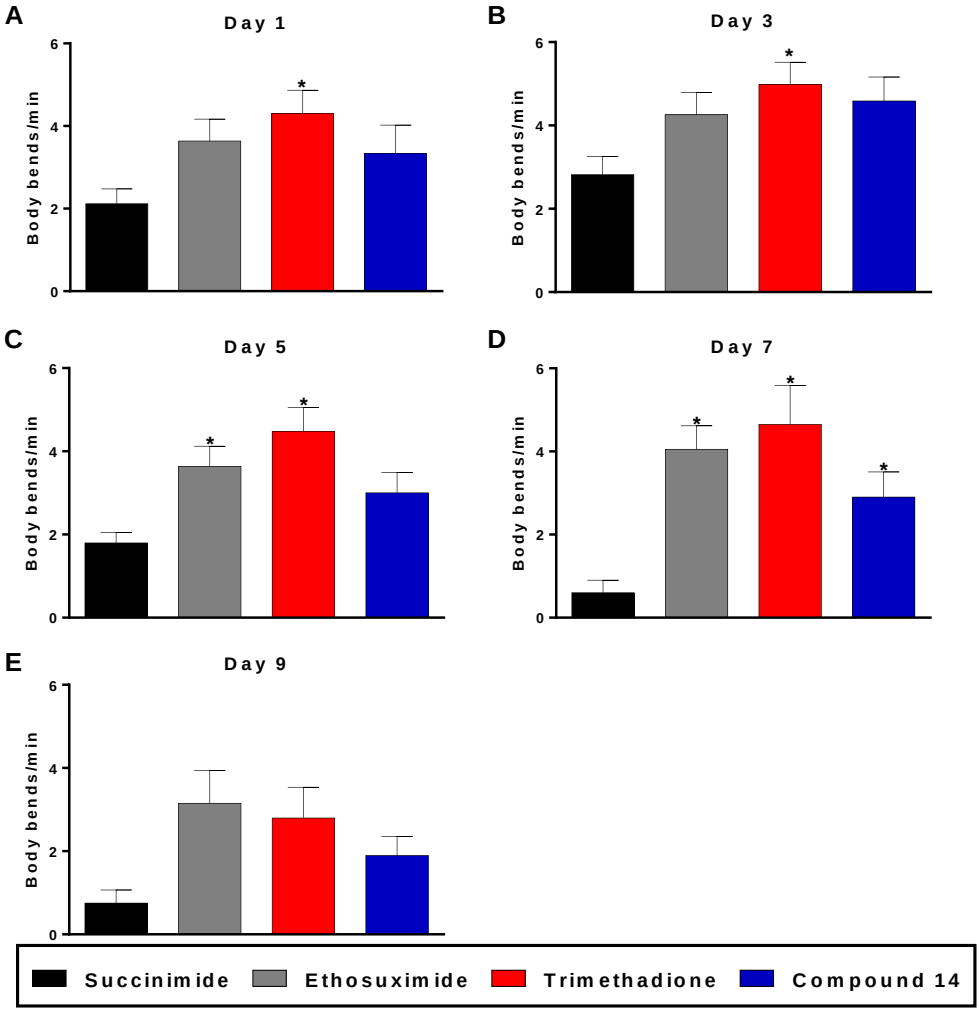

Figure 4.2.11. Trimethadione and compound 14 ameliorates locomotion defects of the CK426 ALS strain. Age-synchronised worms were chronically adminstered 8 mM of respective treatments. (A-D) Trimethadione effected the most consistent improvements in locomotion up to day 7, whereas a significant improvement was only seen with compound 14 treatment at (D) day 7. Data shown was pooled with contributions from Beth Atherton (University of Liverpool) and comparisons were made against the succinimide control via the Kruskal-Wallis test with Dunn's multiple comparisons; *, $p<0.05$. Number of biological replicates for pooled data and *n* (per day per treatment); five, days 1 to 5 all treatments except compound 14 (n = 47 – 50), three, days 1 to 5 compound 14 (n = 28 – 30); two, days 7 and 9 (n = 20).

4.2.5 Comparing bioaccumulation of compounds in chronically-treated CK426 worms

4.2.5.1 Optimisation of extraction conditions

To evaluate the contribution of drug bioaccumulation towards potency differences observed between compound 9 and ethosuximide, 1D ^{1}H NMR spectroscopy was performed on day 1 CK426 worms. As explained in the previous chapter, although there were issues with assessing bioaccumulation from an acute liquid treatment protocol due to the hydrophobic nature of compound 9 (chapter 3, section 3.2.7), these are circumvented with a chronic plate-based treatment procedure herein. As before, singlet peaks with the highest intensity from each compound was selected for analysis as these peaks offer the best signal-to-noise ratios for detection and differentiation from *C. elegans*-derived metabolites.

To establish suitable extraction conditions, a series of experiments were performed prior to preparation and analysis of samples. Previous work conducted by a separate group concluded bead-beating and 80 % methanol as the best tissue disruption method and solvent for the most reproducible extraction of water-soluble metabolites from *C. elegans* (Geier *et al*., 2011). However, the efficiencies of sonication and the acetonitrile extraction solvent were not evaluated therein, hence this was addressed in the current study. By utilising two estimated similarly-sized populations of day 1 CK426 worms, extraction efficiencies of bead-beating and sonication were compared based on the yield of extracted metabolites (Figure 4.2.12).

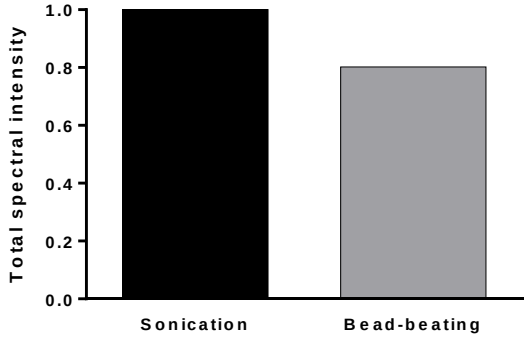

Figure 4.2.12. Comparing the efficiencies of bead-beating and sonication for metabolite extraction from *C. elegans*. Metabolites from *C. elegans* samples of similar estimated sizes were extracted by either approach with AcN and analysed with 1D ^{1}H NMR spectroscopy. Extracted yields were determined by total TSP-scaled ^{1}H spectral intensities which excluded the region occupied by protonated water. Note that although the reference molecule TSP may be added to samples prior to extraction to account for extraction-induced losses, TSP acts as the internal standard for improving estimation of extracted yields when added after extractions herein as the absence of extraction-induced TSP losses results in confidence in the TSP concentration. Extracted yields were compared by normalizing to the higher yield of the two methods. The level of metabolites extracted from bead-beating was about 20% lower, suggesting that sonication may be a better approach. Data shown was from a single extraction of samples from a single preparation.

Sonication appeared to be more efficient as it produced a slightly higher metabolite yield than bead-beating. This was likely a consequence of the procedure being performed *in situ*, reducing number of transfers between plastic ware, and as such, reducing sample losses. However, derived yields should be noted with caution as extracted sample sizes were based on worm population estimations, hence the effect of sample size differences on extracted yield is indeterminate. Despite this caveat, sonication was favoured and was the selected method for extraction herein due to the conveniences associated with it, and the simple fact that less procedural steps lead to reduced sources of error.

To determine the extent of sample loss from sonication, the reference molecule TSP was used as an internal standard which was added either before or after sonication of the samples. Comparison of TSP levels between the two approaches revealed a profound 10-fold reduction due to the extraction procedure, highlighting the importance of accounting for sonication-induced sample losses by co-extracting the internal standard with samples (Figure 4.2.13).

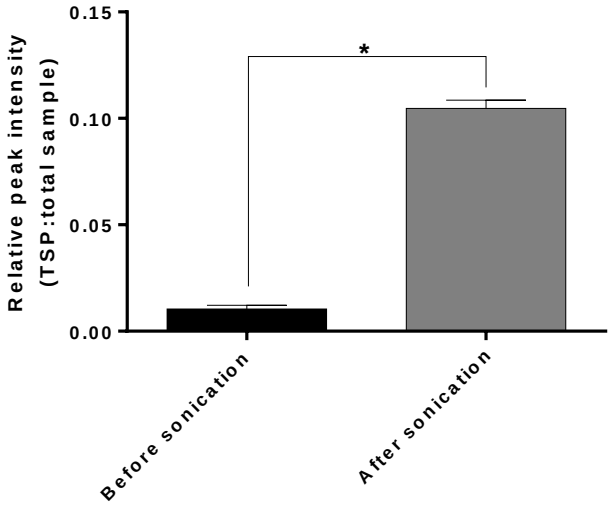

Figure 4.2.13. Extent of sample loss from sonication. The reference compound TSP was added to *C. elegans* samples as an internal standard before or after sonication, followed by analysis with 1D ^{1}H NMR spectroscopy. TSP-derived signals, derived by scaling against total 1D ^{1}H spectral intensities which excluded the protonated water region, were compared between both conditions. Sonication resulted in a 10-fold reduction of TSP as evident from the significant reduction of the compound when added before sonication ($p<0.05$). Results shown are derived from an independent sonication of three biological replicates per condition, with comparisons of TSP signal intensities performed via the unpaired *t* test.

Acetonitrile (AcN) is a recommended extraction solvent for water-soluble metabolites, whereas a mixture of chloroform and methanol is more suitable for lipid metabolites (Beckonert *et al*., 2007). As compound 9 is hydrophobic, AcN might fail to extract it as efficiently as for water-soluble compounds succinimide and ethosuximide. As AcN acts as a solubilising agent for water-soluble metabolites, compound 9 might potentially be excluded from the AcN-metabolite fraction, resulting in NMR undetectability. However, as reproducibility requires keeping conditions as standardised as possible, the feasibility of utilising this extraction solvent for the compound was assessed as illustrated in Figure 2.10 of chapter 2. Briefly, solutions of the compound at the treatment concentration were prepared and subjected to mock extractions with AcN. The compound was detectable with 1D ^{1}H NMR spectroscopy, demonstrating that a proportion of the compound is soluble in the AcN-metabolite fraction (Figure 4.2.14). Additional DMSO in the NMR buffer did not improve the solubility of the compound as its detected level was comparable, further demonstrating that AcN did not reduce extraction efficiency of the compound at the treatment concentration. However, this inference should be taken with caution as AcN might only be an acceptable extraction solvent for the concentration of the compound tested or lower, as the tendency of the compound to precipitate will invariably increase with increasing concentrations.

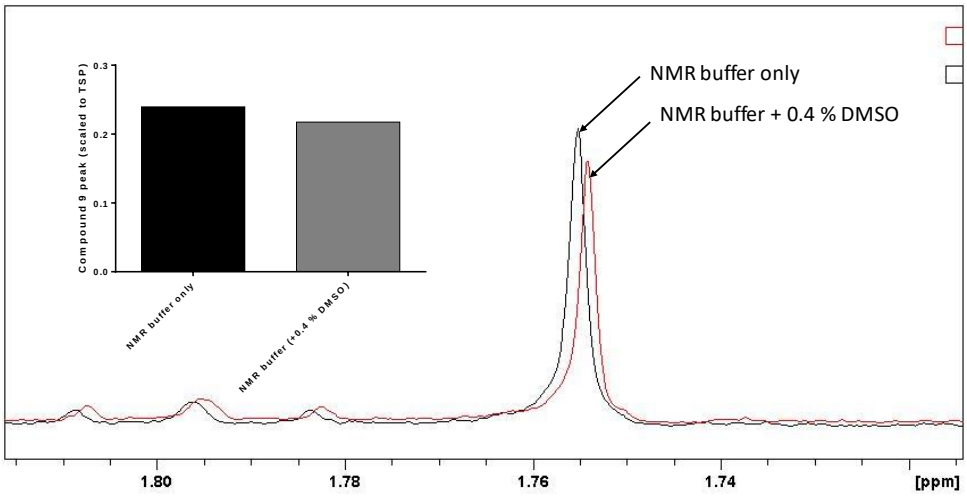

Figure 4.2.14. AcN did not affect the solubility of hydrophobic compound 9 despite being an extraction solvent for water-soluble metabolites. Lyophilised solutions of the compound at 0.05 mM in 0.4 % DMSO were subjected to a mock extraction procedure with AcN without sonication, followed by preparation in NMR buffer with or without additional DMSO. Subsequent centrifugation in order to pellet insoluble components determines if the compound remained solubilised with AcN, and whether additional DMSO was required to promote or improve solubility. 1D ^{1}H NMR spectroscopy of the liquid fraction which corresponds to the metabolite-containing fraction, detected comparable levels of the compound in the presence (red spectrum) and absence (black spectrum) of additional DMSO. This demonstrated that solubility of the compound was not affected with AcN. The result shown is from a single experiment of single preparations. NMR traces shown were scaled to the TSP peak intensity, and arrows indicate the strongest singlet peak from the compound detected from both conditions.

4.2.5.2 Compound 9 failed to bioaccumulate to detectable levels in CK426 worms after chronic treatment

To relate treatment bioaccumulation with phenotypic and pathological observations from neurodegeneration and lifespan analyses as aforementioned (section 4.2.3), chronic treatment of the CK426 worms was carried out at the same concentrations as previously tested. Although protective effects from both ethosuximide and compound 9 appeared to be most consistent at older assessed ages of days 5 to 9 from locomotion (Figure 4.2.2) and neuronal imaging (Figure 4.2.6 and 4.2.7) assays, analysis of bioaccumulation was initially not performed with worms of these ages due to the difficulty in maintaining a large gravid population without progeny contaminations. Although the DNA synthesis inhibitor FUDR can be used to sterilise gravid worms and hence prevent progeny contamination (Mitchell *et al*., 1979), it has been reported to be a confounding factor in lifespan analyses (Anderson *et al*., 2016) and might potentially affect bioaccumulation of the compounds in unknown ways. For these reasons, day 1 was the age selected for analysis.

Following extraction and analysis with 1D ^{1}H NMR spectroscopy, resultant 1D ^{1}H spectra from respective compounds demonstrated detectability of the strongest singlet peaks from unmetabolized succinimide and ethosuximide (Figure 4.2.15), but not of compound 9 (Figure 4.2.16). The compound 9-derived peak coincides with a region occupied by worm metabolites shared across all differentially-treated samples. In addition, the concentration of the externally administered compound was 0.05 mM, which was 160-fold lower than the treatment concentration of 8 mM for both succinimide and ethosuximide. The combination of both factors would have severely reduced the possibility of the detection of the compound. In an attempt to improve detectability of this singlet peak, worms were administered a 40-fold higher concentration of the compound at 2mM, the currently established highest tolerable concentration used in concentration-response assessments as described above (section 4.2.3). Nevertheless, this failed to improve the visibility of the compound-derived signal from internal metabolites (Figure 4.2.16). Due to potential occlusion of the signal due to overlapping peaks from

worm metabolites, other compound-derived peaks occupying separate spectral regions were examined for both low and high concentrations of compound 9. Unfortunately, no distinguishable signals from the compound were visible at either concentration (Figure 4.2.16).

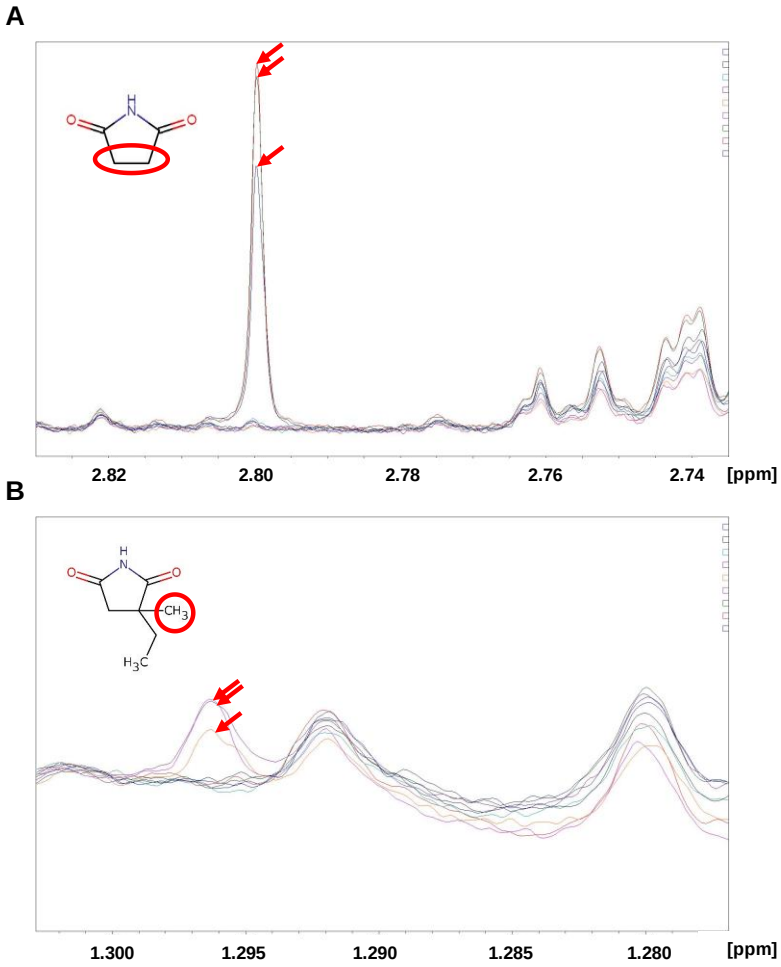

Figure 4.2.15. Detectable traces of succinimide and ethosuximide in treated day 1 CK426 ALS worms. Overlay of spectra from all treatments (8 mM succinimide and ethosuximide, 0.05 mM compound 9) and regions with compound-derived peaks of interest. (A) Succinimide (in 2.82 – 2.74 ppm) and (B) ethosuximide-derived peaks (1.30 – 1.28 ppm) were readily distinguishable only in samples treated with the respective compounds (red arrows). Peaks common to all treatment from *C. elegans* metabolites are shown alongside compound-derived peaks for emphasis. Data shown is from nine ^{1}H spectra from three treatment conditions with three biological replicates each.

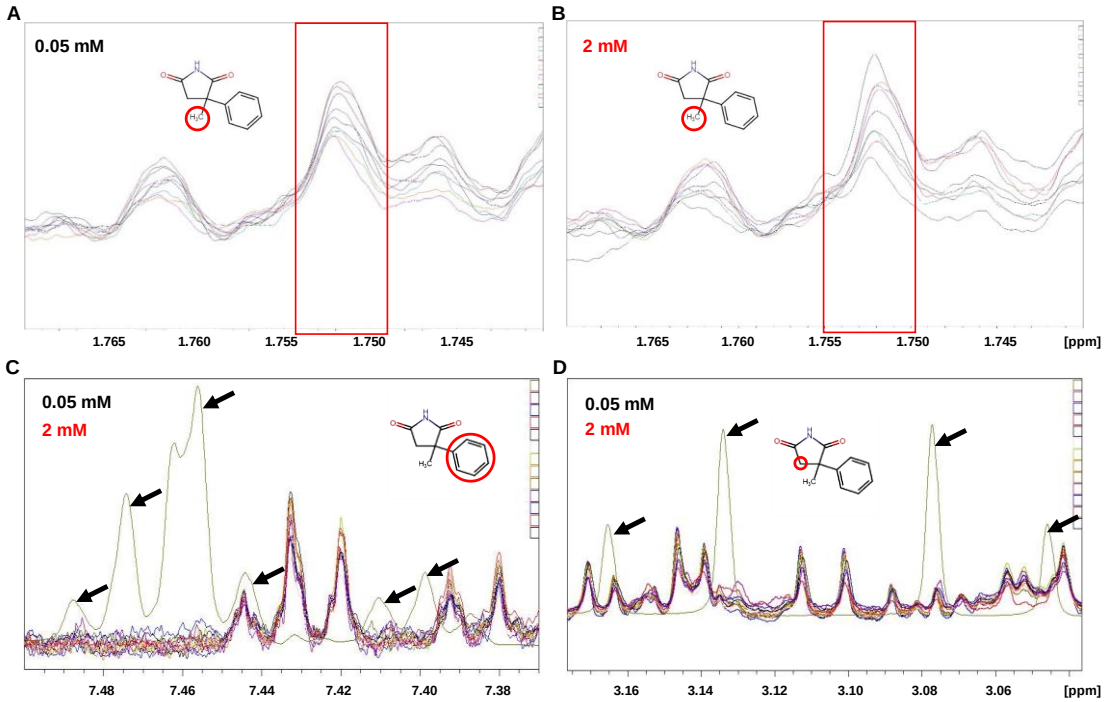

Figure 4.2.16. Compound 9 is undetectable in treated day 1 CK426 ALS worms. Spectra from all treatments were overlaid and specific regions containing compound-derived peaks of interest were focused on to assess the presence of these peaks. The singlet peak with the highest intensity from the compound (boxed region) was indistinguishable in samples treated with both (A) low and (B) high concentrations, as it might be occluded by common worm-derived metabolites. Due to the undetectability of the singlet peak, the presence of other compound-derived multiplet peaks in the (C) aromatic or (D) -CH_2 region were analysed from spectra derived from treatment with both low and high concentrations. To facilitate the ease of peak identification from these multiplets, the reference spectrum of the compound was overlaid with those from treated samples; reference peaks as shown in green and indicated with black arrows. These peaks were also not detectable from samples. Data shown is from nine ^{1}H spectra from three treatment conditions with three biological replicates each.

Since the unmetabolized form of compound 9 was undetectable in day 1 samples, additional analyses were performed on worms aged to day 5 based on the hypothesis that the compound will bioaccumulate to higher levels over time, and to mirror physiological effects of treatment at that age. Comparison between day 1 and 5 samples may additionally facilitate some insights into the kinetics of bioaccumulation, metabolism and clearance. Despite potential effects of FUDR on bioaccumulation, worms were aged in the presence of the compound to maintain a homogenous aged population. Similar to day 1 samples, no traces of compound 9 were observed (results not shown). Given the undetectability of the unmetabolized compound in both younger and older worms, it is possible that metabolism of the compound had occurred and that traces of the compound-derived metabolite(s) could be distinguished to inform about drug accumulation. There has only been one reported *p*-hydroxyphenyl metabolite of compound 9 to date (Dudley *et al*., 1974). Hydroxylation of compound 9 to the metabolite causes a shift of spectral peaks, as ^{1}H NMR peaks from the *p*-hydroxyphenyl moiety of the metabolite were predicted to produce two doublet peaks which distinguish the metabolite from the multiplets derived from the unhydroxylated phenyl of compound 9 (Dudley *et al*., 1974). However, these peaks coincide with a very noisy worm-derived metabolite region of the ^{1}H spectrum and may not be easily distinguished even if present. As with compound 9, the methyl moiety of the metabolite is likely to produce a singlet with the highest intensity; however the spectral region of this peak is unknown and may differ from the unmetabolized compound. To pinpoint the approximate spectral regions occupied by this metabolite-derived peak, the predicted 1D ^{1}H NMR spectra for compound 9 and the metabolite were compared (Appendix 7); refer to chapter 2, section 2.5.4 for details on spectral prediction. Predicted spectra showed a slight upfield spectral shift of the drug metabolite-derived peak. However, no distinct singlet peak was distinguishable from worm-derived metabolite signals in upfield regions from the original compound 9-derived peak on the spectra analysed herein, showing that the metabolite was similarly undetectable.

Although peaks from succinimide and ethosuximide remained detectable in day 5 worms (results not shown), fair comparisons against day 1 samples were not possible as FUDR treatment plates used for aging day 5 worms were not depleted of bacterial food lawns at the time of sample processing. In contrast, bacterial lawns were thick and infected, which were extremely difficult to remove from worm samples during washes as they constitute a bulk of the worm samples. Therefore, it was possible that they have participated in the bioaccumulation and metabolism of the treatments, or they might have influenced bioaccumulation in the worms in some way. In view of this possible confounding factor and the quality of samples analysed, spectra from day 5 worms were not analysed.

To quantify the internal concentrations of unmetabolized succinimide and ethosuximide in day 1 CK426 worms, concentration and sample size standard curves (refer to chapter 2, section 2.6.3.3 and Figure 2.17) were constructed (Figures 4.2.17 and 4.2.18); note that curves were also shown herein for compound 9 for completion. Measured internal concentrations were 206.6 ± 48.89 µM for succinimide and 143.8 ± 39.08 µM for ethosuximide. Although determined concentrations were derived from unmetabolized forms of the compounds, higher values for the inert control succinimide likely verifies the intrinsic bioactivity of ethosuximide. The unapparent physiological effects of compound 9 and its metabolite at age day 1 suggests the possibility of a lack of treatment uptake at that age and might be an explanation for the undetectability of the compound. However, DMSO was easily distinguishable in these samples (not shown), verifying at least carrier uptake by the worms, although it is possible that worms had preferentially taken up DMSO instead of the compound.

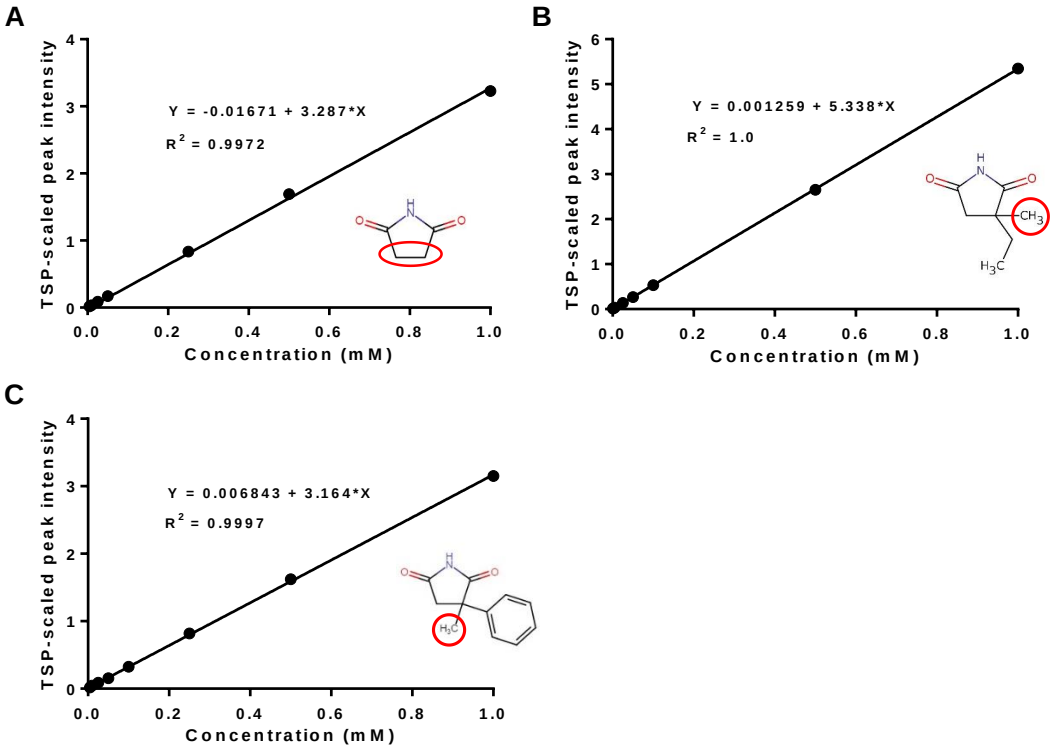

Figure 4.2.17. Standard curves for estimating internal concentration of compounds in *C. elegans* following treatment. A range of concentrations for each compound were analysed with 1D ^{1}H NMR spectroscopy and the resultant spectral intensities of analysed peaks, as derived from indicated regions from each compound, were scaled to the reference compound TSP and plotted against respective concentrations to generate the curves. Data shown was from a single experiment of single preparations.

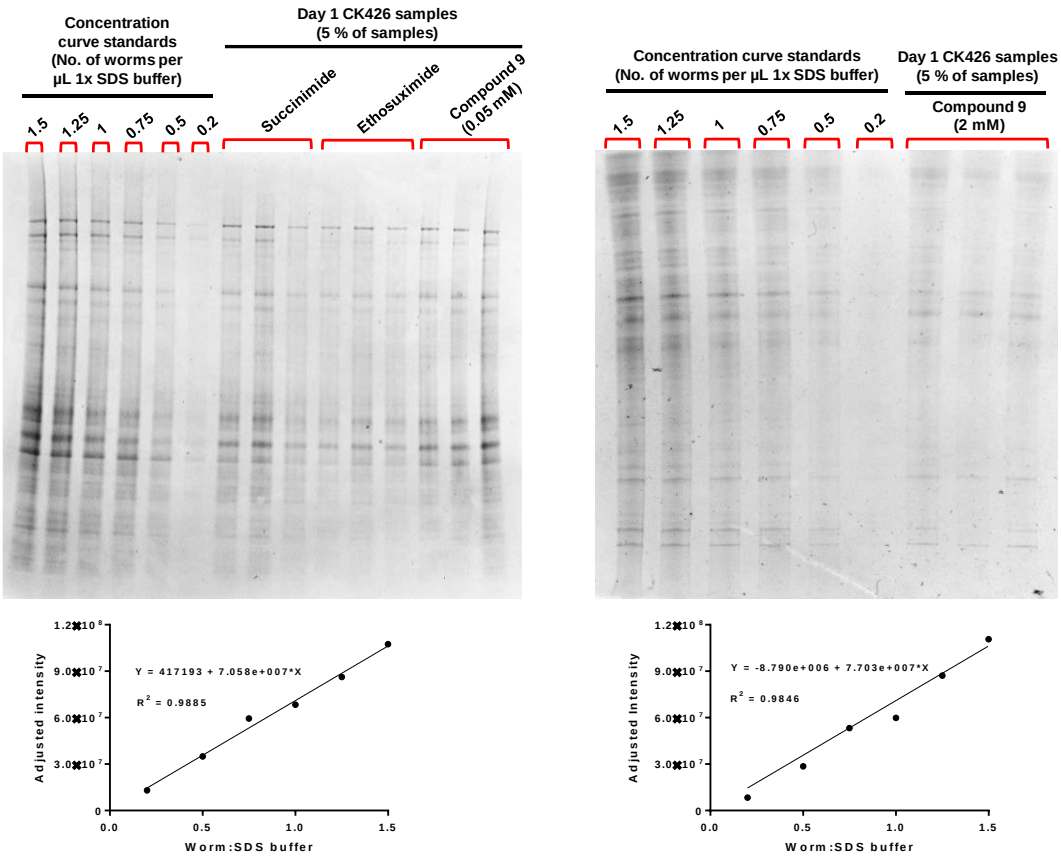

Figure 4.2.18. Sample size estimation from standard curves. Standard curves were generated from the coomassie blue staining intensities of known ratios of day 1 CK426 worms in 1X SDS buffer resolved on SDS-PAGE gel. Samples, which are 5 % of the analysed populations, were resolved and stained alongside standards to preserve staining consistency for accurate interpolation. Shown here are the stained gels and corresponding standard curves below; two gels were analysed due to the number of conditions and replicates required. The number of worms analysed by 1D ^{1}H NMR spectroscopy was extrapolated from interpolated numbers. Data shown was from a single experiment of samples from four treatment conditions with three biological replicates each.

4.3 DISCUSSION

In the preceding chapter, compound 9 was demonstrated to exert a 2-fold enhancement of anticonvulsive potency than ethosuximide and was selected as the candidate molecule for the derivation of secondary compounds. Subsequent work herein verified its neuroprotective and lifespan-extending properties in the CK426 *C. elegans* ALS model. Most importantly, comparable protective effects with ethosuximide were exerted at a concentration which was 160-fold lower than the drug. Unlike ethosuximide whereby neuroprotection and lifespan extension have been reported in various models of neurodegeneration (Tauffenberger *et al*., 2013, Chen *et al*., 2015b, Tiwari *et al*., 2015), these protective effects of compound 9 and/or its methsuximide prodrug have not been documented elsewhere. Hence, the current work presents novel findings of a molecule with much enhanced potency despite it being structurally similar to ethosuximide.

As treatments for epilepsy, ethosuximide is only effective against absence seizures, whereas the methsuximide pro-drug of compound 9 has a broad spectrum of activity and is effective against other seizure types as well (Browne *et al*., 1983, French *et al*., 1958, Dow *et al*., 1958, Carter and Maley, 1957, Wilder and Buchanan, 1981, Hurst, 1996). The striking enhanced potency of compound 9 relative to ethosuximide herein and its wide spectrum of activity in humans may be attributed to increased lipophilicity conferred by its phenyl moiety, as lipophilicity often improves the potency of a molecule *in vitro*. However, increased lipophilicity is additionally associated with undesirable features such as increased toxicity, and reduced solubility, bioavailability, and metabolic stability (Leeson and Springthorpe, 2007), exemplified by the increased toxicity of methsuximide in comparison to ethosuximide. Lipophilicity is defined by the octanol-water distribution coefficients, LogP and LogD, with the latter being a more physiologically relevant measure due to the additional consideration of pH-dependent ionisation states of molecules (van de Waterbeemd *et al*., 1998). In CNS drug discovery, although lipophilicity has been reported to improve brain permeation as shown by a good correlation of predicted LogD values with total drug levels in the brain (Wager *et al*., 2010a), it is the free unbound fraction which is more relevant as it mediates the

therapeutic effect at the biological target(s) (Rankovic, 2015). More importantly, a negative correlation has been reported for LogP and free unbound drug levels in the brain (Gleeson, 2008), which emphasizes the importance of considering the effect of lipophilicity on brain permeation based not on total but on the free unbound drug levels in the brain. In addition, to reiterate the importance of a multiobjective parameter optimisation approach as discussed in the preceding chapter, other parameters such as molecule binding to and efflux by drug transporters such P-glycoprotein affects brain permeation and should be considered alongside lipophilicity of a molecule. This is important for future work when further compounds have been developed from compound 9. Although the (*R*)-enantiomer was successfully generated by the end of the three-step reaction, no further attempts were made to recover it due to insufficient amounts from the tiny scale of the reaction. Hence, findings herein were derived from the racemate of the compound. Although bioactivity and toxicity may differ between enantiomeric forms, characterization work performed herein with the racemate is equally important as enantiomers may interact with each other to produce different biological effects from single enantiomers. Although the enantiomers of compound 9 remain to be characterised herein, chiral effects on not only pharmacological activity, but also on important parameters contributing to the mechanism of action, such as toxicity and ADME properties, should be assessed for a lead molecule derived from compound 9 in the future.

Investigation of bioaccumulated drug levels in the CK426 worms treated with 8 mM ethosuximide revealed an internal ethosuximide concentration of 143.8 ± 39.08 µM in day 1 animals. A separate study reported an internal concentration of approximately 220 µM in WT worms which were chronically-treated with 14 mM of the drug (Evason *et al*., 2005). However, the reported method of measuring bioaccumulated concentrations differ from the approach used herein. Instead of 1D ^{1}H NMR spectroscopy, a commercial immunoassay was utilised to detect and measure the drug levels in the worms. Despite the differences in procedures, the bioaccumulated concentration from a lower externally administered concentration of 8 mM herein does not deviate far, given the previously reported linear relationship between drug plasma levels

and administered doses of the drug (Patsalos, 2005). Although bioaccumulated drug levels is lower than the reported therapeutic range of 280 to 700 µM in human plasma for the treatment of absence seizures (Browne *et al*., 1975), it might be attributed to species differences. Despite the expression of many members of phase I and II metabolism enzymes by *C. elegans*, the detoxification functions of these proteins in the worms are largely not characterised (Lindblom and Dodd, 2006), and metabolism routes and resultant drug metabolites may differ between *C. elegans* and humans.

Unlike ethosuximide, compound 9 was undetectable in CK426 worms at both younger and older ages of days 1 and 5. Undetectability may be partly explained by the known half-lives of the compounds in humans, which were reported to be 38 hours for compound 9 (Porter *et al*., 1979) and 30 to 60 hours for ethosuximide (Buchanan *et al*., 1969). The similar or perhaps even longer half-life of ethosuximide, in addition to the 160-fold difference in treatment concentrations administered to worms, would have likely resulted in a greater bioaccumulation and hence detectability of the drug as opposed to compound 9.

The metabolism of ethosuximide had been extensively studied (Millership *et al*., 2005, Millership *et al*., 1995, Mifsud *et al*., 2001, Preste *et al*., 1974, Pettersen, 1978, Villen *et al*., 1990, Millership *et al*., 1993, Horning *et al*., 1973b, Goulet *et al*., 1976), whereas limited information is available for the metabolic fate of methsuximide aside from its known N-demethylation metabolism to compound 9 (Horning *et al*., 1973a, Dudley *et al*., 1974, Dobrinska and Welling, 1977, Orton and Nicholls, 1972, Nicholls and Orton, 1972). Ethosuximide and compound 9 are the known bioactive species. The main metabolite of ethosuximide is biologically inactive (Preste *et al*., 1974), whereas the activities of methsuximide-derived metabolites have not been documented aside from compound 9. Although a hydroxylated *p*-hydroxyphenyl metabolite of compound 9 is the only reported metabolite of the compound to date, the activity of this metabolite has not been characterised (Dudley *et al*., 1974). Other metabolites of the compound may exist, albeit not documented. In the body, drugs undergo phase I and II biotransformation (Lindblom and Dodd,

2006). Phase I functionalisation reactions occur by hydrolysis, oxidation, or reduction, to reveal or attach functional groups such as hydroxyl (-OH), carboxyl (-COOH), thiol (-SH), amine (-NH), or amino ($-NH_2$) groups to a molecule. The next stage of biotransformation, the phase II detoxification reactions, inactivates and hydrophilizes phase I primary metabolites for subsequent elimination from the body by conjugating endogenous groups such as glucuronide, methyl, and gluthathione to the metabolites. The *p*-hydroxyphenyl metabolite of compound 9 could be an active species which contributes to the biological activity of the compound, as it is hydroxylated and not a phase II conjugated derivative. As shown herein and similar to compound 9, traces of this metabolite were indistinguishable. Although the limit of detection for compound 9 was 5 µM based on observations of the spectra derived for generating the concentration curves herein, whether the compound and/or its metabolite had presumably bioaccumulated below this concentration was difficult to ascertain at this point as their corresponding peaks were occluded by peaks from worm-derived metabolites. However, given that the externally-administered concentration was a 100-fold lower than the detection limit at 0.05 µM, and based on findings herein which showed drastically reduced bioaccumulated µM concentrations of succinimide and ethosuximide in the low hundreds despite an external treatment concentration of 8 mM, the assumption may be made that the compound and/or its metabolite had bioaccumulated below this 5 µM detection threshold. This detectable concentration again differs from reported human plasma levels which ranged approximately from 100 to 260 µM (20 to 50 µg/ml) (Strong *et al*., 1974, Porter *et al*., 1979, Tennison *et al*., 1991). Taken together with findings from ethosuximide, the enhanced potency from the compound was most likely attributed to its chemistry and not simply a consequence of improved bioaccumulation in the worms. Furthermore, it is noteworthy that this presumed internal concentration of less than 5 µM is extremely close to the desired K_D affinity range of femtomole to nanomole concentrations for high affinity ligands, suggesting feasibility of target identification with the compound in comparison to ethosuximide (Terstappen *et al*., 2007).

Active compounds 4 (trimethadione) and 14, previously demonstrated to be less and more potent than ethosuximide respectively from PTZ-induced seizure assays, were selected for analysis of their neuroprotective activities herein to gain an insight into the potential predictive utility of the seizure assay for neuroprotectiveness. Both molecules were neuroprotective as they improved the defective locomotion of the CK426 worms. In corroboration with the protective activity of trimethadione against neurodegeneration, the AED was also previously shown to protect against cell death in primary mouse hippocampal and cortical neuronal cultures (Wildburger *et al*., 2009a). Despite the preservation of bioactivity from both compounds from the PTZ-induced seizure to the neuroprotection assay herein, the extent of neuroprotectiveness relative to ethosuximide did not correlate with the observed differences in anticonvulsive potencies. Previous lifespan analyses showed a 47 % increase of mean lifespan from WT worms treated with 4 mg/mL trimethadione whereas ethosuximide extended a relatively modest extension of 17 % at the same treatment concentration (Evason *et al*., 2005). Furthermore, the active molecule compound 15 was shown to possess a lower anticonvulsant potency than ethosuximide from the seizure assays in the preceding chapter, yet was reported in the same study to extend the mean lifespan by 31 % as opposed to 13 % by ethosuximide at the same concentration of 2 mg/mL. Although lifespan extension was previously shown not to effectively correlate with neuroprotection (Tauffenberger *et al*., 2013), the lifespan findings support at least observations herein that seizure protection may not effectively predict the extent of neuroprotection. As additionally discussed in the preceding chapter, the PTZ seizure model and obtained SAR findings in the current study may only be applicable to a select group of compounds like the succinimide-based compounds, based on SAR discrepancies with a structurally-similar AED levetiracetam which does not exhibit anti-seizure protection in the rodent scPTZ counterpart. Regardless of these caveats and based on the limited findings obtained herein, it seems that neuroprotective activity could at least be predicted from the anticonvulsive activity of the molecules assayed herein. Hence, based on current findings, it served as a useful and more rapid pre-screening approach for potential neuroprotectiveness prior to validation of

these properties in more time-consuming neurodegeneration assays as reported herein.

As illustrated at the beginning of the current chapter, the neuroprotective and/or lifespan extending properties of the AEDs valproic acid (van Bergeijk *et al*., 2006, Pan *et al*., 2005, Kautu *et al*., 2013, Teixeira-Castro *et al*., 2011, Qing *et al*., 2008, Yi *et al*., 2013, Rouaux *et al*., 2007, Crochemore *et al*., 2009, Sugai *et al*., 2004, Monti *et al*., 2010, Monti *et al*., 2012, Kidd and Schneider, 2011, Ximenes *et al*., 2015, Carriere *et al*., 2014, Evason *et al*., 2008), trimethadione (Evason *et al*., 2005, Wildburger *et al*., 2009a), and levetiracetam (Sanchez *et al*., 2012, Bezard *et al*., 2004, Erbaş *et al*., 2016, Musaeus *et al*., 2017) have been demonstrated across a number of studies, and like ethosuximide, they have the potential to be repurposed as treatments for neurodegeneration. Amongst them, the neuroprotective activity of valproic acid has been the most extensively documented as it has been shown to be protective in in models of ALS, PD, AD, spinocerebellar ataxia type 3, and spinal muscular atrophy in cells, *C. elegans*, and rodents. Hence, similar to ethosuximide, valproic acid has neuroprotective activity across a spectrum of neurodegeneration disease models. Note that despite extensive evidence of its neuroprotective properties, it has failed phase III trials for the treatment of ALS, resulting in discontinuation of further development as an ALS therapeutic (Piepers *et al*., 2009). Valproic acid is also associated with a greater range and severity of adverse effects, with hepatotoxicity and teratogenicity being two notable examples (Moshe *et al*., 2015). Additionally, the structural dissimilarity of valproic acid compared to ethosuximide and compound 9 suggests that the latter succinimide-based derivatives may work via distinct sets of mechanisms from valproic acid to protect against neurodegeneration. For these reasons, the current study chose to focus on ethosuximide and compound 9.

Although trimethadione is structurally quite similar to ethosuximide, its neuroprotective properties were assessed in primary mouse hippocampal and cortical neuronal cultures (Wildburger *et al*., 2009a) and not in neurodegeneration models *per se* aside from the work performed herein. In addition, findings herein demonstrated a similar extent of neuroprotection from

the drug when tested at the same concentration as ethosuximide, whereas compound 9 was much more potent. Additionally, trimethadione is no longer prescribed for the treatment of absence seizures due to associated toxicity, hence it may be more suitable for experimental instead of clinical use. Lastly, the neuroprotective properties of levetiracetam have not been as extensively studied as ethosuximide across a range of models, since it showed neuroprotection only in PD and AD models (Bezard *et al*., 2004, Sanchez *et al*., 2012, Erbaş *et al*., 2016). Although it was reported to normalise abnormal EEG patterns in the brains of mild AD patients, no cognitive improvements were mediated (Musaeus *et al*., 2017). Given the better documentation of neuroprotectiveness from ethosuximide in a range of neurodegeneration models, and the enhanced potency of compound 9 as compared to the drug, taken together these justify the decision to utilise compound 9 for further studies rather than trimethadione or levetiracetam.

Unlike ethosuximide, the broad spectrum of neuroprotectiveness from compound 9 has yet to be assessed. Being structurally-similar, however, this may by extension apply to compound 9 as well although further study is warranted. Collaborative plans are currently in place to assess the neuroprotective activity of the compound in the rat AD-like model whereby ethosuximide was shown to mediate neuroprotective and neurogenic properties (Tiwari *et al*., 2015), and in a polyQ expansion model in mouse primary neuronal cells (Massimiliano Stagi, University of Liverpool). As these are rodent models which are generally considered to be the gold standards for preclinical testing, it will be interesting to see if the compound exerts neuroprotection in these clinically-relevant models of neurodegeneration in addition to findings from the CK426 ALS model herein.

CHAPTER 5

MECHANISM OF ETHOSUXIMIDE AND COMPOUND 9

5.1 INTRODUCTION

5.1.1 Mechanism of ethosuximide

The MMOA of ethosuximide remains unelucidated despite being an established AED for the treatment of absence seizures. The drug was thought to mediate its anticonvulsant therapeutic effect by blocking the low-voltage activated T-type calcium channels, as several studies have reported inhibition of low threshold calcium currents mediated by these channels (Coulter *et al*., 1989a, Coulter *et al*., 1990, Coulter *et al*., 1989b, Gomora *et al*., 2001, Lacinova *et al*., 2000). However, other studies have refuted such findings (Sayer *et al*., 1993, Thompson and Wong, 1991, Gross *et al*., 1997, Todorovic and Lingle, 1998, Herrington and Lingle, 1992, Kostyuk *et al*., 1992, Pfrieger *et al*., 1992, Leresche *et al*., 1998, Tsakiridou *et al*., 1995). Phenotypically, work done within our group demonstrated that deletion of the *C. elegans* T-type calcium channel CCA-1 did not affect neuroprotective and lifespan-extending effects of the drug in CK10 FTDP-17 worms (Chen *et al*., 2015b). This was further corroborated by a different study which verified that the drug did not act via these channels to extend the lifespan of WT worms (Collins *et al*., 2008). Although it is possible that CCA-1 may not mediate neuroprotective and/or longevity effects of the drug, these phenotypic findings lend support to the latter group of studies. In addition to putative T-type calcium channel block, evidence has also demonstrated that the drug blocks voltage-gated sodium and potassium channels in giant squid axon, although channel blockade might be in part attributed to a nonspecific effect since extremely high concentrations of the drug of up to 60 mM were administered (Fohlmeister *et al*., 1984). In a different study, therapeutically-relevant concentrations of ethosuximide had no effect on the high frequency sustained repetitive firing of the sodium action potentials in mouse spinal cord neurons, suggesting that sodium channel blockade is not a therapeutic but rather a nonspecific effect of the drug (McLean and Macdonald, 1986).

Ethosuximide was also proposed to mediate its lifespan-extending effects by inhibiting chemosensory function in *C. elegans* (Collins *et al*., 2008). Forward chemical genetic screens identified mutations in chemosensory neuronal genes *che-3* and *osm-3*, which conferred resistance to ethosuximide-induced

toxicity. Furthermore, the *osm-3* mutation increased lifespan and was resistant to further lifespan extension by the drug, strongly supporting this hypothesis. However, work performed within our group on the *dnj-14* ANCL worms contradicts this model, as these worms have sensory defects and reduced instead of extended lifespans (Kashyap *et al*., 2014). Moreover, ethosuximide extended lifespans and improved the sensory function of these worms (Chen *et al*., 2015b), effects which are not consistent with the proposed mechanism of action.

DAF-16 is the *C. elegans* ortholog of the mammalian FOXO transcription factors which has been shown to play a role in mediating neuroprotective and longevity effects of ethosuximide. Work performed within our group has demonstrated that RNAi-mediated silencing of *daf-16* abolished the lifespan extension of *dnj-14* ANCL worms by ethosuximide (Chen *et al*., 2015b). In addition, ethosuximide induced the expression of several FOXO-regulated genes in a mouse neuroblastoma N2A cell line, demonstrating that the role of DAF-16/FOXO in mediating the effects of the drug was conserved from *C. elegans* to mammals. In a separate study, introduction of a null d*af-16* mutation into the genetic background of a A315T TDP-43-expressing transgenic *C. elegans* ALS worms partially diminished the ability of the drug to reduce the number of paralyzed worms and motor neurodegeneration, suggesting that neuroprotection is only partially mediated through DAF-16 (Tauffenberger *et al*., 2013). Contradictory to the abovementioned findings, ethosuximide was reported to significantly extend the lifespans of two different *daf-16* null mutant strains (Evason *et al*., 2005). However, it should be noted that the mean lifespans of these worms were not restored to the same level as ethosuximide-treated WT worms, again suggestive of a partial dependence of the drug on the transcription factor for lifespan extension. DAF-16 and its antagonistic role in the insulin/insulin-like growth factor 1 (IGF-1) signalling (IIS) pathway is described in more detail in section 5.1.3 below.

Ethosuximide was also reported to mediate neuroprotective and neurogenic properties via activation of the PI3K/AKT/Wnt/β-catenin pathway (Tiwari *et al*., 2015). The drug was shown to promote neural stem cell proliferation and

neuronal differentiation in the hippocampus of normal rats. In a rat AD-like model generated by bilateral stereotaxic injection of $A\beta_{42}$ into the hippocampus, ethosuximide further protected against $A\beta_{42}$-induced losses of hippocampal proliferating and neuronal differentiating cells, apoptosis, and cognitive deficits. These effects were attributed to the PI3K/AKT/Wnt/β-catenin pathway, as pharmacological inhibition of the PI3K/AKT axis or RNA interference (RNAi)-mediated silencing of β-catenin blocked ethosuximide-induced hippocampal neuronal differentiation. *In silico* molecular docking predictions additionally suggest interaction of ethosuximide with various components of the pathway.

5.1.2 Mechanism of compound 9

Unlike ethosuximide, there is extremely limited information on the mechanisms of action of compound 9 and its AED pro-drug methsuximide. Like ethosuximide, compound 9 was reported to inhibit the low threshold calcium currents (Coulter *et al*., 1990). The compound was also suggested to block voltage-gated sodium channels like the AED phenytoin (Yaari *et al*., 1986, Zhang *et al*., 1996a). However, this mechanism is unlikely to contribute to the anticonvulsive, neuroprotective, and lifespan-extending effects of the compound observed in worms in the current project, since *C. elegans* does not express these channels.

5.1.3 *C. elegans* DAF-16 and PQM-1 in the IIS pathway

The conserved *C. elegans* IIS pathway mediates lifespan regulation, dauer formation, metabolism, and responses to stress (Barbieri *et al*., 2003). Regulation of this pathway is carried out via the activation or inhibition of the IGF receptor (IGFR) ortholog, DAF-2, by various insulin-like peptides (ILPs) in *C. elegans* (Murphy and Hu, 2013). DAF-2 is a receptor tyrosine kinase which undergoes autophosphorylation and activation of its tyrosine kinase activity when bound by activating ILPs, resulting in the recruitment of AGE-1/PI3K to the plasma membrane via the PI3K adaptor subunit, AAP-1. At the plasma membrane, AGE-1 phosphorylates phosphatidylinositol 4,5-bisphosphate (PIP_2) to phosphatidylinositol 3,4,5-triphosphate (PIP_3), which then recruits the serine/threonine phosphoinositide-dependent kinase PDK-1 to the plasma membrane. AKT-1 and AKT-2, members of the protein kinase B family of

serine/threonine kinases, are subsequently recruited, phosphorylated, and activated by PDK-1. Phosphorylation of cytoplasmic DAF-16 by these kinases promotes binding and cytoplasmic sequestration by the 14-3-3 proteins FTT-2 and PAR-5, preventing nuclear shuttling of the transcription factor and thus rendering it transcriptionally inactive. The IIS pathway is antagonized by DAF-18 phosphatase/tensin homolog (PTEN) phosphatase and PPTR-1/protein phosphatase 2A subunit (PP2A), which dephosphorylates PIP_3 to PIP_2 and reduces AKT-1 phosphorylation respectively, resulting in the disinhibition and nuclear translocation of DAF-16. Aside from the IIS pathway, other cofactors and coregulators also regulate the activity of DAF-16 directly or indirectly, such as the *C. elegans* sirtuins (Landis and Murphy, 2010).

Loss-of-function mutations in *daf-2* and in genes encoding various components of the IIS pathway, such as *age-1*, cause a lifespan extension phenotype which is dependent on DAF-16 activity (Lin *et al*., 1997, Ogg *et al*., 1997, Kenyon *et al*., 1993). To understand how DAF-16 regulates aging, genes dependent on its transcriptional regulation were previously identified from loss-of-function *daf-2* backgrounds (Murphy *et al*., 2003, McElwee *et al*., 2003). DAF-16-regulated genes were categorised into two separate groups which were either up- (Class 1) or down-regulated (Class 2) when DAF-2/IIS was inhibited (Murphy *et al*., 2003). Subsequent work demonstrated that DAF-16 induces Class 1 gene expression dependently on the DAF-16-binding element (T(G/A)TTTAC; DBE) regulatory sequence in promoter regions (Tepper *et al*., 2013). On the other hand, a zinc finger transcription factor PQM-1 regulates primarily Class 2, and Class 1 genes to a lesser extent, dependently of a different regulatory motif, the DAF-16-associated element (CTTATCA; DAE). Both transcription factors were also shown to antagonize each other by exclusive occupation of either the cytoplasm or the nucleus, (Tepper *et al*., 2013). Given these findings, it is interesting that despite the requirement of DAF-16 by ethosuximide to mediate its protective effects, the PQM-1-regulated DAE motif was significantly enriched in the promoter regions of genes which were differentially-regulated by the drug (Chen *et al*., 2015b). In contrast, the DAF-16-regulated DBE motif was not identified, suggesting that

the drug's mechanism of action involves the regulation of DAE-containing genes.

Gene ontology analysis suggest that stress responses are mediated by DAF-16 regulation of Class 1 genes, whereas PQM-1 regulation of primarily Class 2 genes mediates growth and development (Tepper *et al*., 2013). Based on these findings, a model was proposed whereby PQM-1 resides in the nucleus and upregulates Class 2 genes to promote growth and development in physiological conditions, whereas DAF-16 stays sequestered in the cytoplasm. In contrast, stress conditions inhibit DAF-2/IIS and induce nuclear translocation of DAF-16 and cytoplasmic translocation of PQM-1, resulting in Class 1 gene upregulation to combat stress. A schematic of the DAF-2/IIS pathway and the proposed model of how both transcription factors function in antagonistic ways is illustrated in Figure 5.1.1 For obvious reasons, an abridged illustration of this pathway is presented herein. It should be noted that like mammalian FOXOs, DAF-16 has various isoforms and the spatiotemporal expressions and regulations, and their physiological functions remains largely unknown at this point. Adding to this layer of complexity, DAF-16 can also interact with additional coregulators and cofactors from other signalling pathways.

5.1.4 Chapter aims

As shown in the preceding chapter, compound 9 exhibited a 160-fold enhanced neuroprotective and longevity potency as compared to ethosuximide despite their similar structures. Given the largely unknown mechanism of the compound, the primary objective herein is to gain insights on whether the compound shares a similar MMOA as ethosuximide. In lieu of the conflicting evidence of T-type calcium channels as molecular targets of ethosuximide, and because work done previously within the group has excluded the role of these channels in mediating neuroprotective and longevity effects of the drug, a secondary objective is to provide an additional in-house assessment of the contribution of these channels towards the seizure-protecting effect of ethosuximide.

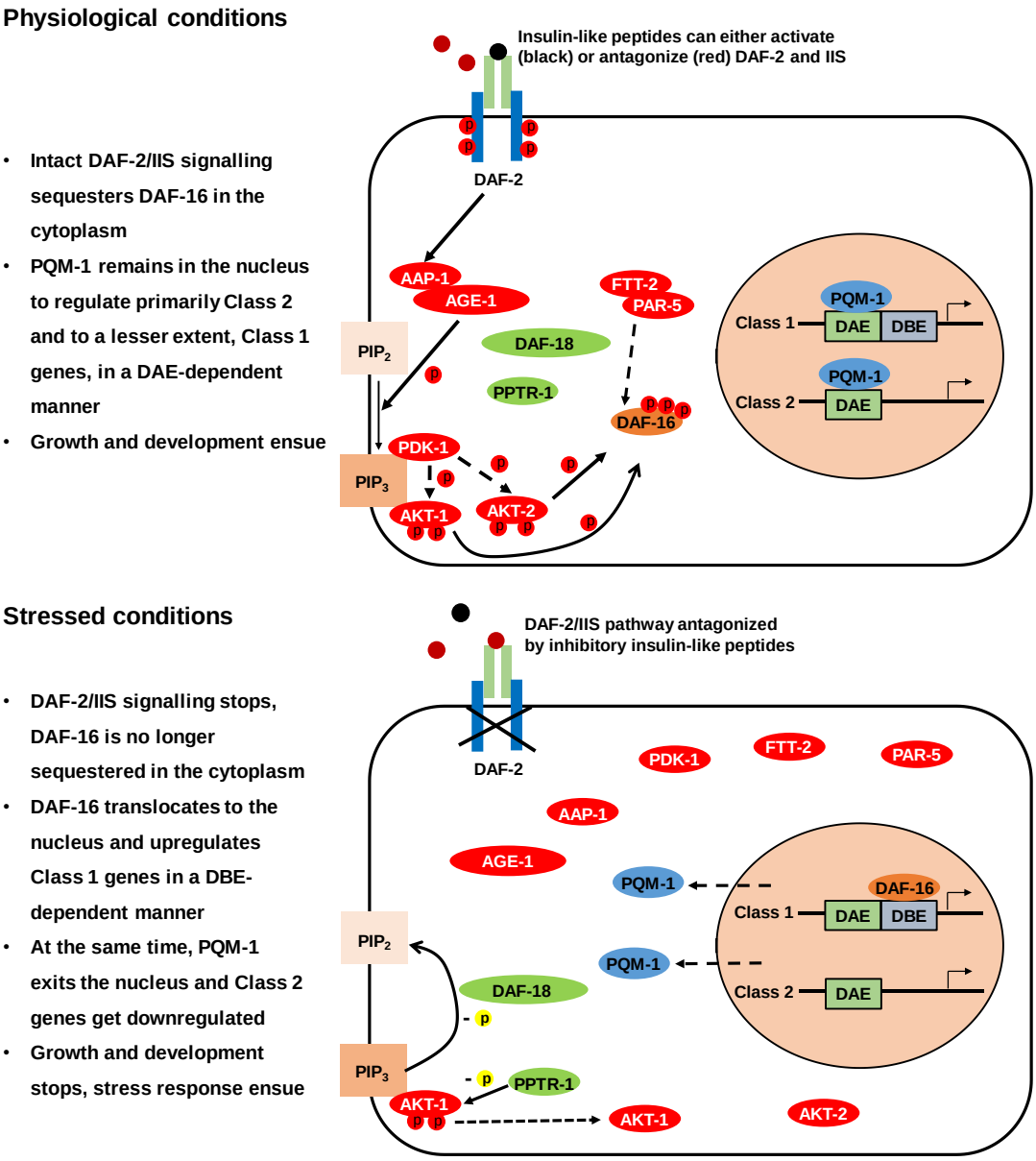

Figure 5.1.1. DAF-2/IIS pathway and antagonistic roles of DAF-16 and PQM-1. Representations of DBE and DAE are based on enrichments in Class 1 and 2 genes; DBE is also found in Class 2 genes but is underrepresented. Although direct binding of transcription factors to associated elements is illustrated herein, gene regulation can occur independently of binding, albeit via unelucidated mechanisms.

5.2 RESULTS

5.2.1 Compound 9 may have a different MMOA from ethosuximide

As reported in the preceding chapter, ethosuximide and compound 9 mediated comparable extents of neuroprotection as evident from both phenotypic improvements of locomotory deficits and direct amelioration of GABAergic neurodegeneration in CK426 worms. Although compound 9 induced a clear extension of lifespan in these worms, the longevity effects of ethosuximide were not pronounced despite previous work reporting otherwise (Chen *et al*., 2015b, Evason *et al*., 2005, Collins *et al*., 2008, Tauffenberger *et al*., 2013). Given that treatment concentrations used were 0.05 and 8 mM for compound 9 and ethosuximide respectively, overall findings indicated the striking enhancement in potency of compound 9 despite its structural similarity to the drug. As AEDs, ethosuximide is only effective for the treatment of absence seizures, whereas the methsuximide pro-drug of compound 9 has a broader spectrum of activity and has anticonvulsive effects against other types of seizures aside from absence seizures (Browne *et al*., 1983, French *et al*., 1958, Dow *et al*., 1958, Carter and Maley, 1957, Wilder and Buchanan, 1981, Hurst, 1996). This suggests that the compound may have a different MMOA than ethosuximide.

To gain insights into this, qPCR analysis was performed on a select handful of genes to compare transcriptional regulatory activities of compound 9 and ethosuximide. Chosen genes for analysis were previously identified to be modulated by ethosuximide in both WT and *dnj-14* ANCL worms from microarray work performed within the group (Chen *et al*., 2015b). An unbiased approach such as microarray would be more ideal for facilitating a wider understanding of the compound's MMOA, but this was not feasible given the time constraints of the current project. Selected genes included a negative control gene *pph-6* which did not change in expression levels in response to ethosuximide, a downregulated gene *tir-1*, and nine of the most upregulated genes *asm-3*, *ugt-25*, *dhs-26*, *ttr-44*, *dod-3*, *dod-6*, *cyp-35B1*/*dod-13*, *cyp*-34A9/*dod*-16, and cyp-*14A3*; a summary of these genes is provided in Table 5.2.1. All of them are DAF-16-dependent upregulated Class 1 genes identified from loss-of-function *daf-2* backgrounds, except *asm-3* and *tir-1* are Class 2

genes which were conversely downregulated (Murphy *et al*., 2003, Tepper *et al*., 2013).

qPCR assessment was carried out on day 7 CK426 worms on the same treatments used to assess both neuroprotective and longevity effects; day 7 was the age selected for analysis as direct protection against GABAergic neurodegeneration was consistent for both compounds at this timepoint. Transcript levels from ethosuximide-treated worms mostly corroborated microarray findings on ethosuximide-upregulated genes, as Class 1 genes *ugt-25*, *dhs-26*, *dod-6*, *cyp-35B1*/*dod-13*, *cyp*-34A9/*dod*-16, and cyp-*14A3* were similarly induced in response to the drug (Figure 5.2.2). Expression levels of the remaining two microarray upregulated genes *asm-3* and *ttr-44*, per contra, were not significantly elevated. Likewise, ethosuximide did not cause a reduction in *tir-1* expression as previously observed. Unlike ethosuximide, compound 9 did not cause any significant modulation of gene expression, aside from the downregulation of *dhs-26* (Figure 5.2.2).

Comparisons between both treatments revealed a more pronounced difference in expression levels as the transcript abundances of all Class 1 genes were strikingly higher from ethosuximide-treated worms as compared to compound 9-treated ones. In contrast, transcript levels of the Class 2 gene *asm-3* were not statistically different between both treatments, whereas the other Class 2 gene *tir-1* was expressed at significantly higher levels by compound 9. From these differences in the transcriptional regulatory activities of both compounds, it is possible that compound 9 may have a different MMOA than ethosuximide.

Microarray findings	*C. elegans* gene	Gene description	Literature	Human ortholog
Upregulated	*asm-3*	Sphingomyelin phosphodiesterase	• Class 2 gene • Acts upstream of DAF-16 to positively regulate DAF-2/IIS pathway in C. elegans (Kim and Sun, 2012)	SMPD1
	dod-3	Unknown protein; Downstream Of DAF-16 (Regulated by DAF-16)	**Class I genes** • Unknown functions of *dod-3* and *dod-6* • *cyp-35B1*/*dod-13, cyp*-34A9/*dod*-16, and cyp-*14A3* encode the cytochrome P450 family members, which are the major enzymes carrying out phase I functionalisation reactions in drug metabolism; phase I reactions mediate hydrolysis, oxidation, or reduction, to reveal or attach functional groups such as hydroxyl (-OH), carboxyl (-COOH), thiol (-SH), amine (-NH), or amino (-NH_2) groups to a molecule • *ugt-25* encodes the phase II UDP-glucuronosyltransferase, which conjugates glucuronide groups to phase I primary metabolites; phase II detoxification reactions inactivates and hydrophilizes molecules to facilitate elimination from the body • *dhs-26* encodes a short chain dehydrogenase which is an oxidoreductase • *ttr-4* encodes a transthyretin-like protein with unknown function	-
	dod-6			-
	cyp-35B1/ *dod-13*	Cytochrome P450; Downstream Of DAF-16 (Regulated by DAF-16)		CYP2A7P1
	cyp-34A9/ *dod*-16			
	ttr-4	Transthyretin-like protein; Downstream Of DAF-16 (Regulated by DAF-16)		-
	cyp-*14A3*	Cytochrome P450		CYP1A2
	ugt-25	UDP-Glucuronosyltransferase		UGT3A1, UGT3A2
	dhs-26	Short chain dehydrogenase		DHRS1
Downregulated	*tir-1*	Sterile alpha and TIR motif-containing protein tir-1	• Class 2 gene • Null mutations suppresses neurodegeneration in *C. elegans* ALS model (Veriepe *et al*, 2015)	SARM1

Table 5.2.1. Genes selected for qPCR analysis. Selected genes were previously shown from microarray analysis to be regulated with ethosuximide treatment in both WT and *dnj-14* ANCL worms (Chen *et al*., 2015b).

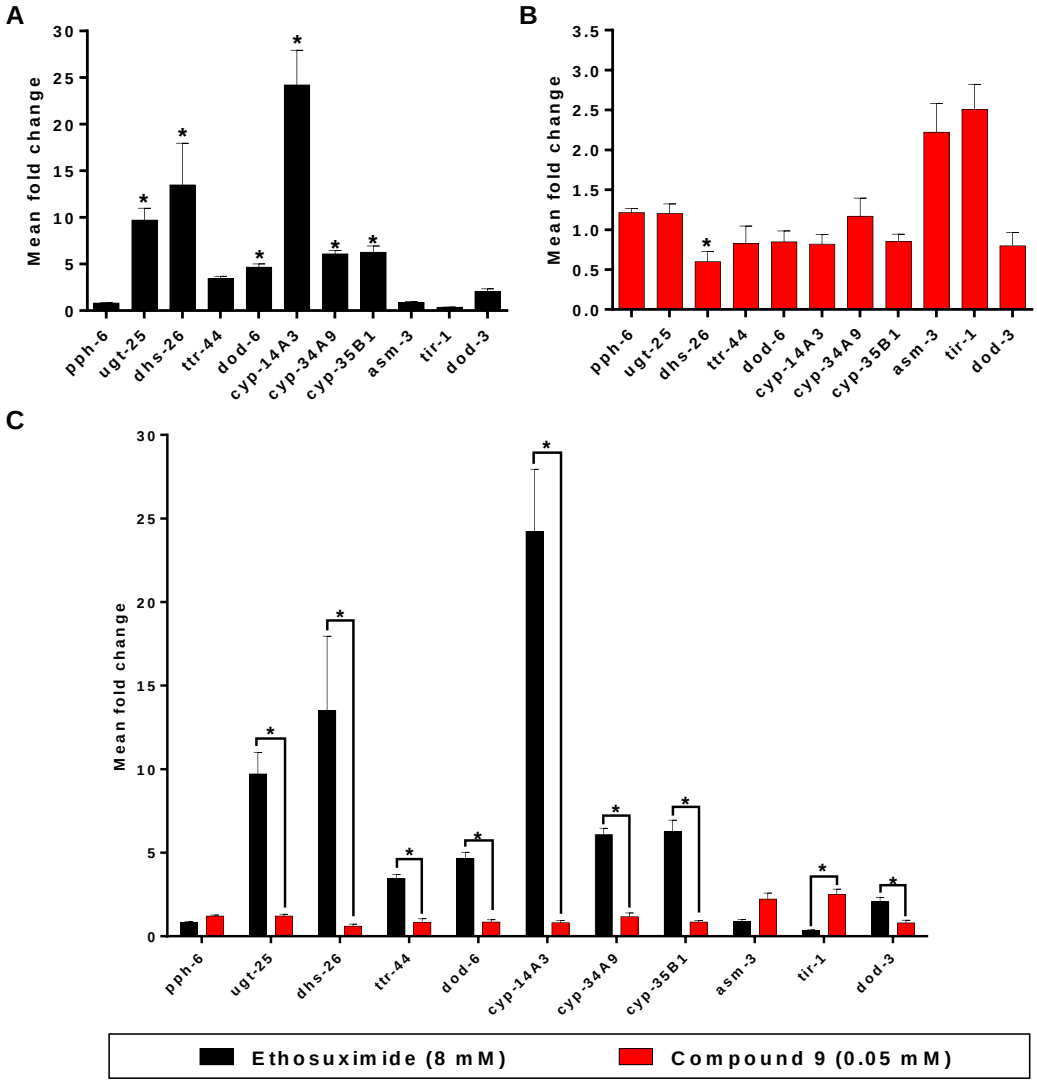

Figure 5.2.2. Gene expression changes by ethosuximide and compound 9. Transcript levels of selected genes were analysed with qPCR in chronically-treated day 7 CK426 worms. (A) Ethosuximide significantly upregulated most transcripts except *ttr-4*, *asm-3*, *tir-1*, and *dod-3* when compared to unchanged levels of the *pph-6* negative control ($p<0.05$), whereas (B) only *dhs-26* expression was significantly reduced by compound 9. (C) Except *tir-1*, expression levels of all genes were higher with ethosuximide than compound 9 treatment ($p<0.05$). Data was pooled from four biological replicates, with three technical replicates per gene and strain. Fold changes were derived from normalization to housekeeping genes (*pmp-3* and *cdc-42*) and respective succinimide and DMSO controls for ethosuximide and compound 9. Analysis was performed with the Kruskal-Wallis test with Dunn's multiple comparisons; *, $p<0.05$.

To gain an additional insight into the MMOA of compound 9 as compared to ethosuximide, metabolome profiles acquired previously by 1D ^{1}H NMR spectroscopy for drug bioaccumulation determination was subjected to further analysis. As discussed in the preceding chapter, both day 1- and 5-treated CK426 worms were processed to determine drug bioaccumulation. However, day 5 samples were of poor quality due to the presence of heavy contamination by the bacterial food source which introduced additional variability. As reliable NMR data depends on good reproducibility between replicates to detect real biological differences, these data are not suitable for further analysis, although the information derived at this later timepoint is potentially more cogent and comparable with day 7 qPCR findings. To get an idea of metabolome differences between the two treatments without contamination, 1D ^{1}H NMR metabolome profiles of day 1 samples were subjected to uni- and multi-variate analyses (Figure 5.2.3). Due to the low number of biological replicates (*nf* = 3), however, analysis was restricted to unsupervised statistical methods to avoid overfitting of discriminant models such as partial least squares discriminant analysis (PLS-DA).

Multivariate principal component analysis (PCA) transformed the 1940-bucketed spectra from 10 to 0.10 ppm, which excluded the protonated water region at 4.8 to 4.6 ppm, into 5 principal components (PCs), with 95 % of the variance between treatments displayed with PC1 and PC2 on the scores plot (Figure 5.2.3). The intra-group clustering pattern on the PCA scores plot provides an indication of the reproducibility within each group, and additionally highlights potential differences between groups based on the clustering distances between them. PCA clustering shown herein suggest larger differences from ethosuximide-treated samples in comparison to succinimide- and compound 9-treated ones, as these samples are clearly distinct in the first PC, which explains 90 % of the total variance between the spectra, from the other treatments. Inspection of the PCA loadings plot highlighted variables or features that give rise to the sample variance, with variables distinct from the main cluster at 0,0 being the most influential (Figure 5.2.3). Univariate ANOVA with *post-hoc* Tukey's analysis confirmed that most of these peaks were significantly different in ethosuximide-treated samples (Figure 5.2.3). With the

exception of features at 0.8925 and 0.8775 ppm which coincided with the spectral region of a drug-derived peak at 0.90 to 0.85 ppm (refer to chapter 3, Figure 3.2.19), the other significant features were unlikely drug-derived and possibly metabolome changes as a result of ethosuximide treatment. Although neuroprotection from compound 9 and ethosuximide were not consistently observed in day 1 CK426 worms, these preliminary findings suggest that ethosuximide induces earlier metabolomic changes, which might relate to a different MMOA.

In summary, findings from both qPCR and preliminary metabolome analyses suggest that compound 9 may have a different MMOA from ethosuximide. qPCR findings were more cogent as compound 9 did not induce the same DAF-16-upregulated Class 1 genes as ethosuximide. Additionally, Class 2 genes modulation seems to differ between both compounds. Taken together, this suggests that the protective effects of compound 9 might not be mediated via a DAF-16-dependent pathway like ethosuximide.

A

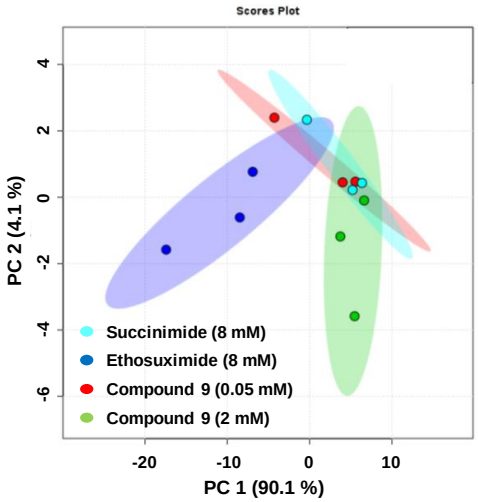

B

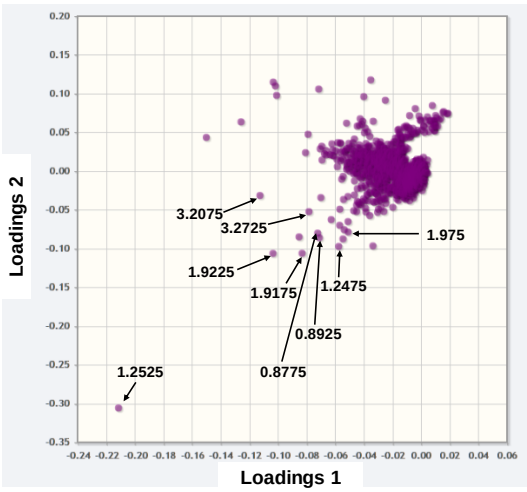

C

Discriminating feature (ppm)	Distance from cluster (0,0)	ANOVA post-hoc analysis (p<0.05)
1.2525	0.371331105	Ethosuximide vs all groups
1.4775	0.15633865	Ethosuximide vs succinimide and 2 mM compound 9
1.3375	0.154615619	Ethosuximide vs 2 mM compound 9
1.4875	0.150028271	NS
1.9225	0.148119829	Ethosuximide vs all groups
1.4925	0.141080651	NS
1.3275	0.140696999	Ethosuximide vs 2 mM compound 9
1.9175	0.134565042	Ethosuximide vs all groups
1.4825	0.127924297	NS
1.4975	0.123065383	NS
1.2575	0.120138539	Ethosuximide vs succinimide and 2 mM compound 9
3.2075	0.116849307	Ethosuximide vs all groups
1.2475	0.11277773	Ethosuximide vs all groups
0.8775	0.111405641	Ethosuximide vs all groups
0.8925	0.107666389	Ethosuximide vs all groups
1.4625	0.104293006	NS
1.1975	0.102971028	Ethosuximide vs all groups
1.1875	0.101996985	Ethosuximide vs succinimide and 0.05 mM compound 9
1.5025	0.09503688	NS
3.2725	0.094127331	Ethosuximide vs all groups

D

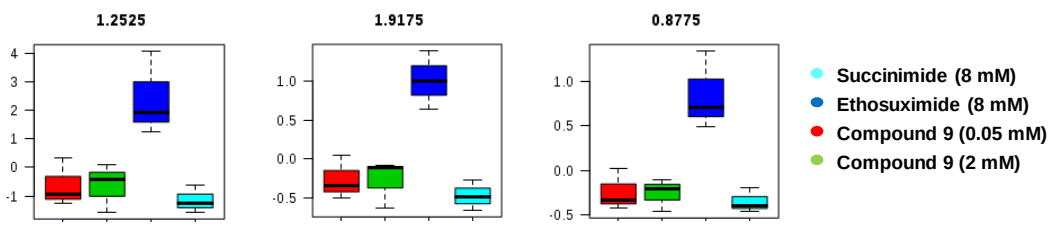

Figure 5.2.3. Uni- and multi-variate analyses of differentially-treated day 1 CK426 samples with ANOVA and PCA. (A) Clustering patterns on PCA scores plot. Shaded areas show 95 % confidence intervals. Although ethosuximide-treated samples (dark blue) appear to cluster away from the other treatments (succinimide, light blue; compound 9, red/green), confidence intervals from all treatments overlap. (B) PCA loadings plot and (C) table with the top twenty discriminating features (ppm) which separated furthest away

from the main cluster (0,0). (C) ANOVA and Tukey's *post-hoc* analysis revealed significant features from ethosuximide-treated samples ($p<0.05$), and those which are significantly different when compared to all other treatments are highlighted in green and indicated on the (B) loadings plot; *p* value of significance was adjusted for multiple testing with the false discovery rate (Benjamini and Hochberg, 1995). (D) Selected box plots demonstrating higher concentrations of significant features from ethosuximide-treated samples (1.2525, 1.9175, and 0.8775 ppm). Data shown is from twelve ^{1}H spectra from four treatment conditions with three biological replicates each; NS, not significant.

5.2.2 Compound 9 requires DAF-16 to exert neuroprotection and lifespan extension

To verify qPCR findings which suggest that the MMOA of compound 9 is not dependent on DAF-16, the neuroprotective and lifespan-extending activities of the compound were re-evaluated in *daf-16* loss-of-function CK426/CZ1200 worms which express a *daf-16* (*mu86*) deletion mutation. These worms were generated by genetic crosses of CK426/CZ1200 and *daf-16* (*mu86*) worms (Lin *et al*., 1997) (refer to chapter 2; section 2.2.1 and Figure 2.1). Note that although both CK426 and CK426/CZ1200 crosses can be performed with *daf-16* mutants, genetic crosses are tedious. For this reason, CK426/CZ1200 worms were crossed as the additional expression of GFP in GABAergic neurons enables further investigation on the effect of loss-of-function *daf-16* on GABAergic motor neuron integrity aside from locomotion and lifespan phenotypes. CK426/CZ1200 worms exhibit locomotion defects and both red pharyngeal and green GABAergic neuronal fluorescence markers from P*myo-2::*dsRED and P*unc-25*::GFP transgenes, whereas *daf-16* (*mu86*) worms have no fluorescent markers or obvious locomotory deficits. Hence, compound mutant progenies from the cross were selected based on CK426/CZ1200-derived markers. F1 progenies heterozygous for the *daf-16* (*mu86*) allele and CK426/CZ1200-derived TDP-43-encoding *TARDBP* and P*unc-25*::GFP transgenes are desired. Due to heterozygosity, hermaphroditic F1 progenies were selected for further propagation based on milder locomotion defects and fainter red pharyngeal and green GABAergic neuronal fluorescence. Homozygous hermaphroditic F2 worms with severe locomotion and bright fluorescences were singled out and further propagated. F3 populations which homogenously displayed these features were genotyped for the presence of the *TARDBP* transgene and homozygosity of the *daf-16* (*mu86*) deletion allele with PCR; genotyping primers were specified in Table 2.3 of chapter 2. Note that human TPD-43 protein expression in the CK426/CZ1200 strain was already previously verified as discussed in the preceding chapter, hence *TARDBP* genotyping was performed herein in place of protein expression confirmation. *daf-16* (*mu86*) homozygosity was verified by the presence of only the deletion allele and not the WT *daf-16* one. PCR primers distinguish between both alleles which either flanked the allelic region or target within the

deletion. The former flanking primers only amplify the *daf-16* (*mu86*) deletion allele of 405 bp, but not the WT one as its product size is too large (11385 bp) for efficient amplification with the PCR conditions used. In contrast, the latter primer pair only amplifies a WT *daf-16* region of 635 bp. As the genomic location of the *TARDBP* transgene was not mapped, only expression but not homozygosity can be confirmed using primers specific for it; *TARDBP* PCR products are 1231 bp. Figure 5.2.4 shows the twice-verified genotype of compound mutant worms prior to analysis.

As reported in the preceding chapter, compound 9 caused a significant 25 % extension of the mean lifespan in CK426 worms as compared to DMSO-treated controls. However, this lifespan-extending effect was abolished in the *daf-16* null CK426/CZ1200 worms herein, as the mean lifespan of compound 9-treated worms were reduced by an insignificant 3 % in comparison to DMSO controls (Figure 5.2.5). This demonstrated that DAF-16 is essential for mediating the longevity effects of compound 9. Similar to the lack of lifespan extension by ethosuximide on CK426 worms as reported in the previous chapter, the drug exhibited no effect on the lifespan of these *daf-16* null worms.

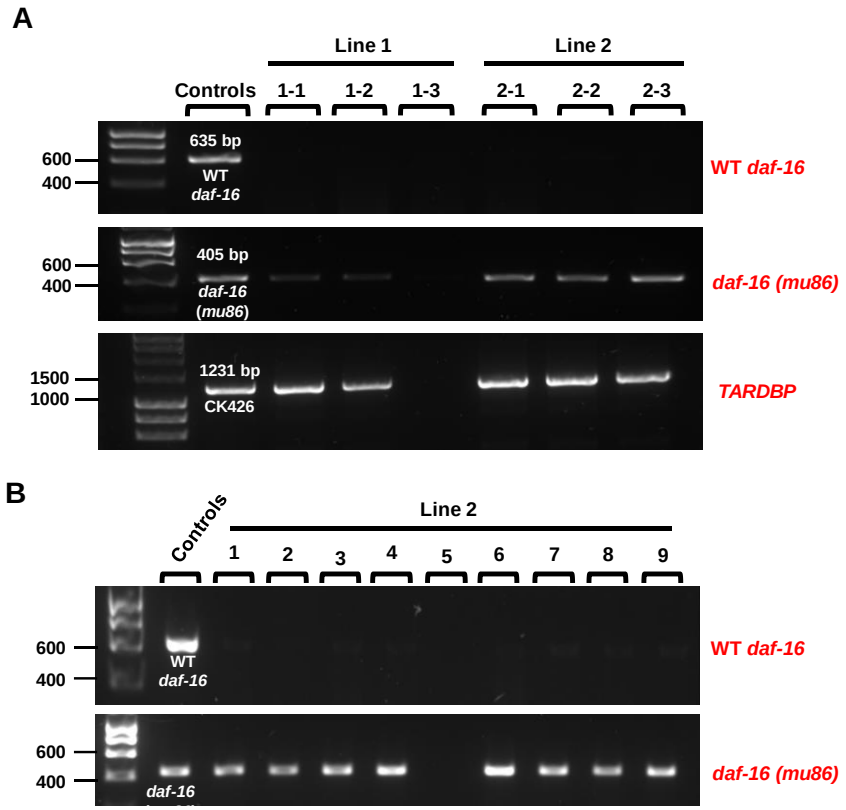

Figure 5.2.4. Agarose gels showing verified genotypes of *daf-16* null CK426/CZ1200 worms. (A) Single worms from two F3 lines were PCR genotyped for *daf-16* (*mu86*) homozygosity and TDP-43-encoding *TARDBP* transgene expression. Primers specific for WT and mutant *daf-16* alleles produce PCR products of 635 and 405 bp respectively, whilst *TARDBP*-specific primers generate 1231 bp products. Products of interest for each gel are indicated beside gels in red. All worms were homozygous for the *daf-16* (*mu86*) allele and express the *TARDBP* transgene. (B) Line 2 worms were further propagated for several generations and reconfirmed for *daf-16* (*mu86*) homozygosity. Progenies displayed poor locomotion and *TARDBP*-associated red pharyngeal co-injected fluorescence marker, hence transgene expression was not re-verified. Note that PCR products from samples 1-3 from (A) and 5 from (B) were not successfully amplified with any of the primers tested, hence no bands were observed.

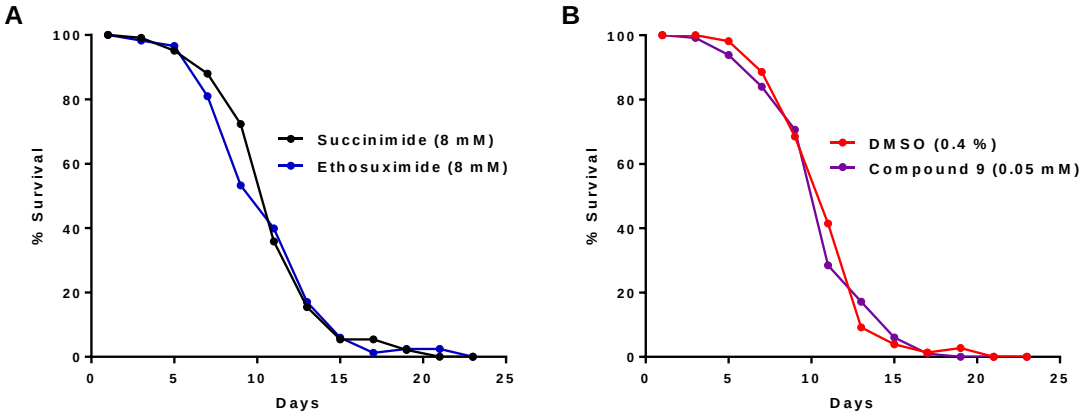

Figure 5.2.5. DAF-16 is essential for lifespan extension by compound 9. Lifespan analyses were performed in chronically-treated *daf-16* null CK426/CZ1200 ALS worms. Worms were scored as dead in the absence of pharyngeal pumping or response to touch, with physically damaged and bagged worms censored from analysis. Both (A) ethosuximide and (B) compound 9 failed to improve the longevity of the CK426 worms in the absence of functional DAF-16 ($p>0.05$). Mean lifespans (number of adulthood days) are as follows: succinimide, 11.70 ± 0.34 (n = 86); ethosuximide, 11.30 ± 0.33 (n = 87); DMSO, 12.03 ± 0.40 (n = 77); compound 9, 11.65 ± 0.32 (n = 86). Data shown was pooled two biological replicates, with comparisons of lifespans carried out with the log-rank test. Total n per biological replicate; first replicate, 46 succinimide, 41 ethosuximide, 36 DMSO, 50 compound 9; second replicate, 40 succinimide, 47 ethosuximide, 40 DMSO, 36 compound 9.

As expected from the known DAF-16 dependency of ethosuximide, loss of functional DAF-16 abolished the drug's neuroprotective effects. This was evident from the failure of the drug to mitigate both locomotion defects of the CK426 worms (Figure 5.2.6), but also cell body losses (Figure 5.2.7) and breaks (Figure 5.2.8) within the inhibitory GABAergic D-type motor neuronal subset. Despite qPCR findings, loss of functional DAF-16 also obliterated these protective effects from compound 9 (Figures 5.2.6 to 5.2.8). Representative images of days 1 and 7 *daf-16* null CK426/CZ1200 worms are shown herein (Figures 5.2.9 and 5.2.10), whilst those of days 3 and 5 worms are shown in Appendices 8 and 9.

Contradictory to qPCR findings, these findings demonstrated that both compound 9 and ethosuximide mediate neuroprotective and longevity properties via a DAF-16-dependent pathway.

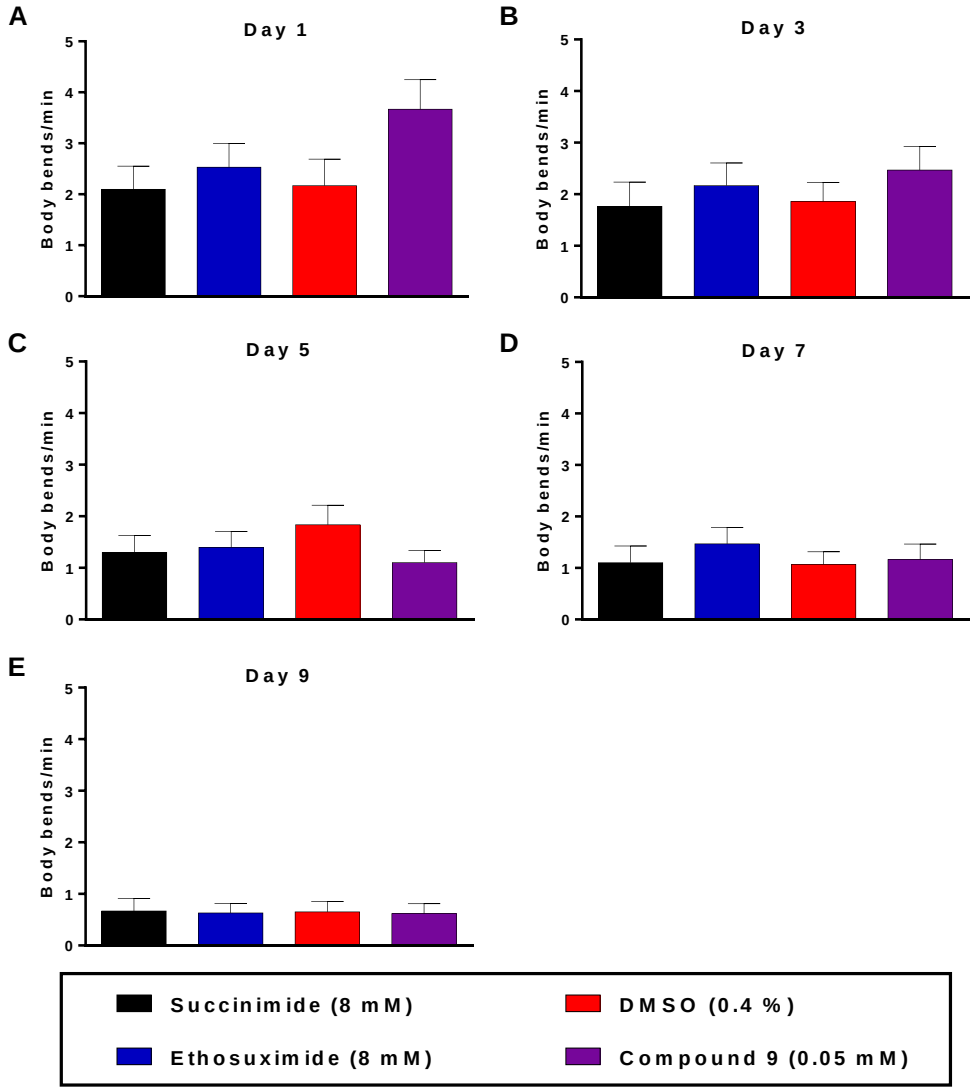

Figure 5.2.6. Compound 9 requires DAF-16 to mitigate locomotion defects of CK426 ALS worms. The *daf-16* gene was deleted in the CK426 genetic background via mating with a *daf-16* null mutant strain to assess the necessity of functional DAF-16 in mediating the protective effects of compound 9 on movement. Similar to ethosuximide, protection by the compound was abolished in the absence of DAF-16 at all assayed ages. Data was pooled from three biological replicates, with comparisons performed via the Kruskal-Wallis test with Dunn's multiple comparisons against succinimide or DMSO controls (n = 26 – 30 worms per treatment per age).

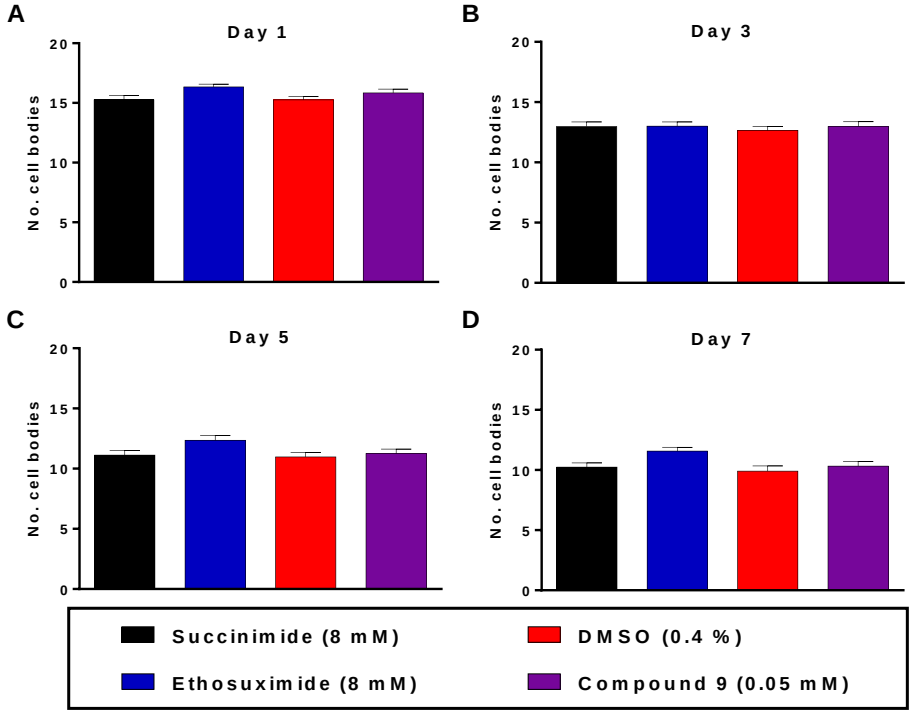

Figure 5.2.7. Compound 9-mediated protection against GABAergic neuronal cell body losses is DAF-16 dependent. The *daf-16* allele was deleted in the GABAergic GFP-expressing CK426/CZ1200 worms through crosses with a *daf-16* null mutant strain. Synchronised worms were chronically treated from the L1 larval stage and scored for the number of intact cell bodies from the D-type GABAergic motor neurons. The loss of DAF-16 completely abolished the ability of both ethosuximide and compound 9 to mitigate cell body losses at all ages. Data was pooled from four biological replicates, with comparisons performed via the Kruskal-Wallis test with Dunn's multiple comparisons against succinimide or DMSO controls (n = 46 – 52 worms per treatment per age).

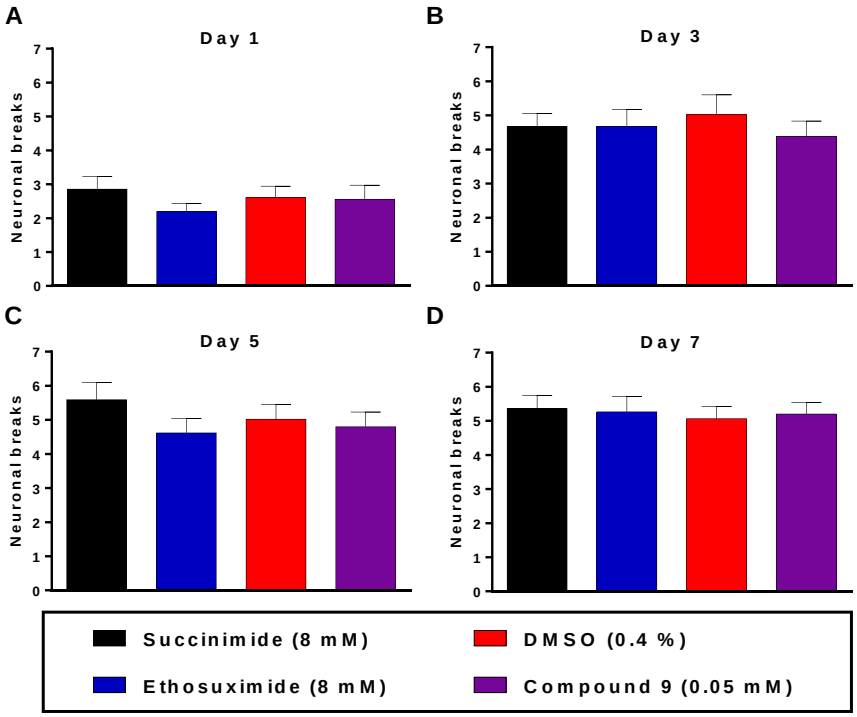

Figure 5.2.8. Protective effect of compound 9 against breaks in GABAergic neurons require DAF-16. Deletion of the *daf-16* allele in CK426/CZ1200 worms was carried out through crosses with a *daf-16* null mutant strain. Synchronised worms were chronically treated from the L1 larval stage and assessed for breaks within the D-type GABAergic motor neurons. At all assayed ages, the loss of *daf-16* prevented reduction of neuronal breaks by both ethosuximide and compound 9 as compared to their respective succinimide and DMSO vehicle controls. Data was pooled from four biological replicates, with comparisons performed via the Kruskal-Wallis test with Dunn's multiple comparisons (n = 46 – 50 worms per treatment per age).

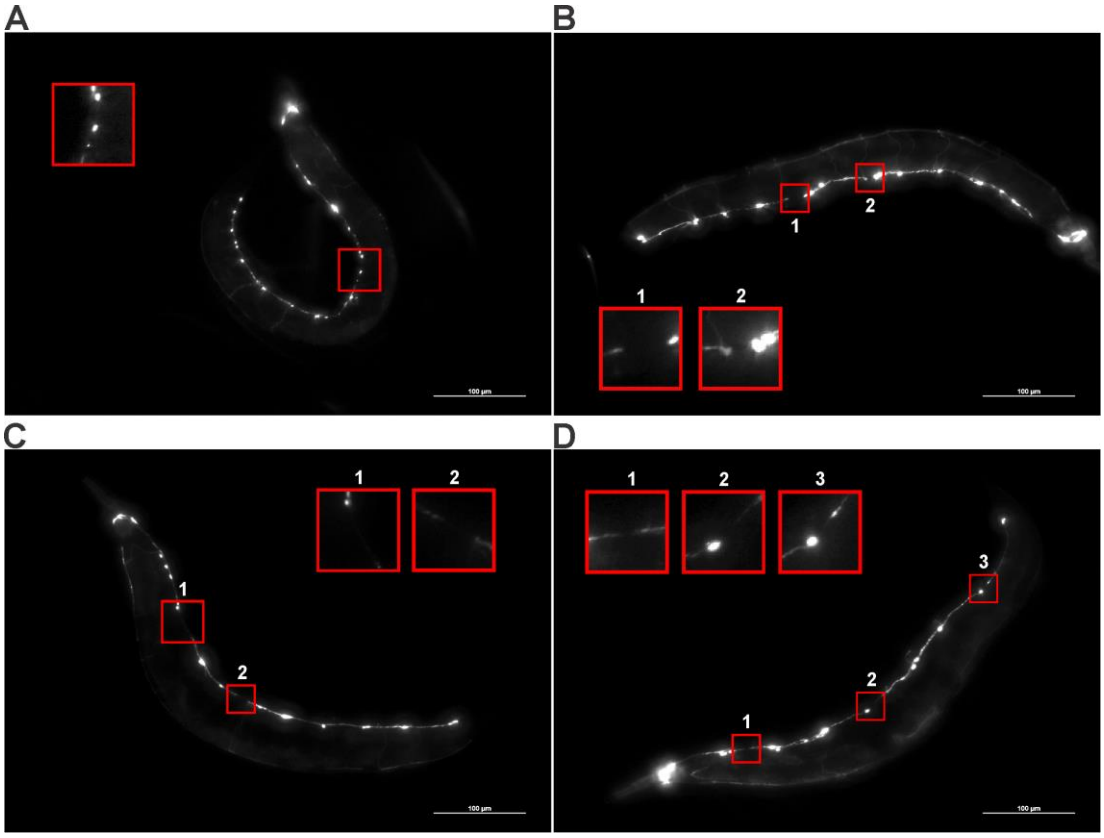

Figure 5.2.9. Representative images of day 1 *daf-16* null CK426/CZ1200 worms. Age-synchronised worms were chronically treated with 8mM (A) succinimide or (B) ethosuximide, (C) 0.4 % DMSO vehicle or (D) 0.05 mM compound 9 in 0.4 % DMSO from the L1 larval stage. Breaks within the D-type GABAergic motor neurons in the ventral nerve cord are indicated and enlarged with red boxes. Images were taken at 200X magnification, scale bars = 100 µm.

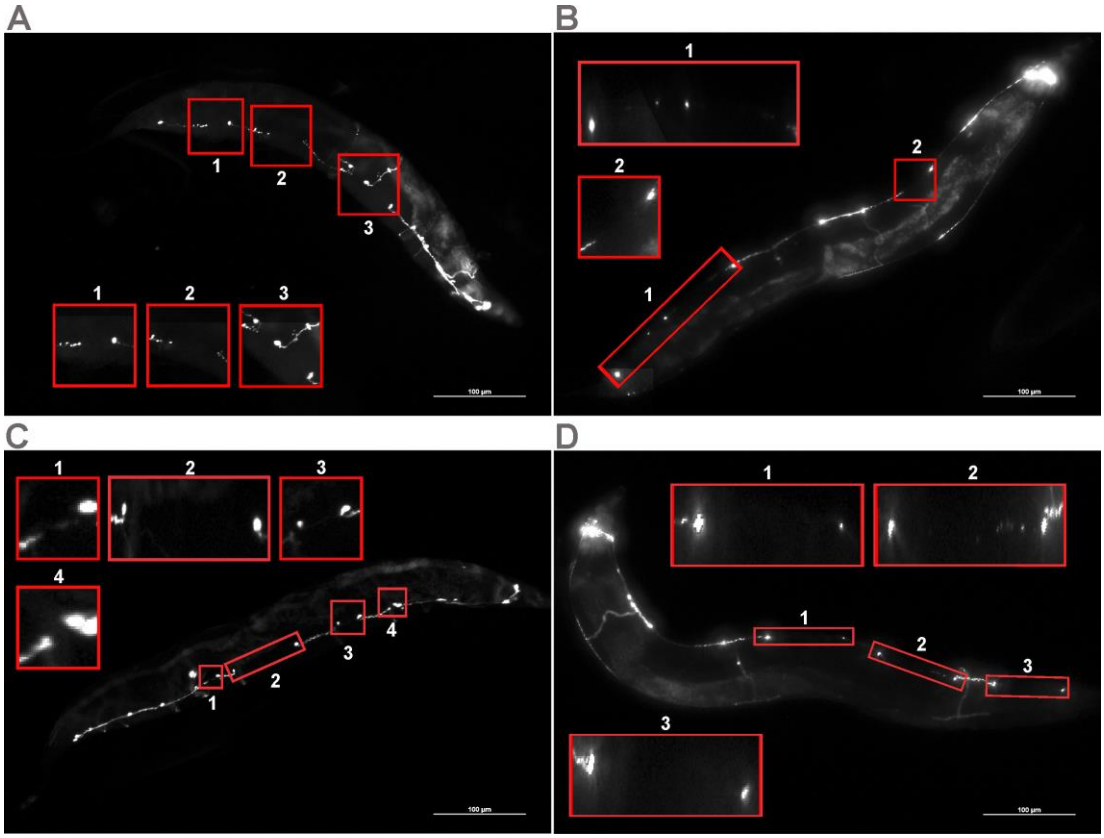

Figure 5.2.10. Representative images of day 7 *daf-16* null CK426/CZ1200 worms. Age-synchronised worms were chronically treated with 8mM (A) succinimide or (B) ethosuximide, (C) 0.4 % DMSO vehicle or (D) 0.05 mM compound 9 in 0.4 % DMSO from the L1 larval stage. Breaks within the D-type GABAergic motor neurons in the ventral nerve cord are indicated and enlarged with red boxes. Images were taken at 200X magnification, scale bars = 100 µm.

5.2.3 Anticonvulsant activity of ethosuximide is not mediated via CCA-1 and DAF-16

Despite being an established antiepileptic drug, the MMOA underlying seizure protection by ethosuximide is not understood. DAF-16 was previously shown to play a role in mediating both lifespan extension and neuroprotection by ethosuximide (Chen *et al*., 2015b, Tauffenberger *et al*., 2013), but its potential role in seizure protection has not been studied or reported. To address this, the anticonvulsive activity of the drug was evaluated on *unc-49* worms which harbour the same null *daf-16* mutation as mentioned in the preceding section (*unc-49*/*daf-16*). Additionally, in view of the controversial role of the T-type calcium channels as mediators of the drug's anticonvulsive effects, a *cca-1* deletion was introduced into the genetic background of the *unc-49* worms (*unc-49*/*cca-1*) herein to enable an in-house insight into whether these channels constitute the drug's defence arsenal against seizures.

These double mutant *unc-49*/*daf-16* and *unc-49*/*cca-1* strains were generated by genetic crosses of the *unc-49* worms with the respective loss-of-function *daf-16* (*mu86*) and *cca-1* (*ad1650*) strains (refer to chapter 2; section 2.2.1 and Figures 2.1 and 2.2). As none of these strains express fluorescence markers, unlike the CK426/CZ1200 worms as aforementioned, progenies from crosses were selected based on the phenotypic markers prior to genotyping. Characteristic to the *unc-49* strain is the "shrinker" phenotype whereby bodily contraction and shortening occurs in response to touch stimulation of either anterior or posterior ends (McLntire *et al*., 1993). Additionally, this strain exhibits reduced thrashes in liquid in comparison to the loss-of-function strains, which display no locomotory abnormality. Furthermore, only *unc-49* worms seize in response to PTZ treatment. As desired heterozygous F1 progenies from these crosses will only possess a single copy of the *unc-49* (*e407*) allele, these worms would technically exhibit milder or no obvious "shrinker" phenotype and higher thrashing rates than parental homozygous *unc-49* worms. Hence, hermaphroditic F1 worms displaying these features were propagated to derive F2 progenies. F2 hermaphrodites with the characteristic *unc-49*-derived "shrinker" phenotype and reduced thrashing rates, indicative of *unc-49* (*e407*) homozygosity, were singled out and propagated for a further

generation before single worm genotyping was performed with PCR to verify homozygosity for *unc-49* (*e407*) and *daf-16* (*mu86*) or *cca-1* (*ad1650*) alleles; genotyping primers specified in Table 2.3 of chapter 2. Both *daf-16* (*mu86*) and *cca-1* (*ad1650*) alleles contain deletions. *cca*-1-targeting primers flank the allele to generate WT and deletion mutant products of 3310 and 930 bp respectively. Primers specific for the WT *daf-16* allele recognize the deleted region, hence PCR products of 1470 bp will only be generated for the WT allele. On the other hand, primers targeting the *daf-16* (*mu86*) allele flanked the allelic region to produce 950 bp products; WT alleles would not be amplified since the 10980 bp deletion is too large. Instead of a deletion, the *unc-49* (*e407*) allele is a C to T point mutation which results in a premature stop codon (Q179stop). To differentiate between the WT and mutated *unc-49* allele, PCR was performed with primers targeting exon 5 of the *unc-49* allele, followed by restriction digestion of products with the enzyme MseI. MseI recognizes the T^TAA sequence and cleaves the WT *unc-49* product at a single site at the exon to generate two 259 and 172 bp fragments. In contrast, the point mutation introduces an additional recognition site at the exon, resulting in cleavage into three 258, 120, and 53 bp fragments. Figures 5.2.11 and 5.2.12 show the verified genotype of three homozygous lines for each double mutant strain. These verified lines were each assessed to check for reproducibility of the observed responses to ethosuximide treatment.

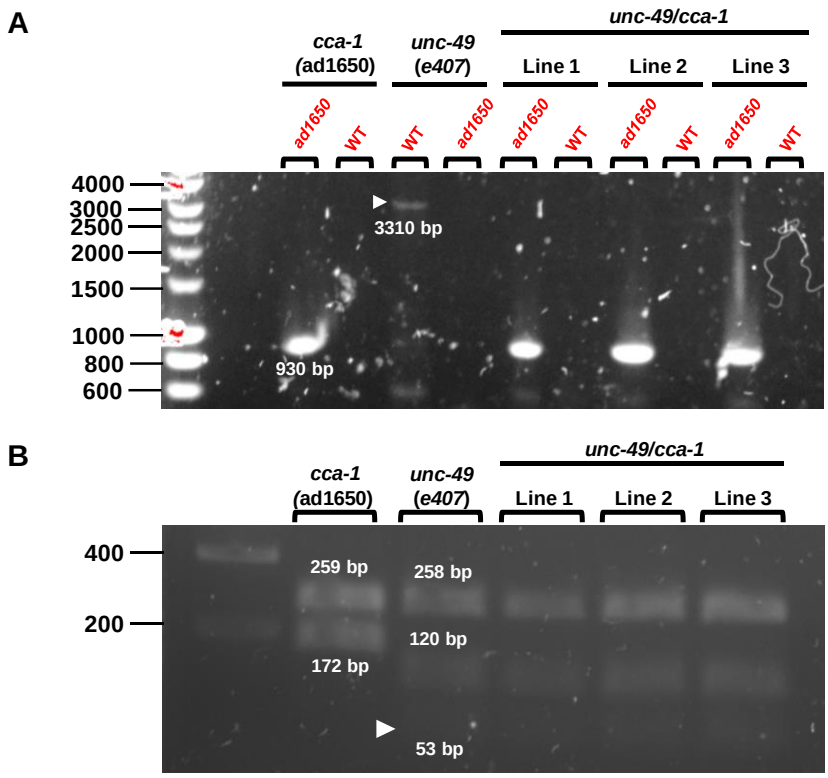

Figure 5.2.11. Agarose gels showing verified genotypes of *unc-49*/*cca-1* lines. Single mutant strains *cca-1* (*ad1650*) and *unc-49* (*e407*) were analysed alongside as reference controls for mutant alleles, and as corresponding controls for WT *unc-49* and *cca-1* alleles. (A) Primers specific for WT and mutant *cca-1* alleles (red) produce PCR products of 3310 and 930 bp respectively. All *unc-49*/*cca-1* lines were homozygous for the *cca-1* (*ad1650*) deletion as only mutant product was detected. (B) Exon 5 of the *unc-49* allele contains the C to T point mutation in the *unc-49* (*e407*) strain and was amplified with PCR. WT and mutant alleles were differentiated with MseI restriction enzyme digestion, which cuts respective PCR products at one and two T^TAA sites to generate two WT and three mutant cleavage products of the specified sizes; the smallest cleaved fragment from mutant product is very faint and indicated with arrow head. Three clear cleavage products were present for all lines, confirming *unc-49* (*e407*) homozygosity. Genotyping was performed by Douglas Grimes (University of Liverpool).

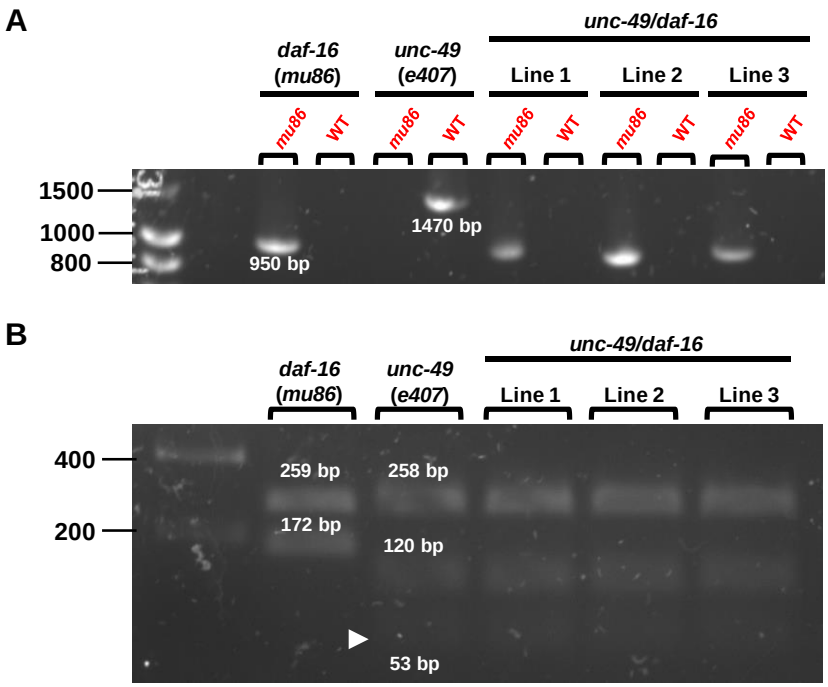

Figure 5.2.12. Agarose gels showing verified genotypes of *unc-49/daf-16* lines. Single mutant strains *daf-16* (mu86) and *unc-49* (*e407*) were analysed alongside as reference controls for mutant alleles, and act as corresponding controls for WT *unc-49* and *daf-16* alleles. (A) Primers specific for WT and mutant daf-*16* alleles (red) produce PCR products of 1470 and 950 bp respectively. All *unc-49*/*daf-16* lines were homozygous for the *daf-16* (mu86) deletion as only mutant product was detected. (B) As before, *unc-49* exon 5 PCR products were digested with the restriction enzyme MseI to distinguish WT and mutant *unc-49* alleles. Three mutant-associated cleavage products were present for all lines, confirming *unc-49* (*e407*) homozygosity. Genotyping was performed by Douglas Grimes (University of Liverpool).

As previously observed in *unc-49* worms, ethosuximide protected against PTZ-induced seizures when worms were acutely treated with the optimal anticonvulsant concentration of 4 mg/mL (28 mM; Figure 5.2.13). At this concentration, the drug also exerted an overall anticonvulsant effect in each *unc-49*/*daf-16* and *unc-49*/*cca-1* line. However, a minority of the assayed population from the *unc-49*/*daf-16* lines was observed to seize at noticeably higher rates and intensities which were akin to succinimide-treated *unc-49* worms. As worms were only acutely treated for this assay, the reduced efficacy of the drug in protecting against induced seizures in a minority of *unc-49*/*daf-16* worms suggest that a longer duration of exposure to the drug may be required to better assess the extent or involvement of the transcription factor in mediating the seizure-protecting activity of ethosuximide. As transcriptional changes are known to occur over a range of timescales in response to different stimuli (Yosef and Regev, 2011), it may well be that the role of DAF-16 in seizure protection is chronic rather than acute. Additionally, elucidating the role of the transcription factor under conditions of chronic treatment may mirror clinical conditions better, since the drug is chronically administered to patients. Although the role of DAF-16 remains unclear at this point, current findings show that neither CCA-1 nor DAF-16 is essential to mediate the acute anticonvulsant activity of the drug.

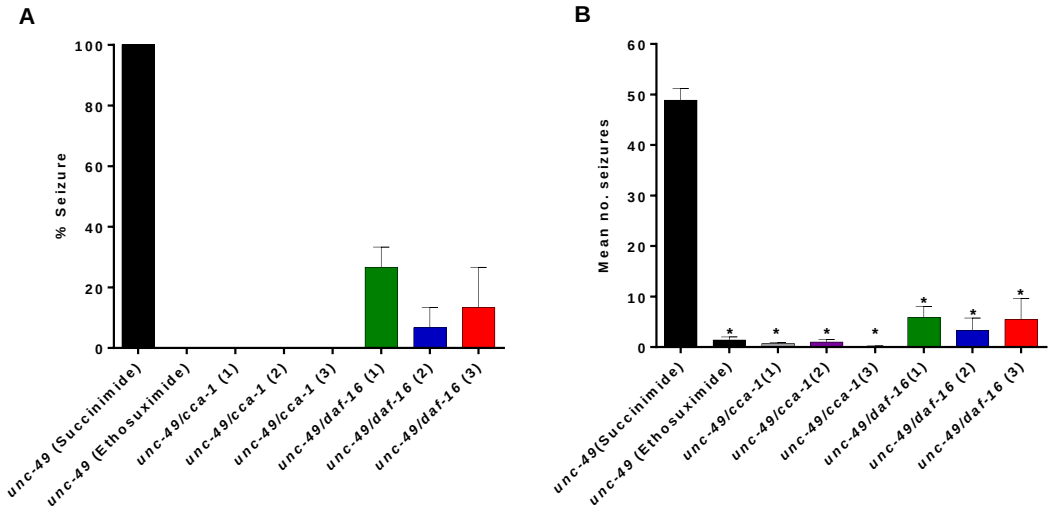

Figure 5.2.13. Identifying putative targets contributing to the antiepileptic activity of ethosuximide. Mutated versions of genes encoding the *C. elegans* homologs of mammalian T-type calcium channel (*cca-1*) and FOXO transcription factors (*daf-16*) were individually introduced into the genetic background of the *unc-49* synaptic transmission mutant strain. Three lines of each double mutant strain were evaluated for the seizure-protecting activity of ethosuximide at the drug concentration of 4 mg/mL. As compared to succinimide-treated *unc-49* worms, ethosuximide reduced (A) percentages of seizing worms and (B) seizure rates of *unc-49* control worms and all *unc-49*/*cca-1* and *unc-49*/*daf-16* double mutant lines ($p<0.05$). In addition, there were no significant differences with these parameters when double mutant lines were compared to the ethosuximide-treated *unc-49* controls ($p>0.05$), thus disclaiming the involvement of CCA-1 and DAF-16 in the antiepileptic mode of action of ethosuximide. Data shown was pooled from three biological replicates, with seizure rates compared via the Kruskal-Wallis test with Dunn's multiple comparison (n = 13 - 15 worms per line and treatment); *, $p<0.05$.

5.3 DISCUSSION

Previous studies have demonstrated the role of the FOXO transcription factor DAF-16 in mediating both neuroprotective and lifespan-extending properties of ethosuximide (Chen *et al*., 2015b, Tauffenberger *et al*., 2013, Evason *et al*., 2005). In contrast, the suggested MMOA of T-type calcium channel blockade by the drug remains controversial (Sayer *et al*., 1993, Thompson and Wong, 1991, Gross *et al*., 1997, Todorovic and Lingle, 1998, Herrington and Lingle, 1992, Kostyuk *et al*., 1992, Pfrieger *et al*., 1992, Leresche *et al*., 1998, Tsakiridou *et al*., 1995, Chen *et al*., 2015b, Coulter *et al*., 1989a, Coulter *et al*., 1989b, Coulter *et al*., 1990, Gomora *et al*., 2001, Lacinova *et al*., 2000). Although compound 9 was also previously shown to inhibit T-type calcium channels (Coulter *et al*., 1990), the MMOAs of the compound or its pro-drug methsuximide remain largely unknown and need to be delineated. To this end, comparisons drawn with ethosuximide herein demonstrated different metabolome profiles and transcriptional regulation of DAF-16-dependent genes between the compounds. Notably, despite these differences, loss of functional DAF-16 abolished all protective effects mediated by both compounds in CK426 worms. Last but not least, findings herein demonstrated that CCA-1 T-type calcium channels and DAF-16 did not mediate the acute anticonvulsant effects of ethosuximide in the seizure-prone *unc-49* worms.

Nearly all genes analysed by qPCR herein are known Class 1 genes which are upregulated dependently on DAF-16 (Murphy *et al*., 2003, Tepper *et al*., 2013). Previous microarray transcriptomic analyses performed within our group demonstrated the upregulation of these genes by ethosuximide in day 6 *dnj-14* ANCL and WT worms (Chen *et al*., 2015b), and was further verified herein in a different model of neurodegeneration in similarly-aged day 7 CK426 ALS worms. Additionally, phenotypic analyses performed in these two models confirmed the DAF-16-dependency of the drug in mediating its protective effects. To gain insights into how DAF-16 may be modulated by ethosuximide, previous work assessed if nuclear translocation of the transcription factor was induced by the drug since this is required for DAF-16 to regulate its gene targets in the nucleus (Chen *et al*., 2015b). Although ethosuximide did not induce observable nuclear translocation of DAF-16 in a GFP-tagged DAF-16-

expressing *C. elegans* strain (Chen *et al*., 2015b), it may not necessarily preclude this occurrence as it was not observed in the long-lived *age-1* (*hx546*) IIS mutant strain either despite the necessity of DAF-16 for lifespan extension in these worms (Dorman *et al*., 1995, Henderson and Johnson, 2001). A high detection threshold was hence proposed to account for the lack of obvious drug-induced DAF-16::GFP nuclear translocation.

Despite the requirement of DAF-16 for ethosuximide to exert neuroprotection and lifespan extension, the role of the transcription factor in the MMOA of the drug remains unclear. As mentioned in the introduction above, the DAE but not DBE motif was found to be overrepresented in the promoter regions of ethosuximide-regulated genes (Chen *et al*., 2015b), suggesting that ethosuximide works via a DAF-16, DAE-dependent but not DBE-dependent manner. This seems paradoxical considering that DAE is regulated by PQM-1 whereas DBE is regulated by DAF-16. Further work will have to be performed to facilitate insights into this.

Ethosuximide was also reported to mediate neuroprotective and neurogenic effects in a rat AD-like model via activation of the PI3K/AKT/Wnt/β-catenin pathway (Tiwari *et al*., 2015), and results herein additionally corroborated its reported DAF-16-dependency (Chen *et al*., 2015b, Tauffenberger *et al*., 2013, Evason *et al*., 2005). Despite the opposing effect of PI3K/AKT on downstream β-catenin and DAF-16/FOXO, physical interaction between *C. elegans* and mammalian BAR-1/β-catenin and DAF-16/FOXO was previously reported to be essential for mediating the responses of the transcription factor to oxidative stress (Essers *et al*., 2005), presenting a paradoxical mechanism of ethosuximide. However, a contradictory study showed an enrichment of DAF-16-induced Class 1 genes in genes upregulated in loss-of-function *bar-1* mutants (van der Bent *et al*., 2014). Conversely, PQM-1-induced Class 2 genes were enriched in the downregulated subset in these mutants, suggesting negative and positive regulation of DAF-16 and PQM-1 activities by BAR-1. Differential spatiotemporal regulation of BAR-1/β-catenin and DAF-16/FOXO may account for the seemingly paradoxical effects of ethosuximide, as the drug may exert different effects depending on the timepoint and

population of cells studied. Such potential spatiotemporal differences can be exemplified by a previous study which uncovered disparities between neuronal and global transcriptomes of IIS *daf-2* and *daf-2*/*daf-16* loss of function mutant strains (Kaletsky *et al*., 2016). Whereas gene ontology terms reflected mainly metabolism-associated functions of differentially-regulated genes from whole animal transcriptomes, neuronal transcriptomic profiles were enriched for neuronal functions. One of the IIS/FOXO-regulated neuronal genes is *fkh-9*, which encodes another FOXO transcription factor FKH-9, and is a known canonical Class 1 gene which was shown from whole worm transcriptome profiles to be upregulated in *daf-2* mutants. Loss-of-function *fkh-9* in *daf-2* mutants hindered axonal regeneration in older worms, which was rescued by pan-neuronal-expression of the gene. In contrast, pan-neuronal expression did not rescue the shortened lifespan in *fkh-9* null *daf-2* mutants, suggesting that the transcription factor regulates lifespan a neuron-independent manner. In addition to such spatiotemporal regulatory differences as exemplified above, the polypharmacology of AEDs may explain this seemingly paradoxical role of ethosuximide. The biological diversities of AEDs are well known, and they have been repurposed for other indications such as neuropathic pain and mood disorders (Bialer, 2012b). Ethosuximide is no exception, and its promiscuity suggests that it can both activate PI3K/AKT/Wnt/β-catenin and a DAF-16-dependent pathway concurrently.

Despite the discrepancies in the preliminary metabolome data and transcriptional regulatory activities between ethosuximide and compound 9, both compounds required DAF-16 to mediate their protective effects. This demonstrated that like ethosuximide, compound 9 also works via a DAF-16-dependent MMOA, although the exact mechanisms remain to be elucidated. These metabolome and transcriptional differences may simply be reflective of the 160-fold difference in concentrations administered for both compounds (8 mM ethosuximide and 0.05 mM compound 9). Additional to the concentration effects, the analysis of day 1 worms instead of older worms may also contribute to the observed metabolome differences, as protective effects were not yet evident at this age. In support of concentration effects, genes encoding the major phase I cytochrome P450 (*cyp-35B1*/*dod13, cyp-34A9*/*dod-16,* and *cyp-*

14A3) and phase II UDP-glucuronosyltransferase (*ugt-25*) drug metabolism enzymes were massively upregulated by ethosuximide but not compound 9. In addition, many AEDs, including ethosuximide, are known inducers of drug metabolism enzymes, and drug metabolism rate in *C. elegans* was previously shown to be concentration-dependent (Zheng *et al*., 2013). Although this does not preclude the possibility that upregulation of these genes is part of the MMOA of ethosuximide, since DAF-16 was previously shown to upregulate phase I and II metabolism enzymes (McElwee *et al*., 2007), these transcriptional changes observed herein were most likely a response to the pharmacological challenge and may be red herrings. Furthermore, findings should be interpreted with caution since only a handful of genes were analysed herein. An unbiased and global transcriptomic or proteomic approach, or a comprehensive metabolomics analysis, will have to be performed in order to infer biologically significant differences between both treatments. In view of spatiotemporal differences as exemplified by the reported disparities in neuronal and whole animal transcriptomes above (Kaletsky *et al*., 2016), unbiased analysis of the neuronal transcriptome and/or metabolome may be a more sophisticated approach to facilitate insights into neurodegenerative changes. However, it is perhaps ideal to combine both neuronal and whole animal analyses to facilitate comparative insights into neuronal-specific and systemic alterations. To best identify MMOA-relevant components, appropriate controls are essential, such as differentially-treated WT and *daf-16* null CK426 worms.

Considering the antagonistic roles of DAF-16 and PQM-1, it will be interesting to investigate the role of the latter, less extensively studied transcription factor in the protective effects of both compounds. Additionally, since the PQM-1-regulated DAE motif was enriched in ethosuximide-regulated genes (Chen *et al*., 2015b), this can provide useful insights into how the drug works via a DAF-16, DAE-dependent manner. Although I attempted to generate *pqm-1* null CK426/CZ1200 mutants by genetic crosses of loss-of-function *pqm-1 (ok485)* worms with the latter, these desired mutants were not successfully obtained. Alternatively, *pqm-1* silencing may be performed via RNAi in CK426 worms to mimic the *pqm-1* loss-of-function background. These loss-of-function *pqm-1*

mutants should be included as controls for MMOA delineation in addition to those mentioned above.

As aforementioned in section 5.1.1, voltage-gated potassium channel inhibition is also a putative mechanism of ethosuximide in addition to the controversial blockade of T-type calcium and voltage-gated sodium channels. As *C. elegans* do not express voltage-gated sodium channels (Hobert, 2013), the action of ethosuximide on this ion channel family cannot be studied in the nematode. However, voltage-gated potassium channels are expressed in the nematodes, and future work can employ chemical reverse genetics with RNAi-silencing of potassium channel genes to assess the anticonvulsant and/or neuroprotective effects of the drug in the absence of these channels.

In summary, findings herein showed that both compound 9 and ethosuximide mediate protective effects DAF-16-dependently. Clinically, the methsuximide AED pro-drug of compound 9 has a broader spectrum of activity due to its anticonvulsant effect against a wider range of seizure types, whereas ethosuximide is only effective against absence seizures. This suggests that despite their dependence on DAF-16, MMOAs between both compounds may differ. Alternatively, the broader spectrum of activity by methsuximide may simply be a result of much enhanced potency, as demonstrated by its active metabolite compound 9 in the preceding chapter. As of now, the MMOAs of both compounds remain unclear and further work needs to be performed to delineate them, especially with regard to neuroprotection.

CHAPTER 6

DISCUSSION

Ethosuximide is a succinimide-like AED approved for the treatment of absence seizures, albeit with an unclear MMOA. Several pre-existing studies have demonstrated its lifespan-extending effects in both WT and ALS *C. elegans* strains (Evason *et al*., 2005, Collins *et al*., 2008, Tauffenberger *et al*., 2013). In addition, it exerted neuroprotection in different models of neurodegeneration in *C. elegans* and rats, demonstrating its potential to be repurposed clinically as a general neuroprotective agent (Tiwari *et al*., 2015, Chen *et al*., 2015b, Tauffenberger *et al*., 2013). The concept of a broadly neuroprotective treatment is extremely appealing given the poor comprehension of disease pathologies underlying neurodegenerative disorders, which is reflected in the numerous clinical trial failures for the most common and widely studied neurodegenerative condition, AD (McDade and Bateman, 2017). Additionally, drug repurposing is an attractive alternative as approved drugs have already been preclinically evaluated and so can be expedited to clinical testing, reducing the lengthy, tedious, and expensive nature of the drug discovery and development process. However, high concentrations and doses of ethosuximide administered in those *in vivo* studies suggest potentially low neuroprotective clinical efficacy and/or potency. High potency is especially important for the purposes of identifying binding targets through a traditional small molecule affinity chromatography approach to facilitate insights into the MMOA, as potency depends on affinity for target(s). However, the necessity for drug derivatisation to immobilize it onto the affinity chromatography column may further reduce its affinity for its target(s), especially since important structural requirements for bioactivity are difficult to extrapolate from pre-existing SAR information due to the diversity of derivatives studied. In view of such potential issues associated with ethosuximide, the broad aims of the current project were to obtain a structurally-similar candidate molecule which exhibits enhanced neuroprotective and/or lifespan-extending potency in comparison to the drug and to obtain more potent derivatives from it in order to facilitate target identification studies.

To achieve these general aims, and considering the difficulty of extrapolating relevant SAR information from previous studies, an in-house assessment of the SAR of ethosuximide was mandatory. This was performed in the current

study with structurally-similar compounds which were identified and selected with chemistry approaches. Given the low to medium throughput of *C. elegans* neurodegeneration assays, the higher throughput PTZ-induced seizure assay in the GABA-defective *unc-49* strain was selected as the primary screening platform of choice. SAR inferences herein do not fully corroborate with previous findings from mammalian systems, but this was most likely a consequence of the diversity of derivatives analysed amongst the different studies. This illustrates the necessity of an in-house SAR assessment, and emphasizes the need for reiterative SAR evaluation per new set of derivatives obtained from the candidate molecule. Given the potential inapplicability of anticonvulsive SAR requirements for neuroprotective and/or lifespan-extending activity, future SAR studies should ideally be performed based on a suitable neurodegeneration readout which has been optimised for a higher throughput format. This can be facilitated with automation, as techniques to automate *C. elegans* handling and for sampling behavioural readouts such as thrashing and lifespan have been developed (Lockery *et al*., 2012, Stroustrup *et al*., 2013, Swierczek *et al*., 2011, Flavell *et al*., 2013, Ben Arous *et al*., 2009, Boyd *et al*., 2010, Buckingham and Sattelle, 2009, Yemini *et al*., 2013, Tsibidis and Tavernarakis, 2007). The feasibility of HTS in *C. elegans* has additionally been demonstrated by various groups (Kwok *et al*., 2006, Burns *et al*., 2006, Sleigh *et al*., 2011, Gosai *et al*., 2010, McCormick *et al*., 2013, Schwendeman and Shaham, 2016, Leung *et al*., 2013, Ellerbrock *et al*., 2004).

In addition to facilitating SAR insights, primary screens in the PTZ seizure assay identified compound 9 as the candidate molecule. The compound exhibited a 2-fold enhanced anticonvulsant potency than ethosuximide, and is the known active metabolite of the AED methsuximide. Although methsuximide also exhibited the same enhancement of potency, compound 9 was selected as the candidate molecule instead since pro-drug activation can be bypassed. Additionally, compound 9 exhibits more desirable pharmacokinetic features as its half-life is 38 hours compared to 1.4 hours for methsuximide (Porter *et al*., 1979), with average 700-fold higher plasma levels in patients on chronic methsuximide treatment (Strong *et al*., 1974).

As neuroprotective and lifespan-extending properties could not be inferred from the seizure assays, compound 9 had to be further assessed for these properties. The model of choice was the transgenic CK426 ALS strain which expresses A315T human TDP-43 (Liachko *et al*., 2010). The compound ameliorated locomotion defects and extended the shortened lifespan of these worms. Furthermore, it protected against degeneration of the D-type GABAergic inhibitory motor neurons, by reducing both GABAergic cell body losses and neuronal breaks. Most importantly, the compound exerted similar extent of protection at a 160-fold lower concentration than ethosuximide, showing an even greater augmentation of potency in neuroprotection as compared to a 2-fold improvement of anticonvulsive potency.

Compound 9 was initially selected as the candidate molecule based on its enhanced anticonvulsive potency compared to ethosuximide, and further demonstrated enhanced potency as well when assessed for both neuroprotective and lifespan-extending effects. This preservation of augmented potency from the compound from the PTZ-induced seizure assay to neurodegeneration and lifespan assays suggest the potential predictive value of the former primary screening platform for neuroprotection and lifespan extension. Additionally, links between seizures and neurodegeneration have been reported and suggested. Further investigation was hence performed with trimethadione and compound 14, which were shown from the seizure assay to possess lower and higher anticonvulsant potency than ethosuximide respectively. Both molecules exhibited neuroprotection by ameliorating the locomotion defects of CK426 ALS worms when administered at the same concentration as ethosuximide. However, extents of protection were similar to ethosuximide, and did not reflect the previously observed anticonvulsive potency differences. This suggest that neuroprotective efficacy and/or potency, and anticonvulsive SAR requirements, may not be directly extrapolated. Regardless, the seizure assay could at least predict for neuroprotectiveness in the compounds studied herein, and provided a relatively higher throughput approach for pre-screening of succinimide-like compounds for neuroprotectiveness and lifespan extension properties at this initial stage.

Although compound 9 exhibited enhanced neuroprotective and lifespan-extending potency than ethosuximide, this may be attributed to improved bioaccumulation in the worms. To invalidate this occurrence, 1D ^{1}H NMR spectroscopy was performed to assess internal drug levels. Ethosuximide bioaccumulated at 143.8 µM in day 1 adult worms, whereas compound 9 was undetectable and indistinguishable from worm-derived internal metabolites even when administered at the highest tolerable concentration. As protective effects of both compounds were not as evident or consistent at age day 1 as compared to later ages of days 5 and older, undetectability may be due to a lack of bioaccumulation; however, traces from the DMSO vehicle were obvious, suggesting otherwise. To mirror physiological effects at later ages and to improve detectability based on the assumption that bioaccumulated levels may increase over time, day 5 samples were additionally analysed. Despite this, the compound remained undetectable. Although the compound may accumulate as its potentially-active *p*-hydroxyphenyl metabolite, traces of the metabolite were not visible even if present. This was inferred from the undetectability of its strongest singlet peak within its predicted spectral region. Aside from this *p*-hydroxyphenyl metabolite, other metabolites have not been documented, albeit possible. To tease out traces of the compound, heteronuclear ^{1}H and ^{13}C NMR spectroscopy may be performed with a ^{13}C-labelled compound 9, which can be synthesized from ^{13}C-labelled precursors. As ^{13}C is of extremely low natural abundance at 1.1 %, isotopic labelling improves detection sensitivity since isotope abundance is synthetically enhanced. In addition, the dynamic range of the ^{13}C resonance is much greater at 250 ppm, as opposed to 15 ppm for the ^{1}H, hence improving the dispersal of signals and reducing the difficulty of peak identification due to overlapping resonances (Bothwell and Griffin, 2011).

For the purposes of target(s) identification and given the poor documentation of the compound's metabolic fate, it is paramount to identify other metabolites of compound 9 aside from its reported *p*-hydroxyphenyl metabolite, and to ascertain whether and which of these metabolites contribute towards the biological effects. This is important as it is possible that compound 9 may not be the primary active species despite being the known active metabolite of

methsuximide. ^{13}C-labelling can facilitate such metabolite studies as traces from the compound can be picked up from new ^{13}C signals which are not present in control samples. In addition, these heteronuclear analyses can facilitate structure elucidation of potential metabolites. However, an inherent problem associated with NMR is its low sensitivity, hence metabolites present in very low concentrations might not even be picked up even with isotopic labelling. An alternative and more sensitive approach is mass spectrometry, which can be combined with pre-separation chromatographic techniques such as HPLC and gas chromatography. Sample pre-separation is important to isolate the parent drug and/or metabolites from endogenous molecules which may mask these signals, and requires prior knowledge of the retention times of parent drug and its metabolites. This information is usually not available for unknown metabolites, however drug metabolism introduces structural and chemical modifications which will generate metabolites of differing molecular weights and polarities, which can be inferred (Holcapek *et al*., 2008). Mass spectrometry data, which provides information on the molecular weights, formula, and fragmentation patterns, can be inferred from to deduce the type of structural modifications made from the parent drug, but are usually inadequate for full structure elucidation of metabolites. Hence, a combination of both NMR and mass spectrometry approaches, both coupled with chromatographic sample pre-separation, is the most ideal approach for achieving this aim.

Despite the possibility of other potentially-active metabolites of compound 9, 1D ^{1}H NMR findings herein demonstrated undetectability of both compound 9 and its *p*-hydroxyphenyl metabolite due the occlusion of their respective signals by internal metabolites. Given the massive 160-fold concentration reduction of externally-administered compound 9 in comparison to ethosuximide, and the bioaccumulated concentration of the latter at 143.8 µM, internal concentrations of the compound and its metabolite were postulated to be below the observed detection limit of 5 µM. Hence, overall findings strongly suggest that the enhanced neuroprotective potency from the compound was not a result of improved bioaccumulation in the worms, justifying its selection as the candidate molecule. However, the protective properties of the

compound were assessed on its racemic form. In consideration of potential differences in activity between the enantiomeric forms of the compound, the current study has attempted to firstly derive its (*R*)-enantiomer through chemical syntheses for chiral comparisons. Despite the successful generation of the enantiomer, the enantiomer was not further purified due to the small scale of the reaction, as recovered amounts would be insufficient for a thorough assessment. Although syntheses reactions were not repeated on a larger scale, it offers a proof of concept for further work. As regulations have enforced mandatory chiral assessments in recognition of chiral-associated differences (Strong, 1999, Daniels *et al*., 1997), this work is crucial for keeping in line with current regulations. In addition to elucidating the active metabolites derived from compound 9 as aforementioned, knowledge of the active enantiomeric form is equally important for facilitating target(s) identification if the compound was to be utilised for this purpose in the near future. It should be emphasized that despite the importance of evaluating the single enantiomers, characterization of the racemate is equally vital as enantiomeric interactions may occur *in vivo* to produce different biological effects.

Work performed in the current study has also attempted to facilitate some insights into the MMOA of compound 9 in juxtaposition with ethosuximide. Although preliminary metabolomics data and transcriptional analysis of a handful of selected known ethosuximide-regulated genes suggested differing MMOAs, both compounds exhibited DAF-16-dependency as loss of functional DAF-16 abolished all protective effects in CK426 ALS worms. Previous microarray work performed in our group showed an enrichment of the PQM-1-regulated DAE motif in genes which were differentially regulated by ethosuximide, suggesting a paradoxical DAF-16- and PQM-1/DAE-dependent MMOA of the drug (Chen *et al*., 2015b). Further work could enable additional insights into the role of PQM-1 by assessing the physiological effects of both compounds in loss-of-function *pqm-1* CK426 worms. As metabolomics and transcriptional analyses were not comprehensively performed herein, these could be investigated more thoroughly with appropriate controls which include control and drug-treated CK426, *daf-16* null CK426, and *pqm-1* null CK426 strains to best pinpoint drug-specific MMOAs. In addition, the neuronal

population may be complementarily examined with these global whole animal analyses to provide further and comparative insights into neuron-specific and systemic neurodegenerative changes. As metabolomics data herein was inferred from day 1 of adulthood when protective effects from both compounds were not consistent or evident as opposed to later ages, further work should utilise older worms to relate back to transcriptional and phenotypic work. Since reliable NMR data relies on good reproducibility to detect real biological differences, much care must be taken to keep the aged samples as free from contamination as possible, as this was a problem herein with data from day 5 samples which could not be relevantly interpreted due to associated heavy contamination. In the current study, the analysed metabolite fraction was extracted with acetonitrile, a recommended solvent for isolating water-soluble metabolites (Beckonert *et al*., 2007). Although work performed herein has demonstrated that it did not cause the hydrophobic compound 9 to precipitate out of the soluble metabolite fraction, future dedicated metabolomics analyses should include the lipidomic fraction for a more comprehensive coverage of the metabolome. The lipidomic fraction could be extracted using a mixture of chloroform/methanol (Beckonert *et al*., 2007).

Although ethosuximide did not induce an observable nuclear translocation of GFP-tagged DAF-16 previously (Chen *et al*., 2015b), it will be interesting to assess if the drug and compound 9 stimulates PQM-1 nuclear exit since this transcription factor resides in the nucleus in physiological conditions; this might facilitate further insights given the known subcellular antagonism of DAF-16 and PQM-1 (Tepper *et al*., 2013). Another possible approach is to administer a combination treatment of ethosuximide and compound 9 to CK426 worms, as an additive effect as opposed to single treatments will suggest potentially differing mechanisms working independently from DAF-16. An extremely tedious and potentially more useful approach would be to perform forward chemical genetic screens with both compounds to identify genes which modify the functional responses to drug treatment. With this approach, worms are mutagenized to introduce random mutations in the genome, followed by phenotypic analysis with drug treatment. Mutations which abolish the protective effects of the compounds can be mapped back to the genes that

they reside in. This approach provides a readout of protein function with systemic effects and may be more informative than assessing transcriptional changes, since the relationships between genes, proteins, and physiological responses are not always straightforward. However, it can be extremely tedious given the potential innumerability of the uncharacterised mutations, especially if age-dependent phenotypes are used as phenotypic readouts. Alternative to the unbiased forward chemical genetics approach, reverse chemical genetics screens can be performed with RNAi-mediated silencing of known genes hypothesized to mediate protective effects of the compounds. Being a directed approach, this is less tedious but may limit the discovery of previously unknown genetic mediators.

Although compound 9 is the known active metabolite of methsuximide and not a novel structure, regulations enable enantiomeric forms of approved drugs to be marketed and patented as new drugs (Strong, 1999, Daniels *et al*., 1997). Hence, the enantiomeric differences in pharmacological activity, toxicity, and pharmacokinetics/pharmacodynamics need to be elucidated if the compound is to be reintroduced as a treatment for neurodegeneration. Although the compound and methsuximide have not been as extensively studied as ethosuximide, pre-existing information might facilitate these chiral evaluations of the compound and expedite the process. Additionally, the initial stages of reiterative compound synthesis and screens can be bypassed, further quickening the developmental process. More importantly, the compound is a more attractive candidate than ethosuximide due to its 160-fold enhanced neuroprotective potency as shown from findings herein. However, its general neuroprotective effects remain to be evaluated as these properties have only been demonstrated in the CK426 ALS model. This will be addressed with on-going work in a rat AD-like model (Tiwari *et al*., 2015) and polyQ expansion model in mouse primary neuronal cells (Massimiliano Stagi, University of Liverpool).

As a final point of consideration, chiral inversion may be a potential issue to address if a single enantiomeric form of compound 9 is to be introduced as a treatment for neurodegeneration in the future (Nguyen *et al*., 2006). Chiral inversion occurs when a single enantiomer is converted into the other

enantiomer or a racemate by *in vivo* processes, and would be problematic if activity and toxicity profiles are altered. Bioisoteres are chemical groups with similar chemical properties and biological effects which can be used to substitute chiral inversion sites in a molecule (Lima and Barreiro, 2005). In addition, such bioisoteric replacements may improve the physicochemical properties of a molecule and reduce toxicity, thereby improving the safety margin of the dosing regimen. This can be exemplified from a previous study which developed compounds possessing both antiseizure and neuroprotective properties (Smith *et al*., 2014). In the mentioned study, bioisoteric replacement of a potential racemization site at a benzylic hydroxyl group with an achiral difluoro group in the active enantiomer of an anticonvulsive and neuroprotective small molecule was performed to prevent chiral inversion into the inactive enantiomer. In addition to preventing racemization, the bioisoteric replacement further improve lipophilicity and topological polar surface area values, parameters known to affect CNS permeation.

As discussed previously, valproic acid, levetiracetam, and trimethadione are other AEDs which have also demonstrated lifespan-extending and/or neuroprotective properties (van Bergeijk *et al*., 2006, Pan *et al*., 2005, Kautu *et al*., 2013, Teixeira-Castro *et al*., 2011, Qing *et al*., 2008, Yi *et al*., 2013, Rouaux *et al*., 2007, Crochemore *et al*., 2009, Sugai *et al*., 2004, Monti *et al*., 2010, Monti *et al*., 2012, Kidd and Schneider, 2011, Ximenes *et al*., 2015, Carriere *et al*., 2014, Evason *et al*., 2008, Wildburger *et al*., 2009a, Sanchez *et al*., 2012, Bezard *et al*., 2004, Erbaş *et al*., 2016, Musaeus *et al*., 2017). In addition, the current project has corroborated the neuroprotective activity of trimethadione in the *C. elegans* CK426 ALS model. Although these AEDs have repurposing potential for treating neurodegenerative diseases, several caveats may limit this as compared to ethosuximide and compound 9. Valproic acid, which has the best characterised lifespan-extending and neuroprotective properties in a range of neurodegeneration models amongst these AEDs, is associated with severe adverse effects such as hepatotoxicity and teratogenicity (Moshe *et al*., 2015). Notably, it has additionally failed phase III trials for ALS treatment (Piepers *et al*., 2009). In comparison to valproic acid and ethosuximide, such protective effects have not been as extensively

characterised for trimethadione and levetiracetam, especially for trimethadione whereby protection and lifespan extension were not demonstrated in neurodegeneration models *per se*. Additionally, trimethadione may serve better use as an experimental compound as it is no longer clinically prescribed for absence seizures due to toxicity. On the other hand, ethosuximide and the methsuximide pro-drug of compound 9 have relatively good safety profiles.

Taking the above reasons into consideration and the enhanced neuroprotective potency of compound 9 as compared to ethosuximide as shown herein, compound 9 may have the best translational and repurposing potential for treating neurodegenerative diseases out of these AEDs. Additionally, compound 9 had likely bioaccumulated below the detection limit of 5 µM, which is extremely close to the desired K_D affinity range of femtomole to nanomole concentrations for high affinity ligands. This suggests that the success of target identification may be greatly improved with the compound as opposed to ethosuximide. Identification of potentially disease-modifying target(s) is extremely important as this can shed light on the underlying mechanisms which contribute to disease pathogenesis, in turn fuelling the development of therapeutics based on a rational, target-driven approach. This is especially important for neurodegenerative diseases, whereby the poorly understood processes of disease pathogenesis are reflected by the unmet need for disease-modifying treatments. The classical small molecule affinity chromatography approach and most alternative target deconvolution methods require molecular derivatisation for immobilisation to a matrix, with the exception of drug affinity responsive target stability (DARTS) which relies on proteolytic degradation and proteolytic sparing of unbound and drug-bound proteins respectively to distinguish drug targets (Lomenick *et al*., 2011, Terstappen *et al*., 2007). Although DARTS may in principle be more feasible for potentially lower-affinity ligands such as ethosuximide, the choice of protease and duration of proteolysis are factors which can affect the success of the approach. Given the requirement for molecular derivatisation of most techniques, the more potent and higher affinity compound 9 has broader utility and prospect for successful target identification, and presents a far better molecule than ethosuximide for this purpose. Regardless, the choice of

approach depends on careful consideration of individual advantages and limitations as these approaches are generally tedious. With any identified binding targets, validation of direct drug-target interaction and the functional effects of target modulation must be performed. The latter is especially important as not all interactions have pharmacological relevance. Reverse chemical genetics validation with RNAi-mediated silencing of the target-encoding transcript is a commonly employed and effective approach to functionally validate the identified target (Terstappen *et al*., 2007).

In addition to reintroducing compound 9 as a new treatment for neurodegeneration, novel structures may potentially be derived from it. Although this alternative approach means having to participate in the lengthy and expensive drug discovery and development process from the beginning, it may result in safer, and more efficacious and potent treatments than compound 9. Regardless of whether compound 9 or potential novel structures will be introduced as neurodegeneration treatments in the future, a major problem which is still plaguing neurodegenerative disorders is the lack of understanding of disease pathogenesis processes. In addition, reliable biomarkers remain to be discovered for disease prognosis, diagnosis, and monitoring of treatment efficacy. Drugs currently approved for neurodegeneration diseases provide symptomatic relief without treating the conditions. Hence, translational work needs to focus on the prodromal or presymptomatic stages to halt disease development or progression.

In conclusion, the work performed herein has identified a compound which displays enhanced neuroprotective potency than ethosuximide which has the potential to be repurposed for treating neurodegenerative diseases. This compound, compound 9, may also facilitate the ease and success of target identification as compared to ethosuximide. Consequently, identified targets may be disease-modifying and thus may be therapeutically intervened in addition to providing insights into disease pathogenic mechanisms. In short, the work performed herein has important contributions towards expediting the translational efforts to treat neurodegenerative diseases.

APPENDICES

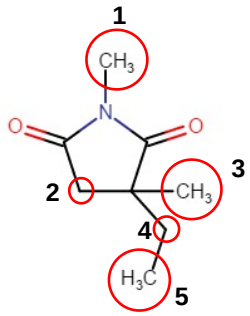

Chemical group no.	^{1}H Chemical shift (ppm)	Peak pattern	Coupling constant
1	2.99	singlet	-
2	1.61 1.72	multiplet multiplet	-
3	1.30	singlet	-
4	2.42 2.62	doublet doublet	$^{2}J_{HH}$ = 16.0 Hz $^{2}J_{HH}$ = 16.0 Hz
5	0.87	triplet	$^{3}J_{HH}$ = 8.0 Hz

Appendix 1. 1D ^{1}H NMR peaks of N-methylated ethosuximide (2,5-Pyrrolidinedione,3-ethyl-1,3-dimethyl).

Reaction 1

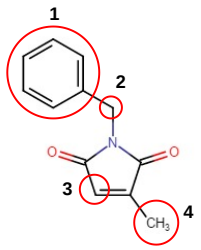

1-Benzyl-3-methylmaleimide

Reaction 2

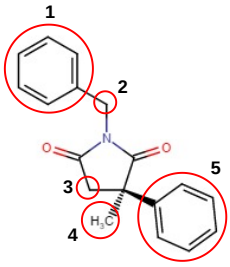

(*R*)-1-Benzyl-3-methyl-3-phenylsuccinimide

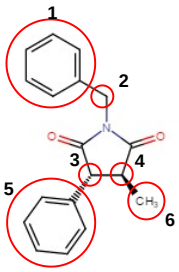

***trans*-1-Benzyl-3-methyl-4-phenylsuccinimide**

Reaction	Product	Chemical group no.	^{1}H Chemical shift (ppm)	Peak pattern	Coupling constant
1	**1-Benzyl-3-methylmaleimide**	1	7.35 – 7.24	multiplet	-
		2	4.65	singlet	-
		3	6.33	quadruplet	$^4J_{HH}$ = 1.8 Hz
		4	2.07	doublet	$^4J_{HH}$ = 1.8 Hz
2	**(*R*)-1-Benzyl-3-methyl-3-phenylsuccinimide**	1 and 5	7.39 – 7.25	multiplet	-
		2	4.72	singlet	-
		3	3.10	doublet	$^2J_{HH}$ = 18.2 Hz
		4	1.69	singlet	-
	***trans*-1-Benzyl-3-methyl-4-phenylsuccinimide**	1 and 5	7.38 – 7.24 7.14 7.4	multiplet doublet doublet	- $^3J_{HH}$ = 7.1 Hz $^3J_{HH}$ = 7.1 Hz
		2	4.69 4.75	doublet doublet	$^2J_{HH}$ = 14.0 Hz $^2J_{HH}$ = 14.0 Hz
		3	3.55	doublet	$^3J_{HH}$ = 6.0 Hz
		4	2.91	quadruplet	$^3J_{HH}$ = 7.2 and 6.6 Hz
		6	1.41	doublet	$^3J_{HH}$ = 7.2 Hz

Appendix 2. 1D ^{1}H NMR peaks of reaction 1 and 2 products from *(R)*-compound 9 synthesis reactions (Shintani *et al*., 2006).

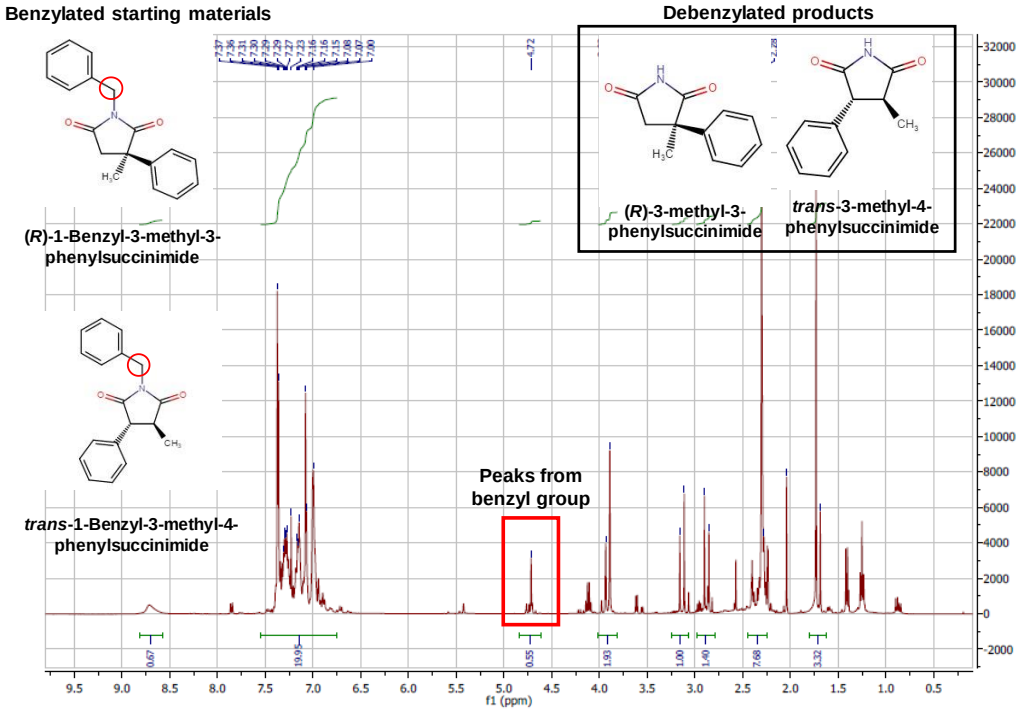

Appendix 3. 1D ^{1}H NMR spectrum of $AlCl_3$-mediated debenzylation of products from reaction 2. Peaks derived from the methylene ($-CH_2$) protons of the benzyl groups were detectable, demonstrating that benzylated compounds were present.

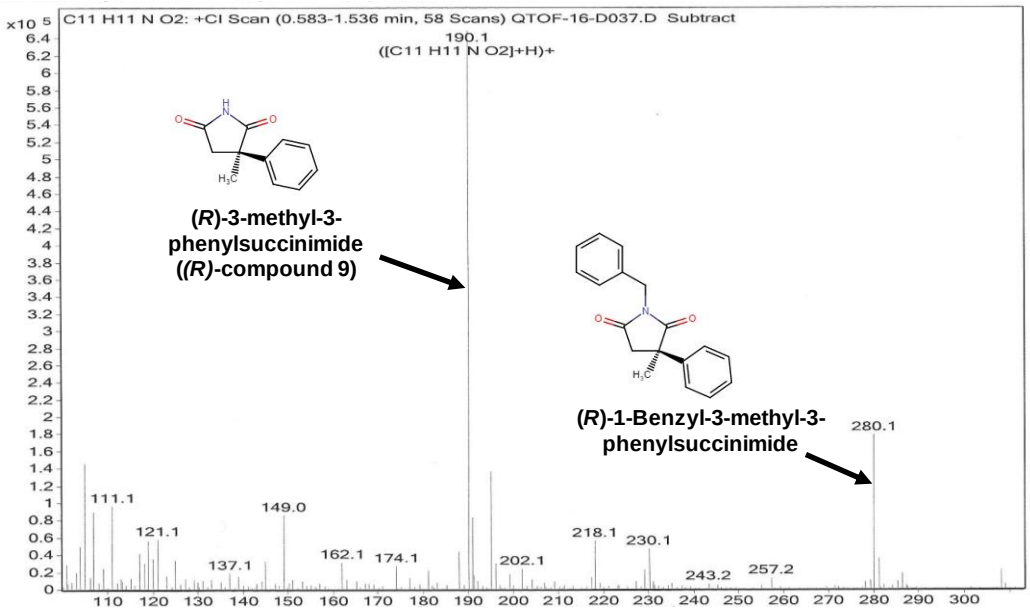

Appendix 4. Mass spectrometry of $AlCl_3$-mediated debenzylation reaction confirmed successful debenzylation of *(R)*-1-benzyl-3-methyl-3-phenylsuccinimide to *(R)*-compound 9. Presence of the benzylated starting material demonstrated that the reaction had not gone into completion.

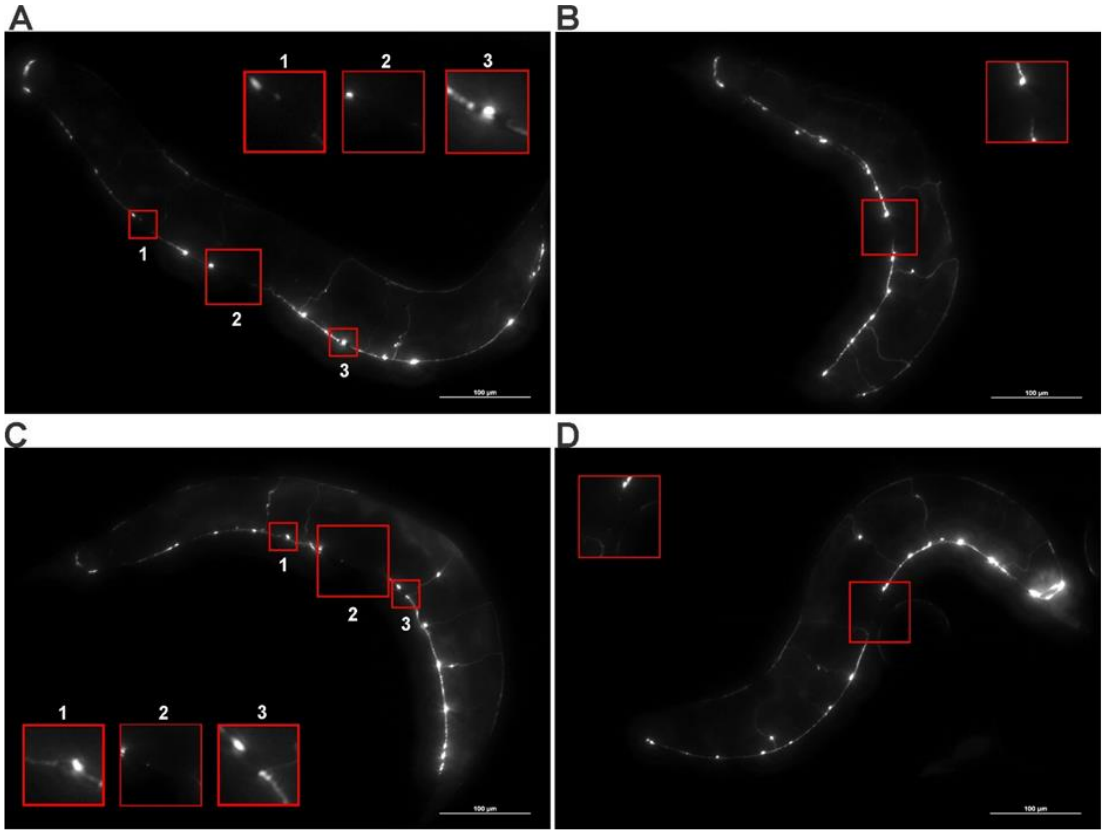

Appendix 5. Representative images of day 3 CK426/CZ1200 worms. Age-synchronised worms were chronically treated with 8mM (A) succinimide or (B) ethosuximide, (C) 0.4 % DMSO vehicle or (D) 0.05 mM compound 9 in 0.4 % DMSO from the L1 larval stage. Breaks within the D-type GABAergic motor neurons in the ventral nerve cord are indicated and emphasized with red boxes. Images were taken at 200X magnification, scale bars = 100 µm.

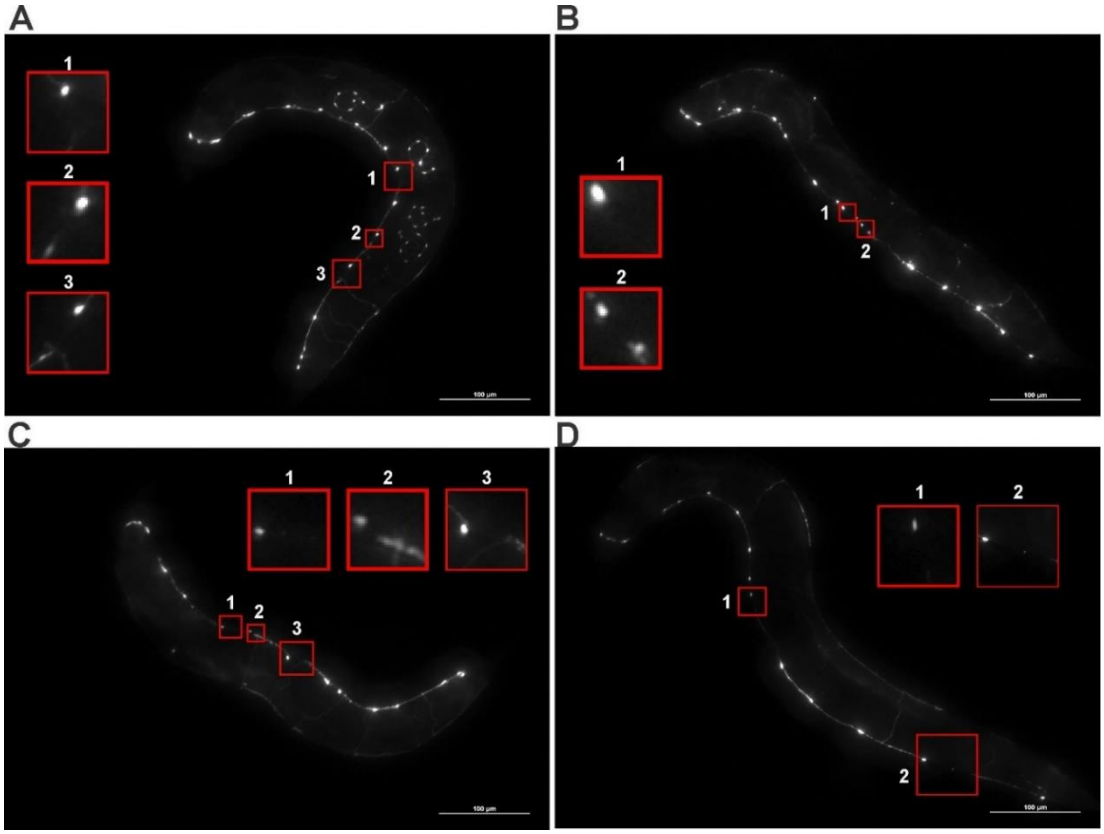

Appendix 6. Representative images of day 5 CK426/CZ1200 worms. Age-synchronised worms were chronically treated with 8mM (A) succinimide or (B) ethosuximide, (C) 0.4 % DMSO vehicle or (D) 0.05 mM compound 9 in 0.4 % DMSO from the L1 larval stage. Breaks within the D-type GABAergic motor neurons in the ventral nerve cord are indicated and emphasized with red boxes. Bagged worms, which contain hatched progenies as shown by the representative image for (A) succinimide-treated worms, were commonly observed at age day 5. Images were taken at 200X magnification, scale bars = 100 µm.

A

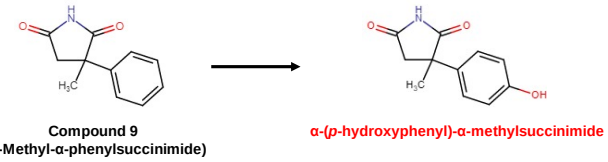

B

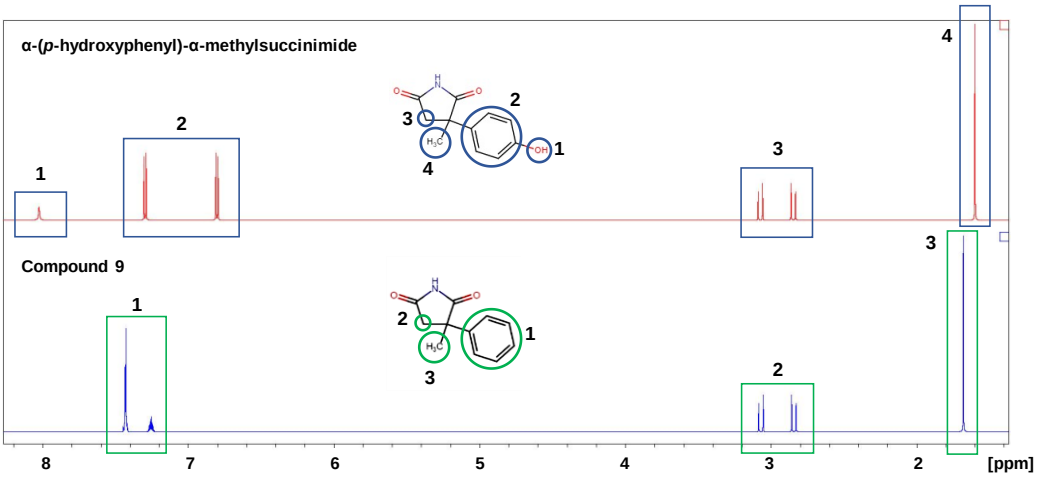

C

Compound	Chemical group no.	^{1}H Chemical shift (ppm)
α-(*p*-hydroxyphenyl)-α-methylsuccinimide	1	8.02
	2	7.29 and 6.80
	3	3.07 and 2.85
	4	1.60
Compound 9	1	7.43 and 7.25
	2	3.07 and 2.84
	3	1.68

Appendix 7. Predicted 1D ^{1}H NMR spectra of compound 9 and its metabolite α-(*p*-hydroxyphenyl)-α-methylsuccinimide. (A) Compound 9 is hydroxylated on its phenyl moiety to α-(*p*-hydroxyphenyl)-α-methylsuccinimide. (B) Hydroxylation causes a change in the spectral pattern of the metabolite in comparison to compound 9. (C) Predicted chemical shifts of peaks from compound 9 and its metabolite. The methyl moiety (compound 9, chemical group 3; metabolite, chemical group 4) produces the peak with the highest intensity for both compound 9 and its metabolite. This metabolite-derived peak is predicted to shift slightly upfield in comparison to the compound 9-derived one. ^{1}H peak resonances were predicted for a resonance frequency of 600 MHz on ACD/I-lab (National Chemical Database Service, UK).

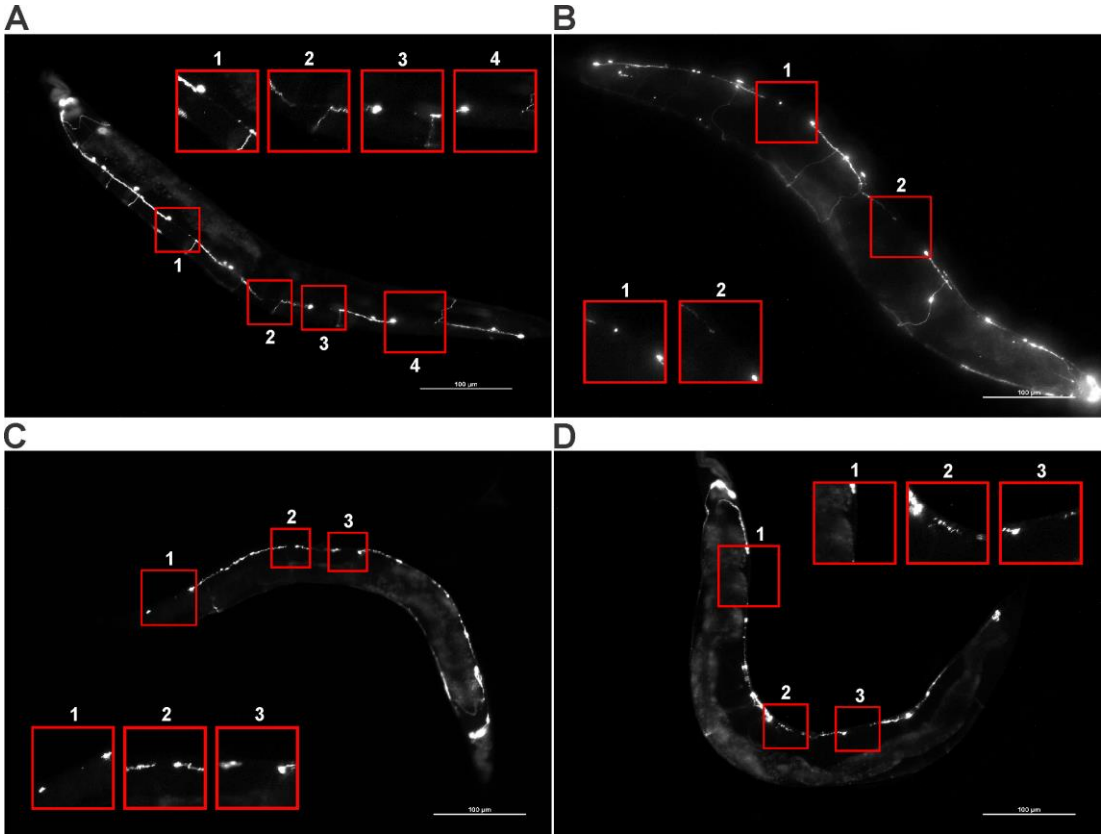

Appendix 8. Representative images of day 3 *daf-16* null CK426/CZ1200 worms. Age-synchronised worms were chronically treated with 8mM (A) succinimide or (B) ethosuximide, (C) 0.4 % DMSO vehicle or (D) 0.05 mM compound 9 in 0.4 % DMSO from the L1 larval stage. Breaks within the D-type GABAergic motor neurons in the ventral nerve cord are indicated and enlarged with red boxes. Images were taken at 200X magnification, scale bars = 100 µm.

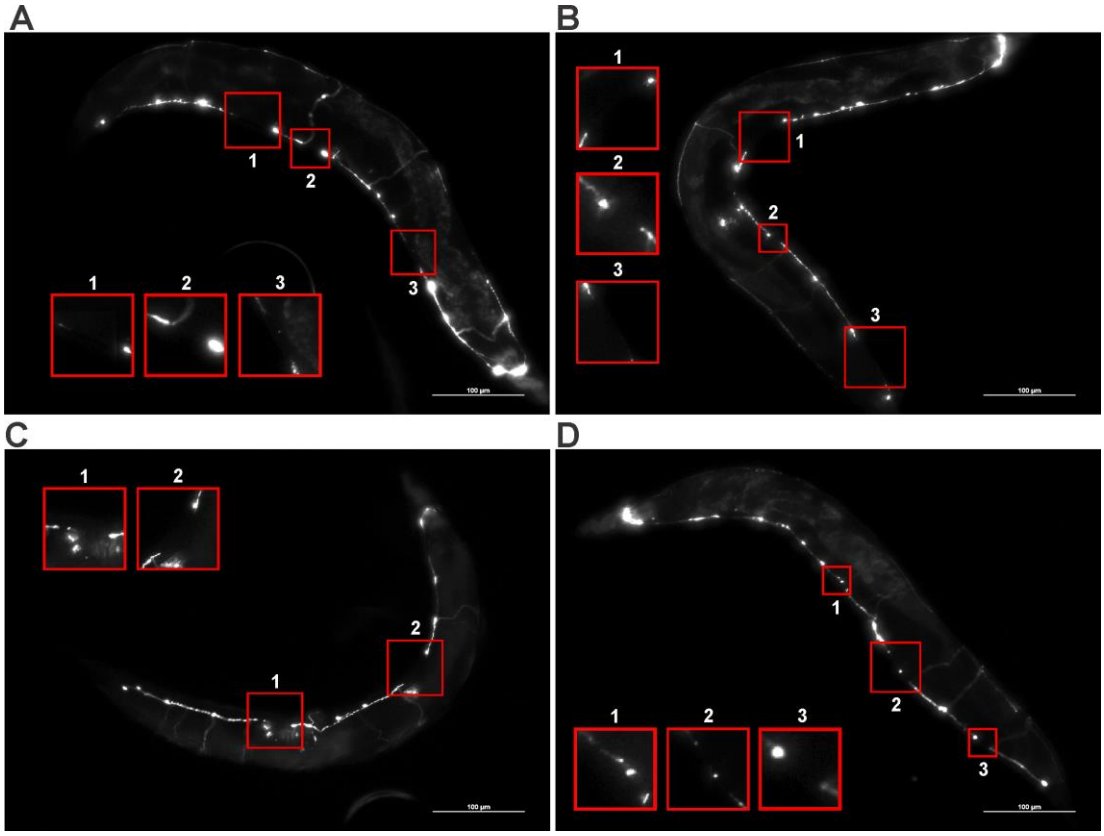

Appendix 9. Representative images of day 5 *daf-16* null CK426/CZ1200 worms. Age-synchronised worms were chronically treated with 8mM (A) succinimide or (B) ethosuximide, (C) 0.4 % DMSO vehicle or (D) 0.05 mM compound 9 in 0.4 % DMSO from the L1 larval stage. Breaks within the D-type GABAergic motor neurons in the ventral nerve cord are indicated and enlarged with red boxes. Images were taken at 200X magnification, scale bars = 100 µm.

REFERENCES

Abbas, S. and Wink, M. (2010) 'Epigallocatechin gallate inhibits beta amyloid oligomerization in Caenorhabditis elegans and affects the daf-2/insulin-like signaling pathway', *Phytomedicine,* 17(11), pp. 902-9.

Abe, K., Aoki, M., Tsuji, S., Itoyama, Y., Sobue, G., Togo, M., Hamada, C., Tanaka, M., Akimoto, M., Nakamura, K., Takahashi, F., Kondo, K., Yoshino, H., Sasaki, H., Yabe, I., Doi, S., Warita, H., Imai, T., Ito, H., Fukuchi, M., Osumi, E., Wada, M., Nakano, I., Morita, M., Ogata, K., Maruki, Y., Ito, K., Kano, O., Yamazaki, M., Takahashi, Y., Ishiura, H., Ogino, M., Koike, R., Ishida, C., Uchiyama, T., Mizoguchi, K., Obi, T., Watanabe, H., Atsuta, N., Aiba, I., Taniguchi, A., Sawada, H., Hazama, T., Fujimura, H., Kusaka, H., Kunieda, T., Kikuchi, H., Matsuo, H., Ueyama, H., Uekawa, K., Ueda, M., Murakami, A., Sumii, R., Kudou, T., Morimoto, K., Yoneoka, T., Hirai, M., Sasaki, K., Terai, H., Natori, T., Matsui, H., Kotani, K., Yoshida, K. and Iwasaki, T. (2017) 'Safety and efficacy of edaravone in well defined patients with amyotrophic lateral sclerosis: a randomised, double-blind, placebo-controlled trial', *The Lancet Neurology,* 16(7), pp. 505-512.

Ahringer, J. (2006) 'Reverse genetics', in *WormBook* [Online]. Available at: http://www.wormbook.org (Accessed: 18 Jan. 2018).

Al-Chalabi, A., van den Berg, L. H. and Veldink, J. (2016) 'Gene discovery in amyotrophic lateral sclerosis: implications for clinical management', *Nature Reviews Neurology,* 13, pp. 96.

Alavez, S., Vantipalli, M. C., Zucker, D. J. S., Klang, I. M. and Lithgow, G. J. (2011) 'Amyloid-binding compounds maintain protein homeostasis during ageing and extend lifespan', *Nature,* 472(7342), pp. 226-229.

Alelyunas, Y. W., Empfield, J. R., McCarthy, D., Spreen, R. C., Bui, K., Pelosi-Kilby, L. and Shen, C. (2010) 'Experimental solubility profiling of marketed CNS drugs, exploring solubility limit of CNS discovery candidate', *Bioorganic & Medicinal Chemistry Letters,* 20(24), pp. 7312-7316.

Amatniek, J. C., Hauser, W. A., DelCastillo-Castaneda, C., Jacobs, D. M., Marder, K., Bell, K., Albert, M., Brandt, J. and Stern, Y. (2006) 'Incidence and predictors of seizures in patients with Alzheimer's disease', *Epilepsia,* 47(5), pp. 867-72.

Anand, R., Gill, K. D. and Mahdi, A. A. (2014) 'Therapeutics of Alzheimer's disease: Past, present and future', *Neuropharmacology,* 76, pp. 27-50.

Anderson, E. N., Corkins, M. E., Li, J.-C., Singh, K., Parsons, S., Tucey, T. M., Sorkaç, A., Huang, H., Dimitriadi, M., Sinclair, D. A. and Hart, A. C. (2016) '*C. elegans* lifespan extension by osmotic stress requires FUdR, base excision repair, FOXO, and sirtuins', *Mechanisms of Ageing and Development,* 154, pp. 30-42.

Aracava, Y., Pereira, E. F., Maelicke, A. and Albuquerque, E. X. (2005) 'Memantine blocks α7* nicotinic acetylcholine receptors more potently than N-methyl-D-aspartate receptors in rat hippocampal neurons', *J Pharmacol Exp Ther,* 312(3), pp. 1195-205.

Arai, T., Hasegawa, M., Akiyama, H., Ikeda, K., Nonaka, T., Mori, H., Mann, D., Tsuchiya, K., Yoshida, M., Hashizume, Y. and Oda, T. (2006) 'TDP-43 is a component of ubiquitin-positive tau-negative inclusions in frontotemporal lobar degeneration and amyotrophic lateral sclerosis', *Biochem Biophys Res Commun,* 351(3), pp. 602-11.

Arya, U., Dwivedi, H. and Subramaniam, J. R. (2009) 'Reserpine ameliorates Aβ toxicity in the Alzheimer's disease model in *Caenorhabditis elegans*', *Exp Gerontol,* 44(6-7), pp. 462-6.

Avendaño-Vázquez, S. E., Dhir, A., Bembich, S., Buratti, E., Proudfoot, N. and Baralle, F. E. (2012) 'Autoregulation of TDP-43 mRNA levels involves interplay between transcription, splicing, and alternative polyA site selection', *Genes & Development,* 26(15), pp. 1679-1684.

Bachmann, K., He, Y., Sarver, J. G. and Peng, N. (2003) 'Characterization of the cytochrome P450 enzymes involved in the in vitro metabolism of ethosuximide by human hepatic microsomal enzymes', *Xenobiotica,* 33(3), pp. 265-76.

Bakchine, S. and Loft, H. (2007) 'Memantine treatment in patients with mild to moderate Alzheimer's disease: results of a randomised, double-blind, placebo-controlled 6-month study', *J Alzheimers Dis,* 11(4), pp. 471-9.

Bamber, B. A., Beg, A. A., Twyman, R. E. and Jorgensen, E. M. (1999) 'The *Caenorhabditis elegans unc-49* locus encodes multiple subunits of a heteromultimeric GABA receptor', *J Neurosci,* 19(13), pp. 5348-59.

Barbieri, M., Bonafe, M., Franceschi, C. and Paolisso, G. (2003) 'Insulin/IGF-I-signaling pathway: An evolutionarily conserved mechanism of longevity from yeast to humans', *Am J Physiol Endocrinol Metab,* 285(5), pp. E1064-71.

Barnard, J. M. (1993) 'Substructure searching methods: Old and new', *Journal of Chemical Information and Computer Sciences,* 33(4), pp. 532-538.

Bateman, R. J., Xiong, C., Benzinger, T. L. S., Fagan, A. M., Goate, A., Fox, N. C., Marcus, D. S., Cairns, N. J., Xie, X., Blazey, T. M., Holtzman, D. M., Santacruz, A., Buckles, V., Oliver, A., Moulder, K., Aisen, P. S., Ghetti, B., Klunk, W. E., McDade, E., Martins, R. N., Masters, C. L., Mayeux, R., Ringman, J. M., Rossor, M. N., Schofield, P. R., Sperling, R. A., Salloway, S. and Morris, J. C. (2012) 'Clinical and biomarker changes in dominantly inherited Alzheimer's disease', *New England Journal of Medicine,* 367(9), pp. 795-804.

Beckonert, O., Keun, H. C., Ebbels, T. M. D., Bundy, J., Holmes, E., Lindon, J. C. and Nicholson, J. K. (2007) 'Metabolic profiling, metabolomic and metabonomic procedures for NMR spectroscopy of urine, plasma, serum and tissue extracts', *Nat. Protocols,* 2(11), pp. 2692-2703.

Bell, J. S., Lonnroos, E., Koivisto, A. M., Lavikainen, P., Laitinen, M. L., Soininen, H. and Hartikainen, S. (2011) 'Use of antiepileptic drugs among community-dwelling persons with Alzheimer's disease in Finland', *J Alzheimers Dis,* 26(2), pp. 231-7.

Bellingham, M. C. (2011) 'A review of the neural mechanisms of action and clinical efficiency of riluzole in treating amyotrophic lateral sclerosis: What have we learned in the last decade?', *CNS Neurosci Ther,* 17(1), pp. 4-31.

Ben Arous, J., Laffont, S. and Chatenay, D. (2009) 'Molecular and sensory basis of a food related two-state behavior in *C. elegans*', *PLoS One,* 4(10), pp. e7584.

Bender, A. and Glen, R. C. (2004) 'Molecular similarity: a key technique in molecular informatics', *Organic & Biomolecular Chemistry,* 2(22), pp. 3204-3218.

Bengzon, J., Mohapel, P., Ekdahl, C. T. and Lindvall, O. (2002) 'Neuronal apoptosis after brief and prolonged seizures', *Progress in brain research,* 135, pp. 111-119.

Benjamini, Y. and Hochberg, Y. (1995) 'Controlling the false discovery rate: a practical and powerful approach to multiple testing', *Journal of the Royal Statistical Society. Series B (Methodological),* 57(1), pp. 289-300.

Bensimon, G., Lacomblez, L. and Meininger, V. (1994) 'A controlled trial of riluzole in amyotrophic lateral sclerosis. ALS/Riluzole Study Group', *N Engl J Med,* 330(9), pp. 585-91.

Berg, A. T., Berkovic, S. F., Brodie, M. J., Buchhalter, J., Cross, J. H., van Emde Boas, W., Engel, J., French, J., Glauser, T. A., Mathern, G. W., Moshe, S. L., Nordli, D., Plouin, P. and Scheffer, I. E. (2010) 'Revised terminology and concepts for organization of seizures and epilepsies: report of the ILAE Commission on Classification and Terminology, 2005-2009', *Epilepsia,* 51(4), pp. 676-85.

Bernardi, S., Scaldaferri, N., Vanacore, N., Trebbastoni, A., Francia, A., D'Amico, A. and Prencipe, M. (2010) 'Seizures in Alzheimer's disease: A retrospective study of a cohort of outpatients', *Epileptic Disord,* 12(1), pp. 16-21.

Bertram, L. and Tanzi, R. E. (2005) 'The genetic epidemiology of neurodegenerative disease', *Journal of Clinical Investigation,* 115(6), pp. 1449-1457.

Bezard, E., Hill, M. P., Crossman, A. R., Brotchie, J. M., Michel, A., Grimee, R. and Klitgaard, H. (2004) 'Levetiracetam improves choreic levodopa-induced dyskinesia in the MPTP-treated macaque', *Eur J Pharmacol,* 485(1-3), pp. 159-64.

Bialer, M. (2012a) 'How did phenobarbital's chemical structure affect the development of subsequent antiepileptic drugs (AEDs)?', *Epilepsia,* 53 Suppl 8, pp. 3-11.

Bialer, M. (2012b) 'Why are antiepileptic drugs used for nonepileptic conditions?', *Epilepsia,* 53 Suppl 7, pp. 26-33.

Bilen, J. and Bonini, N. M. (2005) 'Drosophila as a model for human neurodegenerative disease', *Annu Rev Genet,* 39, pp. 153-71.

Birks, J., Grimley Evans, J., Iakovidou, V. and Tsolaki, M. (2000) 'Rivastigmine for Alzheimer's disease', *Cochrane Database Syst Rev,* (4), pp. Cd001191.

Birks, J. and Harvey, R. J. (2006) 'Donepezil for dementia due to Alzheimer's disease', *Cochrane Database Syst Rev,* (1), pp. Cd001190.

Bothwell, J. H. and Griffin, J. L. (2011) 'An introduction to biological nuclear magnetic resonance spectroscopy', *Biol Rev Camb Philos Soc,* 86(2), pp. 493-510.

Boyd, W. A., McBride, S. J., Rice, J. R., Snyder, D. W. and Freedman, J. H. (2010) 'A high-throughput method for assessing chemical toxicity using a *Caenorhabditis elegans* reproduction assay', *Toxicol Appl Pharmacol,* 245(2), pp. 153-9.

Braungart, E., Gerlach, M., Riederer, P., Baumeister, R. and Hoener, M. C. (2004) '*Caenorhabditis elegans* MPP+ model of Parkinson's disease for high-throughput drug screenings', *Neurodegener Dis,* 1(4-5), pp. 175-83.

Brendel, M., Jaworska, A., Herms, J., Trambauer, J., Rotzer, C., Gildehaus, F. J., Carlsen, J., Cumming, P., Bylund, J., Luebbers, T., Bartenstein, P., Steiner, H., Haass, C., Baumann, K. and Rominger, A. (2015) 'Amyloid-PET predicts inhibition of *de novo* plaque formation upon chronic γ-secretase modulator treatment', *Mol Psychiatry,* 20(10), pp. 1179-1187.

Brenner, S. (1974) 'The genetics of *Caenorhabditis elegans*', *Genetics,* 77(1), pp. 71-94.

Brettschneider, J., Del Tredici, K., Lee, V. M. Y. and Trojanowski, J. Q. (2015) 'Spreading of pathology in neurodegenerative diseases: A focus on human studies', *Nature reviews. Neuroscience,* 16(2), pp. 109-120.

Brodie, M. J., Covanis, A., Gil-Nagel, A., Lerche, H., Perucca, E., Sills, G. J. and White, H. S. (2011) 'Antiepileptic drug therapy: Does mechanism of action matter?', *Epilepsy Behav,* 21(4), pp. 331-41.

Brown, R. H. and Al-Chalabi, A. (2017) 'Amyotrophic Lateral Sclerosis', *New England Journal of Medicine,* 377(2), pp. 162-172.

Browne, T. R., Dreifuss, F. E., Dyken, P. R., Goode, D. J., Penry, J. K., Porter, R. J., White, B. G. and White, P. T. (1975) 'Ethosuximide in the treatment of absence (peptit mal) seizures', *Neurology,* 25(6), pp. 515-24.

Browne, T. R., Feldman, R. G., Buchanan, R. A., Allen, N. C., Fawcett-Vickers, L., Szabo, G. K., Mattson, G. F., Norman, S. E. and Greenblatt, D. J. (1983) 'Methsuximide for complex partial seizures: efficacy, toxicity, clinical pharmacology, and drug interactions', *Neurology,* 33(4), pp. 414-8.

Buchanan, R. A., Fernandez, L. and Kinkel, A. W. (1969) 'Absorption and elimination of ethosuximide in children', *The Journal of Clinical Pharmacology and The Journal of New Drugs,* 9(6), pp. 393-398.

Buckingham, S. D. and Sattelle, D. B. (2009) 'Fast, automated measurement of nematode swimming (thrashing) without morphometry', *BMC Neurosci,* 10, pp. 84.

Buratti, E. and Baralle, F. E. (2012) 'TDP-43: Gumming up neurons through protein-protein and protein-RNA interactions', *Trends Biochem Sci,* 37(6), pp. 237-47.

Burns, A. R., Kwok, T. C., Howard, A., Houston, E., Johanson, K., Chan, A., Cutler, S. R., McCourt, P. and Roy, P. J. (2006) 'High-throughput screening of small molecules for bioactivity and target identification in *Caenorhabditis elegans*', *Nat Protoc,* 1(4), pp. 1906-14.

Burns, A. R., Wallace, I. M., Wildenhain, J., Tyers, M., Giaever, G., Bader, G. D., Nislow, C., Cutler, S. R. and Roy, P. J. (2010) 'A predictive model for drug bioaccumulation and bioactivity in *Caenorhabditis elegans*', *Nat Chem Biol,* 6(7), pp. 549-557.

Byerly, L., Cassada, R. C. and Russell, R. L. (1976) 'The life cycle of the nematode *Caenorhabditis elegans*', *Developmental Biology,* 51(1), pp. 23-33.

Cady, J., Koval, E. D., Benitez, B. A. and *et al*. (2014) 'The *TREM2* variant p.R47H as a risk factor for sporadic amyotrophic lateral sclerosis', *JAMA Neurology,* 71(4), pp. 449-453.

Cahn, R. S., Ingold, C. K. and Prelog, V. (1956) 'The specification of asymmetric configuration in organic chemistry', *Experientia,* 12(3), pp. 81-94.

Caldwell, K. A., Tucci, M. L., Armagost, J., Hodges, T. W., Chen, J., Memon, S. B., Blalock, J. E., DeLeon, S. M., Findlay, R. H., Ruan, Q., Webber, P. J., Standaert, D. G., Olson, J. B. and Caldwell, G. A. (2009) 'Investigating bacterial sources of toxicity as an environmental contributor to dopaminergic neurodegeneration', *PLoS One,* 4(10), pp. e7227.

Calixto, A., Chelur, D., Topalidou, I., Chen, X. and Chalfie, M. (2010a) 'Enhanced neuronal RNAi in *C. elegans* using SID-1', *Nat Methods,* 7(7), pp. 554-9.

Calixto, A., Ma, C. and Chalfie, M. (2010b) 'Conditional gene expression and RNAi using MEC-8-dependent splicing in *C. elegans*', *Nat Methods,* 7(5), pp. 407-11.

Cantó, C. and Auwerx, J. (2009) 'Caloric restriction, SIRT1 and longevity', *Trends in endocrinology and metabolism: TEM,* 20(7), pp. 325-331.

Carniato, D., Schultz, M., Roche, D. and Hallakou-Bozec, S. (2009) *7-Azaindole derivatives as selective 11β-hydroxysteroid dehydrogenase type 1 inhibitors and their preparation, pharmaceutical compositions and use in the treatment of diseases* Patent no. WO2009059666A1. [Online].

Carriere, C. H., Kang, N. H. and Niles, L. P. (2014) 'Neuroprotection by valproic acid in an intrastriatal rotenone model of Parkinson's disease', *Neuroscience,* 267, pp. 114-21.

Carter, C. H. and Maley, M. C. (1957) 'Use of celontin in the treatment of mixed epilepsy', *Neurology,* 7(7), pp. 483-4.

Chamberlin, H. R., Waddell, W. J. and Butler, T. C. (1965) 'A study of the product of demethylation of trimethadione in the control of petit mal epilepsy', *Neurology,* 15, pp. 449-54.

Chartier-Harlin, M. C., Crawford, F., Houlden, H., Warren, A., Hughes, D., Fidani, L., Goate, A., Rossor, M., Roques, P., Hardy, J. and *et al*. (1991) 'Early-onset Alzheimer's disease caused by mutations at codon 717 of the β-amyloid precursor protein gene', *Nature,* 353(6347), pp. 844-6.

Chen, X., Barclay, J. W., Burgoyne, R. D. and Morgan, A. (2015a) 'Using *C. elegans* to discover therapeutic compounds for ageing-associated neurodegenerative diseases', *Chemistry Central Journal,* 9, pp. 65.

Chen, X. and Burgoyne, R. (2012) 'Identification of common genetic modifiers of neurodegenerative diseases from an integrative analysis of diverse genetic screens in model organisms', *BMC Genomics,* 13(1), pp. 71.

Chen, X., McCue, F. H., Wong, S. Q., Kashyap, S. S., Kraemer, B. C., Barclay, J. W., Burgoyne, R. D. and Morgan, A. (2015b) 'Ethosuximide ameliorates neurodegenerative disease phenotypes by modulating DAF-16/FOXO target gene expression', *Mol Neurodegener,* 10(1), pp. 51.

Cheng, C. H., Liu, C. J., Ou, S. M., Yeh, C. M., Chen, T. J., Lin, Y. Y. and Wang, S. J. (2015) 'Incidence and risk of seizures in Alzheimer's disease: A nationwide population-based cohort study', *Epilepsy Res,* 115, pp. 63-6.

Chio, A., Logroscino, G., Traynor, B. J., Collins, J., Simeone, J. C., Goldstein, L. A. and White, L. A. (2013) 'Global epidemiology of amyotrophic lateral sclerosis: A systematic review of the published literature', *Neuroepidemiology,* 41(2), pp. 118-30.

Chow, V. W., Mattson, M. P., Wong, P. C. and Gleichmann, M. (2010) 'An Overview of APP Processing Enzymes and Products', *Neuromolecular medicine,* 12(1), pp. 1-12.

Cirulli, E. T., Lasseigne, B. N., Petrovski, S., Sapp, P. C., Dion, P. A., Leblond, C. S., Couthouis, J., Lu, Y. F., Wang, Q., Krueger, B. J., Ren, Z., Keebler, J., Han, Y., Levy, S. E., Boone, B. E., Wimbish, J. R., Waite, L. L., Jones, A. L., Carulli, J. P., Day-Williams, A. G., Staropoli, J. F., Xin, W. W., Chesi, A., Raphael, A. R., McKenna-Yasek, D., Cady, J., Vianney de Jong, J. M., Kenna, K. P., Smith, B. N., Topp, S.,

Miller, J., Gkazi, A., Al-Chalabi, A., van den Berg, L. H., Veldink, J., Silani, V., Ticozzi, N., Shaw, C. E., Baloh, R. H., Appel, S., Simpson, E., Lagier-Tourenne, C., Pulst, S. M., Gibson, S., Trojanowski, J. Q., Elman, L., McCluskey, L., Grossman, M., Shneider, N. A., Chung, W. K., Ravits, J. M., Glass, J. D., Sims, K. B., Van Deerlin, V. M., Maniatis, T., Hayes, S. D., Ordureau, A., Swarup, S., Landers, J., Baas, F., Allen, A. S., Bedlack, R. S., Harper, J. W., Gitler, A. D., Rouleau, G. A., Brown, R., Harms, M. B., Cooper, G. M., Harris, T., Myers, R. M. and Goldstein, D. B. (2015) 'Exome sequencing in amyotrophic lateral sclerosis identifies risk genes and pathways', *Science,* 347(6229), pp. 1436-41.

Collins, J. J., Evason, K., Pickett, C. L., Schneider, D. L. and Kornfeld, K. (2008) 'The anticonvulsant ethosuximide disrupts sensory function to extend *C. elegans* lifespan', *PLoS Genet,* 4(10), pp. e1000230.

Cook, M., Baker, N., Lanes, S., Bullock, R., Wentworth, C. and Arrighi, H. M. (2015) 'Incidence of stroke and seizure in Alzheimer's disease dementia', *Age Ageing,* 44(4), pp. 695-9.

Corder, E. H., Saunders, A. M., Risch, N. J., Strittmatter, W. J., Schmechel, D. E., Gaskell, P. C., Jr., Rimmler, J. B., Locke, P. A., Conneally, P. M., Schmader, K. E. and *et al*. (1994) 'Protective effect of apolipoprotein E type 2 allele for late onset Alzheimer disease', *Nat Genet,* 7(2), pp. 180-4.

Corder, E. H., Saunders, A. M., Strittmatter, W. J., Schmechel, D. E., Gaskell, P. C., Small, G. W., Roses, A. D., Haines, J. L. and Pericak-Vance, M. A. (1993) 'Gene dose of apolipoprotein E type 4 allele and the risk of Alzheimer's disease in late onset families', *Science,* 261(5123), pp. 921-3.

Coulter, D. A., Huguenard, J. R. and Prince, D. A. (1989a) 'Characterization of ethosuximide reduction of low-threshold calcium current in thalamic neurons', *Ann Neurol,* 25(6), pp. 582-93.

Coulter, D. A., Huguenard, J. R. and Prince, D. A. (1989b) 'Specific petit mal anticonvulsants reduce calcium currents in thalamic neurons', *Neurosci Lett,* 98(1), pp. 74-8.

Coulter, D. A., Huguenard, J. R. and Prince, D. A. (1990) 'Differential effects of petit mal anticonvulsants and convulsants on thalamic neurones: calcium current reduction', *Br J Pharmacol,* 100(4), pp. 800-6.

Crochemore, C., Virgili, M., Bonamassa, B., Canistro, D., Pena-Altamira, E., Paolini, M. and Contestabile, A. (2009) 'Long-term dietary administration of valproic acid does not affect, while retinoic acid decreases, the lifespan of G93A mice, a model for amyotrophic lateral sclerosis', *Muscle & Nerve,* 39(4), pp. 548-552.

Cuyvers, E., Bettens, K., Philtjens, S., Van Langenhove, T., Gijselinck, I., van der Zee, J., Engelborghs, S., Vandenbulcke, M., Van Dongen, J., Geerts, N., Maes, G., Mattheijssens, M., Peeters, K., Cras, P., Vandenberghe, R., De Deyn, P. P., Van Broeckhoven, C., Cruts, M. and Sleegers, K. (2014) 'Investigating the role of rare heterozygous *TREM2* variants in Alzheimer's disease and frontotemporal dementia', *Neurobiology of Aging,* 35(3), pp. 726.e11-726.e19.

Czuczwar, S. J., Ferenc, R., Błaszczyk, B. and Borowicz, K. K. (2007) 'Neuroprotective effects of some newer and potential antiepileptic drugs', *Journal of Pre-Clinical and Clinical Research,* 1(1), pp. 1-5.

Daniels, J. M., Nestmann, E. R. and Kerr, A. (1997) 'Development of stereoisomeric (chiral) drugs: A brief review of scientific and regulatory considerations', *Drug Information Journal,* 31(3), pp. 639-646.

Das, P., Verbeeck, C., Minter, L., Chakrabarty, P., Felsenstein, K., Kukar, T., Maharvi, G., Fauq, A., Osborne, B. A. and Golde, T. E. (2012) 'Transient pharmacologic lowering of Aβ production prior to deposition results in sustained reduction of amyloid plaque pathology', *Molecular Neurodegeneration,* 7(1), pp. 39.

De Strooper, B. and Karran, E. (2016) 'The cellular phase of alzheimer's disease', *Cell,* 164(4), pp. 603-15.

DeJesus-Hernandez, M., Desaro, P., Johnston, A., Ross, O. A., Wszolek, Z. K., Ertekin-Taner, N., Graff-Radford, N. R., Rademakers, R. and Boylan, K. (2011a) 'Novel p.Ile151Val mutation in VCP in a patient of African American descent with sporadic ALS', *Neurology,* 77(11), pp. 1102-1103.

DeJesus-Hernandez, M., Mackenzie, I. R., Boeve, B. F., Boxer, A. L., Baker, M., Rutherford, N. J., Nicholson, A. M., Finch, N. A., Flynn, H., Adamson, J., Kouri, N., Wojtas, A., Sengdy, P., Hsiung, G. Y., Karydas, A., Seeley, W. W., Josephs, K. A., Coppola, G., Geschwind, D. H., Wszolek, Z. K., Feldman, H., Knopman, D. S., Petersen, R. C., Miller, B. L., Dickson, D. W., Boylan, K. B., Graff-Radford, N. R. and Rademakers, R. (2011b) 'Expanded GGGGCC hexanucleotide repeat in noncoding region of C9ORF72 causes chromosome 9p-linked FTD and ALS', *Neuron,* 72(2), pp. 245-56.

Davis, K. L., Thal, L. J., Gamzu, E. R., Davis, C. S., Woolson, R. F., Gracon, S. I., Drachman, D. A., Schneider, L. S., Whitehouse, P. J., Hoover, T. M. and et al. (1992) 'A double-blind, placebo-controlled multicenter study of tacrine for Alzheimer's disease. The Tacrine Collaborative Study Group', *N Engl J Med,* 327(18), pp. 1253-9.

Deng, H. X., Chen, W., Hong, S. T., Boycott, K. M., Gorrie, G. H., Siddique, N., Yang, Y., Fecto, F., Shi, Y., Zhai, H., Jiang, H., Hirano, M., Rampersaud, E., Jansen, G. H., Donkervoort, S., Bigio, E. H., Brooks, B. R., Ajroud, K., Sufit, R. L., Haines, J. L., Mugnaini, E., Pericak-Vance, M. A. and Siddique, T. (2011) 'Mutations in *UBQLN2* cause dominant X-linked juvenile and adult-onset ALS and ALS/dementia', *Nature,* 477(7363), pp. 211-5.

Diekstra, F. P., Van Deerlin, V. M., van Swieten, J. C., Al-Chalabi, A., Ludolph, A. C., Weishaupt, J. H., Hardiman, O., Landers, J. E., Brown, R. H., Jr., van Es, M. A., Pasterkamp, R. J., Koppers, M., Andersen, P. M., Estrada, K., Rivadeneira, F., Hofman, A., Uitterlinden, A. G., van Damme, P., Melki, J., Meininger, V., Shatunov, A., Shaw, C. E., Leigh, P. N., Shaw, P. J., Morrison, K. E., Fogh, I., Chio, A., Traynor, B. J., Czell, D., Weber, M., Heutink, P., de Bakker, P. I., Silani, V., Robberecht, W., van den Berg, L. H. and Veldink, J. H. (2014) 'C9orf72 and UNC13A are shared risk loci for amyotrophic lateral sclerosis and frontotemporal dementia: A genome-wide meta-analysis', *Ann Neurol,* 76(1), pp. 120-33.

Diomede, L., Rigacci, S., Romeo, M., Stefani, M. and Salmona, M. (2013) 'Oleuropein aglycone protects transgenic *C. elegans* strains expressing Aβ42 by reducing plaque load and motor deficit', *PLoS One,* 8(3), pp. e58893.

Dobrinska, M. R. and Welling, P. G. (1977) 'Pharmacokinetics of methsuximide and a major metabolite in dogs', *J Pharm Sci,* 66(5), pp. 688-92.

Dorman, J. B., Albinder, B., Shroyer, T. and Kenyon, C. (1995) 'The *age-1* and *daf-2* genes function in a common pathway to control the lifespan of *Caenorhabditis elegans*', *Genetics,* 141(4), pp. 1399-406.

Dow, R. S., Macfarlane, J. P. and Stevens, J. R. (1958) 'Celontin in patients with refractory epilepsy', *Neurology,* 8(3), pp. 201-201.

Drake, J., Link, C. D. and Butterfield, D. A. (2003) 'Oxidative stress precedes fibrillar deposition of Alzheimer's disease amyloid β-peptide (1-42) in a transgenic *Caenorhabditis elegans* model', *Neurobiol Aging,* 24(3), pp. 415-20.

Dudley, K. H., Bius, D. L. and Waldrop, C. D. (1974) 'Urinary metabolites of N-methyl-alpha-methyl-alpha-phenysuccinimide (methsuximide) in the dog', *Drug Metab Dispos,* 2(2), pp. 113-22.

Duerr, J. S. (2006) 'Immunohistochemistry', in *WormBook* [Online]. Available at: http://www.wormbook.org (Accessed: 18 Jan. 2018).

Ekins, S., Honeycutt, J. D. and Metz, J. T. (2010) 'Evolving molecules using multi-objective optimization: Applying to ADME/Tox', *Drug Discov Today,* 15(11-12), pp. 451-60.

Ellerbrock, B. R., Coscarelli, E. M., Gurney, M. E. and Geary, T. G. (2004) 'Screening for presenilin inhibitors using the free-living nematode, *Caenorhabditis elegans*', *J Biomol Screen,* 9(2), pp. 147-52.

Erbaş, O., Yılmaz, M. and Taşkıran, D. (2016) 'Levetiracetam attenuates rotenone-induced toxicity: A rat model of Parkinson's disease', *Environmental Toxicology and Pharmacology,* 42, pp. 226-230.

Essers, M. A., de Vries-Smits, L. M., Barker, N., Polderman, P. E., Burgering, B. M. and Korswagen, H. C. (2005) 'Functional interaction between β-catenin and FOXO in oxidative stress signaling', *Science,* 308(5725), pp. 1181-4.

Evason, K., Collins, J. J., Huang, C., Hughes, S. and Kornfeld, K. (2008) 'Valproic acid extends *Caenorhabditis elegans* lifespan', *Aging Cell,* 7(3), pp. 305-17.

Evason, K., Huang, C., Yamben, I., Covey, D. F. and Kornfeld, K. (2005) 'Anticonvulsant medications extend worm life-span', *Science,* 307(5707), pp. 258-62.

Farlow, M., Gracon, S. I., Hershey, L. A., Lewis, K. W., Sadowsky, C. H. and Dolan-Ureno, J. (1992) 'A controlled trial of tacrine in Alzheimer's disease. The Tacrine Study Group', *Jama,* 268(18), pp. 2523-9.

Fecto, F., Yan, J., Vemula, S. P., Liu, E., Yang, Y., Chen, W., Zheng, J. G., Shi, Y., Siddique, N., Arrat, H., Donkervoort, S., Ajroud-Driss, S., Sufit, R. L., Heller, S. L., Deng, H. X. and Siddique, T. (2011) '*SQSTM1* mutations in familial and sporadic amyotrophic lateral sclerosis', *Arch Neurol,* 68(11), pp. 1440-6.

Fields, S. and Song, O. (1989) 'A novel genetic system to detect protein-protein interactions', *Nature,* 340(6230), pp. 245-6.

Fire, A., Xu, S., Montgomery, M. K., Kostas, S. A., Driver, S. E. and Mello, C. C. (1998) 'Potent and specific genetic interference by double-stranded RNA in *Caenorhabditis elegans*', *Nature,* 391(6669), pp. 806-811.

Fisher, R. S., van Emde Boas, W., Blume, W., Elger, C., Genton, P., Lee, P. and Engel, J., Jr. (2005) 'Epileptic seizures and epilepsy: Definitions proposed by the International League Against Epilepsy (ILAE) and the International Bureau for Epilepsy (IBE)', *Epilepsia,* 46(4), pp. 470-2.

Flavell, S. W., Pokala, N., Macosko, E. Z., Albrecht, D. R., Larsch, J. and Bargmann, C. I. (2013) 'Serotonin and the neuropeptide PDF initiate and extend opposing behavioral states in *C. elegans*', *Cell,* 154(5), pp. 1023-35.

Florez-McClure, M. L., Hohsfield, L. A., Fonte, G., Bealor, M. T. and Link, C. D. (2007) 'Decreased insulin-receptor signaling promotes the autophagic degradation of β-amyloid peptide in *C. elegans*', *Autophagy,* 3(6), pp. 569-80.

Fogh, I., Ratti, A., Gellera, C., Lin, K., Tiloca, C., Moskvina, V., Corrado, L., Soraru, G., Cereda, C., Corti, S., Gentilini, D., Calini, D., Castellotti, B., Mazzini, L., Querin, G., Gagliardi, S., Del Bo, R., Conforti, F. L., Siciliano, G., Inghilleri, M., Sacca, F., Bongioanni, P., Penco, S., Corbo, M., Sorbi, S., Filosto, M., Ferlini, A., Di Blasio, A. M., Signorini, S., Shatunov, A., Jones, A., Shaw, P. J., Morrison, K. E., Farmer, A. E., Van Damme, P., Robberecht, W., Chio, A., Traynor, B. J., Sendtner, M., Melki, J., Meininger, V., Hardiman, O., Andersen, P. M., Leigh, N. P., Glass, J. D., Overste, D., Diekstra, F. P., Veldink, J. H., van Es, M. A., Shaw, C. E., Weale, M. E., Lewis, C. M., Williams, J., Brown, R. H., Landers, J. E., Ticozzi, N., Ceroni, M., Pegoraro, E., Comi, G. P., D'Alfonso, S., van den Berg, L. H., Taroni, F., Al-Chalabi, A., Powell, J. and Silani, V. (2014) 'A genome-wide association meta-analysis identifies a novel locus at 17q11.2 associated with sporadic amyotrophic lateral sclerosis', *Hum Mol Genet,* 23(8), pp. 2220-31.

Fohlmeister, J. F., Adelman, W. J., Jr. and Brennan, J. J. (1984) 'Excitable channel currents and gating times in the presence of anticonvulsants ethosuximide and valproate', *J Pharmacol Exp Ther,* 230(1), pp. 75-81.

Frank-Cannon, T. C., Alto, L. T., McAlpine, F. E. and Tansey, M. G. (2009) 'Does neuroinflammation fan the flame in neurodegenerative diseases?', *Molecular Neurodegeneration,* 4, pp. 13.

Fraser, A., Kamath, R., Zipperlen, P., Martinez-Campos, M., Sohrmann, M. and Ahringer, J. (2000) 'Functional genomic analysis of *C. elegans* chromosome I by systematic RNA interference', *Nature,* 408.

Freischmidt, A., Wieland, T., Richter, B., Ruf, W., Schaeffer, V., Muller, K., Marroquin, N., Nordin, F., Hubers, A., Weydt, P., Pinto, S., Press, R., Millecamps, S., Molko, N., Bernard, E., Desnuelle, C., Soriani, M. H., Dorst, J., Graf, E., Nordstrom, U., Feiler, M. S., Putz, S., Boeckers, T. M., Meyer, T., Winkler, A. S., Winkelman, J., de Carvalho, M., Thal, D. R., Otto, M., Brannstrom, T., Volk, A. E., Kursula, P., Danzer, K. M., Lichtner, P., Dikic, I., Meitinger, T., Ludolph, A. C., Strom, T. M., Andersen, P. M. and Weishaupt, J. H. (2015) 'Haploinsufficiency of

TBK1 causes familial ALS and fronto-temporal dementia', *Nat Neurosci,* 18(5), pp. 631-6.

French, E. G., Rey-Bellet, J. and Lennox, W. G. (1958) 'Methsuximide in psychomotor and petit-mal seizures', *New England Journal of Medicine,* 258(18), pp. 892-894.

Förstl, H., Burns, A., Levy, R., Cairns, N., Luthert, P. and Lantos, P. (1992) 'Neurologic signs in Alzheimer's disease: Results of a prospective clinical and neuropathologic study', *Archives of Neurology,* 49(10), pp. 1038-1042.

Gaitatzis, A. and Sander, J. W. (2013) 'The long-term safety of antiepileptic drugs', *CNS Drugs,* 27(6), pp. 435-55.

Geier, F. M., Want, E. J., Leroi, A. M. and Bundy, J. G. (2011) 'Cross-platform comparison of *Caenorhabditis elegans* tissue extraction strategies for comprehensive metabolome coverage', *Anal Chem,* 83(10), pp. 3730-6.

'Genome sequence of the nematode *C. elegans*: A platform for investigating biology', (1998) *Science,* 282(5396), pp. 2012-8.

Gidalevitz, T., Krupinski, T., Garcia, S. and Morimoto, R. I. (2009) 'Destabilizing protein polymorphisms in the genetic background direct phenotypic expression of mutant SOD1 toxicity', *PLoS Genet,* 5(3), pp. e1000399.

Gilling, K. E., Jatzke, C., Hechenberger, M. and Parsons, C. G. (2009) 'Potency, voltage-dependency, agonist concentration-dependency, blocking kinetics and partial untrapping of the uncompetitive N-methyl-D-aspartate (NMDA) channel blocker memantine at human NMDA (GluN1/GluN2A) receptors', *Neuropharmacology,* 56(5), pp. 866-875.

Gitcho, M. A., Baloh, R. H., Chakraverty, S., Mayo, K., Norton, J. B., Levitch, D., Hatanpaa, K. J., White, C. L., 3rd, Bigio, E. H., Caselli, R., Baker, M., Al-Lozi, M. T., Morris, J. C., Pestronk, A., Rademakers, R., Goate, A. M. and Cairns, N. J. (2008) 'TDP-43 A315T mutation in familial motor neuron disease', *Ann Neurol,* 63(4), pp. 535-8.

Gitler, A. D., Dhillon, P. and Shorter, J. (2017) 'Neurodegenerative disease: Models, mechanisms, and a new hope', *Disease Models & Mechanisms,* 10(5), pp. 499.

Gleeson, M. P. (2008) 'Generation of a set of simple, interpretable ADMET rules of thumb', *J Med Chem,* 51(4), pp. 817-34.

Glenner, G. G. and Wong, C. W. (1984) 'Alzheimer's disease: Initial report of the purification and characterization of a novel cerebrovascular amyloid protein', *Biochem Biophys Res Commun,* 120, pp. 885-890.

Global Health and Aging (2017) [PDF]. Available at: http://www.who.int/ageing/publications/global_health.pdf (Accessed: 15 Sep. 2017).

Goate, A., Chartier-Harlin, M. C., Mullan, M., Brown, J., Crawford, F., Fidani, L., Giuffra, L., Haynes, A., Irving, N., James, L. and *et al*. (1991) 'Segregation of a missense mutation in the amyloid precursor protein gene with familial Alzheimer's disease', *Nature,* 349(6311), pp. 704-6.

Goedert, M. and Jakes, R. (2005) 'Mutations causing neurodegenerative tauopathies', *Biochimica et Biophysica Acta (BBA) - Molecular Basis of Disease,* 1739(2), pp. 240-250.

Goedert, M., Spillantini, M. G., Cairns, N. J. and Crowther, R. A. (1992) 'Tau proteins of alzheimer paired helical filaments: Abnormal phosphorylation of all six brain isoforms', *Neuron,* 8(1), pp. 159-168.

Goedert, M., Spillantini, M. G., Jakes, R., Rutherford, D. and Crowther, R. A. (1989) 'Multiple isoforms of human microtubule-associated protein tau: Sequences and localization in neurofibrillary tangles of Alzheimer's disease', *Neuron,* 3(4), pp. 519-526.

Gomora, J. C., Daud, A. N., Weiergraber, M. and Perez-Reyes, E. (2001) 'Block of cloned human T-type calcium channels by succinimide antiepileptic drugs', *Mol Pharmacol,* 60(5), pp. 1121-32.

Gonzalez-Moragas, L., Roig, A. and Laromaine, A. (2015) '*C. elegans* as a tool for in vivo nanoparticle assessment', *Advances in Colloid and Interface Science,* 219, pp. 10-26.

Goren, M. Z. and Onat, F. (2007) 'Ethosuximide: From bench to bedside', *CNS Drug Rev,* 13(2), pp. 224-39.

Gosai, S. J., Kwak, J. H., Luke, C. J., Long, O. S., King, D. E., Kovatch, K. J., Johnston, P. A., Shun, T. Y., Lazo, J. S., Perlmutter, D. H., Silverman, G. A. and Pak, S. C. (2010) 'Automated high-content live animal drug screening using c-elegans expressing the aggregation prone serpin α1-antitrypsin Z', *Plos One,* 5(11).

Goulet, J. R., Kinkel, A. W. and Smith, T. C. (1976) 'Metabolism of ethosuximide', *Clinical Pharmacology & Therapeutics,* 20(2), pp. 213-218.

Gross, R. A., Covey, D. F. and Ferrendelli, J. A. (1997) 'Voltage-dependent calcium channels as targets for convulsant and anticonvulsant alkyl-substituted thiobutyrolactones', *J Pharmacol Exp Ther,* 280(2), pp. 686-94.

Grossberg, G. T., Manes, F., Allegri, R. F., Gutiérrez-Robledo, L. M., Gloger, S., Xie, L., Jia, X. D., Pejović, V., Miller, M. L., Perhach, J. L. and Graham, S. M. (2013) 'The safety, tolerability, and efficacy of once-daily memantine (28 mg): A multinational, randomized, double-blind, placebo-controlled trial in patients with moderate-to-severe alzheimer's disease taking cholinesterase inhibitors', *CNS Drugs,* 27(6), pp. 469-478.

Groticke, I., Hoffmann, K. and Loscher, W. (2008) 'Behavioral alterations in a mouse model of temporal lobe epilepsy induced by intrahippocampal injection of kainate', *Exp Neurol,* 213(1), pp. 71-83.

Guerreiro, R., Wojtas, A., Bras, J., Carrasquillo, M., Rogaeva, E., Majounie, E., Cruchaga, C., Sassi, C., Kauwe, J. S. K., Younkin, S., Hazrati, L., Collinge, J., Pocock, J., Lashley, T., Williams, J., Lambert, J.-C., Amouyel, P., Goate, A., Rademakers, R., Morgan, K., Powell, J., St. George-Hyslop, P., Singleton, A. and Hardy, J. (2012) '*TREM2* variants in Alzheimer's disease', *New England Journal of Medicine,* 368(2), pp. 117-127.

Gurney, M. E., Pu, H., Chiu, A. Y., Dal Canto, M. C., Polchow, C. Y., Alexander, D. D., Caliendo, J., Hentati, A., Kwon, Y. W., Deng, H. X. and *et al*. (1994) 'Motor neuron degeneration in mice that express a human Cu,Zn superoxide dismutase mutation', *Science,* 264(5166), pp. 1772-5.

Gutierrez-Zepeda, A., Santell, R., Wu, Z., Brown, M., Wu, Y., Khan, I., Link, C. D., Zhao, B. and Luo, Y. (2005) 'Soy isoflavone glycitein protects against beta amyloid-induced toxicity and oxidative stress in transgenic *Caenorhabditis elegans*', *BMC Neurosci,* 6, pp. 54.

Halliday, M. and Mallucci, G. R. (2015) 'Review: Modulating the unfolded protein response to prevent neurodegeneration and enhance memory', *Neuropathol Appl Neurobiol,* 41(4), pp. 414-27.

Halliday, M., Radford, H., Sekine, Y., Moreno, J., Verity, N., le Quesne, J., Ortori, C. A., Barrett, D. A., Fromont, C., Fischer, P. M., Harding, H. P., Ron, D. and Mallucci, G. R. (2015) 'Partial restoration of protein synthesis rates by the small molecule ISRIB prevents neurodegeneration without pancreatic toxicity', *Cell Death Dis,* 6, pp. e1672.

Halliday, M., Radford, H., Zents, K. A. M., Molloy, C., Moreno, J. A., Verity, N. C., Smith, E., Ortori, C. A., Barrett, D. A., Bushell, M. and Mallucci, G. R. (2017) 'Repurposed drugs targeting eIF2α-P-mediated translational repression prevent neurodegeneration in mice', *Brain,* 140(6), pp. 1768-1783.

Hamamichi, S., Rivas, R. N., Knight, A. L., Cao, S., Caldwell, K. A. and Caldwell, G. A. (2008) 'Hypothesis-based RNAi screening identifies neuroprotective genes in a Parkinson's disease model', *Proc Natl Acad Sci U S A,* 105(2), pp. 728-33.

Han, S. K., Lee, D., Lee, H., Kim, D., Son, H. G., Yang, J. S., Lee, S. V. and Kim, S. (2016) 'OASIS 2: Online application for survival analysis 2 with features for the analysis of maximal lifespan and healthspan in aging research', *Oncotarget,* 7(35), pp. 56147-56152.

Han, S. S., Williams, L. A. and Eggan, K. C. (2011) 'Constructing and deconstructing stem cell models of neurological disease', *Neuron,* 70(4), pp. 626-44.

Hardy, J. and Allsop, D. (1991) 'Amyloid deposition as the central event in the aetiology of Alzheimer's disease', *Trends Pharmacol Sci,* 12(10), pp. 383-8.

Hauser, W. A., Annegers, J. F. and Rocca, W. A. (1996) 'Descriptive epidemiology of epilepsy: Contributions of population-based studies from Rochester, Minnesota', *Mayo Clin Proc,* 71(6), pp. 576-86.

Henderson, S. T. and Johnson, T. E. (2001) '*daf-16* integrates developmental and environmental inputs to mediate aging in the nematode *Caenorhabditis elegans*', *Curr Biol,* 11(24), pp. 1975-80.

Herrington, J. and Lingle, C. J. (1992) 'Kinetic and pharmacological properties of low voltage-activated Ca^{2+} current in rat clonal (GH3) pituitary cells', *J Neurophysiol,* 68(1), pp. 213-32.

Heyman, A., Wilkinson, W. E., Hurwitz, B. J., Helms, M. J., Haynes, C. S., Utley, C. M. and Gwyther, L. P. (1987) 'Early-onset Alzheimer's disease: Clinical predictors of institutionalization and death', *Neurology,* 37(6), pp. 980-4.

Hirose, T., Nakano, Y., Nagamatsu, Y., Misumi, T., Ohta, H. and Ohshima, Y. (2003) 'Cyclic GMP-dependent protein kinase EGL-4 controls body size and lifespan in *C. elegans*', *Development,* 130(6), pp. 1089.

Hobert, O. (2013) 'The neuronal genome of *Caenorhabditis elegans*', in *WormBook* [Online]. Available at: http://www.wormbook.org (Accessed: 15 Sep. 2017).

Hoglinger, G. U., Melhem, N. M., Dickson, D. W., Sleiman, P. M. A., Wang, L. S., Klei, L., Rademakers, R., de Silva, R., Litvan, I., Riley, D. E., van Swieten, J. C., Heutink, P., Wszolek, Z. K., Uitti, R. J., Vandrovcova, J., Hurtig, H. I., Gross, R. G., Maetzler, W., Goldwurm, S., Tolosa, E., Borroni, B., Pastor, P., Cantwell, L. B., Han, M. R., Dillman, A., van der Brug, M. P., Gibbs, J. R., Cookson, M. R., Hernandez, D. G., Singleton, A. B., Farrer, M. J., Yu, C. E., Golbe, L. I., Revesz, T., Hardy, J., Lees, A. J., Devlin, B., Hakonarson, H., Muller, U., Schellenberg, G. D. and Grp, P. S. P. G. S. (2011) 'Identification of common variants influencing risk of the tauopathy progressive supranuclear palsy', *Nature Genetics,* 43(7), pp. 699-U125.

Holcapek, M., Kolarova, L. and Nobilis, M. (2008) 'High-performance liquid chromatography-tandem mass spectrometry in the identification and determination of phase I and phase II drug metabolites', *Analytical and Bioanalytical Chemistry,* 391(1), pp. 59-78.

Holliday, J. D., Hu, C. Y. and Willett, P. (2002) 'Grouping of coefficients for the calculation of inter-molecular similarity and dissimilarity using 2D fragment bit-strings', *Comb Chem High Throughput Screen,* 5(2), pp. 155-66.

Hoogewijs, D., Houthoofd, K., Matthijssens, F., Vandesompele, J. and Vanfleteren, J. R. (2008) 'Selection and validation of a set of reliable reference genes for quantitative *sod* gene expression analysis in *C. elegans*', *BMC Molecular Biology,* 9(1), pp. 9.

Hoozemans, J. J., van Haastert, E. S., Eikelenboom, P., de Vos, R. A., Rozemuller, J. M. and Scheper, W. (2007) 'Activation of the unfolded protein response in Parkinson's disease', *Biochem Biophys Res Commun,* 354(3), pp. 707-11.

Hoozemans, J. J. M., van Haastert, E. S., Nijholt, D. A. T., Rozemuller, A. J. M., Eikelenboom, P. and Scheper, W. (2009) 'The unfolded protein response is activated in pretangle neurons in Alzheimer's disease hippocampus', *American Journal of Pathology,* 174(4), pp. 1241-1251.

Horning, M. G., Butler, C., Harvey, D. J., Hill, R. M. and Zion, T. E. (1973a) 'Metabolism of N,2-dimethyl-2-phenylsuccinimide (methsuximide) by the epoxide-diol pathway in rat, guinea pig and human', *Res Commun Chem Pathol Pharmacol,* 6(2), pp. 565-78.

Horning, M. G., Stratton, C., Nowlin, J., Harvey, D. J. and Hill, R. M. (1973b) 'Metabolism of 2-ethyl-2-methylsuccinimide (ethosuximide) in the rat and human', *Drug Metabolism and Disposition,* 1(3), pp. 569.

Hsiung, G. Y., DeJesus-Hernandez, M., Feldman, H. H., Sengdy, P., Bouchard-Kerr, P., Dwosh, E., Butler, R., Leung, B., Fok, A., Rutherford, N. J., Baker, M., Rademakers, R. and Mackenzie, I. R. (2012) 'Clinical and pathological features of familial frontotemporal dementia caused by C9ORF72 mutation on chromosome 9p', *Brain,* 135(Pt 3), pp. 709-22.

Hubbard, B. P. and Sinclair, D. A. (2014) 'Small molecule SIRT1 activators for the treatment of aging and age-related diseases', *Trends in Pharmacological Sciences,* 35(3), pp. 146-154.

Hughes, J. R. (2009) 'Absence seizures: A review of recent reports with new concepts', *Epilepsy Behav,* 15(4), pp. 404-12.

Hurst, D. L. (1996) 'Methsuximide therapy of juvenile myoclonic epilepsy', *Seizure,* 5(1), pp. 47-50.

Imfeld, P., Bodmer, M., Schuerch, M., Jick, S. S. and Meier, C. R. (2013) 'Seizures in patients with Alzheimer's disease or vascular dementia: A population-based nested case-control analysis', *Epilepsia,* 54(4), pp. 700-7.

Irizarry, M. C., Jin, S., He, F., Emond, J. A., Raman, R., Thomas, R. G., Sano, M., Quinn, J. F., Tariot, P. N., Galasko, D. R., Ishihara, L. S., Weil, J. G. and Aisen, P. S. (2012) 'Incidence of new-onset seizures in mild to moderate Alzheimer disease', *Arch Neurol,* 69(3), pp. 368-72.

Irwin, J. J. and Shoichet, B. K. (2005) 'ZINC - a free database of commercially available compounds for virtual screening', *J Chem Inf Model,* 45(1), pp. 177-82.

Jack, C. R., Knopman, D. S., Jagust, W. J., Shaw, L. M., Aisen, P. S., Weiner, M. W., Petersen, R. C. and Trojanowski, J. Q. (2010) 'Hypothetical model of dynamic biomarkers of the Alzheimer's pathological cascade', *Lancet neurology,* 9(1), pp. 119.

Jagota, S. and Rajadas, J. (2012) 'Effect of phenolic compounds against Aβ aggregation and Aβ-induced toxicity in transgenic *C. elegans*', *Neurochem Res,* 37(1), pp. 40-8.

Jakel, R. J., Schneider, B. L. and Svendsen, C. N. (2004) 'Using human neural stem cells to model neurological disease', *Nat Rev Genet,* 5(2), pp. 136-144.

Jellinger, K. A. (2010) 'Basic mechanisms of neurodegeneration: A critical update', *J Cell Mol Med,* 14(3), pp. 457-87.

Jeong, H., Cohen, D. E., Cui, L., Supinski, A., Savas, J. N., Mazzulli, J. R., Yates, J. R., 3rd, Bordone, L., Guarente, L. and Krainc, D. (2012) 'Sirt1 mediates neuroprotection from mutant huntingtin by activation of the TORC1 and CREB transcriptional pathway', *Nat Med,* 18(1), pp. 159-65.

Jia, F., Kato, M., Dai, H., Xu, A., Okuda, T., Sakurai, E., Okamura, N., Lovenberg, T. W., Barbier, A., Carruthers, N. I., Iinuma, K. and Yanai, K. (2006) 'Effects of histamine H_3 antagonists and donepezil on learning and mnemonic deficits induced by pentylenetetrazol kindling in weanling mice', *Neuropharmacology,* 50(4), pp. 404-11.

Jiang, M., Wang, J., Fu, J., Du, L., Jeong, H., West, T., Xiang, L., Peng, Q., Hou, Z., Cai, H., Seredenina, T., Arbez, N., Zhu, S., Sommers, K., Qian, J., Zhang, J., Mori, S., Yang, X. W., Tamashiro, K. L., Aja, S., Moran, T. H., Luthi-Carter, R., Martin, B., Maudsley, S., Mattson, M. P., Cichewicz, R. H., Ross, C. A., Holtzman, D. M., Krainc, D. and Duan, W. (2012) 'Neuroprotective role of Sirt1 in mammalian models of Huntington's disease through activation of multiple Sirt1 targets', *Nat Med,* 18(1), pp. 153-8.

Jin, Y., Jorgensen, E., Hartwieg, E. and Horvitz, H. R. (1999) 'The *Caenorhabditis elegans* gene *unc-25* encodes glutamic acid decarboxylase and is required for synaptic transmission but not synaptic development', *J Neurosci,* 19(2), pp. 539-48.

Johnson, B. S., Snead, D., Lee, J. J., McCaffery, J. M., Shorter, J. and Gitler, A. D. (2009a) 'TDP-43 is intrinsically aggregation-prone, and amyotrophic lateral sclerosis-linked mutations accelerate aggregation and increase toxicity', *J Biol Chem,* 284(30), pp. 20329-39.

Johnson, J. O., Mandrioli, J., Benatar, M., Abramzon, Y., Van Deerlin, V. M., Trojanowski, J. Q., Gibbs, J. R., Brunetti, M., Gronka, S., Wuu, J., Ding, J., McCluskey, L., Martinez-Lage, M., Falcone, D., Hernandez, D. G., Arepalli, S., Chong, S., Schymick, J. C., Rothstein, J., Landi, F., Wang, Y. D., Calvo, A., Mora, G., Sabatelli, M., Monsurro, M. R., Battistini, S., Salvi, F., Spataro, R., Sola, P., Borghero, G., Galassi, G., Scholz, S. W., Taylor, J. P., Restagno, G., Chio, A. and Traynor, B. J. (2010) 'Exome sequencing reveals *VCP* mutations as a cause of familial ALS', *Neuron,* 68(5), pp. 857-64.

Johnson, J. O., Pioro, E. P., Boehringer, A., Chia, R., Feit, H., Renton, A. E., Pliner, H. A., Abramzon, Y., Marangi, G., Winborn, B. J., Gibbs, J. R., Nalls, M. A., Morgan, S., Shoai, M., Hardy, J., Pittman, A., Orrell, R. W., Malaspina, A., Sidle, K. C., Fratta, P., Harms, M. B., Baloh, R. H., Pestronk, A., Weihl, C. C., Rogaeva, E., Zinman, L., Drory, V. E., Borghero, G., Mora, G., Calvo, A., Rothstein, J. D., Drepper, C., Sendtner, M., Singleton, A. B., Taylor, J. P., Cookson, M. R., Restagno, G., Sabatelli, M., Bowser, R., Chio, A. and Traynor, B. J. (2014) 'Mutations in the *Matrin 3* gene cause familial amyotrophic lateral sclerosis', *Nat Neurosci,* 17(5), pp. 664-666.

Johnson, J. R., Ferdek, P., Lian, L. Y., Barclay, J. W., Burgoyne, R. D. and Morgan, A. (2009b) 'Binding of UNC-18 to the N-terminus of syntaxin is essential for neurotransmission in *Caenorhabditis elegans*', *Biochem J,* 418(1), pp. 73-80.

Jonsson, T., Atwal, J. K., Steinberg, S., Snaedal, J., Jonsson, P. V., Bjornsson, S., Stefansson, H., Sulem, P., Gudbjartsson, D., Maloney, J., Hoyte, K., Gustafson, A., Liu, Y., Lu, Y., Bhangale, T., Graham, R. R., Huttenlocher, J., Bjornsdottir, G., Andreassen, O. A., Jonsson, E. G., Palotie, A., Behrens, T. W., Magnusson, O. T., Kong, A., Thorsteinsdottir, U., Watts, R. J. and Stefansson, K. (2012a) 'A mutation in *APP* protects against Alzheimer's disease and age-related cognitive decline', *Nature,* 488(7409), pp. 96-9.

Jonsson, T., Stefansson, H., Steinberg, S., Jonsdottir, I., Jonsson, P. V., Snaedal, J., Bjornsson, S., Huttenlocher, J., Levey, A. I., Lah, J. J., Rujescu, D., Hampel, H., Giegling, I., Andreassen, O. A., Engedal, K., Ulstein, I., Djurovic, S., Ibrahim-Verbaas, C., Hofman, A., Ikram, M. A., van Duijn, C. M., Thorsteinsdottir, U., Kong, A. and Stefansson, K. (2012b) 'Variant of *TREM2* associated with the risk of Alzheimer's disease', *New England Journal of Medicine,* 368(2), pp. 107-116.

Jorgensen, E. M. (2005) 'GABA', in *WormBook* [Online]. Available at: http://www.wormbook.org (Accessed: 15 Sep. 2017).

Jorgensen, E. M. and Mango, S. E. (2002) 'The art and design of genetic screens: *Caenorhabditis elegans*', *Nat Rev Genet,* 3(5), pp. 356-369.

Kaletsky, R., Lakhina, V., Arey, R., Williams, A., Landis, J., Ashraf, J. and Murphy, C. T. (2016) 'The *C. elegans* adult neuronal IIS/FOXO transcriptome reveals adult phenotype regulators', *Nature,* 529(7584), pp. 92-96.

Kaletta, T. and Hengartner, M. O. (2006) 'Finding function in novel targets: *C. elegans* as a model organism', *Nature Reviews Drug Discovery,* 5(5), pp. 387-398.

Kalia, L. V. and Lang, A. E. (2015) 'Parkinson's disease', *The Lancet,* 386(9996), pp. 896-912.

Kamath, R. S. and Ahringer, J. (2003) 'Genome-wide RNAi screening in *Caenorhabditis elegans*', *Methods,* 30(4), pp. 313-21.

Kamath, R. S., Martinez-Campos, M., Zipperlen, P., Fraser, A. G. and Ahringer, J. (2001) 'Effectiveness of specific RNA-mediated interference through ingested double-stranded RNA in *Caenorhabditis elegans*', *Genome Biol,* 2.

Kaminski, K. and Obniska, J. (2008) 'Design, synthesis, and anticonvulsant activity of N-phenylamino derivatives of 3,3-dialkyl-pyrrolidine-2,5-diones and hexahydro-isoindole-1,3-diones', *Bioorg Med Chem,* 16(9), pp. 4921-31.

Kaminski, K., Obniska, J., Chlebek, I., Liana, P. and Pekala, E. (2013) 'Synthesis and biological properties of new N-Mannich bases derived from 3-methyl-3-phenyl- and 3,3-dimethyl-succinimides. Part V', *Eur J Med Chem,* 66, pp. 12-21.

Karuppagounder, S. S., Pinto, J. T., Xu, H., Chen, H. L., Beal, M. F. and Gibson, G. E. (2009) 'Dietary supplementation with resveratrol reduces plaque pathology in a transgenic model of Alzheimer's disease', *Neurochem Int,* 54(2), pp. 111-8.

Kashyap, S. S., Johnson, J. R., McCue, H. V., Chen, X., Edmonds, M. J., Ayala, M., Graham, M. E., Jenn, R. C., Barclay, J. W., Burgoyne, R. D. and Morgan, A. (2014) '*Caenorhabditis elegans dnj-14*, the orthologue of the *DNAJC5* gene mutated in adult onset neuronal ceroid lipofuscinosis, provides a new platform for neuroprotective drug screening and identifies a SIR-2.1-independent action of resveratrol', *Human Molecular Genetics*.

Kautu, B. B., Carrasquilla, A., Hicks, M. L., Caldwell, K. A. and Caldwell, G. A. (2013) 'Valproic acid ameliorates *C. elegans* dopaminergic neurodegeneration with implications for ERK-MAPK signaling', *Neuroscience letters,* 541, pp. 116-119.

Kenna, K. P., Landers, J. E. and Ticozzi, N. (2017) 'Chapter 3 - Genetics of Amyotrophic Lateral Sclerosis A2 - Boulis, Nicholas', in O'Connor, D. & Donsante, A. (eds.) *Molecular and Cellular Therapies for Motor Neuron Diseases*: Academic Press, pp. 43-59.

Kennedy, S., Wang, D. and Ruvkun, G. (2004) 'A conserved siRNA-degrading RNase negatively regulates RNA interference in *C. elegans*', *Nature,* 427(6975), pp. 645-649.

Kenyon, C., Chang, J., Gensch, E., Rudner, A. and Tabtiang, R. (1993) 'A *C. elegans* mutant that lives twice as long as wild type', *Nature,* 366(6454), pp. 461-4.

Keowkase, R., Aboukhatwa, M. and Luo, Y. (2010) 'Fluoxetine protects against amyloid-beta toxicity, in part via *daf-16* mediated cell signaling pathway, in *Caenorhabditis elegans*', *Neuropharmacology,* 59(4-5), pp. 358-65.

Khan, A., Marson, C. M. and Porter, R. A. (2001) 'SYnthesis of exocyclic enamides via stereocontrolled allylic isomerization and 1,3-transposition', *Synthetic Communications,* 31(11), pp. 1753-1764.

Khanna, M. R., Kovalevich, J., Lee, V. M., Trojanowski, J. Q. and Brunden, K. R. (2016) 'Therapeutic strategies for the treatment of tauopathies: Hopes and challenges', *Alzheimers Dement,* 12(10), pp. 1051-1065.

Khurana, V. and Lindquist, S. (2010) 'Modelling neurodegeneration in *Saccharomyces cerevisiae*: Why cook with baker's yeast?', *Nat Rev Neurosci,* 11(6), pp. 436-449.

Kidd, S. K. and Schneider, J. S. (2011) 'Protective effects of valproic acid on the nigrostriatal dopamine system in a 1-methyl-4-phenyl-1,2,3,6-tetrahydropyridine mouse model of Parkinson's disease', *Neuroscience,* 194, pp. 189-194.

Kim, D., Nguyen, M. D., Dobbin, M. M., Fischer, A., Sananbenesi, F., Rodgers, J. T., Delalle, I., Baur, J. A., Sui, G., Armour, S. M., Puigserver, P., Sinclair, D. A. and Tsai, L. H. (2007a) 'SIRT1 deacetylase protects against neurodegeneration in models for Alzheimer's disease and amyotrophic lateral sclerosis', *Embo j,* 26(13), pp. 3169-79.

Kim, Y. and Sun, H. (2012) 'ASM-3 acid sphingomyelinase functions as a positive regulator of the DAF-2/AGE-1 signaling pathway and serves as a novel anti-aging target', *PLOS ONE,* 7(9), pp. e45890.

Kim, H. J., Kim, N. C., Wang, Y. D., Scarborough, E. A., Moore, J., Diaz, Z., MacLea, K. S., Freibaum, B., Li, S., Molliex, A., Kanagaraj, A. P., Carter, R., Boylan, K. B., Wojtas, A. M., Rademakers, R., Pinkus, J. L., Greenberg, S. A., Trojanowski, J. Q., Traynor, B. J., Smith, B. N., Topp, S., Gkazi, A. S., Miller, J., Shaw, C. E., Kottlors, M., Kirschner, J., Pestronk, A., Li, Y. R., Ford, A. F., Gitler, A. D., Benatar, M., King, O. D., Kimonis, V. E., Ross, E. D., Weihl, C. C., Shorter, J. and Taylor, J. P. (2013) 'Mutations in prion-like domains in hnRNPA2B1 and hnRNPA1 cause multisystem proteinopathy and ALS', *Nature,* 495(7442), pp. 467-73.

Kim, H. J., Raphael, A. R., LaDow, E. S., McGurk, L., Weber, R. A., Trojanowski, J. Q., Lee, V. M., Finkbeiner, S., Gitler, A. D. and Bonini, N. M. (2014) 'Therapeutic modulation of eIF2α phosphorylation rescues TDP-43 toxicity in amyotrophic lateral sclerosis disease models', *Nat Genet,* 46(2), pp. 152-60.

Kim, J., Onstead, L., Randle, S., Price, R., Smithson, L., Zwizinski, C., Dickson, D. W., Golde, T. and McGowan, E. (2007b) 'Aβ40 inhibits amyloid deposition *in vivo*', *J Neurosci,* 27(3), pp. 627-33.

Klein, C. and Westenberger, A. (2012) 'Genetics of Parkinson's disease', *Cold Spring Harbor Perspectives in Medicine,* 2(1), pp. a008888.

Klopmand, G. (1992) 'Concepts and applications of molecular similarity'. In: M. A. Johnson and G. M. Maggiora, eds., *Journal of Computational Chemistry,* 1st ed. New York: John Wiley & Sons, pp. 539-540.

Klunk, W. E., Covey, D. F. and Ferrendelli, J. A. (1982a) 'Anticonvulsant properties of alpha, gamma, and alpha, gamma-substituted gamma-butyrolactones', *Molecular Pharmacology,* 22(2), pp. 438.

Klunk, W. E., Covey, D. F. and Ferrendelli, J. A. (1982b) 'Comparison of epileptogenic properties of unsubstituted and beta-alkyl-substituted gamma-butyrolactones', *Mol Pharmacol,* 22(2), pp. 431-7.

Klunk, W. E., Covey, D. F. and Ferrendelli, J. A. (1982c) 'Structure-activity relationships of alkyl-substituted gamma-butyrolactones and succinimides', *Mol Pharmacol,* 22(2), pp. 444-50.

Knapp, M. J., Knopman, D. S., Solomon, P. R., Pendlebury, W. W., Davis, C. S. and Gracon, S. I. (1994) 'A 30-week randomized controlled trial of high-dose tacrine in patients with Alzheimer's disease. The Tacrine Study Group', *Jama,* 271(13), pp. 985-91.

Koppers, M., van Blitterswijk, M. M., Vlam, L., Rowicka, P. A., van Vught, P. W., Groen, E. J., Spliet, W. G., Engelen-Lee, J., Schelhaas, H. J., de Visser, M., van der Kooi, A. J., van der Pol, W. L., Pasterkamp, R. J., Veldink, J. H. and van den Berg, L. H. (2012) '*VCP* mutations in familial and sporadic amyotrophic lateral sclerosis', *Neurobiol Aging,* 33(4), pp. 837.e7-13.

Kostyuk, P. G., Molokanova, E. A., Pronchuk, N. F., Savchenko, A. N. and Verkhratsky, A. N. (1992) 'Different action of ethosuximide on low- and high-threshold calcium currents in rat sensory neurons', *Neuroscience,* 51(4), pp. 755-8.

Kraemer, B. C. and Schellenberg, G. D. (2007) 'SUT-1 enables tau-induced neurotoxicity in *C. elegans*', *Human Molecular Genetics,* 16(16), pp. 1959-1971.

Kraemer, B. C., Zhang, B., Leverenz, J. B., Thomas, J. H., Trojanowski, J. Q. and Schellenberg, G. D. (2003) 'Neurodegeneration and defective neurotransmission in a *Caenorhabditis elegans* model of tauopathy', *Proceedings of the National Academy of Sciences of the United States of America,* 100(17), pp. 9980-9985.

Kremer, B., Goldberg, P., Andrew, S. E., Theilmann, J., Telenius, H., Zeisler, J., Squitieri, F., Lin, B., Bassett, A., Almqvist, E., Bird, T. D. and Hayden, M. R. (1994) 'A worldwide study of the Huntington's disease mutation: The sensitivity and specificity of measuring cag repeats', *New England Journal of Medicine,* 330(20), pp. 1401-1406.

Kwiatkowski, T. J., Jr., Bosco, D. A., Leclerc, A. L., Tamrazian, E., Vanderburg, C. R., Russ, C., Davis, A., Gilchrist, J., Kasarskis, E. J., Munsat, T., Valdmanis, P., Rouleau, G. A., Hosler, B. A., Cortelli, P., de Jong, P. J., Yoshinaga, Y., Haines, J. L., Pericak-Vance, M. A., Yan, J., Ticozzi, N., Siddique, T., McKenna-Yasek, D., Sapp, P. C., Horvitz, H. R., Landers, J. E. and Brown, R. H., Jr. (2009) 'Mutations in the *FUS/TLS* gene on chromosome 16 cause familial amyotrophic lateral sclerosis', *Science,* 323(5918), pp. 1205-8.

Kwok, T. C. Y., Ricker, N., Fraser, R., Chan, A. W., Burns, A., Stanley, E. F., McCourt, P., Cutler, S. R. and Roy, P. J. (2006) 'A small-molecule screen in *C. elegans* yields a new calcium channel antagonist', *Nature,* 441(7089), pp. 91-95.

Lacinova, L., Klugbauer, N. and Hofmann, F. (2000) 'Regulation of the calcium channel α_{1G} subunit by divalent cations and organic blockers', *Neuropharmacology,* 39(7), pp. 1254-66.

Lacomblez, L., Bensimon, G., Leigh, P. N., Guillet, P. and Meininger, V. (1996) 'Dose-ranging study of riluzole in amyotrophic lateral sclerosis. Amyotrophic Lateral Sclerosis/Riluzole Study Group II', *Lancet,* 347(9013), pp. 1425-31.

Lai, C. H., Chou, C. Y., Ch'ang, L. Y., Liu, C. S. and Lin, W. C. (2000) 'Identification of novel human genes evolutionarily conserved in *Caenorhabditis elegans* by comparative proteomics', *Genome Research,* 10(5), pp. 703-713.

Landis, J. N. and Murphy, C. T. (2010) 'Integration of diverse inputs in the regulation of *Caenorhabditis elegans* DAF-16/FOXO', *Dev Dyn,* 239(5), pp. 1405-12.

Lasoń, W., Chlebicka, M. and Rejdak, K. (2013) 'Research advances in basic mechanisms of seizures and antiepileptic drug action', *Pharmacological Reports,* 65(4), pp. 787-801.

Later Life in the United Kingdom (2017) [PDF]. Available at: http://www.ageuk.org.uk/Documents/EN-GB/Factsheets/Later_Life_UK_factsheet.pdf?dtrk=true (Accessed: 15 Sep. 2017).

Lee, E. B., Lee, V. M. Y. and Trojanowski, J. Q. (2011) 'Gains or losses: Molecular mechanisms of TDP43-mediated neurodegeneration', *Nature Reviews. Neuroscience,* 13(1), pp. 38-50.

Leeson, P. D. and Springthorpe, B. (2007) 'The influence of drug-like concepts on decision-making in medicinal chemistry', *Nat Rev Drug Discov,* 6(11), pp. 881-890.

Lehmann, J., Smith, R. V. and Langer, S. Z. (1983) 'Stereoisomers of apomorphine differ in affinity and intrinsic activity at presynaptic dopamine receptors modulating [^{3}H]dopamine and [^{3}H]acetylcholine release in slices of cat caudate', *European Journal of Pharmacology,* 88(1), pp. 81-88.

Leresche, N., Parri, H. R., Erdemli, G., Guyon, A., Turner, J. P., Williams, S. R., Asprodini, E. and Crunelli, V. (1998) 'On the action of the anti-absence drug ethosuximide in the rat and cat thalamus', *J Neurosci,* 18(13), pp. 4842-53.

Letemendia, F. and Pampiglione, G. (1958) 'Clinical and electroencephalographic observations in Alzheimer's disease', *Journal of Neurology, Neurosurgery & Psychiatry,* 21(3), pp. 167.

Leung, C. K., Wang, Y., Malany, S., Deonarine, A., Nguyen, K., Vasile, S. and Choe, K. P. (2013) 'An ultra high-throughput, whole-animal screen for small molecule modulators of a specific genetic pathway in *Caenorhabditis elegans*', *PLOS ONE,* 8(4), pp. e62166.

Levy-Lahad, E., Wasco, W., Poorkaj, P., Romano, D. M., Oshima, J., Pettingell, W. H., Yu, C. E., Jondro, P. D., Schmidt, S. D., Wang, K. and *et al*. (1995) 'Candidate gene for the chromosome 1 familial Alzheimer's disease locus', *Science,* 269(5226), pp. 973-7.

Li, J. and Le, W. (2013) 'Modeling neurodegenerative diseases in *Caenorhabditis elegans*', *Experimental Neurology,* 250(0), pp. 94-103.

Liachko, N. F., Guthrie, C. R. and Kraemer, B. C. (2010) 'Phosphorylation promotes neurotoxicity in a *C. elegans* model of TDP-43 proteinopathy', *The Journal of neuroscience : the official journal of the Society for Neuroscience,* 30(48), pp. 16208-16219.

Lima, L. M. and Barreiro, E. J. (2005) 'Bioisosterism: A useful strategy for molecular modification and drug design', *Curr Med Chem,* 12(1), pp. 23-49.

Lin, K., Dorman, J. B., Rodan, A. and Kenyon, C. (1997) '*daf-16*: An HNF-3/forkhead family member that can function to double the life-span of *Caenorhabditis elegans*', *Science,* 278(5341), pp. 1319-22.

Lin, M. T. and Beal, M. F. (2006) 'Mitochondrial dysfunction and oxidative stress in neurodegenerative diseases', *Nature,* 443(7113), pp. 787-95.

Lindblom, T. H. and Dodd, A. K. (2006) 'Xenobiotic detoxification in the nematode *Caenorhabditis elegans*', *J Exp Zool A Comp Exp Biol,* 305(9), pp. 720-30.

Link, C. D. (1995) 'Expression of human β-amyloid peptide in transgenic *Caenorhabditis elegans*', *Proceedings of the National Academy of Sciences of the United States of America,* 92(20), pp. 9368-9372.

Link, C. D., Taft, A., Kapulkin, V., Duke, K., Kim, S., Fei, Q., Wood, D. E. and Sahagan, B. G. (2003) 'Gene expression analysis in a transgenic *Caenorhabditis elegans* Alzheimer's disease model', *Neurobiol Aging,* 24(3), pp. 397-413.

Liu, J., Banskota, A. H., Critchley, A. T., Hafting, J. and Prithiviraj, B. (2015) 'Neuroprotective effects of the cultivated Chondrus crispus in a *C. elegans* model of Parkinson's disease', *Mar Drugs,* 13(4), pp. 2250-66.

Liu-Yesucevitz, L., Bilgutay, A., Zhang, Y.-J., Vanderwyde, T., Citro, A., Mehta, T., Zaarur, N., McKee, A., Bowser, R., Sherman, M., Petrucelli, L. and Wolozin, B. (2010) 'Tar DNA Binding Protein-43 (TDP-43) associates with stress granules: Analysis of cultured cells and pathological brain tissue', *PLOS ONE,* 5(10), pp. e13250.

Lockery, S. R., Hulme, S. E., Roberts, W. M., Robinson, K. J., Laromaine, A., Lindsay, T. H., Whitesides, G. M. and Weeks, J. C. (2012) 'A microfluidic device for whole-animal drug screening using electrophysiological measures in the nematode *C. elegans*', *Lab on a Chip,* 12(12), pp. 2211-2220.

Lomenick, B., Hao, R., Jonai, N., Chin, R. M., Aghajan, M., Warburton, S., Wang, J., Wu, R. P., Gomez, F., Loo, J. A., Wohlschlegel, J. A., Vondriska, T. M., Pelletier, J., Herschman, H. R., Clardy, J., Clarke, C. F. and Huang, J. (2009) 'Target identification using drug affinity responsive target stability (DARTS)', *Proceedings of the National Academy of Sciences,* 106(51), pp. 21984-21989.

Lomenick, B., Olsen, R. W. and Huang, J. (2011) 'Identification of direct protein targets of small molecules', *ACS Chemical Biology,* 6(1), pp. 34-46.

Lozsadi, D. A. and Larner, A. J. (2006) 'Prevalence and causes of seizures at the time of diagnosis of probable Alzheimer's disease', *Dement Geriatr Cogn Disord,* 22(2), pp. 121-4.

Lublin, A., Isoda, F., Patel, H., Yen, K., Nguyen, L., Hajje, D., Schwartz, M. and Mobbs, C. (2011) 'FDA-approved drugs that protect mammalian neurons from glucose toxicity slow aging dependent on CBP and protect against proteotoxicity', *PLoS ONE,* 6(11), pp. e27762.

Löscher, W. (2011) 'Critical review of current animal models of seizures and epilepsy used in the discovery and development of new antiepileptic drugs', *Seizure,* 20(5), pp. 359-368.

Loy, C. and Schneider, L. (2006) 'Galantamine for Alzheimer's disease and mild cognitive impairment', *Cochrane Database Syst Rev,* (1), pp. Cd001747.

Mackenzie, I. R., Bigio, E. H., Ince, P. G., Geser, F., Neumann, M., Cairns, N. J., Kwong, L. K., Forman, M. S., Ravits, J., Stewart, H., Eisen, A., McClusky, L., Kretzschmar, H. A., Monoranu, C. M., Highley, J. R., Kirby, J., Siddique, T., Shaw, P. J., Lee, V. M. and Trojanowski, J. Q. (2007) 'Pathological TDP-43 distinguishes sporadic amyotrophic lateral sclerosis from amyotrophic lateral sclerosis with *SOD1* mutations', *Ann Neurol,* 61(5), pp. 427-34.

Majounie, E., Renton, A. E., Mok, K., Dopper, E. G., Waite, A., Rollinson, S., Chio, A., Restagno, G., Nicolaou, N., Simon-Sanchez, J., van Swieten, J. C., Abramzon, Y., Johnson, J. O., Sendtner, M., Pamphlett, R., Orrell, R. W., Mead, S., Sidle, K. C., Houlden, H., Rohrer, J. D., Morrison, K. E., Pall, H., Talbot, K., Ansorge, O., Hernandez, D. G., Arepalli, S., Sabatelli, M., Mora, G., Corbo, M., Giannini, F., Calvo, A., Englund, E., Borghero, G., Floris, G. L., Remes, A. M., Laaksovirta, H., McCluskey, L., Trojanowski, J. Q., Van Deerlin, V. M., Schellenberg, G. D., Nalls, M. A., Drory, V. E., Lu, C. S., Yeh, T. H., Ishiura, H., Takahashi, Y., Tsuji, S., Le Ber, I., Brice, A., Drepper, C., Williams, N., Kirby, J., Shaw, P., Hardy, J., Tienari, P. J., Heutink, P., Morris, H. R., Pickering-Brown, S. and Traynor, B. J. (2012) 'Frequency of the *C9orf72* hexanucleotide repeat expansion in patients with amyotrophic lateral sclerosis and frontotemporal dementia: A cross-sectional study', *Lancet Neurol,* 11(4), pp. 323-30.

Manning, J. P., Richards, D. A., Leresche, N., Crunelli, V. and Bowery, N. G. (2004) 'Cortical-area specific block of genetically determined absence seizures by ethosuximide', *Neuroscience,* 123(1), pp. 5-9.

Marescaux, C., Vergnes, M. and Depaulis, A. (1992) 'Genetic absence epilepsy in rats from Strasbourg - a review', *J Neural Transm Suppl,* 35, pp. 37-69.

Maruyama, H., Morino, H., Ito, H., Izumi, Y., Kato, H., Watanabe, Y., Kinoshita, Y., Kamada, M., Nodera, H., Suzuki, H., Komure, O., Matsuura, S., Kobatake, K., Morimoto, N., Abe, K., Suzuki, N., Aoki, M., Kawata, A., Hirai, T., Kato, T., Ogasawara, K., Hirano, A., Takumi, T., Kusaka, H., Hagiwara, K., Kaji, R. and Kawakami, H. (2010) 'Mutations of optineurin in amyotrophic lateral sclerosis', *Nature,* 465(7295), pp. 223-6.

Marvanova, M. and Nichols, C. D. (2007) 'Identification of neuroprotective compounds of *Caenorhabditis elegans* dopaminergic neurons against 6-OHDA', *J Mol Neurosci,* 31(2), pp. 127-37.

Masters, C. L., Simms, G., Weinman, N. A., Multhaup, G., McDonald, B. L. and Beyreuther, K. (1985) 'Amyloid plaque core protein in Alzheimer's disease and Down syndrome', *Proc Natl Acad Sci U S A,* 82, pp. 4245-4249.

McColl, G., Roberts, B. R., Pukala, T. L., Kenche, V. B., Roberts, C. M., Link, C. D., Ryan, T. M., Masters, C. L., Barnham, K. J., Bush, A. I. and Cherny, R. A. (2012) 'Utility of an improved model of amyloid-beta ($A\beta_{1-42}$) toxicity in *Caenorhabditis elegans* for drug screening for Alzheimer's disease', *Mol Neurodegener,* 7, pp. 57.

McCormick, A. V., Wheeler, J. M., Guthrie, C. R., Liachko, N. F. and Kraemer, B. C. (2013) 'Dopamine D2 receptor antagonism suppresses tau aggregation and neurotoxicity', *Biological Psychiatry,* 73(5), pp. 464-471.

McDade, E. and Bateman, R. J. (2017) 'Stop Alzheimer's before it starts', *Nature,* 547(7662), pp. 153-155.

McElwee, J., Bubb, K. and Thomas, J. H. (2003) 'Transcriptional outputs of the *Caenorhabditis elegans* forkhead protein DAF-16', *Aging Cell,* 2(2), pp. 111-21.

McElwee, J. J., Schuster, E., Blanc, E., Piper, M. D., Thomas, J. H., Patel, D. S., Selman, C., Withers, D. J., Thornton, J. M., Partridge, L. and Gems, D. (2007) 'Evolutionary conservation of regulated longevity assurance mechanisms', *Genome Biology,* 8(7), pp. R132.

McLean, M. J. and Macdonald, R. L. (1986) 'Sodium valproate, but not ethosuximide, produces use- and voltage-dependent limitation of high frequency repetitive firing of action potentials of mouse central neurons in cell culture', *J Pharmacol Exp Ther,* 237(3), pp. 1001-11.

McLntire, S. L., Jorgensen, E. and Horvitz, H. R. (1993) 'Genes required for GABA function in *Caenorhabditis elegans*', *Nature,* 364(6435), pp. 334-337.

Mead, R. J., Higginbottom, A., Allen, S. P., Kirby, J., Bennett, E., Barber, S. C., Heath, P. R., Coluccia, A., Patel, N., Gardner, I., Brancale, A., Grierson, A. J. and Shaw, P. J. (2013) 'S[+] Apomorphine is a CNS penetrating activator of the Nrf2-ARE pathway with activity in mouse and patient fibroblast models of amyotrophic lateral sclerosis', *Free Radical Biology & Medicine,* 61, pp. 438-452.

Mendez, M. F., Catanzaro, P., Doss, R. C., R, A. R. and Frey, W. H., 2nd (1994) 'Seizures in Alzheimer's disease: Clinicopathologic study', *J Geriatr Psychiatry Neurol,* 7(4), pp. 230-3.

Mifsud, J., Collier, P. S. and Millership, J. S. (2001) 'The pharmacokinetics of ethosuximide enantiomers in the rat', *Biopharmaceutics & Drug Disposition,* 22(2), pp. 83-89.

Miller, C. A. and Long, L. M. (1953) 'Anticonvulsants. IV. An Investigation of α-(Substituted phenyl)-succinimides', *Journal of the American Chemical Society,* 75(24), pp. 6256-6258.

Miller, C. A., Scholl, H. I. and Long, L. M. (1951) 'Anticonvulsants.1 II. A Study of N-R-α,β-Substituted Succinimides', *Journal of the American Chemical Society,* 73(12), pp. 5608-5610.

Millership, J. S., Collier, P. S., Hamilton, J. T., McRoberts, W. C. and Mifsud, J. (1995) 'Chiral aspects of the metabolism of ethosuximide', *Chirality,* 7(3), pp. 173-80.

Millership, J. S., Mifsud, J. and Collier, P. S. (1993) 'The metabolism of ethosuximide', *European Journal of Drug Metabolism and Pharmacokinetics,* 18(4), pp. 349-353.

Millership, J. S., Mifsud, J., Galea, D., McRoberts, W. C. and Hamilton, J. T. (2005) 'Chiral aspects of the human metabolism of ethosuximide', *Biopharm Drug Dispos,* 26(6), pp. 225-32.

Mitchell, D. H., Stiles, J. W., Santelli, J. and Sanadi, D. R. (1979) 'Synchronous growth and aging of *Caenorhabditis elegans* in the presence of fluorodeoxyuridine', *J Gerontol,* 34(1), pp. 28-36.

Mitchell, P., Mould, R., Dillon, J., Glautier, S., Andrianakis, I., James, C., Pugh, A., Holden-Dye, L. and O'Connor, V. (2010) 'A differential role for neuropeptides in acute and chronic adaptive responses to alcohol: Behavioural and genetic analysis in *Caenorhabditis elegans*', *PLOS ONE,* 5(5), pp. e10422.

Monti, B., Gatta, V., Piretti, F., Raffaelli, S. S., Virgili, M. and Contestabile, A. (2010) 'Valproic acid is neuroprotective in the rotenone rat model of Parkinson's disease: Involvement of α-synuclein', *Neurotoxicity Research,* 17(2), pp. 130-141.

Monti, B., Mercatelli, D. and Contestabile, A. (2012) 'Valproic acid neuroprotection in 6-OHDA lesioned rat, a model for parkinson's disease', *HOAJ Biology,* 1(1).

Monti, B., Polazzi, E. and Contestabile, A. (2009) 'Biochemical, molecular and epigenetic mechanisms of valproic acid neuroprotection', *Curr Mol Pharmacol,* 2(1), pp. 95-109.

Moreno, J. A., Halliday, M., Molloy, C., Radford, H., Verity, N., Axten, J. M., Ortori, C. A., Willis, A. E., Fischer, P. M., Barrett, D. A. and Mallucci, G. R. (2013) 'Oral treatment targeting the unfolded protein response prevents neurodegeneration and clinical disease in prion-infected mice', *Science Translational Medicine,* 5(206).

Moreno, J. A., Radford, H., Peretti, D., Steinert, J. R., Verity, N., Martin, M. G., Halliday, M., Morgan, J., Dinsdale, D., Ortori, C. A., Barrett, D. A., Tsaytler, P., Bertolotti, A., Willis, A. E., Bushell, M. and Mallucci, G. R. (2012) 'Sustained translational repression by eIF2α-P mediates prion neurodegeneration', *Nature,* 485(7399), pp. 507-11.

Mori, K., Weng, S. M., Arzberger, T., May, S., Rentzsch, K., Kremmer, E., Schmid, B., Kretzschmar, H. A., Cruts, M., Van Broeckhoven, C., Haass, C. and Edbauer, D. (2013) 'The *C9orf72* GGGGCC repeat is translated into aggregating dipeptide-repeat proteins in FTLD/ALS', *Science,* 339(6125), pp. 1335-8.

Morley, J. F., Brignull, H. R., Weyers, J. J. and Morimoto, R. I. (2002) 'The threshold for polyglutamine-expansion protein aggregation and cellular toxicity is dynamic and influenced by aging in *Caenorhabditis elegans*', *Proc Natl Acad Sci U S A,* 99(16), pp. 10417-22.

Moshe, S. L., Perucca, E., Ryvlin, P. and Tomson, T. (2015) 'Epilepsy: New advances', *Lancet,* 385(9971), pp. 884-98.

Muller, C. J., Bankstahl, M., Groticke, I. and Loscher, W. (2009) 'Pilocarpine vs. lithium-pilocarpine for induction of status epilepticus in mice: Development of spontaneous seizures, behavioral alterations and neuronal damage', *Eur J Pharmacol,* 619(1-3), pp. 15-24.

Muni, I. A., Altshuler, C. H. and Neicheril, J. C. (1973) 'Identification of a blood metabolite of methsuximide by GLC-mass spectrometry', *Journal of Pharmaceutical Sciences,* 62(11), pp. 1820-1823.

Murphy, C. T. and Hu, P. J. (2013) 'Insulin/insulin-like growth factor signaling in *C. elegans.*', in *WormBook* [Online]. Available at: http://www.wormbook.org (Accessed: 15 Sep. 2017).

Murphy, C. T., McCarroll, S. A., Bargmann, C. I., Fraser, A., Kamath, R. S., Ahringer, J., Li, H. and Kenyon, C. (2003) 'Genes that act downstream of DAF-16 to influence the lifespan of *Caenorhabditis elegans*', *Nature,* 424(6946), pp. 277-83.

Murphy, M. P. and LeVine, H. (2010) 'Alzheimer's disease and the β-amyloid peptide', *Journal of Alzheimer's disease : JAD,* 19(1), pp. 311.

Murrell, J., Farlow, M., Ghetti, B. and Benson, M. D. (1991) 'A mutation in the amyloid precursor protein associated with hereditary Alzheimer's disease', *Science,* 254(5028), pp. 97-9.

Musaeus, C. S., Shafi, M. M., Santarnecchi, E., Herman, S. T. and Press, D. Z. (2017) 'Levetiracetam alters oscillatory connectivity in Alzheimer's disease', *J Alzheimers Dis,* 58(4), pp. 1065-1076.

Neumann, M., Sampathu, D. M., Kwong, L. K., Truax, A. C., Micsenyi, M. C., Chou, T. T., Bruce, J., Schuck, T., Grossman, M., Clark, C. M., McCluskey, L. F., Miller, B. L., Masliah, E., Mackenzie, I. R., Feldman, H., Feiden, W., Kretzschmar, H. A., Trojanowski, J. Q. and Lee, V. M. Y. (2006) 'Ubiquitinated TDP-43 in frontotemporal lobar degeneration and amyotrophic lateral sclerosis', *Science,* 314(5796), pp. 130.

Ngugi, A. K., Bottomley, C., Kleinschmidt, I., Sander, J. W. and Newton, C. R. (2010) 'Estimation of the burden of active and life-time epilepsy: A meta-analytic approach', *Epilepsia,* 51(5), pp. 883-90.

Nguyen, L. A., He, H. and Pham-Huy, C. (2006) 'Chiral drugs: An overview', *International Journal of Biomedical Science : IJBS,* 2(2), pp. 85-100.

Nicholls, P. J. and Orton, T. C. (1972) 'The physiological disposition of ^{14}C-methsuximide in the rat', *Br J Pharmacol,* 45(1), pp. 48-59.

Noskova, L., Stranecky, V., Hartmannova, H., Pristoupilova, A., Baresova, V., Ivanek, R., Hulkova, H., Jahnova, H., van der Zee, J., Staropoli, J. F., Sims, K. B., Tyynela, J., Van Broeckhoven, C., Nijssen, P. C., Mole, S. E., Elleder, M. and Kmoch, S. (2011) 'Mutations in *DNAJC5*, encoding cysteine-string protein alpha, cause autosomal-dominant adult-onset neuronal ceroid lipofuscinosis', *Am J Hum Genet,* 89(2), pp. 241-52.

Obniska, J., Chlebek, I. and Kaminski, K. (2012) 'Synthesis and anticonvulsant properties of new mannich bases derived from 3,3-disubstituted pyrrolidine-2,5-diones. Part IV', *Arch Pharm (Weinheim),* 345(9), pp. 713-22.

Obniska, J., Kaminski, K., Skrzynska, D. and Pichor, J. (2009) 'Synthesis and anticonvulsant activity of new N-[(4-arylpiperazin-1-yl)-alkyl] derivatives of 3-phenyl-pyrrolidine-2,5-dione', *Eur J Med Chem,* 44(5), pp. 2224-33.

Obniska, J., Kopytko, M., Zagorska, A., Chlebek, I. and Kaminski, K. (2010) 'Synthesis and anticonvulsant properties of new Mannich bases derived from 3-aryl-pyrrolidine-2,5-diones. Part 1', *Arch Pharm (Weinheim),* 343(6), pp. 333-41.

Oeda, T., Shimohama, S., Kitagawa, N., Kohno, R., Imura, T., Shibasaki, H. and Ishii, N. (2001) 'Oxidative stress causes abnormal accumulation of familial amyotrophic lateral sclerosis-related mutant SOD1 in transgenic *Caenorhabditis elegans*', *Hum Mol Genet,* 10(19), pp. 2013-23.

Ogg, S., Paradis, S., Gottlieb, S., Patterson, G. I., Lee, L., Tissenbaum, H. A. and Ruvkun, G. (1997) 'The Fork head transcription factor DAF-16 transduces insulin-like metabolic and longevity signals in *C. elegans*', *Nature,* 389(6654), pp. 994-9.

Orr, H. T. (2012) 'Polyglutamine neurodegeneration: Expanded glutamines enhance native functions', *Current Opinion in Genetics & Development,* 22(3), pp. 251-255.

Orr, M. E., Sullivan, A. C. and Frost, B. (2017) 'A brief overview of tauopathy: Causes, consequences, and therapeutic strategies', *Trends in Pharmacological Sciences,* 38(7), pp. 637-648.

Orton, T. C. and Nicholls, P. J. (1972) 'Effect in rats of subacute administration of ethosuximide, methsuximide and phensuximide on hepatic microsomal enzymes and porphyrin turnover', *Biochemical Pharmacology,* 21(16), pp. 2253-2261.

Pai, M. Y., Lomenick, B., Hwang, H., Schiestl, R., McBride, W., Loo, J. A. and Huang, J. (2015) 'Drug Affinity Responsive Target Stability (DARTS) for small molecule target identification', *Methods in molecular biology (Clifton, N.J.),* 1263, pp. 287-298.

Paiva, F. A., Bonomo Lde, F., Boasquivis, P. F., de Paula, I. T., Guerra, J. F., Leal, W. M., Silva, M. E., Pedrosa, M. L. and Oliveira Rde, P. (2015) 'Carqueja (*Baccharis trimera*) protects against oxidative stress and β-amyloid-induced toxicity in *Caenorhabditis elegans*', *Oxid Med Cell Longev,* 2015, pp. 740162.

Paloneva, J., Manninen, T., Christman, G., Hovanes, K., Mandelin, J., Adolfsson, R., Bianchin, M., Bird, T., Miranda, R., Salmaggi, A., Tranebjærg, L., Konttinen, Y. and Peltonen, L. (2002) 'Mutations in two genes encoding different subunits of a receptor signaling complex result in an identical disease phenotype', *The American Journal of Human Genetics,* 71(3), pp. 656-662.

Palop, J. J., Chin, J., Roberson, E. D., Wang, J., Thwin, M. T., Bien-Ly, N., Yoo, J., Ho, K. O., Yu, G. Q., Kreitzer, A., Finkbeiner, S., Noebels, J. L. and Mucke, L. (2007) 'Aberrant excitatory neuronal activity and compensatory remodeling of inhibitory hippocampal circuits in mouse models of Alzheimer's disease', *Neuron,* 55(5), pp. 697-711.

Pan, T., Li, X., Xie, W., Jankovic, J. and Le, W. (2005) 'Valproic acid-mediated Hsp70 induction and anti-apoptotic neuroprotection in SH-SY5Y cells', *FEBS Letters,* 579(30), pp. 6716-6720.

Parker, J. A., Arango, M., Abderrahmane, S., Lambert, E., Tourette, C., Catoire, H. and Neri, C. (2005) 'Resveratrol rescues mutant polyglutamine cytotoxicity in nematode and mammalian neurons', *Nat Genet,* 37(4), pp. 349-350.

Patsalos, P. N. (2005) 'Properties of antiepileptic drugs in the treatment of idiopathic generalized epilepsies', *Epilepsia,* 46 Suppl 9, pp. 140-8.

Peskind, E. R., Potkin, S. G., Pomara, N., Ott, B. R., Graham, S. M., Olin, J. T. and McDonald, S. (2006) 'Memantine treatment in mild to moderate Alzheimer disease: A 24-week randomized, controlled trial', *Am J Geriatr Psychiatry,* 14(8), pp. 704-15.

Pettersen, J. E. (1978) 'Urinary metabolites of 2-ethyl-2-methylsuccinimide (ethosuximide) studied by combined gas chromatography mass spectrometry', *Biological Mass Spectrometry,* 5(11), pp. 601-603.

Pfrieger, F. W., Veselovsky, N. S., Gottmann, K. and Lux, H. D. (1992) 'Pharmacological characterization of calcium currents and synaptic transmission between thalamic neurons in vitro', *J Neurosci,* 12(11), pp. 4347-57.

Piepers, S., Veldink, J. H., de Jong, S. W., van der Tweel, I., van der Pol, W. L., Uijtendaal, E. V., Schelhaas, H. J., Scheffer, H., de Visser, M., de Jong, J. M., Wokke, J. H., Groeneveld, G. J. and van den Berg, L. H. (2009) 'Randomized sequential trial of valproic acid in amyotrophic lateral sclerosis', *Ann Neurol,* 66(2), pp. 227-34.

Pitkanen, A. and Kubova, H. (2004) 'Antiepileptic drugs in neuroprotection', *Expert Opin Pharmacother,* 5(4), pp. 777-98.

Polymenidou, M., Lagier-Tourenne, C., Hutt, K. R., Huelga, S. C., Moran, J., Liang, T. Y., Ling, S. C., Sun, E., Wancewicz, E., Mazur, C., Kordasiewicz, H., Sedaghat, Y., Donohue, J. P., Shiue, L., Bennett, C. F., Yeo, G. W. and Cleveland, D. W. (2011) 'Long pre-mRNA depletion and RNA missplicing contribute to neuronal vulnerability from loss of TDP-43', *Nat Neurosci,* 14(4), pp. 459-68.

Porta-de-la-Riva, M., Fontrodona, L., Villanueva, A. and Cerón, J. (2012) 'Basic *Caenorhabditis elegans* Methods: Synchronization and Observation', *Journal of Visualized Experiments : JoVE,* (64), pp. 4019.

Porsteinsson, A. P., Grossberg, G. T., Mintzer, J. and Olin, J. T. (2008) 'Memantine treatment in patients with mild to moderate Alzheimer's disease already receiving a cholinesterase inhibitor: A randomized, double-blind, placebo-controlled trial', *Curr Alzheimer Res,* 5(1), pp. 83-9.

Porter, R. J., Penry, J. K., Lacy, J. R., Newmark, M. E. and Kupferberg, H. J. (1979) 'Plasma concentrations of phensuximide, methsuximide, and their metabolites in relation to clinical efficacy', *Neurology,* 29(11), pp. 1509-13.

Poupaert, J. H., Vandervorst, D., Guiot, P., Moustafa, M. M. and Dumont, P. (1984) 'Structure-activity relationships of phenytoin-like anticonvulsant drugs', *J Med Chem,* 27(1), pp. 76-8.

Preste, P. G., Westerman, C. E., Das, N. P., Wilder, B. J. and Duncan, J. H. (1974) 'Identification of 2-ethyl-2-methyl-3-hydroxysuccinimide as a major metabolite of ethosuximide in humans', *Journal of Pharmaceutical Sciences,* 63(3), pp. 467-469.

Qing, H., He, G., Ly, P. T., Fox, C. J., Staufenbiel, M., Cai, F., Zhang, Z., Wei, S., Sun, X., Chen, C. H., Zhou, W., Wang, K. and Song, W. (2008) 'Valproic acid inhibits Aβ production, neuritic plaque formation, and behavioral deficits in Alzheimer's disease mouse models', *J Exp Med,* 205(12), pp. 2781-9.

Quinn, N. (1995) 'Fortnightly Review: Drug treatment of Parkinson's disease', *BMJ,* 310(6979), pp. 575.

Rankovic, Z. (2015) 'CNS drug design: Balancing physicochemical properties for optimal brain exposure', *Journal of Medicinal Chemistry,* 58(6), pp. 2584-2608.

Rao, S. C., Dove, G., Cascino, G. D. and Petersen, R. C. (2009) 'Recurrent seizures in patients with dementia: Frequency, seizure types, and treatment outcome', *Epilepsy Behav,* 14(1), pp. 118-20.

Rayaprolu, S., Mullen, B., Baker, M., Lynch, T., Finger, E., Seeley, W. W., Hatanpaa, K. J., Lomen-Hoerth, C., Kertesz, A., Bigio, E. H., Lippa, C., Josephs, K. A., Knopman, D. S., White, C. L., Caselli, R., Mackenzie, I. R., Miller, B. L., Boczarska-Jedynak, M., Opala, G., Krygowska-Wajs, A., Barcikowska, M., Younkin, S. G., Petersen, R. C., Ertekin-

Taner, N., Uitti, R. J., Meschia, J. F., Boylan, K. B., Boeve, B. F., Graff-Radford, N. R., Wszolek, Z. K., Dickson, D. W., Rademakers, R. and Ross, O. A. (2013) '*TREM2* in neurodegeneration: Evidence for association of the p.R47H variant with frontotemporal dementia and Parkinson's disease', *Molecular Neurodegeneration,* 8(1), pp. 19.

Reisberg, B., Doody, R., Stöffler, A., Schmitt, F., Ferris, S. and Möbius, H. J. (2003) 'Memantine in Moderate-to-Severe Alzheimer's Disease', *New England Journal of Medicine,* 348(14), pp. 1333-1341.

Renton, A. E., Chio, A. and Traynor, B. J. (2014) 'State of play in amyotrophic lateral sclerosis genetics', *Nat Neurosci,* 17(1), pp. 17-23.

Renton, A. E., Majounie, E., Waite, A., Simon-Sanchez, J., Rollinson, S., Gibbs, J. R., Schymick, J. C., Laaksovirta, H., van Swieten, J. C., Myllykangas, L., Kalimo, H., Paetau, A., Abramzon, Y., Remes, A. M., Kaganovich, A., Scholz, S. W., Duckworth, J., Ding, J., Harmer, D. W., Hernandez, D. G., Johnson, J. O., Mok, K., Ryten, M., Trabzuni, D., Guerreiro, R. J., Orrell, R. W., Neal, J., Murray, A., Pearson, J., Jansen, I. E., Sondervan, D., Seelaar, H., Blake, D., Young, K., Halliwell, N., Callister, J. B., Toulson, G., Richardson, A., Gerhard, A., Snowden, J., Mann, D., Neary, D., Nalls, M. A., Peuralinna, T., Jansson, L., Isoviita, V. M., Kaivorinne, A. L., Holtta-Vuori, M., Ikonen, E., Sulkava, R., Benatar, M., Wuu, J., Chio, A., Restagno, G., Borghero, G., Sabatelli, M., Heckerman, D., Rogaeva, E., Zinman, L., Rothstein, J. D., Sendtner, M., Drepper, C., Eichler, E. E., Alkan, C., Abdullaev, Z., Pack, S. D., Dutra, A., Pak, E., Hardy, J., Singleton, A., Williams, N. M., Heutink, P., Pickering-Brown, S., Morris, H. R., Tienari, P. J. and Traynor, B. J. (2011) 'A hexanucleotide repeat expansion in C9ORF72 is the cause of chromosome 9p21-linked ALS-FTD', *Neuron,* 72(2), pp. 257-68.

Revett, T. J., Baker, G. B., Jhamandas, J. and Kar, S. (2013) 'Glutamate system, amyloid β peptides and tau protein: Functional interrelationships and relevance to Alzheimer disease pathology', *Journal of Psychiatry & Neuroscience : JPN,* 38(1), pp. 6-23.

Risse, S. C., Lampe, T. H., Bird, T. D., Nochlin, D., Sumi, S. M., Keenan, T., Cubberley, L., Peskind, E. and Raskind, M. A. (1990) 'Myoclonus, seizures, and paratonia in Alzheimer disease', *Alzheimer Dis Assoc Disord,* 4(4), pp. 217-25.

Rogaev, E. I., Sherrington, R., Rogaeva, E. A., Levesque, G., Ikeda, M., Liang, Y., Chi, H., Lin, C., Holman, K., Tsuda, T. and *et al*. (1995) 'Familial Alzheimer's disease in kindreds with missense mutations in a gene on chromosome 1 related to the Alzheimer's disease type 3 gene', *Nature,* 376(6543), pp. 775-8.

Romanelli, M. F., Morris, J. C., Ashkin, K. and Coben, L. A. (1990) 'Advanced Alzheimer's disease is a risk factor for late-onset seizures', *Arch Neurol,* 47(8), pp. 847-50.

Rosen, D. R., Siddique, T., Patterson, D., Figlewicz, D. A., Sapp, P., Hentati, A., Donaldson, D., Goto, J., O'Regan, J. P., Deng, H. X. and *et al*. (1993) 'Mutations in Cu/Zn superoxide dismutase gene are associated with familial amyotrophic lateral sclerosis', *Nature,* 362(6415), pp. 59-62.

Ross, C. A. and Tabrizi, S. J. (2011) 'Huntington's disease: From molecular pathogenesis to clinical treatment', *Lancet Neurol,* 10(1), pp. 83-98.

Rouaux, C., Panteleeva, I., Rene, F., de Aguilar, J. L. G., Echaniz-Laguna, A., Dupuis, L., Menger, Y., Boutillier, A. L. and Loeffler, J. P. (2007) 'Sodium valproate exerts neuroprotective effects in vivo through CREB-binding protein-dependent mechanisms but does not improve survival in an amyotrophic lateral sclerosis mouse model', *Journal of Neuroscience,* 27(21), pp. 5535-5545.

Rual, J. F., Ceron, J., Koreth, J., Hao, T., Nicot, A. S., Hirozane-Kishikawa, T., Vandenhaute, J., Orkin, S. H., Hill, D. E., van den Heuvel, S. and Vidal, M. (2004) 'Toward improving *Caenorhabditis elegans* phenome mapping with an ORFeome-based RNAi library', *Genome Res,* 14(10b), pp. 2162-8.

Ruan, Q., Harrington, A. J., Caldwell, K. A., Caldwell, G. A. and Standaert, D. G. (2010) 'VPS41, a protein involved in lysosomal trafficking, is protective in *Caenorhabditis elegans* and mammalian cellular models of Parkinson's disease', *Neurobiol Dis,* 37(2), pp. 330-8.

Rubinsztein, D. C. (2006) 'The roles of intracellular protein-degradation pathways in neurodegeneration', *Nature,* 443(7113), pp. 780-6.

Rybka, S., Obniska, J., Rapacz, A., Filipek, B. and Kaminski, K. (2014) 'Synthesis, physicochemical, and anticonvulsant properties of new N-Mannich bases derived from pyrrolidine-2,5-dione and its 3-methyl analog', *Arch Pharm (Weinheim),* 347(10), pp. 768-76.

Saari, W. S., King, S. W. and Lotti, V. J. (1973) 'Synthesis and biological activity of (6aS)-10,11-dihydroxyaporphine, the optical antipode of apomorphine', *Journal of Medicinal Chemistry,* 16(2), pp. 171-172.

Saha, S., Guillily, M. D., Ferree, A., Lanceta, J., Chan, D., Ghosh, J., Hsu, C. H., Segal, L., Raghavan, K., Matsumoto, K., Hisamoto, N., Kuwahara, T., Iwatsubo, T., Moore, L., Goldstein, L., Cookson, M. and Wolozin, B. (2009) 'LRRK2 modulates vulnerability to mitochondrial dysfunction in *Caenorhabditis elegans*', *J Neurosci,* 29(29), pp. 9210-8.

Samann, J., Hegermann, J., von Gromoff, E., Eimer, S., Baumeister, R. and Schmidt, E. (2009) 'Caenorhabditits elegans LRK-1 and PINK-1 act antagonistically in stress response and neurite outgrowth', *J Biol Chem,* 284(24), pp. 16482-91.

Samson, W. N., van Duijn, C. M., Hop, W. C. and Hofman, A. (1996) 'Clinical features and mortality in patients with early-onset Alzheimer's disease', *Eur Neurol,* 36(2), pp. 103-6.

Sanchez, P. E., Zhu, L., Verret, L., Vossel, K. A., Orr, A. G., Cirrito, J. R., Devidze, N., Ho, K., Yu, G.-Q., Palop, J. J. and Mucke, L. (2012) 'Levetiracetam suppresses neuronal network dysfunction and reverses synaptic and cognitive deficits in an Alzheimer’s disease model', *Proceedings of the National Academy of Sciences,* 109(42), pp. E2895-E2903.

Santulli, L., Coppola, A., Balestrini, S. and Striano, S. (2016) 'The challenges of treating epilepsy with 25 antiepileptic drugs', *Pharmacological Research,* 107, pp. 211-219.

Satyal, S. H., Schmidt, E., Kitagawa, K., Sondheimer, N., Lindquist, S., Kramer, J. M. and Morimoto, R. I. (2000) 'Polyglutamine aggregates alter protein folding homeostasis in *Caenorhabditis elegans*', *Proc Natl Acad Sci U S A,* 97(11), pp. 5750-5.

Sayer, R. J., Brown, A. M., Schwindt, P. C. and Crill, W. E. (1993) 'Calcium currents in acutely isolated human neocortical neurons', *J Neurophysiol,* 69(5), pp. 1596-606.

Scarmeas, N., Honig, L. S., Choi, H. and *et al*. (2009) 'Seizures in Alzheimer disease: Who, when, and how common?', *Archives of Neurology,* 66(8), pp. 992-997.

Schlachetzki, J. C. M., Saliba, S. W. and Oliveira, A. C. P. d. (2013) 'Studying neurodegenerative diseases in culture models', *Revista Brasileira de Psiquiatria,* 35, pp. S92-S100.

Schmid, C. D., Sautkulis, L. N., Danielson, P. E., Cooper, J., Hasel, K. W., Hilbush, B. S., Sutcliffe, J. G. and Carson, M. J. (2002) 'Heterogeneous expression of the triggering receptor expressed on myeloid cells-2 on adult murine microglia', *J Neurochem,* 83(6), pp. 1309-20.

Schmidt, D. and Schachter, S. C. (2014) 'Drug treatment of epilepsy in adults', *Bmj-British Medical Journal,* 348, pp. 18.

Schulz, A., Kohlschütter, A., Mink, J., Simonati, A. and Williams, R. (2013) 'NCL diseases — clinical perspectives', *Biochimica et Biophysica Acta (BBA) - Molecular Basis of Disease,* 1832(11), pp. 1801-1806.

Schuske, K., Beg, A. A. and Jorgensen, E. M. (2004) 'The GABA nervous system in *C. elegans*', *Trends Neurosci,* 27(7), pp. 407-14.

Schwendeman, A. R. and Shaham, S. (2016) 'A high-throughput small molecule screen for *C. elegans* linker cell death inhibitors', *PLOS ONE,* 11(10), pp. e0164595.

Scotter, E. L., Chen, H.-J. and Shaw, C. E. (2015) 'TDP-43 proteinopathy and als: Insights into disease mechanisms and therapeutic targets', *Neurotherapeutics,* 12(2), pp. 352-363.

Selkoe, D. J. and Hardy, J. (2016) 'The amyloid hypothesis of Alzheimer's disease at 25 years', *EMBO Molecular Medicine,* 8(6), pp. 595-608.

Settivari, R., Levora, J. and Nass, R. (2009) 'The divalent metal transporter homologues SMF-1/2 mediate dopamine neuron sensitivity in *Caenorhabditis elegans* models of manganism and parkinson disease', *J Biol Chem,* 284(51), pp. 35758-68.

Shatunov, A., Mok, K., Newhouse, S., Weale, M. E., Smith, B., Vance, C., Johnson, L., Veldink, J. H., van Es, M. A., van den Berg, L. H., Robberecht, W., Van Damme, P., Hardiman, O., Farmer, A. E., Lewis, C. M., Butler, A. W., Abel, O., Andersen, P. M., Fogh, I., Silani, V., Chio, A., Traynor, B. J., Melki, J., Meininger, V., Landers, J. E., McGuffin, P., Glass, J. D., Pall, H., Leigh, P. N., Hardy, J., Brown, R. H., Jr., Powell, J. F., Orrell, R. W., Morrison, K. E., Shaw, P. J., Shaw, C. E. and Al-Chalabi, A. (2010) 'Chromosome 9p21 in sporadic amyotrophic lateral sclerosis in the UK and seven other countries: A genome-wide association study', *Lancet Neurol,* 9(10), pp. 986-94.

Sheridan, R. P. and Kearsley, S. K. (2002) 'Why do we need so many chemical similarity search methods?', *Drug Discovery Today,* 7(17), pp. 903-911.

Sherrington, R., Rogaev, E. I., Liang, Y., Rogaeva, E. A., Levesque, G., Ikeda, M., Chi, H., Lin, C., Li, G., Holman, K., Tsuda, T., Mar, L., Foncin, J. F., Bruni, A. C., Montesi, M. P., Sorbi, S., Rainero, I., Pinessi, L., Nee, L., Chumakov, I., Pollen, D., Brookes, A., Sanseau, P., Polinsky, R. J., Wasco, W., Da Silva, H. A., Haines, J. L., Perkicak-Vance, M. A., Tanzi, R. E., Roses, A. D., Fraser, P. E., Rommens, J. M. and St George-Hyslop, P. H. (1995) 'Cloning of a gene bearing missense mutations in early-onset familial Alzheimer's disease', *Nature,* 375(6534), pp. 754-60.

Sherzai, D., Losey, T., Vega, S. and Sherzai, A. (2014) 'Seizures and dementia in the elderly: Nationwide Inpatient Sample 1999-2008', *Epilepsy Behav,* 36, pp. 53-6.

Shintani, R., Duan, W.-L. and Hayashi, T. (2006) 'rhodium-catalyzed asymmetric construction of quaternary carbon stereocenters: Ligand-dependent regiocontrol in the 1,4-addition to substituted maleimides', *Journal of the American Chemical Society,* 128(17), pp. 5628-5629.

Simmer, F., Tijsterman, M., Parrish, S., Koushika, S. P., Nonet, M. L., Fire, A., Ahringer, J. and Plasterk, R. H. (2002) 'Loss of the putative RNA-directed RNA polymerase RRF-3 makes *C. elegans* hypersensitive to RNAi', *Curr Biol,* 12(15), pp. 1317-9.

Sjogren, T., Sjogren, H. and Lindgren, A. G. (1952) 'Morbus Alzheimer and morbus Pick; A genetic, clinical and patho-anatomical study', *Acta Psychiatr Neurol Scand Suppl,* 82, pp. 1-152.

Sleigh, J. N. (2010) 'Functional analysis of nematode nicotinic receptors', *Bioscience Horizons: The International Journal of Student Research,* 3(1), pp. 29-39.

Sleigh, J. N., Buckingham, S. D., Esmaeili, B., Viswanathan, M., Cuppen, E., Westlund, B. M. and Sattelle, D. B. (2011) 'A novel *Caenorhabditis elegans* allele, *smn-1(cb131)*, mimicking a mild form of spinal muscular atrophy, provides a convenient drug screening platform highlighting new and pre-approved compounds', *Human Molecular Genetics,* 20(2), pp. 245-260.

Smith, G. R., Brenneman, D. E., Zhang, Y., Du, Y. and Reitz, A. B. (2014) 'Small-molecule anticonvulsant agents with potent in vitro neuroprotection and favorable drug-like properties', *J Mol Neurosci,* 52(3), pp. 446-58.

Smith, H. L. and Mallucci, G. R. (2016) 'The unfolded protein response: mechanisms and therapy of neurodegeneration', *Brain,* 139(8), pp. 2113-2121.

Smith, J. V. and Luo, Y. (2003) 'Elevation of oxidative free radicals in Alzheimer's disease models can be attenuated by Ginkgo biloba extract EGb 761', *J Alzheimers Dis,* 5(4), pp. 287-300.

Son, A. Y., Biagioni, M. C., Kaminski, D., Gurevich, A., Stone, B. and Di Rocco, A. (2016) 'Parkinson's disease and cryptogenic epilepsy', *Case Reports in Neurological Medicine,* 2016, pp. 3745631.

Spillantini, M. G., Crowther, R. A., Jakes, R., Hasegawa, M. and Goedert, M. (1998) 'α-Synuclein in filamentous inclusions of Lewy bodies from Parkinson's disease and dementia with lewy bodies', *Proc Natl Acad Sci U S A,* 95(11), pp. 6469-73.

Spillantini, M. G., Schmidt, M. L., Lee, V. M., Trojanowski, J. Q., Jakes, R. and Goedert, M. (1997) 'α-synuclein in Lewy bodies', *Nature,* 388(6645), pp. 839-40.

Squiban, B., Belougne, J., Ewbank, J. and Zugasti, O. (2012) 'Quantitative and automated high-throughput genome-wide rnai screens in *C. elegans*', *Journal of Visualized Experiments : JoVE,* (60), pp. 3448.

Sreedharan, J., Blair, I. P., Tripathi, V. B., Hu, X., Vance, C., Rogelj, B., Ackerley, S., Durnall, J. C., Williams, K. L., Buratti, E., Baralle, F., de Belleroche, J., Mitchell, J. D., Leigh, P. N., Al-Chalabi, A., Miller, C. C., Nicholson, G. and Shaw, C. E. (2008) 'TDP-43 mutations in familial and sporadic amyotrophic lateral sclerosis', *Science,* 319(5870), pp. 1668-72.

Stiernagle, T. (2006) 'Maintenance of *C. elegans*', in *WormBook* [Online]. Available at: http://www.wormbook.org (Accessed: 18 Jan. 2018).

Strittmatter, W. J., Saunders, A. M., Schmechel, D., Pericak-Vance, M., Enghild, J., Salvesen, G. S. and Roses, A. D. (1993) 'Apolipoprotein E: High-avidity binding to β-amyloid and increased frequency of type 4 allele in late-onset familial Alzheimer disease', *Proc Natl Acad Sci U S A,* 90(5), pp. 1977-81.

Strong, J. M., Abe, T., Gibbs, E. L. and Atkinson, A. J. (1974) 'Plasma-levels of methsuximide and N-demethylmethsuximide during methsuximide therapy', *Neurology,* 24(3), pp. 250-255.

Strong, M. (1999) 'FDA policy and regulation of stereoisomers: Paradigm shift and the future of safer, more effective drugs', *Food Drug Law J,* 54(3), pp. 463-87.

Stroustrup, N., Ulmschneider, B. E., Nash, Z. M., Lopez-Moyado, I. F., Apfeld, J. and Fontana, W. (2013) 'The *Caenorhabditis elegans* lifespan machine', *Nat Meth,* 10(7), pp. 665-670.

Stumpfe, D. and Bajorath, J. (2011) 'Similarity searching', *Wiley Interdisciplinary Reviews-Computational Molecular Science,* 1(2), pp. 260-282.

Stutzbach, L. D., Xie, S. X., Naj, A. C., Albin, R., Gilman, S., Lee, V. M., Trojanowski, J. Q., Devlin, B. and Schellenberg, G. D. (2013) 'The unfolded protein response is activated in disease-affected brain regions in progressive supranuclear palsy and Alzheimer's disease', *Acta Neuropathol Commun,* 1, pp. 31.

Sugai, F., Yamamoto, Y., Miyaguchi, K., Zhou, Z., Sumi, H., Hamasaki, T., Goto, M. and Sakoda, S. (2004) 'Benefit of valproic acid in suppressing disease progression of ALS model mice', *European Journal of Neuroscience,* 20(11), pp. 3179-3183.

Sulkava, R. (1982) 'Alzheimer's disease and senile dementia of Alzheimer type. A comparative study', *Acta Neurol Scand,* 65(6), pp. 636-50.

Sutphin, G. L. and Kaeberlein, M. (2009) 'Measuring *Caenorhabditis elegans* life span on solid media', *Journal of Visualized Experiments : JoVE,* (27), pp. 1152.

Suzuki, N., Aoki, M., Warita, H., Kato, M., Mizuno, H., Shimakura, N., Akiyama, T., Furuya, H., Hokonohara, T., Iwaki, A., Togashi, S., Konno, H. and Itoyama, Y. (2010) 'FALS with FUS mutation in Japan, with early onset, rapid progress and basophilic inclusion', *J Hum Genet,* 55(4), pp. 252-4.

Swierczek, N. A., Giles, A. C., Rankin, C. H. and Kerr, R. A. (2011) 'High-throughput behavioral analysis in *C. elegans*', *Nat Meth,* 8(7), pp. 592-598.

Tabara, H., Grishok, A. and Mello, C. C. (1998) 'RNAi in *C. elegans*: Soaking in the genome sequence', *Science,* 282(5388), pp. 430-1.

Tabet, N. (2006) 'Acetylcholinesterase inhibitors for Alzheimer’s disease: Anti-inflammatories in acetylcholine clothing!', *Age and Ageing,* 35(4), pp. 336-338.

Takei, K., Watanabe, K., Yuki, S., Akimoto, M., Sakata, T. and Palumbo, J. (2017) 'Edaravone and its clinical development for amyotrophic lateral sclerosis', *Amyotroph Lateral Scler Frontotemporal Degener,* 18(sup1), pp. 5-10.

Tan, C. F., Eguchi, H., Tagawa, A., Onodera, O., Iwasaki, T., Tsujino, A., Nishizawa, M., Kakita, A. and Takahashi, H. (2007) 'TDP-43 immunoreactivity in neuronal inclusions in familial amyotrophic lateral sclerosis with or without *SOD1* gene mutation', *Acta Neuropathol,* 113(5), pp. 535-42.

Tariot, P. N., Farlow, M. R., Grossberg, G. T., Graham, S. M., McDonald, S. and Gergel, I. (2004) 'Memantine treatment in patients with moderate to severe Alzheimer disease already receiving donepezil: A randomized controlled trial', *Jama,* 291(3), pp. 317-24.

Tateishi, T., Hokonohara, T., Yamasaki, R., Miura, S., Kikuchi, H., Iwaki, A., Tashiro, H., Furuya, H., Nagara, Y., Ohyagi, Y., Nukina, N., Iwaki, T., Fukumaki, Y. and Kira, J. (2010) 'Multiple system degeneration with basophilic inclusions in Japanese ALS patients with FUS mutation', *Acta Neuropathol,* 119(3), pp. 355-64.

Tauffenberger, A., Julien, C. and Parker, J. A. (2013) 'Evaluation of longevity enhancing compounds against transactive response DNA-binding protein-43 neuronal toxicity', *Neurobiol Aging,* 34(9), pp. 2175-82.

Teixeira-Castro, A., Ailion, M., Jalles, A., Brignull, H. R., Vilaça, J. L., Dias, N., Rodrigues, P., Oliveira, J. F., Neves-Carvalho, A., Morimoto, R. I. and Maciel, P. (2011) 'Neuron-specific proteotoxicity of mutant ataxin-3 in *C. elegans*: Rescue by the DAF-16 and HSF-1 pathways', *Human Molecular Genetics,* 20(15), pp. 2996-3009.

Tennison, M. B., Greenwood, R. S. and Miles, M. V. (1991) 'Methsuximide for intractable childhood seizures', *Pediatrics,* 87(2), pp. 186-9.

Tepper, R. G., Ashraf, J., Kaletsky, R., Kleemann, G., Murphy, C. T. and Bussemaker, H. J. (2013) 'PQM-1 complements DAF-16 as a key transcriptional regulator of DAF-2-mediated development and longevity', *Cell,* 154(3), pp. 676-690.

Terstappen, G. C., Schlupen, C., Raggiaschi, R. and Gaviraghi, G. (2007) 'Target deconvolution strategies in drug discovery', *Nat Rev Drug Discov,* 6(11), pp. 891-903.

Thompson, S. M. and Wong, R. K. (1991) 'Development of calcium current subtypes in isolated rat hippocampal pyramidal cells', *J Physiol,* 439, pp. 671-89.

Timmons, L., Court, D. L. and Fire, A. (2001) 'Ingestion of bacterially expressed dsRNAs can produce specific and potent genetic interference in *Caenorhabditis elegans*', *Gene,* 263(1-2), pp. 103-12.

Timmons, L. and Fire, A. (1998) 'Specific interference by ingested dsRNA', *Nature,* 395.

Tiwari, S. K., Seth, B., Agarwal, S., Yadav, A., Karmakar, M., Gupta, S. K., Choubey, V., Sharma, A. and Chaturvedi, R. K. (2015) 'Ethosuximide induces hippocampal neurogenesis and reverses cognitive deficits in amyloid-β toxin induced Alzheimer's rat model via PI3K/Akt/Wnt/β-catenin pathway', *Journal of Biological Chemistry*.

Todorovic, S. M. and Lingle, C. J. (1998) 'Pharmacological properties of T-type Ca^{2+} current in adult rat sensory neurons: Effects of anticonvulsant and anesthetic agents', *J Neurophysiol,* 79(1), pp. 240-52.

Tollervey, J. R., Curk, T., Rogelj, B., Briese, M., Cereda, M., Kayikci, M., Konig, J., Hortobagyi, T., Nishimura, A. L., Zupunski, V., Patani, R., Chandran, S., Rot, G., Zupan, B., Shaw, C. E. and Ule, J. (2011) 'Characterizing the RNA targets and position-dependent splicing regulation by TDP-43', *Nat Neurosci,* 14(4), pp. 452-8.

Tomson, T. and Villen, T. (1994) 'Ethosuximide enantiomers in pregnancy and lactation', *Ther Drug Monit,* 16(6), pp. 621-3.

Treusch, S., Hamamichi, S., Goodman, J. L., Matlack, K. E., Chung, C. Y., Baru, V., Shulman, J. M., Parrado, A., Bevis, B. J., Valastyan, J. S., Han, H., Lindhagen-Persson, M., Reiman, E. M., Evans, D. A., Bennett, D. A., Olofsson, A., DeJager, P. L., Tanzi, R. E., Caldwell, K. A., Caldwell, G. A. and Lindquist, S. (2011) 'Functional links between Aβ toxicity, endocytic trafficking, and Alzheimer's disease risk factors in yeast', *Science,* 334(6060), pp. 1241-5.

Trojnar, M. K., Malek, R., Chroscinska, M., Nowak, S., Blaszczyk, B. and Czuczwar, S. J. (2002) 'Neuroprotective effects of antiepileptic drugs', *Pol J Pharmacol,* 54(6), pp. 557-66.

Tsakiridou, E., Bertollini, L., de Curtis, M., Avanzini, G. and Pape, H. C. (1995) 'Selective increase in T-type calcium conductance of reticular thalamic neurons in a rat model of absence epilepsy', *J Neurosci,* 15(4), pp. 3110-7.

Tsibidis, G. D. and Tavernarakis, N. (2007) 'Nemo: A computational tool for analyzing nematode locomotion', *BMC Neurosci,* 8, pp. 86.

van Bergeijk, J., Haastert, K., Grothe, C. and Claus, P. (2006) 'Valproic acid promotes neurite outgrowth in PC12 cells independent from regulation of the survival of motoneuron protein', *Chemical Biology & Drug Design,* 67(3), pp. 244-247.

Van Cauwenberghe, C., Van Broeckhoven, C. and Sleegers, K. (2015) 'The genetic landscape of Alzheimer disease: Clinical implications and perspectives', *Genetics In Medicine,* 18, pp. 421.

van de Waterbeemd, H., Camenisch, G., Folkers, G., Chretien, J. R. and Raevsky, O. A. (1998) 'Estimation of blood-brain barrier crossing of drugs using molecular size and shape, and H-bonding descriptors', *J Drug Target,* 6(2), pp. 151-65.

van der Bent, M. L., Sterken, M. G., Volkers, R. J. M., Riksen, J. A. G., Schmid, T., Hajnal, A., Kammenga, J. E. and Snoek, L. B. (2014) 'Loss-of-function of β-catenin bar-1 slows development and activates the Wnt pathway in *Caenorhabditis elegans*', *Scientific Reports,* 4, pp. 4926.

van Dyck, C. H., Schmitt, F. A. and Olin, J. T. (2006) 'A responder analysis of memantine treatment in patients with Alzheimer disease maintained on donepezil', *Am J Geriatr Psychiatry,* 14(5), pp. 428-37.

van Es, M. A., Veldink, J. H., Saris, C. G., Blauw, H. M., van Vught, P. W., Birve, A., Lemmens, R., Schelhaas, H. J., Groen, E. J., Huisman, M. H., van der Kooi, A. J., de Visser, M., Dahlberg, C., Estrada, K., Rivadeneira, F., Hofman, A., Zwarts, M. J., van Doormaal, P. T., Rujescu, D., Strengman, E., Giegling, I., Muglia, P., Tomik, B., Slowik, A., Uitterlinden, A. G., Hendrich, C., Waibel, S., Meyer, T., Ludolph, A. C., Glass, J. D., Purcell, S., Cichon, S., Nothen, M. M., Wichmann, H. E., Schreiber, S., Vermeulen, S. H., Kiemeney, L. A., Wokke, J. H., Cronin, S., McLaughlin, R. L., Hardiman, O., Fumoto, K., Pasterkamp, R. J., Meininger, V., Melki, J., Leigh, P. N., Shaw, C. E., Landers, J. E., Al-Chalabi, A., Brown, R. H., Jr., Robberecht, W., Andersen, P. M., Ophoff, R. A. and van den Berg, L. H. (2009) 'Genome-wide association study identifies 19p13.3 (*UNC13A*) and 9p21.2 as susceptibility loci for sporadic amyotrophic lateral sclerosis', *Nat Genet,* 41(10), pp. 1083-7.

van Ham, T. J., Thijssen, K. L., Breitling, R., Hofstra, R. M. W., Plasterk, R. H. A. and Nollen, E. A. A. (2008) '*C. elegans* model identifies genetic modifiers of α-synuclein inclusion formation during aging', *PLOS Genetics,* 4(3), pp. e1000027.

van Rheenen, W. and Shatunov, A. and Dekker, A. M. and McLaughlin, R. L. and Diekstra, F. P. and Pulit, S. L. and van der Spek, R. A. and Vosa, U. and de Jong, S. and Robinson, M. R. and Yang, J. and Fogh, I. and van Doormaal, P. T. and Tazelaar, G. H. and Koppers, M. and Blokhuis, A. M. and Sproviero, W. and Jones, A. R. and Kenna, K. P. and van Eijk, K. R. and Harschnitz, O. and Schellevis, R. D. and Brands, W. J. and Medic, J. and Menelaou, A. and Vajda, A. and Ticozzi, N. and Lin, K. and Rogelj, B. and Vrabec, K. and Ravnik-Glavac, M. and Koritnik, B. and Zidar, J. and Leonardis, L. and Groselj, L. D. and Millecamps, S. and Salachas, F. and Meininger, V. and de Carvalho, M. and Pinto, S. and Mora, J. S. and Rojas-Garcia, R. and Polak, M. and Chandran, S. and Colville, S. and Swingler, R. and Morrison, K. E. and Shaw, P. J. and Hardy, J. and Orrell, R. W. and Pittman, A. and Sidle, K. and Fratta, P. and Malaspina, A. and Topp, S. and Petri, S. and Abdulla, S. and Drepper, C. and Sendtner, M. and Meyer, T. and Ophoff, R. A. and Staats, K. A. and Wiedau-Pazos, M. and Lomen-Hoerth, C. and Van Deerlin, V. M. and Trojanowski, J. Q. and Elman, L. and McCluskey, L. and Basak, A. N. and Tunca, C. and Hamzeiy, H. and Parman, Y. and Meitinger, T. and Lichtner, P. and Radivojkov-Blagojevic, M. and Andres, C. R. and Maurel, C. and Bensimon, G. and Landwehrmeyer, B. and Brice, A. and Payan, C. A. and Saker-Delye, S. and Durr, A. and Wood, N. W. and Tittmann, L. and Lieb, W. and Franke, A. and Rietschel, M. and Cichon, S. and Nothen, M. M. and Amouyel, P. and Tzourio, C. and Dartigues, J. F. and Uitterlinden, A. G. and Rivadeneira, F. and Estrada, K. and Hofman, A. and Curtis, C. and Blauw, H. M. and van der Kooi, A. J. and de Visser, M. and Goris, A. and Weber, M. and Shaw, C. E. and Smith, B. N. and Pansarasa, O. and Cereda, C. and Del Bo, R. and Comi, G. P. and D'Alfonso, S. and Bertolin, C. and Soraru, G. and Mazzini, L. and Pensato, V. and Gellera, C. and Tiloca,

C. and Ratti, A. and Calvo, A. and Moglia, C. and Brunetti, M. and Arcuti, S. and Capozzo, R. and Zecca, C. and Lunetta, C. and Penco, S. and Riva, N. and Padovani, A. and Filosto, M. and Muller, B. and Stuit, R. J. and Blair, I. and Zhang, K. and McCann, E. P. and Fifita, J. A. and Nicholson, G. A. and Rowe, D. B. and Pamphlett, R. and Kiernan, M. C. and Grosskreutz, J. and Witte, O. W. and Ringer, T. and Prell, T. and Stubendorff, B. and Kurth, I. and Hubner, C. A. and Leigh, P. N. and Casale, F. and Chio, A. and Beghi, E. and Pupillo, E. and Tortelli, R. and Logroscino, G. and Powell, J. and Ludolph, A. C. and Weishaupt, J. H. and Robberecht, W. and Van Damme, P. and Franke, L. and Pers, T. H. and Brown, R. H. and Glass, J. D. and Landers, J. E. and Hardiman, O. and Andersen, P. M. and Corcia, P. and Vourc'h, P. and Silani, V. and Wray, N. R. and Visscher, P. M. and de Bakker, P. I. and van Es, M. A. and Pasterkamp, R. J. and Lewis, C. M. and Breen, G. and Al-Chalabi, A. and van den Berg, L. H. and Veldink, J. H. (2016) 'Genome-wide association analyses identify new risk variants and the genetic architecture of amyotrophic lateral sclerosis', *Nat Genet,* 48(9), pp. 1043-8.

Vance, C., Rogelj, B., Hortobágyi, T., De Vos, K. J., Nishimura, A. L., Sreedharan, J., Hu, X., Smith, B., Ruddy, D., Wright, P., Ganesalingam, J., Williams, K. L., Tripathi, V., Al-Saraj, S., Al-Chalabi, A., Leigh, P. N., Blair, I. P., Nicholson, G., de Belleroche, J., Gallo, J.-M., Miller, C. C. and Shaw, C. E. (2009) 'Mutations in FUS, an RNA processing protein, cause familial amyotrophic lateral sclerosis type 6', *Science (New York, N.Y.),* 323(5918), pp. 1208-1211.

Vanden Broeck, L., Callaerts, P. and Dermaut, B. (2014) 'TDP-43-mediated neurodegeneration: Towards a loss-of-function hypothesis?', *Trends Mol Med,* 20(2), pp. 66-71.

Ved, R., Saha, S., Westlund, B., Perier, C., Burnam, L., Sluder, A., Hoener, M., Rodrigues, C. M., Alfonso, A., Steer, C., Liu, L., Przedborski, S. and Wolozin, B. (2005) 'Similar patterns of mitochondrial vulnerability and rescue induced by genetic modification of α-synuclein, parkin, and DJ-1 in *Caenorhabditis elegans*', *J Biol Chem,* 280(52), pp. 42655-42668.

Veriepe, J., Fossouo, L. and Parker, J. A. (2015) 'Neurodegeneration in *C. elegans* models of ALS requires TIR-1/Sarm1 immune pathway activation in neurons', *Nat Commun,* 6, pp. 7319.

Villen, T., Bertilsson, L. and Sjoqvist, F. (1990) 'Nonstereoselective disposition of ethosuximide in humans', *Ther Drug Monit,* 12(5), pp. 514-6.

Volicer, L., Smith, S. and Volicer, B. J. (1995) 'Effect of seizures on progression of dementia of the Alzheimer type', *Dementia,* 6(5), pp. 258-63.

Vossel, K. A., Beagle, A. J., Rabinovici, G. D., Shu, H., Lee, S. E., Naasan, G., Hegde, M., Cornes, S. B., Henry, M. L., Nelson, A. B., Seeley, W. W., Geschwind, M. D., Gorno-Tempini, M. L., Shih, T., Kirsch, H. E., Garcia, P. A., Miller, B. L. and Mucke, L. (2013) 'Seizures and epileptiform activity in the early stages of Alzheimer disease', *JAMA Neurol,* 70(9), pp. 1158-66.

Wager, T. T., Chandrasekaran, R. Y., Hou, X., Troutman, M. D., Verhoest, P. R., Villalobos, A. and Will, Y. (2010a) 'Defining desirable central nervous system drug space through the alignment of molecular properties, in vitro ADME, and safety attributes', *ACS Chem Neurosci,* 1(6), pp. 420-34.

Wager, T. T., Hou, X., Verhoest, P. R. and Villalobos, A. (2010b) 'Moving beyond rules: The development of a central nervous system multiparameter optimization (CNS MPO) approach to enable alignment of druglike properties', *ACS Chem Neurosci,* 1(6), pp. 435-49.

Walker, G., Houthoofd, K., Vanfleteren, J. R. and Gems, D. (2005) 'Dietary restriction in *C. elegans*: From rate-of-living effects to nutrient sensing pathways', *Mech Ageing Dev,* 126(9), pp. 929-37.

Wang, H., Lim, P. J., Yin, C., Rieckher, M., Vogel, B. E. and Monteiro, M. J. (2006) 'Suppression of polyglutamine-induced toxicity in cell and animal models of Huntington's disease by ubiquilin', *Hum Mol Genet,* 15(6), pp. 1025-41.

Watanabe, T., Tahara, M. and Todo, S. (2008) 'The novel antioxidant edaravone: From bench to bedside', *Cardiovasc Ther,* 26(2), pp. 101-14.

Weininger, D. (1988) 'SMILES, a chemical language and information system. 1. Introduction to methodology and encoding rules', *Journal of Chemical Information and Computer Sciences,* 28(1), pp. 31-36.

White, H. S. (2003) 'Preclinical development of antiepileptic drugs: Past, present, and future directions', *Epilepsia,* 44, pp. 2-8.

Wildburger, N. C., Lin-Ye, A., Baird, M. A., Lei, D. and Bao, J. (2009a) 'Neuroprotective effects of blockers for T-type calcium channels', *Molecular Neurodegeneration,* 4, pp. 44-44.

Wildburger, N. C., Lin-Ye, A., Baird, M. A., Lei, D. B. and Bao, J. X. (2009b) 'Neuroprotective effects of blockers for T-type calcium channels', *Molecular Neurodegeneration,* 4.

Wilder, B. J. and Buchanan, R. A. (1981) 'Methsuximide for refractory complex partial seizures', *Neurology,* 31(6), pp. 741-4.

Williams, S. N., Locke, C. J., Braden, A. L., Caldwell, K. A. and Caldwell, G. A. (2004) 'Epileptic-like convulsions associated with LIS-1 in the cytoskeletal control of neurotransmitter signaling in *Caenorhabditis elegans*', *Hum Mol Genet,* 13(18), pp. 2043-59.

Williams-Gray, C. H. and Worth, P. F. (2016) 'Parkinson's disease', *Medicine,* 44(9), pp. 542-546.

Wong, P. C., Cai, H., Borchelt, D. R. and Price, D. L. (2002) 'Genetically engineered mouse models of neurodegenerative diseases', *Nat Neurosci,* 5(7), pp. 633-9.

World Alzheimer Report (2016) [PDF]. Available at: https://www.alz.co.uk/research/WorldAlzheimerReport2016.pdf (Accessed: 15 Sep. 2017).

Wu, C. H., Fallini, C., Ticozzi, N., Keagle, P. J., Sapp, P. C., Piotrowska, K., Lowe, P., Koppers, M., McKenna-Yasek, D., Baron, D. M., Kost, J. E., Gonzalez-Perez, P., Fox, A. D., Adams, J., Taroni, F., Tiloca, C., Leclerc, A. L., Chafe, S. C., Mangroo, D., Moore, M. J., Zitzewitz, J. A., Xu, Z. S., van den Berg, L. H., Glass, J. D., Siciliano, G., Cirulli, E. T., Goldstein, D. B., Salachas, F., Meininger, V., Rossoll, W., Ratti, A.,

Gellera, C., Bosco, D. A., Bassell, G. J., Silani, V., Drory, V. E., Brown, R. H., Jr. and Landers, J. E. (2012) 'Mutations in the profilin 1 gene cause familial amyotrophic lateral sclerosis', *Nature,* 488(7412), pp. 499-503.

Wu, Y., Li, X., Zhu, J. X., Xie, W., Le, W., Fan, Z., Jankovic, J. and Pan, T. (2011) 'Resveratrol-activated AMPK/SIRT1/autophagy in cellular models of Parkinson's disease', *Neurosignals,* 19(3), pp. 163-74.

Xia, J. and Wishart, D. S. (2002) 'Using MetaboAnalyst 3.0 for comprehensive metabolomics data analysis', *Current Protocols in Bioinformatics*: John Wiley & Sons, Inc.

Ximenes, J. C., Neves, K. R., Leal, L. K., do Carmo, M. R., Brito, G. A., Naffah-Mazzacoratti Mda, G., Cavalheiro, E. A. and Viana, G. S. (2015) 'Valproic acid neuroprotection in the 6-OHDA model of Parkinson's disease is possibly related to its anti-inflammatory and hdac inhibitory properties', *J Neurodegener Dis,* 2015, pp. 313702.

Xu, Z. S. (2012) 'Does a loss of TDP-43 function cause neurodegeneration?', *Mol Neurodegener,* 7, pp. 27.

Yaari, Y., Selzer, M. E. and Pincus, J. H. (1986) 'Phenytoin: Mechanisms of its anticonvulsant action', *Ann Neurol,* 20(2), pp. 171-84.

Yamanaka, K., Okubo, Y., Suzaki, T. and Ogura, T. (2004) 'Analysis of the two p97/VCP/Cdc48p proteins of *Caenorhabditis elegans* and their suppression of polyglutamine-induced protein aggregation', *J Struct Biol,* 146(1-2), pp. 242-50.

Yemini, E., Jucikas, T., Grundy, L. J., Brown, A. E. and Schafer, W. R. (2013) 'A database of *Caenorhabditis elegans* behavioral phenotypes', *Nat Methods,* 10(9), pp. 877-9.

Yi, J. P., Zhang, L., Tang, B. S., Han, W. W., Zhou, Y. F., Chen, Z., Jia, D. D. and Jiang, H. (2013) 'Sodium valproate alleviates neurodegeneration in SCA3/MJD via suppressing apoptosis and rescuing the hypoacetylation levels of histone H3 and H4', *Plos One,* 8(1).

Yosef, N. and Regev, A. (2011) 'Impulse control: Temporal dynamics in gene transcription', *Cell,* 144(6), pp. 886-896.

Zhang, Y. F., Gibbs, J. W. and Coulter, D. A. (1996a) 'Anticonvulsant drug effects on spontaneous thalamocortical rhythms in vitro: Valproic acid, clonazepam, and α-methyl-α-phenylsuccinimide', *Epilepsy Research,* 23(1), pp. 37-53.

Zhang, Y. F., Gibbs, J. W., 3rd and Coulter, D. A. (1996b) 'Anticonvulsant drug effects on spontaneous thalamocortical rhythms in vitro: Ethosuximide, trimethadione, and dimethadione', *Epilepsy Res,* 23(1), pp. 15-36.

Zheng, S. Q., Ding, A. J., Li, G. P., Wu, G. S. and Luo, H. R. (2013) 'Drug absorption efficiency in caenorhbditis elegans delivered by different methods', *PLOS ONE,* 8(2), pp. e56877.

Zimmerman, F. T. and Burgemeister, B. B. (1958) 'A new drug for petit mal epilepsy', *Neurology,* 8(10), pp. 769-75.